

Foldamers and chromophores

Citation for published version (APA):

Sinkeldam, R. W. (2006). *Foldamers and chromophores*. [Phd Thesis 1 (Research TU/e / Graduation TU/e), Chemical Engineering and Chemistry]. Technische Universiteit Eindhoven. <https://doi.org/10.6100/IR602533>

DOI:

[10.6100/IR602533](https://doi.org/10.6100/IR602533)

Document status and date:

Published: 01/01/2006

Document Version:

Publisher's PDF, also known as Version of Record (includes final page, issue and volume numbers)

Please check the document version of this publication:

- A submitted manuscript is the version of the article upon submission and before peer-review. There can be important differences between the submitted version and the official published version of record. People interested in the research are advised to contact the author for the final version of the publication, or visit the DOI to the publisher's website.
- The final author version and the galley proof are versions of the publication after peer review.
- The final published version features the final layout of the paper including the volume, issue and page numbers.

[Link to publication](#)

General rights

Copyright and moral rights for the publications made accessible in the public portal are retained by the authors and/or other copyright owners and it is a condition of accessing publications that users recognise and abide by the legal requirements associated with these rights.

- Users may download and print one copy of any publication from the public portal for the purpose of private study or research.
- You may not further distribute the material or use it for any profit-making activity or commercial gain
- You may freely distribute the URL identifying the publication in the public portal.

If the publication is distributed under the terms of Article 25fa of the Dutch Copyright Act, indicated by the "Taverne" license above, please follow below link for the End User Agreement:

www.tue.nl/taverne

Take down policy

If you believe that this document breaches copyright please contact us at:

openaccess@tue.nl

providing details and we will investigate your claim.

FOLDAMERS AND CHROMOPHORES

PROEFSCHRIFT

ter verkrijging van de graad van doctor aan de
Technische Universiteit Eindhoven, op gezag van de
Rector Magnificus, prof.dr.ir. C.J. van Duijn, voor een
commissie aangewezen door het College voor
Promoties in het openbaar te verdedigen
op donderdag 23 maart 2006 om 16.00 uur

door

Renatus Wilhelmus Sinkeldam

geboren te Purmerend

Dit proefschrift is goedgekeurd door de promotor:

prof.dr. E.W. Meijer

Copromotor:

dr. J.A.J.M. Vekemans

This research has been financially supported by the Council for Chemical Sciences of the Netherlands Organization for Scientific Research (NWO-CW).

Omslagontwerp: R. W. Sinkeldam. Based on a picture from the helical staircase designed by Giuseppe Momo (Musei Vaticani, Rome, 1932).

Druk: Universiteitsdrukkerij, Technische Universiteit Eindhoven

A catalogue record is available from the Library Eindhoven University of Technology

ISBN-10: 90-386-3047-6

ISBN-13: 978-90-386-3047-2

Contents

Chapter 1:	Helical backbones based on intramolecular secondary interactions	01
1.1	Introduction	02
1.2	Natural α -helices and their β -peptide analogues	02
1.3	Structurally constraint synthetic helices	03
1.4	Synthetic foldamers based on solvophobicity and π - π interactions	04
1.5	Aromatic oligoamides: intramolecular hydrogen bonding and π - π stacking	06
1.6	Aromatic oligo-ureas	09
1.7	The poly(ureidophthalimide) design	11
1.8	Aim of the thesis	12
1.9	Outline of the thesis	13
1.10	References	14
Chapter 2:	Synthesis of 3,6-disubstituted phthalimides	17
2.1	Introduction	18
2.2	Alternative synthetic approaches towards 3,6-diaminophthalimides	19
2.3	A novel versatile methodology for the synthesis of 3,6-diaminophthalimides	22
2.4	A brief investigation on foldamers with an aliphatic periphery	25
2.5	Conclusions	28
2.6	Experimental	29
2.7	References	39
Chapter 3:	Anthraquinones as a novel backbone	41
3.1	Introduction	42
3.2	Alternating anthraquinone-ureidophthalimide copolymer	42
3.3	A brief 'urea-scrambling' investigation	44
3.4	Towards an anthraquinone homopolymer	47
3.5	Towards a triangular helical anthraquinone foldamer	50
3.6	Conclusions	55
3.7	Experimental	56
3.8	References	64
Chapter 4:	Foldamers decorated with chromophores	65
4.1	Introduction: peripheral functionalization with chromophores	66
4.2	Ureidophthalimide foldamer decorated with OPV3 chromophores	67
4.3	Ureidophthalimide foldamer decorated with OPV4 chromophores	73
4.4	Ureidophthalimide foldamer decorated with D- π -A chromophores	78
4.5	Conclusions	81
4.6	Outlook	82
4.7	Experimental	83
4.8	References	90

Chapter 5:	Helical architectures in water	93
5.1	Introduction: inspired by Nature	94
5.2	Synthesis	95
5.3	UV-vis and CD spectroscopy	97
5.4	Conclusions	101
5.5	Polu(ureidophthalimide)s: what have we learned?	102
5.6	Experimental	104
5.7	References	107
Chapter 6:	Indigo: synthesis of a new soluble n-type material	109
6.1	Introduction	110
6.2	A brief history on the synthesis of indigo	113
6.3	Towards soluble indigo derivatives, the isatin pathway	114
6.4	A Friedel-Crafts precursor as the key intermediate	115
6.5	Soluble <i>N,N'</i> -diacetylidigo derivatives	116
6.6	Photophysical characterization of the novel indigos	119
6.7	Is <i>N,N'</i> -diacetylidigo a new n-type material suitable for organic solar cells?	121
6.8	Conclusions	125
6.9	Experimental	126
6.10	References	134
Summary		137
Samenvatting		139
Curriculum Vitae		141
Dankwoord		142

Chapter 1

Helical backbones based on intramolecular secondary interactions

Abstract

Many biomolecules have dynamically ordered architectures and the helical shape is abundant in Nature. Numerous artificially designed architectures are reported to mimic the transition from a random coil to a helical secondary structure. These structures are referred to as foldamers: oligomers that can adopt a conformationally ordered state in solution. In this respect β -peptides occupy a special position since they resemble the naturally occurring α -helix most closely. A number of design strategies have led to novel helical architectures in which folding is based on secondary interactions like hydrogen bonding and solvophobicity. The synthetic nature of these structures also allowed the extensive use of π - π interactions. All architectures have one thing in common: the formation of secondary structures relies on a clever design of the primary structure. In this first chapter, a review on foldamers is presented.

1.1 Introduction

Synthetic organic chemistry has advanced to such high level that complicated structures have become available by skillful hands employing multi-step syntheses.¹ However, the interdisciplinary research of today and the future demands chemistry that incorporates design elements that go beyond the covalent bond. Three-dimensional control over molecular structures is not only of interest in the mimicry of the immense complexity of natural systems, but may also find use in the field of molecular electronics^{2,3}. With an apparent simple toolbox consisting of secondary interactions like hydrogen bonding and π - π stacking, the supramolecular chemist strives towards complete control over supramolecular architectures.

A fascinating example in which supramolecular interactions are employed to gain control over the secondary structure is the foldamer.⁴ The term foldamer was defined by Moore in 2001 who stated: *"A foldamer is any oligomer that folds into a conformationally ordered state in solution, the structures of which are stabilized by a collection of noncovalent interactions between nonadjacent monomer units."*^{4e}

This field is characterized by the search for the optimal blend of covalent chemistry and supramolecular interactions. The reversible nature of foldamers requires structural elements capable of forming intramolecular non-covalent interactions. Excellent examples are the natural α -helices and their β -peptide analogues, both relying on hydrogen bonding and solvophobicity. Synthetic foldamer designs that combine the latter two secondary interactions with aromatic structural elements may expect additional stabilization based on π - π interactions.

The various approaches presented in this chapter underline the importance of the design of the primary structure in pursuing the desired secondary structure in a controlled manner. For an excellent and comprehensive review the reader is referred to ref. 4a and 4e.

1.2 Natural α -helices and their synthetic β -peptide analogues

Probably all foldamer research is inspired by the vast number and complexity of molecular shapes in nature and in particular the helix has gained a lot of attention. This shape can for example be recognized in DNA and RNA. The best known natural helical architecture is the α -helix (Figure 1.1) of which Pauling determined its right handedness by X-ray analysis in 1951.⁵

Previous studies of natural peptides indicated that folding from random coil into the helical secondary structure is the result of numerous subtle interactions of the backbone, side chains, and solvent, which are difficult to control.⁶ Besides solvophobic effects, hydrogen bonding proved to have a great impact on the formation of secondary structures. It was found that approximately 90% of all polar groups in the interior of a protein are involved in hydrogen bonding interactions.⁷ Individual hydrogen bonds are weak but directional, and their combined strength exceeds that of the sum of all single hydrogen bonds.⁸ The combination of solvophobicity, hydrogen bonding, and Van der Waals interactions determines the shape and

stability of the architecture. A detailed study on the folding of proteins from random coil to ordered secondary structures was reported by Zimm and Bragg.⁹ The high degree of complexity in the folding process of proteins prompted chemists to develop more simple systems that allow a detailed study of the interactions governing folding. Eventually, this knowledge may lead to the control of the folding process.

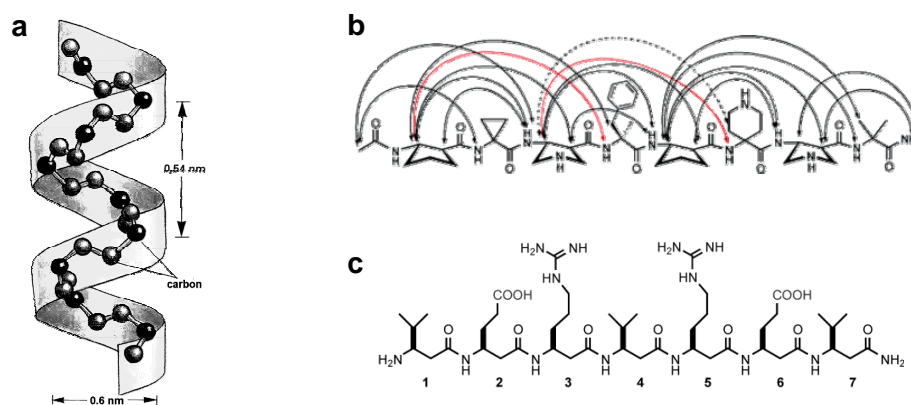


Figure 1.1: a) A cartoon of a natural α -helix constructed from 9 amino acids. b) An example of a β -peptide by Gellman¹¹ et al., wherein the arrows indicate NOE interactions. c) A β -peptide capable of folding as reported by Seebach¹² et al..

Of all synthetic helical architectures the β -peptides resemble the natural α -helix the most.¹⁰ Similar to the α -helix, their folding into the secondary architecture relies on hydrophobicity and intramolecular hydrogen bonding between non-adjacent amino acids. The choice for β -peptides to mimic and study the folding into, and the stability of helical systems is logical from the organic chemist's point of view. The extra carbon in the β -amino-acid building block that constitutes the backbone of the β -peptide is a valuable anchor point for synthetic derivatization. The β -peptides are extensively studied by Seebach¹¹ and Gellman¹². Several functionalities are incorporated in the backbone to influence the properties of the secondary architecture (Figure 1.1).

Characterization of the structures is typically performed by 2D-NMR, X-ray analysis, and circular dichroism (CD) spectroscopy. Especially the NOE contacts between distinguishable protons form a proof of the secondary structure in solution. Remarkably, helical architectures comprising β -peptides proved more stable than their α -peptide counterparts.^{12b} This is encouraging news for a completely synthetic approach.

1.3 Structurally constrained synthetic helices

Besides natural helical architectures, many synthetic analogues have been developed. A class of non-natural helical architectures that has enjoyed interest for almost 60 years are the helicenes.

These ortho-fused aromatic rings were first reported in the 1950's by Newman.¹³ Since then many different synthetic strategies have been developed to obtain at these structures.¹⁴ After six *ortho*-fusions of benzene rings the system is irreversibly forced to adopt a helical conformation due to structural constraints (Figure 1.2, left). With the fusion of a seventh unit the handedness of the helical architecture cannot be interchanged.

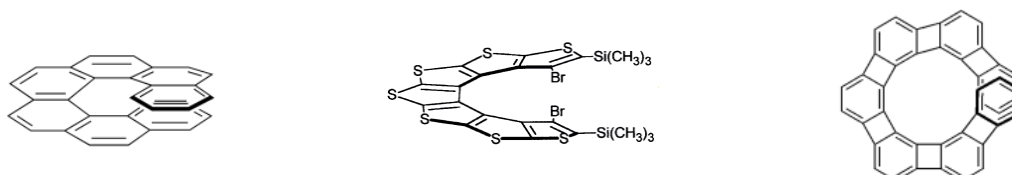


Figure 1.2: Helicenes: of hexahelicene (left), heptathiophene (center) and [7] heliphene (right).

Since there are no structural influences that favor one handedness over the other the result will be a racemic mixture of P- and M-helicenes. In spite of the difficulties, Newman reported the resolution of hexahelicene by selective complexation with one of the enantiomers of 2-(2,4,5,7-tetranitro-9-fluorenylideneaminoxy)propionic acid.¹³ The same approach has been employed by Wynberg *et al* in solution and in conjunction with column and thin-layer chromatography.¹⁵

This design is not limited to benzene rings alone. Heterohelicenes based on thiophene have been studied as well.^{15,16} Temperature dependent ¹H-NMR study on [7]heliphene (Figure 1.2, right) indicated a remarkably low energy barrier of 12.6 kcal/mol for inversion of the helical handedness.¹⁷ However, by increasing the number of annealed rings, the stability increases.

The helicenes are inspirational to the field of foldamers since they demonstrate that structural constraints are an important aspect in the design of helical architectures. Moreover, helicenes have incorporated π - π interactions capable of stabilizing the architecture. However, they cannot be referred to as foldamers since the structural constraints hamper unfolding.

1.4 Synthetic foldamers based on solvophobicity and π - π interactions

The designs described in this paragraph also rely on structural constraints for folding, albeit that there is now enough structural freedom to unfold. The structural freedom requires these structures to rely even more on solvophobicity and π - π stacking since no elements capable of hydrogen bonding are present.

Based on the dipole-induced *transoid* preference of the 2,2'-bipyridine unit helical architectures with an interior cavity of 2.5 Å in diameter have been prepared by Lehn *et al.* with oligomers consisting of alternating *meta*-linked pyrimidine and pyridine units (Figure 1.3, left).^{18,19} Replacement of the pyrimidine unit by a pyridazine also rendered a helical architecture. However, due to the *para-meta* substitution pattern in this case a larger inner diameter is present (Figure 1.3, center).²⁰ Substitution of the pyridine units in the first design by 1,8-naphthyridine units enlarged the inner diameter to ~5 Å (Figure 1.3, right).²¹ This set of

helical oligo-*N*-heterocycles nicely demonstrates that the diameter of the interior can be customized by selecting the right building blocks.

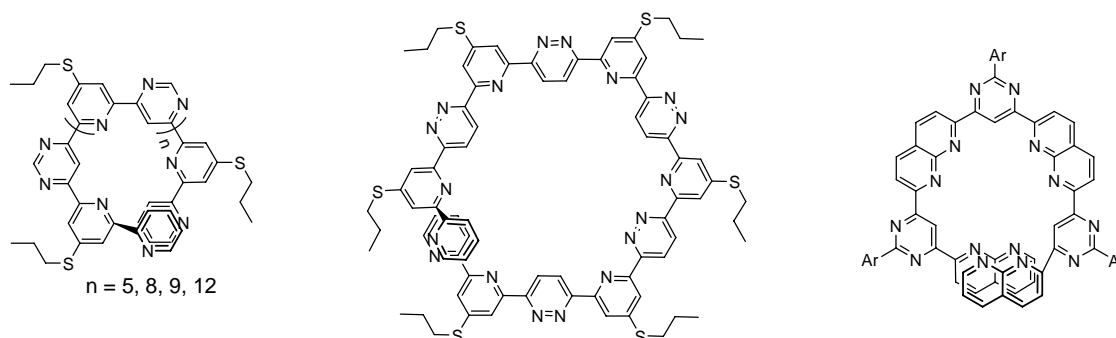


Figure 1.3: Aromatic *N*-heterocyclic helices based on π - π interactions. *Meta*-linked pyrimidine-pyridines (left), alternating pyridazine-pyridines (center) and alternating 1,8-naphthyridine-pyrimidines (right).

Another type of foldamer that relies on the combination of solvophobicity and π - π interactions has been extensively studied by Moore and coworkers. Their oligo(*meta*-phenylene-ethynylene) (*mPE*) constructs, capable of folding into helical structures, were reported for the first time in 1997.²² Prior to that, macrocycles based on the same design principle were reported.²³ The initial folding in *mPE*s is purely based on solvophobic effects (Figure 1.4). Of course, the design is such that the conformational freedom of the ethynyl linkers is restricted to a favorable *cisoid* or an unfavorable *transoid* conformation depending on the solvent. In a 'poor' solvent (e.g. acetonitrile) the system is prone to shield the apolar benzene moieties from the solvent by adopting an all *cisoid* conformation and thereby inducing folding. The large π -system stabilizes the formed architectures, while the polar ethyleneoxide side chains ensure solubility in acetonitrile.

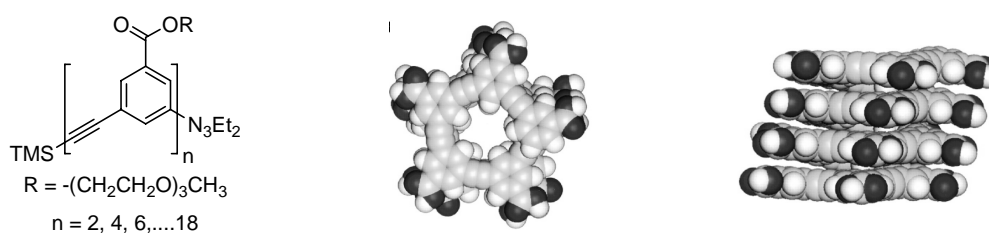


Figure 1.4: The oligo(*mPE*) as designed by Moore and coworkers. Chemical structure (left), and models: top view (center), side view (right) with $n = 18$, $R = H$. The end groups have been omitted for clarity.

The helix formation in the solid state was confirmed by X-ray analysis²⁴ and in solution by characteristic differences in chemical shift in $^1\text{H-NMR}$, measured in chloroform for the random coil and in acetonitrile for the folded structure. Electron spin resonance (ESR) measurements on double spin labeled analogues of the oligo(*mPE*) in ethyl acetate were consistent with a helical organization.²⁵ Furthermore, a UV-vis study of the oligomers in chloroform-acetonitrile mixtures revealed a difference in packing of the chromophores with a concomitant

hypochromic effect; a powerful indicator of oriented chromophores commonly seen in DNA, RNA and other polymers.^{26,27} In later reports the changes in the UV-vis spectrum upon changing chloroform-acetonitrile ratios were combined with fluorescence spectroscopy.²⁸ Circular dichroism²⁹ studies on similar oligomers with chiral ethyleneoxide side chains revealed a large bisignate Cotton effect, suggesting the presence of helical architectures with preferred handedness. The latter aggregated into larger helical columns in highly polar aqueous acetonitrile solutions, as was proven by sergeants and soldiers³⁰ experiments in combination with CD spectroscopy.³¹

The first reported achiral *m*PE could obviously not be analyzed with CD spectroscopy since there was no preference of one helical handedness over the other. However, a preferred handedness was induced by the introduction of a hydrophobic chiral guest that fits in the inner void of the helical architecture.³² Even a 'guest' that exceeds the length of the helix in the shape of a dumbbell³³ has been used successfully. A similar oligo(*m*PE) decorated with apolar chiral side chains revealed a large bisignate Cotton effect in heptane, indicative for the presence of helical architectures, and the absence of a Cotton effect in chloroform, suggesting a random coil conformation or an attained equilibrium between P and M helices.³⁴

The polar solvent in all former studies was acetonitrile, but introduction of longer ethyleneoxide side chains allowed measurements in water.³⁵ Besides ethyleneoxides to ensure solubility in water, a cationic amphiphilic poly(*m*PE) has been synthesized and studied on the air water interface³⁶ and in aqueous³⁷ solutions.

Although less widespread, the synthesis³⁸ and NMR study³⁹ of chiral oligo(*ortho*-PE) capable of adopting a helical conformation in solution have been reported.^{40,41} The results obtained with different aromatic *N*-heterocycles, the oligo(*m*PE) and oligo(*o*PE) systems demonstrate that in a smart design based on limited conformational freedom, additional functionalities such as hydrogen bonding units to direct folding are not needed to induce folding. However, additional external structural elements capable of hydrogen bonding between adjacent repeat units were used to strengthen the folded conformation of *m*PE.⁴² Solvent denaturation experiments indicated an increased stability of the folded structure of approximately 1 kcal/mol by one such hydrogen bonding interaction.⁴³ Introduction of hydrogen bonding units on every repeat unit even caused the structure to fold in chloroform, in which a random coil formation was expected.⁴⁴

1.5 Aromatic oligoamides: intramolecular hydrogen bonding and π - π stacking

To exploit the combination of hydrogen bonding and π - π interactions, structural features are needed which are present in the research on aromatic oligoamides.^{4bc} In these designs amide substituted aryls can fold due to the intramolecular hydrogen bonding capabilities of the amide. After one turn the helix may be stabilized by additional π - π interactions.

The most straightforward design was presented by Gong and coworkers. ^1H , ^1H -NOESY NMR studies on their crescent oligomers too small to reach one turn nevertheless confirmed the curved structure.⁴⁵ Later studies on longer oligomers showed that controlled coupling of *para* and *meta* linked units allows control over the size of the internal cavity (Figure 1.5).^{46,47} The dynamic folding and unfolding of the system was revealed by temperature dependent ^1H , ^1H -NOESY NMR.⁴⁸ In addition, the same design principle also gave access to the synthesis of macrocycles.⁴⁹

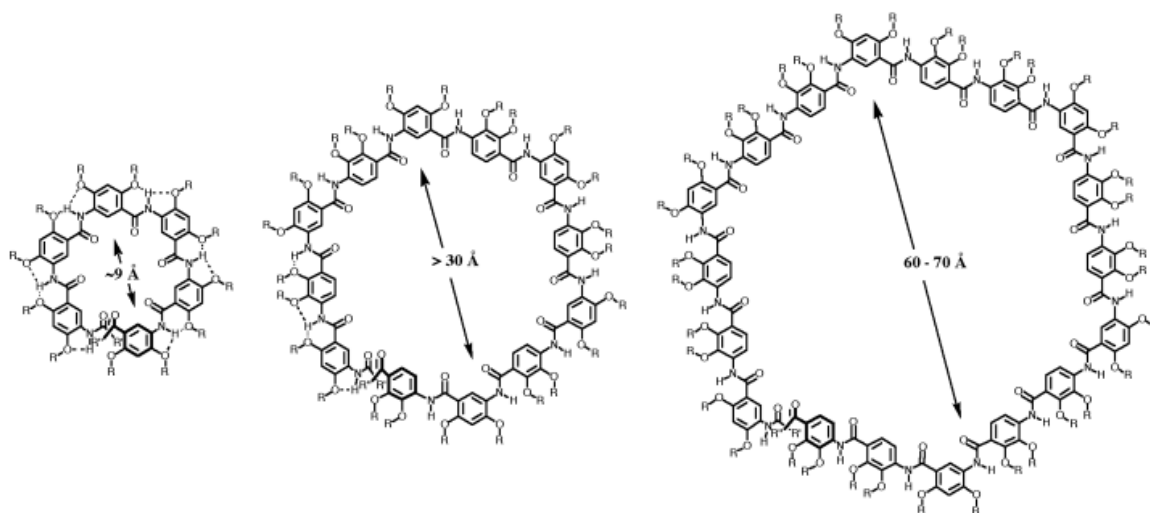


Figure 1.5: Control over the interior diameter (d) of oligo-amides. All *meta*-coupled units, $d = \sim 9 \text{ \AA}$ (left), alternating *meta-para*-coupled units, $d = > 30 \text{ \AA}$ (center), and *meta-para-para* repetition, $d = 60\text{-}70 \text{ \AA}$ (right).

All *para*-connected *N*-alkylated poly(benzamide) no longer has amide hydrogens available for hydrogen bonding. However, face to edge interactions of the benzene units still allow folding into helical architectures comprising three units per turn.⁵⁰

A whole range of new designs emerged through the incorporation of *N*-aromatic heterocycles. In these systems the nitrogen plays the role of hydrogen bond acceptor and thereby assists the direction of the folding. Probably one of the earliest designs based on anthranilamides was reported by Hamilton *et al.* in 1994.⁵¹ Helix formation is nucleated with the incorporation of 2,6-pyridinedicarboxamide as a turning point (Figure 1.6, left) since oligo(anthranilamides) tend to form linear strands.⁵² In later research the introduction of unit E as a central turning point gave access to a two turn helix (Figure 1.6, right).⁵³

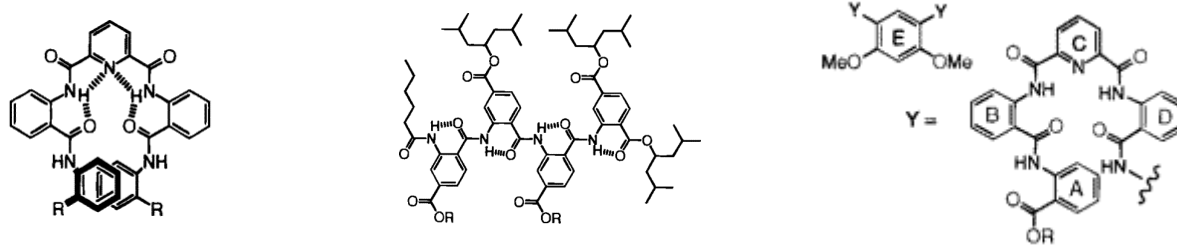


Figure 1.6: Anthranilamide based designs by Hamilton. The pyridine turn unit (left), linear strand (center), and the two turn helix (right).

The use of pyridines in oligoamides to direct folding can also be found in the work of Lehn and coworkers. Intermolecular hydrogen bonding interactions between the templating cyanurate and the oligo(isophthalamide) backbone induce folding into a helical secondary structure (Figure 1.7, left).⁵⁴ An apparently small alteration of the backbone allows folding without the need of cyanurate as a template (Figure 1.7, right).⁵⁵ The secondary architectures have been extensively studied in solution by numerous NMR techniques.⁵⁶

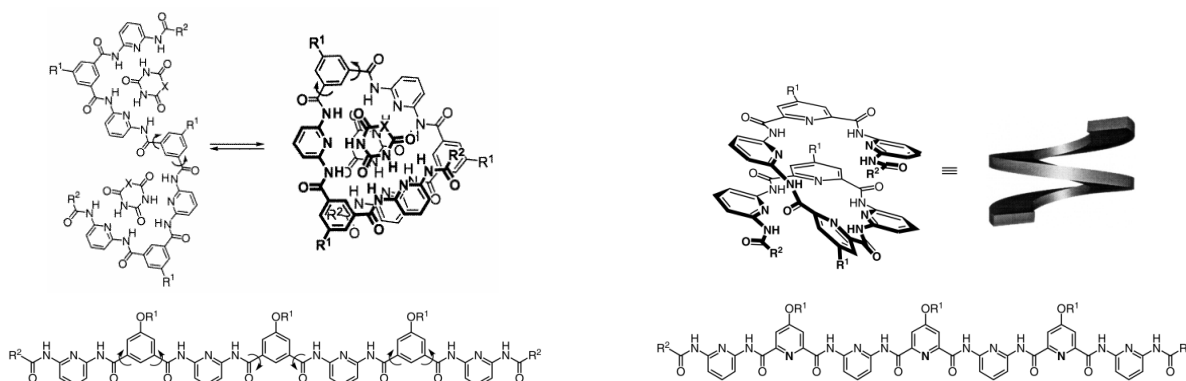


Figure 1.7: Lehn's cyanurate templated folding of isophthalamide (left), and self-directed folding of oligo(pyridine-dicarboxamide) (right).

These two designs prove that subtle changes in the structural motif of the backbone can make the difference between autonomous folding or the requirement for a template to induce folding. Moreover, studies on the oligo(pyridine-dicarboxamide) revealed the unique formation of intertwined helices in solution and in the solid state.^{57,58} Partial oxidation of the pyridine nitrogens to the corresponding *N*-oxide oligomers did not hamper double helix formation.⁵⁹ In addition, deprotonation of the amide protons in the oligo(pyridine-dicarboxamide) (Figure 1.7, right) resulted in an excellent tridentate ligand for transition metals (*e.g.* Cu^{2+} , Ni^{2+}) giving rise to helical metal complexes in the solid state.⁶⁰ X-ray diffraction of the formed crystals indicated that only two of the seven pyridine rings take part in the complexation. The secondary architecture of oligo(pyridine-dicarboxamide) proved to be sensitive towards protonation. Under neutral conditions the system adopts a helical architecture with the amide carbonyls

pointing outwards. With the addition of four equivalents of triflic acid (TfOH) the intramolecular hydrogen bonding is lost and the system adopts a linear structure. Addition of another three equivalents of TfOH protonates all pyridine rings. Remarkably, the system arranges into a helix again. ^1H , ^1H -NOESY experiments indicated an organization in which the amide carbonyls are now pointing inwards and form hydrogen bonds with the protonated pyridine moieties.⁶¹

The scope of the aromatic oligoamide design was expanded by Huc *et al.* with the use of oligo(quinoline). Although the system is based on a similar hydrogen bonding interaction the inner void is smaller due to the 60° bend of the consecutive units instead of the approximate 120° bend introduced by the *meta*-linked oligo(pyridine-dicarboxamide). Besides linear polymers, polymerization of 8-amino-2-quinolinecarboxylic acid easily yielded the cyclo-trimer and the cyclo-tetramer.⁶² A stepwise approach, however, gave access to the dimer, tetramer and octamer (Figure 1.8).⁶³ Especially the latter proved to adopt a very stable helical conformation in solution as determined by ^1H , ^1H -ROESY NMR experiments.

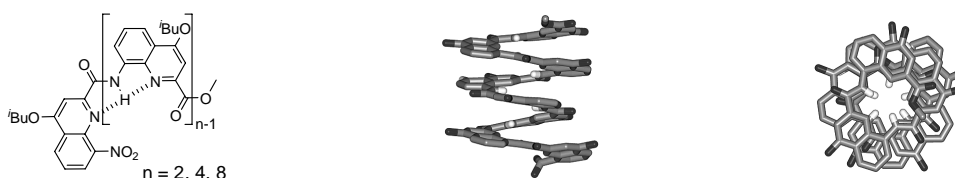


Figure 1.8: The oligo(quinoline) as designed by Huc and coworkers (left), its crystal structure: side view (center), and top view (right). The ^iBuO -groups have been omitted for clarity.

Derivatization of the ester end group of the achiral backbone with the chiral (*R*)-phenylethylamino function, resulted in a preference for one helical handedness as was established by CD spectroscopy.⁶⁴ In this manner a series of chiral end groups has been investigated.⁶⁵ The preference for one helical handedness could also be induced by connecting two quinoline tetramers (Figure 1.8) to 1,5-diaminoanthraquinone without disrupting the continuity of the hydrogen bonding network.⁶⁶ The anthraquinone unit serves as a helical inversion center. Steric hindrance dictates that the helices will be formed on both sides of the anthraquinone plane, as was determined by X-ray diffraction analysis. Hence, both a *P* and an *M* helix are formed, thereby rendering an overall achiral assembly. Furthermore, preliminary studies have shown that a somewhat altered oligo(quinoline) can accommodate one molecule of water in its cavity.⁶⁷

1.6 Aromatic oligo-ureas

Urea functionalities have already been incorporated in aliphatic peptidomimetic backbones to induce folding.^{68,69} However, foldamers based on aromatic oligo-ureas are very uncommon,

judged from the limited number of publications that addresses this design principle. Similar to the aromatic oligoamides (Section 1.5) also in this design hydrogen bonding is used to direct the folding and π - π interactions may further stabilize the secondary architecture.

To the best of our knowledge the first report on this design principle comes from Shudo and coworkers.^{70,71} In this very straightforward construct five benzene rings are *meta*-linked *via* *N,N'*-dimethylureas. Besides urea linkers, guanidine linkers have been used as well. Due to the methyl groups on the urea functionality hydrogen bonding is excluded, forcing the oligomer to rely for folding on π - π interactions only. X-ray analysis revealed the existence both the M and the P helices. The observed chemical shift in ¹H-NMR measurements in CDCl₃ at high-field (~6.1 ppm) fits with the expected shielding effect of stacked benzene moieties in a helical architecture.

Interestingly, two designs have been reported that are not yet studied experimentally. The first one is from Zimmerman and coworkers. Their research on heterocyclic ureas is expected to eventually give access to oligo(1,8-naphthyridinyurea), which should be able to undergo a concentration dependent sheet-to-helix transition in which the urea goes from a *cisoid* to a *transoid* conformation (Figure 1.9).⁷²

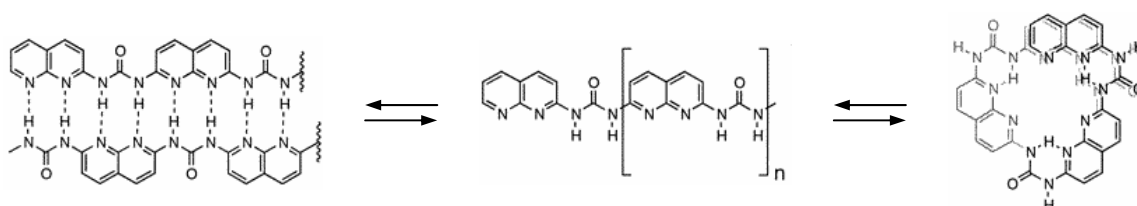


Figure 1.9: Potential helix-to-sheet transitions based on hypothetical oligo(naphthyridinyurea).

Also Gong and coworkers aim for a foldamer based on aromatic oligo-ureas.^{4b} In their design two ester functions (Figure 1.10, left) or the combination of an ester and an ether function (center) are incorporated as hydrogen bonding acceptors for the urea hydrogens, rendering a *cisoid* conformation for the ureas. This results –in combination with *meta*-linked benzene moieties– in a highly curved backbone prone to fold.

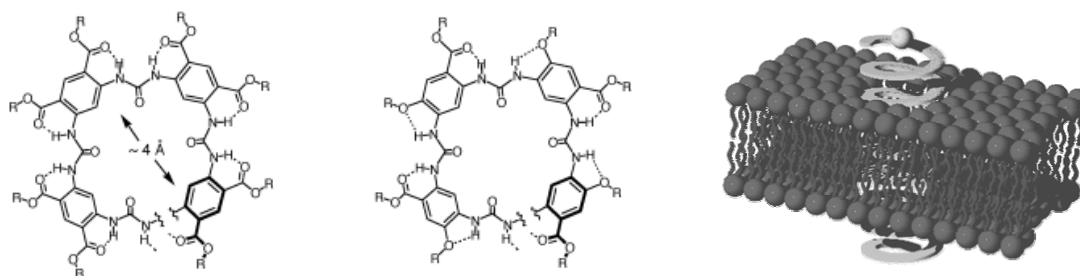


Figure 1.10: Oligoureas with peripheral esters (left), a combination of peripheral esters and ethers (center) as designed by Gong et al., and a cartoon of the envisaged transmembrane ion channel (right).

The size of the neutral, electrostatically negative inner void may be suitable for ion binding and/or transport. This design may give access to synthetic ion channels.⁷³ It is logical to choose this type of structure since transmembrane segments of most protein channels are thought to be helical.⁷⁴

1.7 The poly(ureidophthalimide) design

The following design is reported by Judith van Gorp from our laboratory and comprises phthalimide units linked *via para*-positioned urea functionalities (Figure 1.11).⁷⁵ The consecutive monomeric units introduce a curvature in the ureidophthalimide backbone due to intramolecular hydrogen bonding of *cisoid* urea protons with the adjacent imide carbonyl oxygens. This interaction renders an almost 120° bend, thereby nucleating folding.

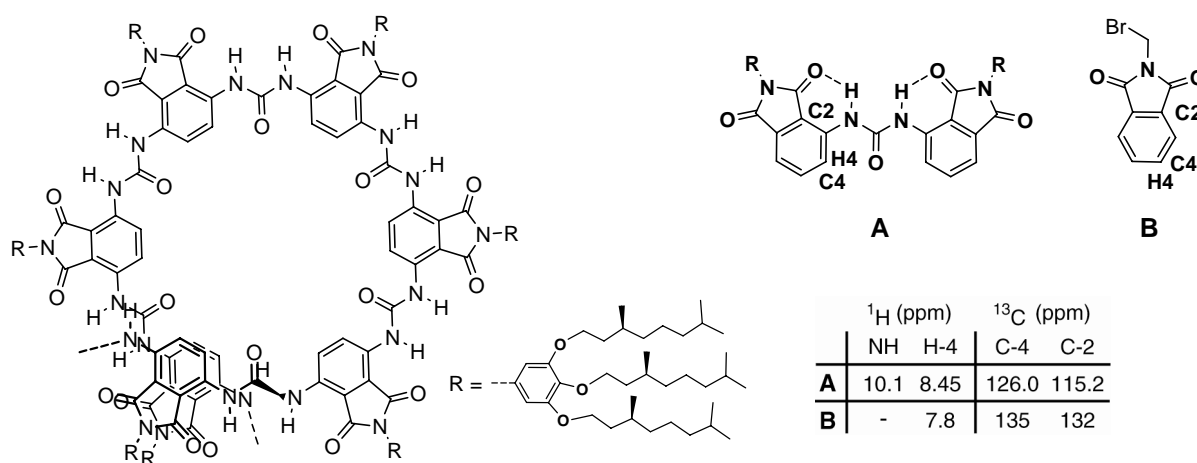


Figure 1.11: One turn of the poly(ureidophthalimide) (left), and model urea compound **A** and reference phthalimide **B**⁷⁶ with ¹H- and ¹³C-NMR data measured in CDCl₃ (right).

In CDCl₃ the position of the urea hydrogens in ¹H NMR at 10.1 ppm is a clear indication of hydrogen bonding with the adjacent in plane imide carbonyls. This interaction brings the system into a planar conformation which, in turn, positions H-4 in close proximity to the carbonyl oxygen of the urea function (Figure 1.11). The anisotropic deshielding of the carbonyl oxygen has a marked influence on the position of H-4 located at 8.5 ppm. The planar conformation and the accompanying intramolecular hydrogen bonding are also reflected in the relative shielding of C-2 and C-4 in **A** compared to reference phthalimide **B** in ¹³C-NMR. The outcome of this NMR study on the model compound strongly indicates a planar conformation with a *cisoid* oriented urea linker required for folding of longer oligomers. Furthermore, the characteristic deshielding in ¹H-NMR of the NH and H-4 protons is also observed for the polymer.

The assumed folding into a helical architecture is in agreement with circular dichroism studies of the foldamer in THF which revealed a bisignate Cotton effect with a zero crossing

that coincided with the absorption maximum in the UV-vis spectrum. However, the measurements in CHCl_3 were CD silent, suggesting a random coil conformation. Moreover, studies in heptane proved the stacking of shorter oligomers (< 1 turn) to larger chiral aggregates. Model studies indicated that by folding an inner void is constructed with a diameter of ~ 14 Å for the hollow core⁷⁷, somewhat larger than the ~ 9 Å for Moore's *m*-phenylene ethynylene system³³ (Figure 1.4).

The most striking difference with the previously mentioned designs is the procedure required to obtain longer oligomers. All previously discussed designs rely on a stepwise lengthening of the oligomers, which is very advantageous for the detailed study of the folding process. However, formation of long oligomers requires many laborious steps. The synthesis of poly(ureidophthalimide) is based on a (co)polymerization and, therefore, immediately gives access to longer oligomers. The disadvantage, of course, is that the result of the polymerization by definition renders a broad mixture of oligomeric lengths ranging typically from the dimer to the 30-mer. This issue has been addressed by attempts to synthesize oligomers of definite length by a semi-stepwise approach^{78,79} as was reported by Tom de Greef.⁸⁰ However, unexpected urea scrambling afforded preferentially polymeric species.⁸¹

The potential for the introduction of a variety of functionalities on the imide nitrogen (R group, Figure 1.11), predestined to organize along the helical backbone, make this design unique and highly attractive for further research.

1.8 Aim of the thesis

The structures and structural elements depicted throughout this chapter have been a great inspiration for the research described in this thesis. However, all current systems are optimized for detailed studies on the actual folding process. The building blocks only comprise functionalities essential for the folding into helical architectures. The aim of this thesis is to go one step further by exploitation of the secondary structure with the incorporation of functionality that may influence the folding but is not strictly required for helicity. An excellent starting point is the recently designed poly(ureidophthalimide) foldamer (Figure 1.11). The monomer that gives access to this polymer is already equipped with an anchor point for the introduction of functionality. The scope, however, is limited to functionalities of interest in the field of molecular electronics *i.e.* chromophores and to functionalities that allow studies in an aqueous environment to mimic the natural α -helix. Attempts to substitute the phthalimide unit with novel anthraquinones keeping the initial basis for secondary interactions intact will also be part of the scope. Besides the foldamer itself, part of the research described in this thesis will focus on the development of a new n-type chromophore, incorporating the indigo moiety, which may find its use in the organizing properties of a foldamer suitable for application in organic solar cells.

1.9 Outline of the thesis

To extend the scope of the recently developed poly(ureidophthalimide) foldamer a novel synthetic strategy had to be developed. In chapter 2, the role of 3,6-bis(acetylamino)phthalic anhydride as the key precursor for the high yielding introduction of virtually any imide-*N*-functionality is discussed. Furthermore, how these new intermediates give access to the corresponding 3,6-diaminophthalimides, that are required as polymeric precursors for the poly(ureidophthalimide) foldamers, is described.

A more detailed mechanistic investigation, presented in Chapter 3, should give more insight into the formation of a non-perfectly alternating copolymer during reaction of 3,6-diisocyanatophthalimide with 1,4-diamino-anthraquinone. To circumvent the problem with copolymerization new lipophilic and hydrophilic anthraquinone based polymer precursors are discussed that may give access to an anthraquinone homopolymer.

In chapter 4 a detailed study of OPV (oligophenylenevinylene) functionalized periphery of poly(ureidophthalimide) is presented. The influence of the large OPV π -system on folding is investigated with UV-vis and CD studies in CHCl_3 , THF, and heptane. Comparison of temperature dependent CD studies in THF and heptane has been undertaken to get more insight into the dynamics of the secondary structure. Several CD experiments have been conducted to gain more understanding of the influence of the solvent on the shape and stability of the supramolecular architecture. Furthermore, the preliminary results are discussed with a foldamer decorated with donor-acceptor chromophores, potentially suitable for a nonlinear optics (NLO) study.

To be able to mimic the versatile natural α -helix with poly(ureidophthalimide) peripheral decoration with hydrophilic oligo(ethyleneoxide) side chains that ensure solubility in water is envisaged, as is described in chapter 5. The presence of chirality in the side chains far remote from the ureidophthalimide core enable a UV-vis and CD spectroscopy study of the polymer in water. In addition, the ethyleneoxide tails also allow a UV-vis and CD study in THF, which allows comparison with the previously synthesized lipophilic foldamer.

Finally, the research described in chapter 6 is not concerned with the helical architecture itself but rather focuses on the development of a new n-type chromophore that in future research may be incorporated in the poly(ureidophthalimide) system to benefit from the controlled peripheral alignment. Inspiration for the new material is derived from the ancient dye indigo, which is known for its notorious insolubility. Previously unreported functionalization of indigo was programmed to allow alteration of its intrinsic small band gap. More importantly, functionalization had to result in processable indigo derivatives. After extensive photophysical investigations of the new materials, the construction of the first bulk-heterojunction organic solar cell comprised of a modified indigo as an n-type material in combination with poly(phenylenevinylene) (PPV) as the p-type material is described.

1.10 References

- 1) Two striking examples: (a) Brevetoxin A: Nicolaou K. C.; Yang Z.; Shi G.; Gunzner J. L.; Agrios K. A.; Gartner P. *Nature* **1998**, 392, 264-9. (b) Taxol: Nicolaou, K. C.; Yang, Z.; Liu, J. J.; Ueno, H.; Nantermet, P. G.; Guy, R. K.; Claiborne, C. F.; Renaud, J.; Couladouros, E. A.; Paulvannan K. *Nature* **1994**, 367, 630-4.
- 2) Meijer, E. W.; Schenning, A. P. H. J. *Nature* **2002**, 419, 353-4.
- 3) Schenning, A. P. H. J.; Meijer, E. W. *Chem. Commun.* **2005**, 3245-8.
- 4) Review articles on foldamers: (a) Block, M. A. B.; Kaiser, C.; Khan, A.; Hecht, S. *Top. Curr. Chem.* **2005**, 89. (b) Sanford, A. R.; Yamato, K.; Yang, X.; Han, Y.; and Gong, B. *Eur. J. Biochem.* **2004**, 271, 1416-25. (c) Huc, I. *Eur. J. Org. Chem.* **2004**, 17-29. (d) Schmuck, C. *Angew. Chem. Int. Ed.* **2003**, 2448-52. (e) Hill, D. J.; Mio, M. J.; Prince, R. B.; Hughes, T. S.; Moore, J. S. *Chem. Rev.* **2001**, 101, 3893-4011. (f) Gellman, S. H. *Acc. Chem. Res.* **1998**, 31, 173.
- 5) Pauling, L.; Corey, R.B.; Branson, H.R. *Proc. Natl. Acad. Sci. USA.*, **1951**, 37, 205-11.
- 6) (a) Kritzer, J. A.; Tirado-Rives, J.; Hart, S. A.; Lear, J. D.; Jorgensen, W. L.; and Schepartz, A. *J. Am. Chem. Soc.* **2005**, 127, 167-78. (b) Dill, K. A.; Chan, H. S. *Nat. Struct. Biol.* **1997**, 4, 10-9. (c) Levinthal, C. *J. Chim. Phys.* **1968**, 65, 44-5.
- 7) Chothia, C. *Nature*, **1975**, 254, 304-8.
- 8) Jeffrey, G.A.; Saenger, W. *Hydrogen bonding in biological structures*; Springer Verlag: Berlin, **1994**.
- 9) Zimm, B.H.; Bragg, J.K. *J. Chem. Phys.* **1959**, 31, 526-35.
- 10) Review articles on helical β -peptides: (a) Martinek, T. A.; Fülöp, F. *Eur. J. Biochem.* **2003**, 270, 3657-66. (b) Cheng, R. P.; Gellman, S. H.; and DeGrado, W. F. *Chem. Rev.* **2001**, 101, 3219-32. (c) DeGrado, W. F.; Schneider, J. P.; Hamuro, Y. *J. Peptide Res.* **1999**, 54, 206-17.
- 11) A selection of recent articles: (a) Appella, D. H.; Christianson, L. A.; Klein, D. A.; Powell, D. R.; Huang, X.; Barchi Jr, J. J.; and Gellman, S. H. *Nature*, **1997**, 387, 381-4. (b) Appella, D. H.; Christianson, L. A.; Karle, I. L.; Powell, D. R.; and Gellman, S. H. *J. Am. Chem. Soc.* **1996**, 118, 13071-2.
- 12) A selection of recent articles: (a) Reuping, M.; Mahajan, Y. R.; Jaun, B.; and Seebach, D. *Chem. Eur. J.* **2004**, 10, 1607-15. (b) Seebach, D.; and Matthews, J. L. *Chem. Commun.* **1997**, 2015-22.
- 13) Newman, M.S.; Lutz, W. B.; Lednicer, D. *J. Am. Chem. Soc.* **1955**, 77, 3420-1.
- 14) For review articles: (a) Urbano, A. *Angew. Chem. Int. Ed.* **2003**, 42, 3986-9. (b) Meurer, K. P.; Vögtle, F. *Top. Curr. Chem.* **1985**, 127, 1-76. (c) Laarhoven, W. H.; Prinsen, W. J. C. *Top. Curr. Chem.* **1984**, 125, 63-130. (d) Von Richard, H. M. *Angew. Chem.* **1974**, 86, 727-38.
- 15) Wynberg, H.; Groen, M. B.; *J. Am. Chem. Soc.* **1968**, 90, 5338-41.
- 16) Rajca, A.; Wang, H.; Pink, M.; Rajca, S. *Angew. Chem. Int. Ed.* **2000**, 39, 4481-3.
- 17) (a) Han, S.; Anderson, D. R.; Bond, A. D.; Chu, H. V.; Disch, R. L.; Holmes, D.; Schulman, J. M.; Teat, S. J.; Vollhardt, K. P. C.; Whitener, G. D. *Angew. Chem. Int. Ed.* **2002**, 41, 3227-30. (b) Han, S.; Bond, A. D.; Disch, R. L.; Holmes, D.; Schulman, J. M.; Teat, S. J.; Vollhardt, K. P. C.; Whitener, G. D. *Angew. Chem. Int. Ed.* **2002**, 41, 3223-7.
- 18) Hanan, G. S.; Lehn J.-M.; Kyritsakas, N.; Fischer, J. J. *Chem. Soc., Chem. Commun.* **1995**, 765-6.
- 19) Ohkita, M.; Lehn, J.-M.; Baum, G.; Fenske, D. *Chem. Eur. J.* **1999**, 5, 3471-81.
- 20) Cuccia, L. A.; Lehn, J.-M.; Homo, J. C.; Schmutz, M. *Angew. Chem. Int. Ed.* **2000**, 39, 233-7.
- 21) Petitjean, A.; Cuccia, L. A.; Lehn, J.-M.; Nierengarten, H.; Schmutz, M. *Angew. Chem. Int. Ed.* **2002**, 41, 1195-8.
- 22) Nelson, J. C.; Saven, J. G.; Moore, J. S.; and Wolynes, P. G. *Science*, **1997**, 277, 1793-6.
- 23) Zhang, J.; Pesak, D. J.; Ludwick, J. L.; Moore, J. S. *J. Am. Chem. Soc.* **1994**, 116, 4227-39.
- 24) Mio, M. J.; Prince, R. B.; Moore, J. S.; Kuebel, C.; Martin, D. C. *J. Am. Chem. Soc.* **2000**, 122, 6134-5.
- 25) Matsuda, K.; Stone, M. T.; and Moore, J. S., *J. Am. Chem. Soc.* **2002**, 124, 11836-7.

- 26) Bloomfield, V. A.; Crothers, D. M.; Tinoco, I. *Physical Chemistry of Nucleic acids*; Harper & Row, New York, 1974.
- 27) Cantor, C. R.; Schimmel, P. R. *Biophysical Chemistry*; Freeman, New York, 1980.
- 28) Prince, R. B.; Saven, J. G.; Wolynes, P. G.; Moore, S. J. *J. Am. Chem. Soc.* **1999**, *121*, 3114-21.
- 29) Prince, R. B.; Brunsveld, L.; Meijer, E. W.; Moore, J. S. *Angew. Chem. Int. Ed.* **2000**, *39*, 228-30.
- 30) Green, M. M.; Reidy, M. P.; Johnson, R. D.; Darling, G.; O'Leary, D. J.; Willson, G. J. *Am. Chem. Soc.* **1989**, *111*, 6452-4.
- 31) Brunsveld, L.; Meijer, E. W.; Prince, R. B.; and Moore, J. S. *J. Am. Chem. Soc.* **2001**, *123*, 7978-84.
- 32) Prince, R. B.; Barnes, S. A.; and Moore, J. S., *J. Am. Chem. Soc.* **2000**, *122*, 2758-62.
- 33) Tanatani, A.; Hughes, T. S.; Moore, J. S. *Angew. Chem. Int. Ed.* **2002**, *41*, 325-8.
- 34) Brunsveld, L.; Prince, R. B.; Meijer, E. W.; Moore, J. S. *Org. Lett.* **2000**, *2*, 1525-8.
- 35) Stone, M. T.; and Moore, S. J., *Org. Lett.* **2004**, *6*, 469-72.
- 36) Arnt, L.; Tew, G. N. *J. Am. Chem. Soc.* **2002**, *124*, 7664-5.
- 37) Arnt, L.; Tew, G. N. *Macromolecules* **2004**, *37*, 1283-8.
- 38) Jones, T. V.; Blatchly, R. A.; Tew, G. N. *Org. Lett.* **2003**, *5*, 3297-9.
- 39) Jones, T. V.; Slutsky, M. M.; Laos, R. de Greef, T. F. A.; Tew, G. N. *J. Am. Chem. Soc.* **2005**, *127*, ASAP.
- 40) Grubbs, R. H.; Kratz, D. *Chem. Ber.* **1993**, *126*, 149-57.
- 41) Shotwell, S.; Windscheif, P. M.; Smith, M. D.; Bunz, U. H. F. *Org. Lett.* **2004**, *6*, 4151-4.
- 42) Yang, X.; Yuan, L.; Yamato, K.; Brown, A. L.; Feng, W.; Furukawa, M.; Cheng Zeng, X.; Gong, B. *J. Am. Chem. Soc.* **2004**, *126*, 3148-62.
- 43) Cary, J. M.; Moore, J. S. *Org. Lett.* **2002**, *4*, 4663-6.
- 44) Yang, X.; Brown, A. L.; Furukawa, M.; Li, S.; Gardinier, W. E.; Bukowski, E. J.; Bright, F. V.; Zheng, C.; Zeng, X. C.; Gong, B. *Chem. Commun.* **2003**, 56-7.
- 45) Zhu, J.; Parra, R. B.; Zeng, H.; Skrzypczak-Jankun, E.; Cheng Zeng, X.; Gong, B. *J. Am. Chem. Soc.* **2000**, *122*, 4219-20.
- 46) Gong, B. *Chem. Eur. J.* **2001**, *7*, 4336-42.
- 47) Gong, B.; Zeng, H.; Zhu, L.; Han, Y.; Cheng, S.; Furukawa, M.; Parra, R. D.; Kovalevsky, A. Y.; Mills, J. L.; Skrzypczak-Jankun, E.; Martinovic, S.; Smith, R. D.; Zheng, C.; Szyperski, T.; Cheng Zeng, X. *Proc. Natl. Acad. Sci. U. S. A.* **2002**, *99*, 11583-8.
- 48) Yuan, L.; Zeng, H.; Yamato, K.; Sanford, A. R.; Feng, W.; Atreya, H. S.; Sukumaran, D. K.; Szyperski, T.; Gong, B. *J. Am. Chem. Soc.* **2004**, *126*, 16528-37.
- 49) Yuan, L.; Feng, W.; Yamato, K.; Sanford, A. R.; Xu, D.; Guo, H.; Gong, B. *J. Am. Chem. Soc.* **2004**, *126*, 11120-1.
- 50) Tanatani, A.; Yokoyama, A.; Azumaya, I.; Takakura, Y.; Mitsui, C.; Shiro, M.; Uchiyama, M.; Muranaka, A.; Kobayashi, N.; Yokozawa, T. *J. Am. Chem. Soc.* **2005**, *127*, 8553-61.
- 51) Hamuro, Y.; Geib, S. J.; Hamilton, A. D. *Angew. Chem.* **1994**, *106*, 465-7.
- 52) Hamuro, Y.; Geib, S. J.; Hamilton, A. D. *J. Am. Chem. Soc.* **1996**, *118*, 7529-41.
- 53) Hamuro, Y.; Geib, S. J.; Hamilton, A. D. *J. Am. Chem. Soc.* **1997**, *119*, 10587-93.
- 54) Berl, V.; Krische, M. J.; Huc, I.; Lehn, J.-M.; Schmutz, M. *Chem. Eur. J.* **2000**, *6*, 1938-46.
- 55) Berl, V.; Huc, I.; Khoury, R. G.; Lehn, J.-M. *Chem. Eur. J.* **2001**, *7*, 2798-809.
- 56) Dolain, C.; Grélard, A.; Laguerre, M.; Jiang, H.; Maurizot, V.; Huc, I. *Chem. Eur. J.* **2005**, *11*, 6135-44.
- 57) Berl, V.; Huc, I.; Khoury, R. G.; Krische, M. J.; Lehn, J.-M. *Nature* **2000**, *407*, 720-3.
- 58) Berl, V.; Huc, I.; Khoury, R. G.; Lehn, J.-M. *Chem. Eur. J.* **2001**, *7*, 2810-20.
- 59) Dolain, C.; Zhan, C.; Léger, J.-M.; Daniels, L.; Huc, I. *J. Am. Chem. Soc.* **2005**, *127*, 2400-1.
- 60) Maurizot, V.; Linti, G.; Huc, I. *Chem. Commun.* **2004**, 924-5.
- 61) Dolain, C.; Maurizot, V.; Huc, I. *Angew. Chem. Int. Ed.* **2003**, *42*, 2738-40.
- 62) Jiang, H.; Léger, J.-M.; Guionneau, P.; Huc, I. *Org. Lett.* **2004**, *6*, 2985-8.

- 63) Jiang, H.; Léger, J-M.; Huc, I. *J. Am. Chem. Soc.* **2003**, *125*, 3448-9.
- 64) Jiang, H.; Dolain, C.; Léger, J-M.; Gornitzka, H.; Huc, I. *J. Am. Chem. Soc.* **2004**, *126*, 1034-5.
- 65) Dolain, C.; Jiang, H.; Léger, J-M.; Guionneau, P.; Huc, I. *J. Am. Chem. Soc.* **2005**, *127*, 12943-51.
- 66) Maurizot, V.; Dolain, C.; Leydet, Y.; Léger, J-M.; Guionneau, P.; Huc, I. *J. Am. Chem. Soc.* **2004**, *126*, 10049-52.
- 67) Garric, J.; Léger, J-M.; Huc, I. *Angew. Chem. Int. Ed.* **2005**, *44*, 1954-8.
- 68) (a) Violet, A.; Averlant-Petit, M.C.; Semetey, V.; Hemmerlin, C.; Casimir, R.; Graff, R.; Marraud, M.; Briand, J.-P.; Rognan, D.; Guichard, G. *J. Am. Chem. Soc.* **2005**, *127*, 2156-64. (b) Semetey, V.; Didierjean, C.; Briand, J.-P.; Aubry, A.; Guichard, G. *Angew. Chem., Int. Ed* **2002**, *41*, 1895-8.
- 69) (a) Burgess, K.; Ibarzo, J.; Linthicum, D. S.; Shin, H.; Shitangkoon, A.; Totani, R.; Zhang, A. *J. Am. Chem. Soc.* **1997**, *119*, 1556-64. (b) Burgess, K.; Linthicum, D. S.; Shin, H. *Angew. Chem., Int. Ed. Eng.* **1995**, *34*, 907-9.
- 70) Tanatani, A.; Kagechika, H.; Azumaya, I.; Fukutomi, R.; Ito, Y.; Yamaguchi, K.; Shudo, K. *Tetrahedron Lett.* **1997**, *38*, 4425-8.
- 71) Yamaguchi, K.; Matsumura, G.; Kagechika, H.; Azumaya, I.; Ito, Y.; Itai, A.; Shudo, K. *J. Am. Chem. Soc.* **1991**, *113*, 5474-5.
- 72) Corbin, P. S.; Zimmerman, S. C.; Thiessen, P. A.; Hawryluk, N. A.; Murray, T. J. *J. Am. Chem. Soc.* **2001**, *123*, 10475-88.
- 73) A selection of recent reviews on synthetic ion channels: (a) Sakai, N.; Mareda, J.; and Matile, S. *Acc. Chem. Res.* **2005**, *38*, 79-87. (b) Matile, S.; Som, A.; and Sordé N. *Tetrahedron*, **2004**, *60*, 6405-35. (c) Gokel, G. W.; Schlesinger, P. H.; Djedovič, N. K.; Ferdani, R.; Harder, E. C.; Hu, J.; Leevy, W. M.; Pajewska, J.; Pajewski, R.; and Weber, M. E. *Bioorg. Med. Chem.* **2004**, *12*, 1291-1304. (d) Koert, U.; Al-Momani, L.; Pfeifer, J. R. *Synthesis*, **2004**, 1129-46. (e) Koert, U.; and Reiß, P. *J. Supramol. Chem.* **2003**, *2*, 29-37.
- 74) B. Hille, *Ionic Channels of excitable Membranes*, 2nd ed.; Sinauer: Sunderland, MA, 1992; pp 244-245.
- 75) van Gorp, J. J.; Vekemans, J. A. J. M.; Meijer, E. W. *Chem. Commun.* **2004**, 60-1.
- 76) Pouchert, C. J.; Behnke, J. *The Aldrich library of 13C and 1H Spectra* **1993**, p1460-A, Aldrich Chemical Company Inc.
- 77) van Gorp, J. J.; Thesis, Eindhoven University of Technology: *Helices by Hydrogen Bonding*, **2004**.
- 78) Aratani, N; Tsuda, A.; Osuka, A. *Synlett* **2001**, *11*, 1663-74.
- 79) Aratani, N; Osuka, A. *Macromol. Rapid Commun.* **2001**, *22*, 725-40.
- 80) De Greef, T. F. A. Graduation report: *Towards stepwise synthesis of well-defined ureidophthalimide oligomers*; Eindhoven University of Technology, 2004.
- 81) A tentative mechanism for urea scrambling is presented in chapter 3, section 3.3.

Chapter 2

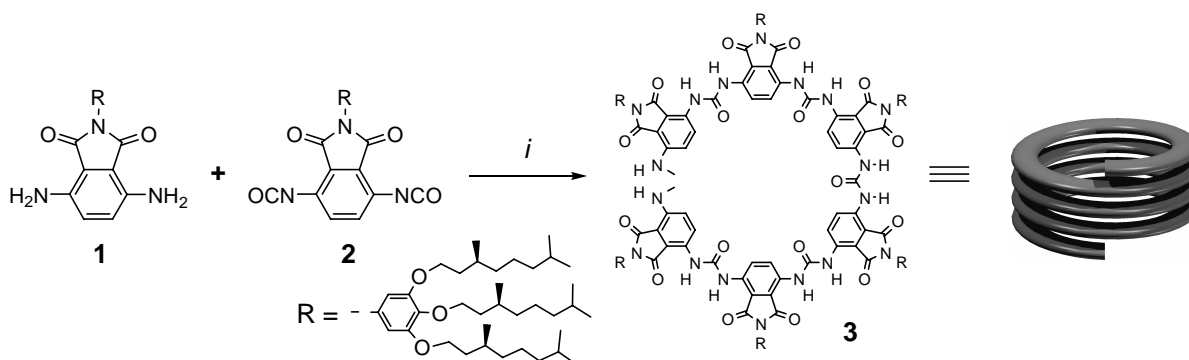
Synthesis of 3,6-disubstituted phthalimides

Abstract

To extend the scope of the poly(ureidophthalimide) foldamers (Chapter 1, Section 1.6), introduction of peripheral functionality predetermined to organize along the helical backbone was envisaged. Since the current synthetic methodology has proven to be insufficient, new approaches have been investigated for the synthesis of the 3,6-diaminophthalimide polymer precursor. The most successful strategy involves 3,6-bis(acetylamino)phthalic anhydride as the key intermediate. The phthalimide formation is a two-step process comprising a ring opening followed by a ring closure. In contrast to its predecessor 3,6-dinitrophthalic anhydride, which was very reactive towards ring opening, the reactivity of 3,6-bis(acetylamino)phthalic anhydride is more balanced with faster ring closure. The new synthetic methodology gave access to a poly(ureidophthalimide) decorated with a single chiral aliphatic tail per unit. To investigate whether folding still occurs without peripheral aromatic functionality the compound was subjected to a brief CD study. Measurements in THF and heptane showed a bisignate Cotton effect indicative of the presence of helical architectures. In contrast to previously measured poly(ureidophthalimides) a Cotton effect is observed in CHCl₃. This observation in combination with the temperature independent Cotton effect in three solvents may be attributed to the positioning of the chiral center close to the core.

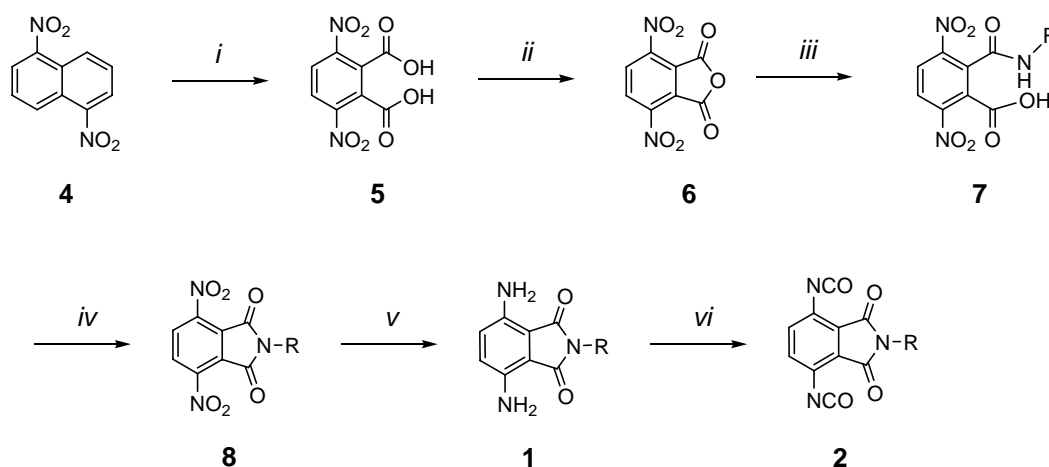
2.1 Introduction

As was described in Chapter 1, poly(ureidophthalimide) **3** (Scheme 2.1) can be categorized as a foldamer since it can fold into a conformationally ordered state in solution.¹ Recently, Judith van Gorp reported the synthesis of the first ureidophthalimide based foldamer originating from 3,6-diaminophthalimide and the corresponding diisocyanate.² Purification by column chromatography allowed separation of the longer oligomers from the shorter oligomers. Circular dichroism studies of the fraction containing only longer oligomers (on average 30 units) revealed a bisignate Cotton effect in THF and heptane, indicative of folding into a helical architecture. Studies in heptane showed aggregation of the shorter oligomers into chiral aggregates as well. However, no folding was observed in CHCl_3 , in agreement with a random coil conformation.



Scheme 2.1: Synthesis of polymer building blocks **1** and **2**. i) DMAP (1.0 equiv.), PhCH_3 , reflux.

Many synthetic approaches have been investigated to arrive at 3,6-diamino-phthalimides.³ The only successful method started from 1,5-dinitronaphthalene (**4**), which could be converted into 3,6-dinitrophthalic acid (**5**) in 25% yield under harsh conditions (Scheme 2.2).^{4,5}



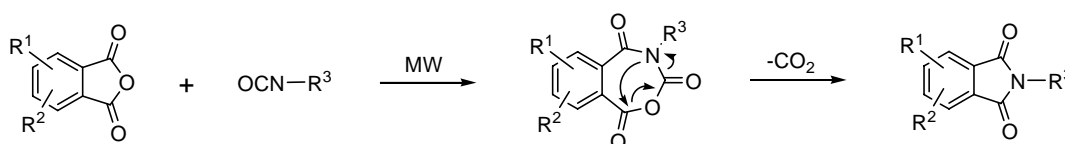
Scheme 2.2: Synthesis of polymer building blocks **1** and **2**. i) HNO_3 , H_2SO_4 , 80°C . ii) Ac_2O , 100°C , 10 min. iii) H_2NR , CH_3CN , rt. iv) Ac_2O , 100°C . v) H_2 , Pd/C, EtOAc/EtOH, rt. vi) COCl_2 , PhCH_3 , rt to reflux.

Subsequent anhydride formation could be achieved by reaction with acetic anhydride furnishing 3,6-dinitrophthalic anhydride (**6**). This synthon is very reactive towards primary aromatic amines, which can be ascribed to the electron withdrawing nature of the nitro functionalities enhancing the electrophilicity of the carbonyl moieties. Ring opening leads to the formation of intermediate amic acid **7**. This could be transformed into the desired phthalimide **8** by an acetic anhydride assisted ring closure at elevated temperatures. A subsequent palladium mediated hydrogenation of dinitro compound **8** gives diamine **1** which in turn is converted into the corresponding diisocyanate **2** by phosgene treatment.

In spite of the facile synthetic approach depicted above the yields for the introduction of aromatic amines were typically around 40-60%. The introduction of aliphatic amines was a complete failure. To expand the scope of the foldamer studies, decoration of the core with a variety of functionalities is required. Incorporation of chromophores (Chapter 4) and functionalities that ensure solubility in water (Chapter 5) have been envisaged. The limitation of the approach depicted in scheme 2.2 demanded the development of a new synthetic methodology. However, synthesis of phthalimides with a substitution pattern similar to **1** is not trivial and a general method is not available.

2.2 Alternative synthetic approaches towards 3,6-diaminophthalimides

In our first approach the use of microwave (MW) assisted synthesis is employed to increase the yield for the incorporation of aromatic amines and to enable introduction of aliphatic amines. The high yielding microwave assisted formation of a range of phthalimides with different substitution patterns by reaction of substituted phthalic anhydrides with aromatic as well as aliphatic isocyanates has been previously reported.⁶ The reaction is typically performed in dimethylacetamide with reaction times of 1 to 2 minutes. It is remarkable that the mechanism assumes a nucleophilic attack of the isocyanate nitrogen (Scheme 2.3). Perhaps, the mechanism has a more concerted nature, including attack of the nitrogen with a simultaneous nucleophilic attack of the formed carboxylate on the electrophilic isocyanate carbon. The subsequent formation of a 7 membered ring that is prone to lose carbon dioxide is considered to be the main driving force for the phthalimide formation.

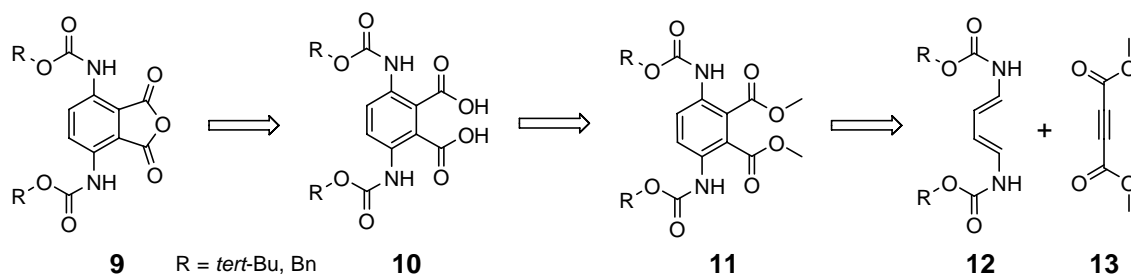


Scheme 2.3: MW-assisted synthesis of substituted phthalimides.

Although no examples with the 3,6-disubstitution pattern are given, attempts have been made to reproduce these results with 3,6-dinitrophthalic anhydride (**6**, Scheme 2.2) and various

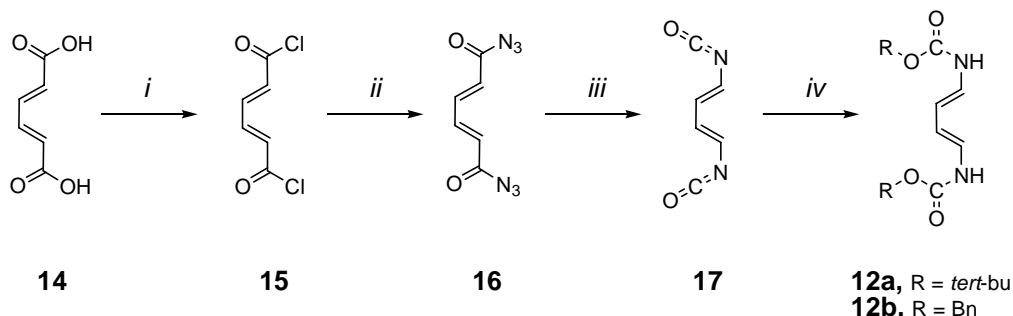
isocyanates. The results were disappointing since no or hardly any phthalimide product was obtained. However, control experiments with compounds mentioned in the original paper gave the desired products in excellent yields. It seems that the intrinsic imbalance of 3,6-dinitrophthalic anhydride in reactivity between fast ring opening and the slow ring closure cannot be leveled by MW assisted synthesis.

The nitro functionalities in phthalic anhydride enhance the ring opening step but at the same time slow down the ring closure generating the phthalimide system. Conversion of the electron withdrawing nitro functionality is envisaged to bring the two step phthalimide formation more in balance. We aimed for a carbamate function since this allows facile conversion into the desired diamino-phthalimides **1** (Scheme 2.2). With anhydride **9** (Scheme 2.4) a variety of 3,6-bis(aminoprotected)phthalimides should become available. The key step in the retro synthetic analysis is a Diels-Alder reaction of commercial acetylene **13** with diene **12**.^{7,8} Saponification of diester **11** should give the corresponding diacid **10**, which in turn may provide anhydride **9** by exposure to acetic anhydride. A very attractive consequence of this approach is the circumvention of the synthesis of dinitrophthalic acid (**5**, Scheme 2.2).



Scheme 2.4: Retro synthetic approach towards anhydride **9**.

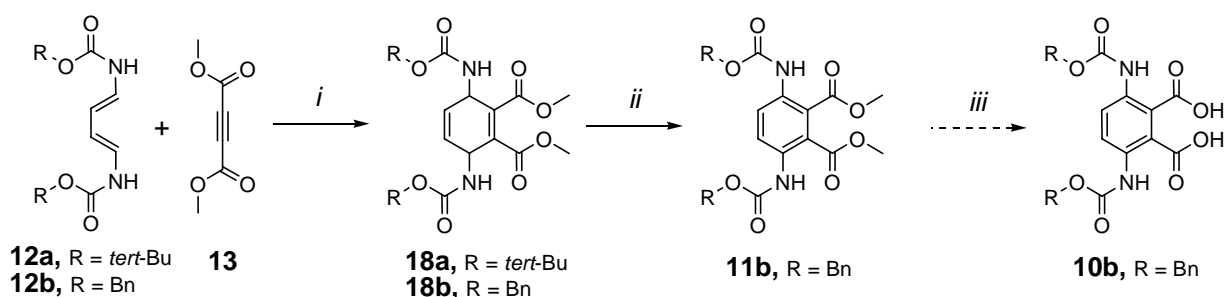
Diene **12** can be synthesized starting from commercially available *trans, trans*-muconic acid **14**. Diacid **14** is converted in diacid chloride **15** by reaction with thionyl chloride (Scheme 2.5).



Scheme 2.5: 4 Step syntheses to dicarbamates **12**. i) SOCl_2 , DCM, reflux, 48 h. ii) NaN_3 , CHCl_3 , H_2O , 4° , 2 h. iii) PhCH_3 , reflux, 1 h. iv) *tert*-BuOH or BnOH, PhCH_3 , $40\text{--}80^\circ\text{C}$, 1 h.

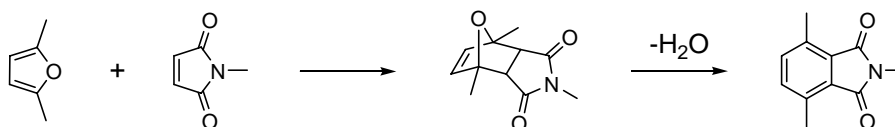
Subsequently, compound **15** is reacted with sodium azide furnishing diacylazide **16** which in turn is transformed to diisocyanate **17** by a Curtius rearrangement at elevated temperatures. Reaction of diisocyanate **17** with *tert*-butanol or benzyl alcohol gave carbamates **12a** and **12b**, respectively.

Dienes **12a** and **12b** are reacted with commercially available diester **13** giving Diels-Alder adducts **18a** and **18b** (Scheme 2.6). Unfortunately, oxidation (aromatization) to dicarbamate **11** proved to be only possible when the R-group is a benzyl (**18b**). In case of the *tert*-butyl group (**18a**) elimination of one of the *N*-Boc groups, leaving a tri-substituted benzene, seems unpreventable under the same conditions. Moreover, oxidation to the aromatic system only proved to take place when *ortho*-chloranil was used as the oxidant. This is most likely due to the favorable *ortho* positioning of the two carbonyls, which are ideally located for taking up two hydrogens in a concerted fashion from the pre-aromatic cyclohexadiene moiety in **18**. Other organic oxidants like dichlorodicyano-*para*-benzoquinone (DDQ) lacking this typical carbonyl positioning do not furnish the desired aromatic analogues of **18**. Hydrolysis of the two methyl esters was more challenging than expected. So far it seems that only one of the methyl esters can be hydrolyzed.



Scheme 2.6: Towards phthalic acid **10**. i) DMF, 90°C, **18a**: 18 h, >90% based on ¹H-NMR; **18b**: 7 h, ~94%. ii) *o*-chloranil, C₂Cl₄, 110°C, 65 h, 49%. iii) NaOH, H₂O, reflux.

Another route, also relying on a Diels-Alder approach, is the reaction of 2,5-dimethylfuran with *N*-methylmaleimide rendering 3,6-disubstituted methylphthalimide (Scheme 2.7).⁹ Although this results in a 3,6-disubstituted phthalimide, the strategy seems to be limited to the reaction as mentioned. Synthetic problems might arise with the derivatization of 2,5-dimethylfuran or its precursors. This strategy also demands early introduction of potentially large and highly functional complex moieties.

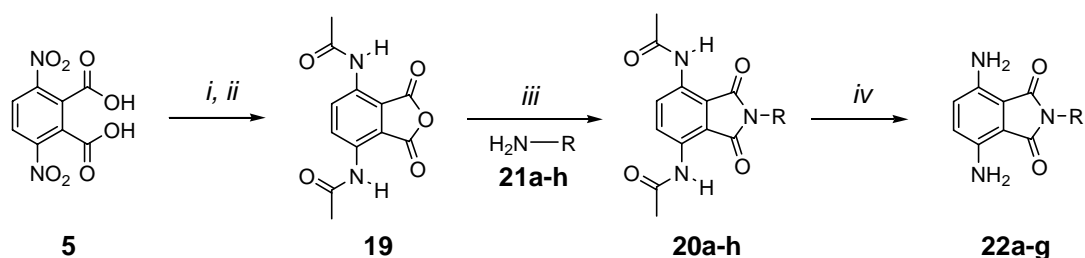


Scheme 2.7: Synthesis of 3,6-dimethyl-*N*-methylphthalimide.

In spite of all efforts to develop a new synthetic methodology to arrive at 3,6-disubstituted phthalimides the use of the 3,6-dinitrophthalic anhydride precursor still seems the best choice.

2.3 A novel versatile methodology for the synthesis of 3,6-diaminophthalimides

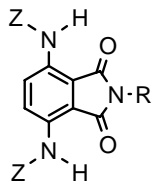
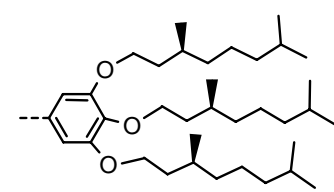
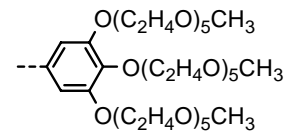
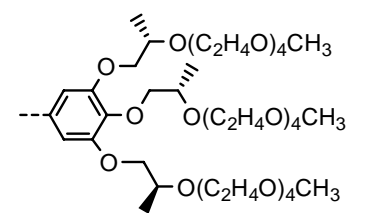
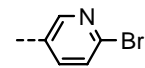
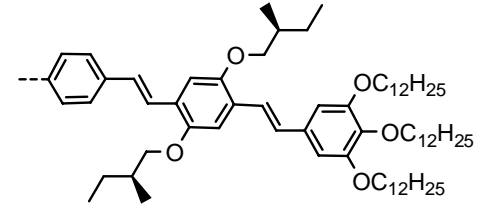
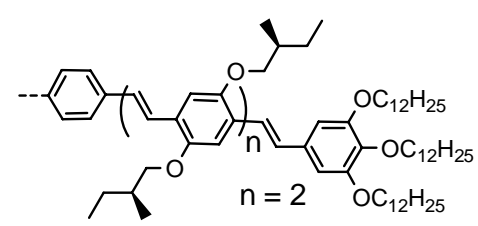
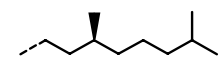
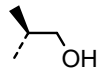
Similar to the strategy depicted in scheme 2.4 also in this approach the electron withdrawing nitro functionalities in anhydride **6** that facilitate ring opening are converted into mildly electron releasing moieties that will increase the rate of the ring closure in the two-step phthalimide formation. Novel synthon 3,6-bis(acetylamino)phthalic anhydride (**19**) is synthesized to balance the imide formation. In scheme 2.8 a straightforward methodology for the synthesis of 3,6-diaminophthalimide building blocks **22** employing 3,6-bis(acetylamino)phthalic anhydride **19** as a key intermediate is presented.



Scheme 2.8: A new synthetic methodology for the synthesis of 3,6-diaminophthalimides **22a-g**. *i)* H_2 , Pd/C, MeOH, rt, 17 h. *ii)* Ac_2O , DMF, 100°C. *iii)* H_2N-R (**21a-h**, Table 1), dioxane, reflux, 17 h. *iv)* 1.6 M HCl, dioxane, reflux.

Compound **19** is obtained *via* a palladium mediated catalytic reduction of 3,6-dinitrophthalic acid **5**, followed by exposure of the unstable 3,6-diaminophthalic acid intermediate to acetic anhydride.¹⁰ Subsequent reaction of **19** with primary amines in dioxane at reflux affords a wide variety of 3,6-bis(acetylamino)phthalimides (**20a-h**) in good to almost complete conversion (Table 2.1). Besides aromatic amines the incorporation of aliphatic amines was equally successful. All phthalimides were purified by column chromatography or crystallization. The final step towards the desired monomeric building blocks for the foldamer is the removal of the *N*-acetyl functionalities. Exposure of 3,6-bis(acetylamino)phthalimides (**20a-g**) to a 1.6 M solution of HCl in aqueous dioxane at reflux furnishes the corresponding 3,6-diaminophthalimides **22a-g** in 75-95%.

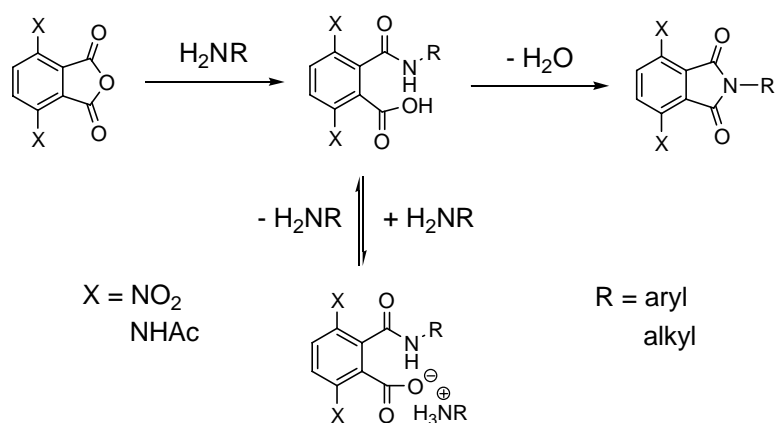
Table 2.1: Yields obtained for 3,6-bis(acetylamino)phthalimides (**20a-h**) and the corresponding 3,6-diaminophthalimides (**22a-g**).

	 20 , Z = COCH ₃ 22 , Z = H	Imides 20	Imides 22
		R	yield (%) ^a
a		86	91
b		80	83
c		90	95
d		85 ^c	~70 ^d
e		91	81
f	 n = 2	87	75
g		83	90
h		86	--

^a isolated yield for the 3,6-diacetylaminophthalimides; ^b isolated yield for the 3,6-diaminophthalimides; ^c based on ¹H-NMR, isolated: 68%; ^d based on ¹H-NMR

We have found that the outcome of imide formation is strongly governed by the substituents on the anhydride and the nature of the *N*-source to be incorporated. This revealed that 3,6-bis(acetylamino)phthalic anhydride (**19**) is more suitable than 3,6-dinitrophthalic anhydride (**6**). This may be rationalized by the mechanism of the reaction.

The formation of the phthalimide most likely proceeds *via* two steps, starting with a ring opening reaction involving a nucleophilic attack of the amine on the carbonyl carbon of the phthalic anhydride (Scheme 2.9). The second step is the ring closure to the phthalimide system with concomitant release of water. The remaining carboxylic acid functionality of the amic acid intermediate formed after the first step readily protonates the amine giving an organic salt, as observed in ¹H-NMR. Although not observed in our research, the formation of an isoimide by dehydration of the amic acid followed by a Dimroth¹¹ rearrangement to the imide has been reported.^{12,13}



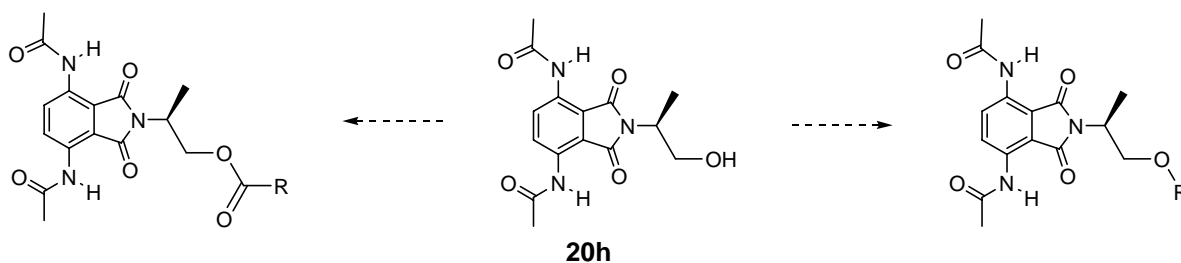
Scheme 2.9: A tentative mechanism for the formation of phthalimides.

In case of aromatic amines the organic salt is in equilibrium with the free acid. However, when aliphatic amines are employed, the intermediate is trapped as the organic salt. This is due to the combination of the electron withdrawing nature of the nitro groups, which enhances the acidity of the carboxylic acid and the higher basicity of the aliphatic amines compared to the aromatic ones. Consequently, conversion of the electron withdrawing nitro function into the electron-donating acetamide strongly improves the ring closure reaction.

From table 1 the broad scope of the methodology towards imides **20** and **22** becomes obvious. Not only weakly nucleophilic aromatic amines **21a-f** but also strongly nucleophilic aliphatic amines **21g-h** were successfully incorporated. Even the more sterically demanding amine **21h** was integrated in a good yield. In addition, in the case of synthon **20h** derivatization prior to removal of the acetyl groups is envisaged. The list covers the introduction of hydrophobic **a, d-h** as well as hydrophilic **b-c** functionalities. The current strategy via 3,6-bis(acetylamino)phthalic anhydride (**19**) has clearly proven to be superior to our previously

reported approach (Scheme 2.1) starting from 3,6-dinitrophthalic anhydride (**6**). To summarize, with this library of novel 3,6-diaminophthalimides in hand, the synthesis and study of a wide range of appealing foldamers are viable.

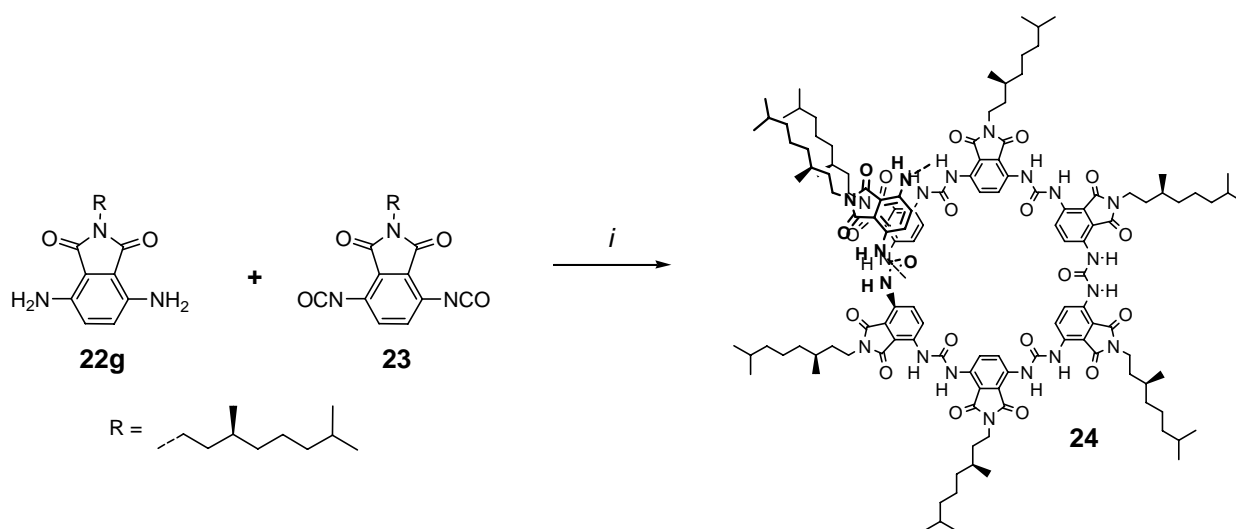
Although not yet further exploited, compound **20h** is an attractive synthon for further derivatization to a wide variety of 3,6-diaminophthalimides. Since synthon **20h** already possesses the desired chirality to facilitate CD spectroscopy, the peripheral functionality of choice does not necessarily need to contain a stereocenter. Relatively simple synthetic strategies can be developed to introduce the peripheral functionality. An obvious strategy would be the formation of an ester linkage by reaction with an acid or acid-chloride. However, preference should be given to a chemically more stable ether linkage by exploitation of the Williamson- or Mitsunobu-etherification (Scheme 2.10). Besides these two options, the generation of a linker based on a carbamate function by reaction of **20h** with an isocyanate may have potential.



Scheme 2.10: Potential linking strategies for the introduction of peripheral functionality.

2.4 A brief investigation on foldamers with an aliphatic periphery

This novel synthetic route (Scheme 2.8) gave access to the anticipated diamine **22g**, bearing a single chiral aliphatic tail. Polymerization of diamine **22g** with the corresponding diisocyanate **23** in refluxing toluene in the presence of 4-dimethylaminopyridine (DMAP) furnished poly(ureidophthalimide) **24** (Scheme 2.11). This polymer serves as a model system for the polymers that may become accessible with 3,6-bis(acetylamino)phthalimide **20h** (Table 2.1). Polymer **24** is the first poly(ureidophthalimide) which is functionalized with a purely aliphatic periphery. The tails ensure solubility in common organic solvents. The presence of a chiral center allows circular dichroism studies. Although polymer **24** may serve as a test case for prospective polymers based on **20h**, it must be noted that the chiral center in the latter is located even less remotely from the backbone.



Scheme 2.11: Synthesis of polymer **24** bearing an aliphatic periphery. i) DMAP (1.0 equiv.), PhCH_3 , reflux, 17 h.

Polymer **24** was separated by column chromatography over silica gel, with an ethyl acetate / heptane mixture as the solvent, into two fractions. The first fraction (~30 w%) is an enrichment of higher molecular weight oligomers with lengths from 4-21 units, whereas the second fraction (~70 w%) mostly contains the lower molecular weight oligomers with lengths from 1-13 as is determined by GPC (Figure 2.1a).

Fraction **24a**, containing the longer oligomers, was studied with UV-vis and CD spectroscopy. When dissolved in THF, fraction **24a** shows two absorption maxima located at 305 and 400 nm (Figure 2.1b). Although small, a clear CD effect is present in the same solvent with a zero crossing at 315 nm. The absorption band at 400 nm does not show a Cotton effect. Elevation of the temperature to 50 °C, does not affect the Cotton effect. It must be noted that 3,6-bis(acetylamino)phthalimide **20g** is CD silent in THF and in heptane.

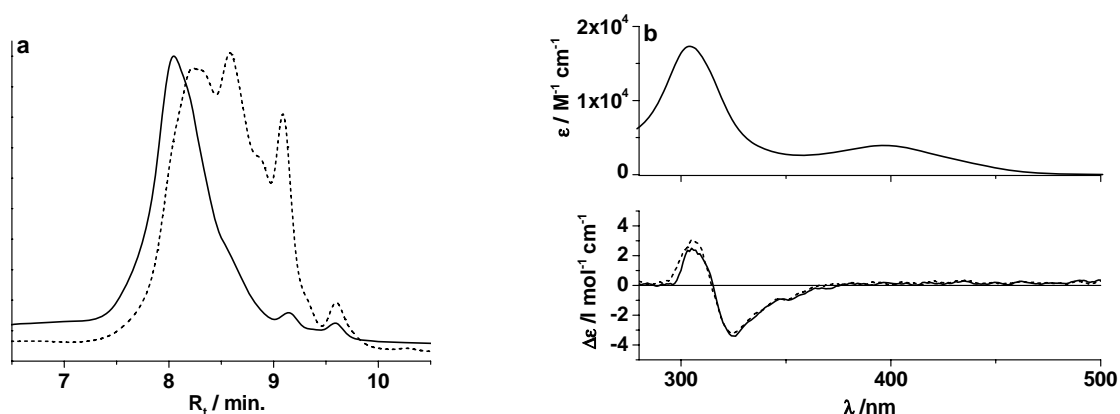


Figure 2.1: a) Normalized GPC (CHCl_3 , 310 nm, mixed-D, polystyrene internal standard) traces of fraction **24a** (black line), fraction **24b** (dashed line); b) UV-vis and CD spectra of fraction **24a** in THF (1.0×10^{-4} M, based on monomeric Mw) at 20 °C (black line) and 50 °C (dashed line).

UV-vis and CD analysis of fraction **24a** dissolved in heptane reveals maxima at the same wavelength as in THF (305 and 400 nm) (Figure 2.2a). Although still small, the intensity of the Cotton effect in heptane is somewhat larger compared to that in THF. Like in THF, raising the temperature in heptane to 80 °C for 1 hour has no influence on the Cotton effect. In contrast to previously synthesized hydrophobic ureidophthalimide polymers that showed no CD effect in chloroform², this polymer does (Figure 2.2b). Circular dichroism measurements of **24a** in CHCl₃ show a small but clear Cotton effect. The effect asymmetrically decreases upon raising the temperature but does not disappear entirely. It must be noted that **22g** is CD silent in CHCl₃ and therefore it is reasonable to assume that the CD effect is the result of preferred helicity at the foldamer level.

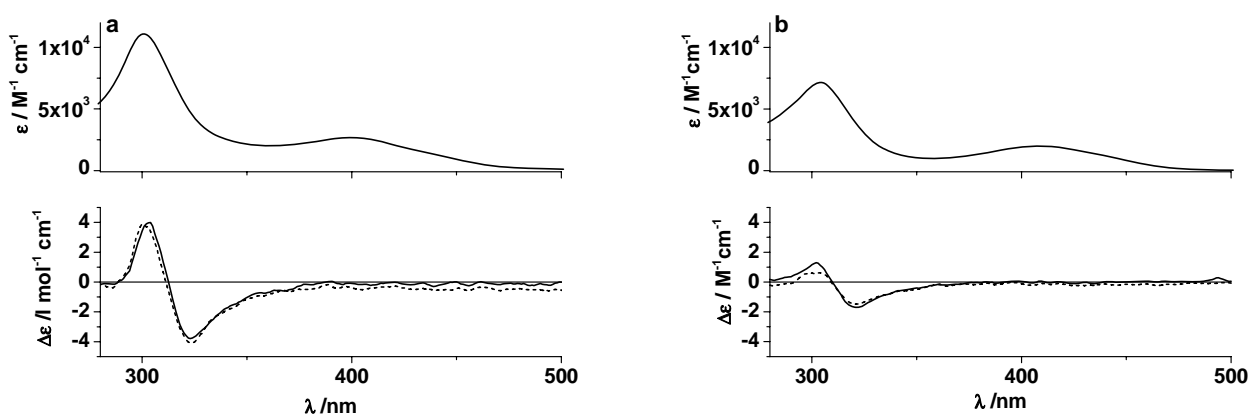


Figure 2.2: a) UV-vis and CD spectra of fraction **24a** in heptane ($1.1 \cdot 10^{-4}$ M) at 20 °C (black line) and 80 °C (dashed line). b) UV-vis and CD spectra of fraction **24a** in CHCl₃ ($1.3 \cdot 10^{-4}$ M) at 20 °C (black line) and 80 °C (dashed line).

There is a marked difference in foldameric character between the poly(ureidophthalimide)s **3** (Scheme 2.1) and **24a**, which can be attributed to differences in their structural features. The system decorated with just aliphatic tails has a far less space demanding periphery as compared to the aromatic ones where every aromatic core is decorated with three chiral alkyl tails. Therefore, the number of chiral centers per monomeric unit is also less, resulting in a lower 'chiral density'. Another obvious difference is the absence of aromatic units, and hence the lack of any possible π - π interactions. These structural differences might account for the lower intensity of the Cotton effect. However, the new polymer has the chiral center located very close to the core, in principle resulting in a higher impact of the chirality. This may account for the stability of the secondary architecture at elevated temperatures and the presence of a Cotton effect in chloroform. In addition, the temperature independent Cotton effect might also be explained by the lower solubility of this system compared to poly(ureidophthalimide) **3** rendering unfolding unfavorable. Moreover, the broad nature of the NMR signals for **24a** in CHCl₃ and THF with and without additional hexafluoroisopropanol to break up hydrogen

bonds, indicates the presence of highly aggregated species rendering characterization difficult. According to Moore's foldamer definition¹ polymer **24a** does not belong to the class of foldamers since the putative helical architecture seems to lack dynamics and reversibility based on the temperature dependent CD spectra in various solvents.

2.5 Conclusions

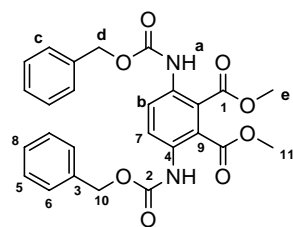
Synthesis of 3,6-disubstituted phthalimides is not trivial and is supported by only a few literature precedents. Modification of the previously reported approach (Scheme 2.2) as depicted in Scheme 2.3 has proven to be a viable method to synthesize a variety of different 3,6-diamino-phthalimides. This success can be attributed to the introduced kinetic balance between ring opening and ring closure in the two-step phthalimide formation by substituting the nitro functionalities in **6** for the bisacetylamino functionalities in **19**. Since there are no longer synthetic drawbacks for the introduction of primary amines, virtually any poly-ureidophthalimide foldamer can be synthesized.

The alternative route to circumvent the use of 1,5-dinitronaphthalene has so far been more troublesome than expected. Saponification of the methyl ester proved to be the bottleneck (Scheme 2.8). Presumably an acid catalyzed hydrolysis of a *tert*-butyl ester will be more convenient. Although the route has fallen short, there is still enough potential for further investigation.

With the new synthetic methodology to arrive at novel 3,6-diaminophthalimides the anticipated chiral polymer precursors **22g** became accessible. This led to the formation of poly (ureidophthalimide) only bearing a single chiral aliphatic tail per monomeric unit. Preliminary CD experiments show Cotton effects indicative for helical architectures. The Cotton effects in THF and heptane are small, however, they do not vanish upon raising the temperature. In contrast to the monomer, the polymer does display a Cotton effect in CHCl₃. This is remarkable since all ureidophthalimide polymers previously synthesized were CD silent in CHCl₃. This effect can most likely be attributed to the proximity of the chiral center to the core.

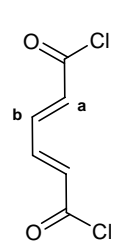
2.6 Experimental

General. All starting materials were obtained from commercial suppliers and used as received. All moisture sensitive reactions were performed under an atmosphere of dry argon. Dry tetrahydrofuran was obtained by distillation from Merck molecular sieves (4 Å), triethylamine was dried on Merck molecular sieves (4 Å). Analytical thin layer chromatography was performed on Kieselgel F-254 precoated silica plates. Visualization was accomplished with UV light. Column chromatography was carried out on Merck silica gel 60 (70-230 mesh or 230-400 mesh ASTM). ¹H-NMR and ¹³C-NMR spectra were recorded on a Varian Mercury, 400 MHz for ¹H-NMR and 100 MHz for ¹³C-NMR, or on a Varian Gemini, 300 MHz for ¹H-NMR and 75 MHz for ¹³C-NMR. Proton chemical shifts are reported in ppm downfield from tetramethylsilane (TMS) and carbon chemical shifts in ppm downfield from TMS using the resonance of the deuterated solvent as internal standard. Elemental analyses were carried out using a Perkin Elmer 2400. Matrix assisted laser desorption/ionization mass spectra were obtained using α -cyano-4-hydroxycinnamic acid as the matrix on a PerSeptive Biosystems Voyager-DE PRO spectrometer. GPC measurements on the oligomeric mixtures were performed on a mixed D column (PL gel 5 μ m, 200-400.000 g/mol), with a flow of 1 ml/min, and chloroform as the eluting solvent. The injection volume was 50 μ l and UV detection (254, 310, or 420 nm) was applied. Molecular weights and polydispersity indices were calculated from a polystyrene standard. IR spectra were measured on a Perkin Elmer 1600 FT-IR. UV/vis spectra were measured on a Perkin Elmer Lambda 40 spectrometer, using (HELMA) quartz cuvettes (path length 1 cm). Circular dichroism spectra were recorded on a Jasco J600 equipped with a Jasco PTC-348WI temperature controller. All ϵ en $\Delta\epsilon$ values are calculated per mole monomeric phthalimide units.

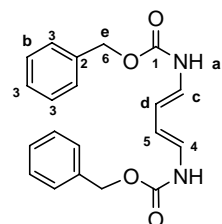


Dimethyl 3,6-bis(benzyloxycarbonylamino)phthalate (11b). Diels-Alder adduct **18b** was redissolved in $\text{Cl}_2\text{C}=\text{CCl}_2$ (6 mL), and tetrachloro-1,2-benzoquinone (5.670 g, 23.058 mmol) was added and the suspension was heated to 110°C for 65 h under continuous stirring. The mixture was filtered over a glass filter with hyflo and rinsed with CHCl_3 to remove excess of oxidant and the corresponding tetrachloro-1,2-dihydroquinone. The filtrate was concentrated *in vacuo* and redissolved in Et_2O and the organic phase washed with aqueous saturated K_2CO_3 . The combined organic layers were dried over MgSO_4 , filtered and concentrated. Subsequent purification by column chromatography (silica gel, 5 v% EtOAc in CHCl_3 , $R_f = 0.3$) and crystallization (50% EtOAc in heptane) gave **11b** as an off-white solid (2.08 g, 4.22 mmol, 49%). ¹H-NMR (300 MHz, CDCl_3) δ (ppm) = 8.51 (br s, 2H, a), 8.24 (s, 2H, b), 7.34-7.28 (m, 10H, c), 5.11 (s, 4H, d), 3.76 (s, 6H, e); ¹³C-NMR (CDCl_3) δ (ppm) = 167.7 (1), 153.5 (2), 135.9 and 133.4 (3 or 4), 128.7, 128.6 and 128.5 (3 \times CH, 5, 6 or 7), 124.7 (8), 119.6 (9), 67.4 (10), 53.1 (11); FT-IR σ (cm^{-1}) = 3370, 3034, 2953, 1737, 1705, 159, 1509, 1455, 1203, 1124, 1065, 1003, 745, 698.

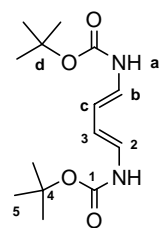
Di-*t*-butyl (1E,3E)-buta-1,3-diene-1,4-diylldicarbamate (12a) and dibenzyl (1E,3E)-buta-1,3-diene-1,4-diylldicarbamate (12b). *Trans-trans*-muconic acid **14** (1.134 g, 7.940 mmol) was dissolved in dry CH_2Cl_2 (30 mL) and DMF (2 drops) and SOCl_2 (1.52 mL, 21.16 mmol) were added. The mixture was refluxed for 39 h under continuous stirring. Concentration of the reaction mixture *in vacuo* gave *trans, trans*-muconic acid



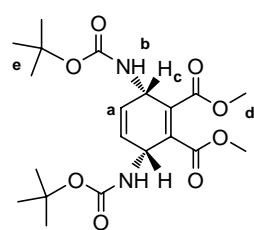
chloride **15** (1.423 g, 7.95 mmol, 100%) as a grey solid. $^1\text{H-NMR}$ (300 MHz, CDCl_3) δ (ppm) = 7.51-7.41 (m, 2H, **a**), 6.61-6.51 (m, 2H, **b**). The grey solid (2.086 g, 11.641 mmol) was dissolved in CHCl_3 (12 mL) and drop wise added to a solution of NaN_3 (2.043 g, 31.430 mmol) in water (8 mL) over a period of two hours at 4°C under continuous stirring. The reaction mixture was poured in a separating funnel and the aqueous layer was discarded. The organic layer was consecutively washed with 10% aq. NaHCO_3 solution (15 mL) and water (15 mL). The organic layer was dried over MgSO_4 and filtered over a glass filter. The dried CH_2Cl_2 layer was heated to reflux and slowly substituted for toluene by using a Dean-Stark setup allowing the temperature to rise to 80°C .



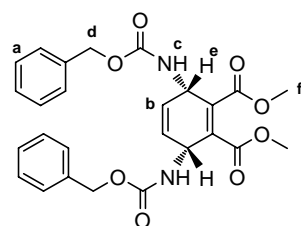
The di-acylazide **16** underwent a Curtius rearrangement to the corresponding diisocyanate **17**. The temperature was still kept at 80°C upon dropwise addition of benzyl alcohol (3.0 mL, 29.102 mmol) for 1.5 hours under continuous stirring. The reaction was monitored by IR. Concentration of the reaction mixture *in vacuo* followed by washing over a glass filter with CHCl_3 (3×20 mL) gave **12b** as a sparingly soluble off-white solid (2.722 g, 7.724 mmol, 66%). $^1\text{H-NMR}$ (300 MHz, DMSO) δ (ppm) = 9.55 (d, 2H, $J = 9.6$ Hz, **a**), 7.37 (m, 10H, **b**), 6.42 (t, 2H, $J = 10.6$ Hz, **c**), 5.69 (d, 2H, $J = 10.2$ Hz, **d**), 5.08 (s, 4H, **e**); $^{13}\text{C-NMR}$ (CDCl_3) δ (ppm) = 157.6 (**1**), 140.8 (**2**), 132.6 (**3**), 132.2 (**3**), 132.1 (**3**), 128.1 (**4**), 113.7 (**5**), 70.1 (**6**); FT-IR σ (cm^{-1}) = 3288, 3064, 3034, 1692, 1647, 1505, 1453, 1269, 1227, 1058, 1008, 954, 764, 721, 736, 692; **m.p.** = decomposition $>230^\circ\text{C}$; **Analysis**, $\text{C}_{20}\text{H}_{20}\text{N}_2\text{O}_4$, calculated: C, 68.17; H, 5.72; N, 7.95; found: C, 68.40; H, 5.98; N, 8.12.



The same procedure with diacid chloride **15** (1.381 g, 7.709 mmol) and NaN_3 (1.353 g, 20.814 mmol) and substitution benzyl alcohol by *tert*-butanol (~ 3 mL, ~ 2.4 g, 32.4 mmol) gave **di-tert-butyl (1E,3E)-buta-1,3-diene-1,4-diyldicarbamate (12a)** as an off-white solid (1.3 g, 4.7 mmol, 61 %). $^1\text{H-NMR}$ (300 MHz, DMSO- d_6) δ (ppm) = 9.12 (d, 2H, $J = 9.9$ Hz, **a**), 6.33 (t, 2H, $J = 10.2$ Hz, **b**), 5.60 (d, 2H, $J = 11.5$, **c**), 1.41 (s, 18H, **d**); $^{13}\text{C-NMR}$ (CDCl_3) δ (ppm) = 153.6 (**1**), 124.6 (**2**), 109.7 (**3**), 79.8 (**4**), 29.0 (**5**); FT-IR σ (cm^{-1}) = 3349, 2990, 1688, 1641, 1489, 1269, 1152, 1054, 965, 860, 767, 774, 759; **m.p.** = decomposition $>260^\circ\text{C}$; **Analysis**, $\text{C}_{14}\text{H}_{24}\text{N}_2\text{O}_4$, calculated: C, 59.13; H, 8.51; N, 9.85; found: C, 58.83; H, 8.23; N, 10.25.

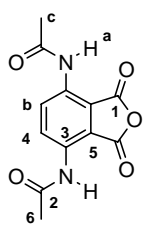


Dimethyl 3,6-bis(tert-butoxycarbonylamino)-3,6-dihydrophthalate (18a). A solution of **di-tert-butyl (1E,3E)-buta-1,3-diene-1,4-diyldicarbamate 12a** (3.01 g, 8.54 mmol), di-ester **13** (1.3 mL, 10.3 mmol) and dihydroquinone (9.88 mg, 0.09 mmol) in DMF (15 mL) was heated for 18 h at 90°C under continuous stirring. The reaction mixture was concentrated *in vacuo* yielding the Diels-Alder adduct **18a** as a solid ($> 90\%$ as was determined by $^1\text{H-NMR}$) and was used as such. $^1\text{H NMR}$ (300 MHz, DMSO- d_6) δ (ppm) = 5.86 (s, 2H, **a**), 5.14 (d, 2H, $J = 8.1$ Hz, **b**), 4.88 (d, 2H, $J = 8.8$ Hz, **c**), 3.78 (s, 6H, **d**), 1.44 (s, 9H, **e**).



Dimethyl 3,6-bis(benzyloxycarbonylamino)-3,6-dihydrophthalate (18b). A solution of **dibenzyl (1E,3E)-buta-1,3-diene-1,4-diyldicarbamate 12b** (3.01 g, 8.54 mmol), di-ester **13** (1.3 mL, 10.3 mmol) and dihydroquinone (9.88 mg, 0.09 mmol) in DMF (15 mL) was heated for 7 h at 90°C under continuous stirring. The reaction mixture was concentrated *in vacuo* yielding the Diels-

Alder adduct **18b** as a solid (4.81 g, 9.73 mmol, ~94%). $^1\text{H NMR}$ (300 MHz, DMSO- d_6) δ (ppm) = 7.35-7.23 (m, 10H, **a**), 7.13 (d, 2H, $J = 9.1$ Hz, **b**), 5.86 (s, 2H, **c**), 5.11-4.97 (m, 4H, **d**), 4.87 (d, 2H, $J = 8.0$ Hz, **e**), 3.61 (s, 6H, **f**) + traces of DMF.

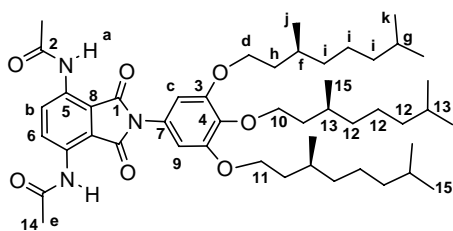


3,6-Bis(acetylamino)phthalic anhydride (19). Pd/C (0.215 g, 0.20 mmol of a 10 w% Pd on carbon) was added to 3,6-dinitrophthalic acid (**5**) The suspension was purged with nitrogen for 30 minutes under continuous stirring. Subsequently, the mixture was placed under a hydrogen atmosphere of 1 bar for 17 h under continuous stirring. The crude reaction mixture was filtered over paper and the residue was washed with methanol.

Concentration of the organic filtrate yielded a green residue, which in turn, was suspended in a mixture of DMF (40 mL) and acetic anhydride (120 mL). The suspension was stirred at room temperature under an argon atmosphere for 2 h until complete dissolved en then the solution was stirred at 90 °C for 1.5 h. After concentration in vacuo the residue was suspended in hot Et₂O (50 mL). The mixture was allowed to cool to 5 °C and then filtered over a Büchner funnel. The solid was washed with Et₂O (3 × 25 mL) giving **19** (0.317 g, 1.207 mmol, 60 %) as a light brown solid.

GC-MS (80-320 °C): $R_t = 10.01$ min, purity ≈ 99 %; $\text{C}_{12}\text{H}_{10}\text{N}_2\text{O}_5$, m/z calculated: 262.06, found: 262, and characteristic fragments: 220, 178 and 43. $^1\text{H-NMR}$ (400 MHz, DMSO- d_6): δ (ppm) = 9.83 (s, 2H, 2 × NH, **a**), 8.29 (s, 2H, 2 × H_{ar} , **b**), 2.17 (s, 6H, 2 × CH_3 , **c**); $^{13}\text{C-NMR}$ (DMSO- d_6 , 50 MHz): δ (ppm) = 169.0 (**1**), 161.8 (**2**), 133.0 (**3**), 130.3 ($\text{H}_{\text{Car}}\text{C}_{\text{ar}}\text{N}$, **4**), 118.8 ($\text{C}_{\text{ar}}\text{C}=\text{O}$, **5**), 23.8 (**6**); **FT-IR** (ATR) σ (cm^{-1}) = 3350 (N-H), 3115 (Ar-H), 1839, 1782 (C=O, anhydride), 1679 (C=O, amide), 1637, 1612, 1554, 1496 (C-C, aromatic), 1442, 1366, 1318, 1289, 1257, 1199, 1153, 1038, 1017, 992, 919, 893, 862, 755, 741; **UV-vis** (CHCl_3 , 4.6×10^{-5} M): λ_{max} = 264, 286, 296 and 388 nm.

General procedure for the synthesis of 3,6-bis(acetylamino)phthalimides (20a-h). A suspension of 3,6-bis(acetylamino)phthalic anhydride **19** and amine **21a-h** (1.0 equiv.) in dioxane (0.15 M) was stirred under reflux. The crude reaction mixture was concentrated and the residue purified by crystallization or column chromatography over silica gel.

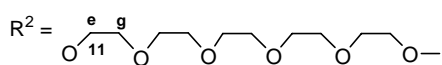
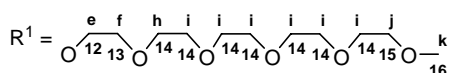
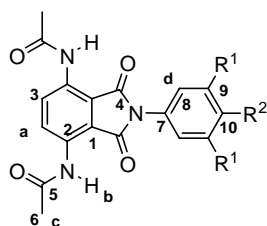


3,6-Bis(acetylamino)-N-(3,4,5-tri-(S)-3,7-dimethyloctyloxyphenyl)phthalimide (20a). **19** (0.052 g, 0.199 mmol) and amine **21a**

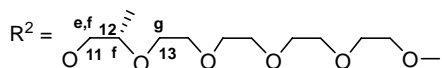
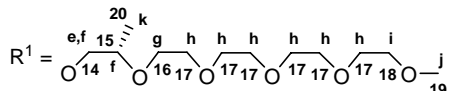
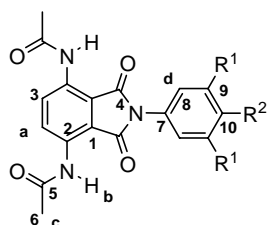
(0.135 g, 0.240 mmol) were used. After 46 h of reflux the solvent was removed by evaporation under vacuum. Purification by column chromatography (silica gel, 40 v% EtOAc in heptane, $R_f = 0.3$) rendered **20a** (0.137 g, 0.170 mmol, 86%) as a yellow sticky solid.

GPC (mixed D, CHCl_3 , 254 nm): $R_t = 8.67$ min. $^1\text{H-NMR}$ (400 MHz, CDCl_3): $\delta = 9.37$ (s, 2H, **a**), 8.78 (s, 2H, **b**), 6.57 (s, 2H, **c**), 4.05-3.97 (m, 6H, **d**), 2.24 (s, 6H, **e**), 1.89-1.82 (m, 3H, **f**), 1.71-1.67 (m, 3H, **g**), 1.64-1.49 (m, 6H, **h**), 1.36-1.11 (m, 18 H, **i**), 0.94-0.92 (ds, 9H, **j**), 0.88-0.85 (m, 18H, **k**); $^{13}\text{C-NMR}$ (75 MHz, CDCl_3): $\delta = 169.2$ and 168.8 (**1**, **2**), 153.8 (**3**), 138.6 (**4**), 133.4 (**5**), 127.8 (**6**), 125.8 (**7**), 114.0 (**8**), 105.5 (**9**), 72.1 (**10**), 67.9 (**11**), 39.7-36.6 and 25.0 (**12**), 30.1-28.3 (**13**), 25.0 (**14**), 23.0-19.9 (**15**); **FT-IR** σ (cm^{-1}) = 3345 (N-H), 2954 and 2927 and 2870 (C-H), 1766, 1731 and 1694 (imide, C=O), 1666 (amide, C=O), 1629, 1597 and 1543 and 1497 (aromatic C-C), 1469, 1439, 1421, 1376, 1304, 1263, 1236 (ether, aryl-O-alkyl), 1173, 1116, 1043,

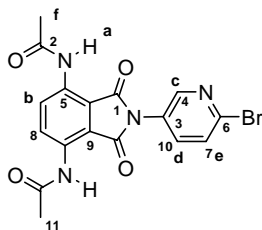
1016, 973, 941, 902, 841, 825, 762, 729, 691; **MS** (MALDI-TOF), m/z calculated: 805.56, measured: 805.53; **Analysis**, $C_{48}H_{75}N_3O_7$, calculated: C, 71.52; H, 9.38; N, 5.21; found: C, 71.86; H, 9.54; N, 5.21; **UV-vis** ($CHCl_3$, 4.27×10^{-5} M): λ_{max} = 275, 291 and 392 nm.



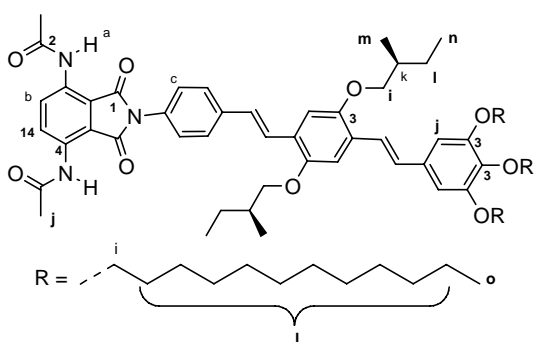
3,6-Bis(acetylamino)-N-(3,4,5-tris(2-(2-(2-(2-methoxyethoxy))-ethoxy)-ethoxy)-ethoxy)-phenyl)-phthalimide (20b). **19** (0.150 g, 0.570 mmol) and amine **21b** (0.545 g, 0.646 mmol) were used. The mixture was refluxed for 21 h. Purification by column chromatography (silica gel, 10 *v%* heptane in 1,2-dimethoxyethane, R_f = 0.3) gave **20b** (0.496 g, 0.456 mmol, 80%) as a viscous orange oil. R_t (GPC, mixed D, 254 nm, $CHCl_3$) = 8.40 min. **1H -NMR** (400 MHz, $CDCl_3$): δ = 9.34 (s, 2H, **b**), 8.72 (s, 2H, **a**), 6.69 (s, 2H, **d**), 4.22-4.18 (m, 6H, **f**), 3.88 (t, 4H, J = 4.8 Hz, **g**), 3.83 (t, 2H, J = 4.9 Hz, **h**), 3.74-3.72 (m, 6H, **i**), 3.68-3.62 (m, 36H, **j**), 3.56-3.52 (m, 6H, **k**), 3.37-3.36 (ds, 9H, **l**), 2.24 (s, 6H, **c**); **^{13}C -NMR** (75 MHz, $CDCl_3$): δ = 168.9 and 168.1 (**4**, **5**), 152.7 (**9**), 138.3 (**10**), 133.1 (**2**), 127.2 (**3**), 125.9 (**7**), 113.6 (**1**), 106.2 (**8**), 72.4 (**11**), 71.9 (**15**), 70.8-70.5 (**14**), 69.5 (**13**), 69.0 (**12**), 58.9 (**16**), 24.7 (**6**); **FT-IR** σ (cm^{-1}) = 3362 (N-H), 2871 (C-H), 2243, 1766, 1753 and 1702 (imide and amide), 1636, 1616, 1596 and 1548 and 1491 (aromatic C-C), 1438, 1394, 1368, 1351, 1299, 1239, 1173, 1098 (ether), 1037, 945, 907, 845, 751, 685, 666; **MS** (MALDI-TOF), m/z calculated: 1087.53, measured: 1110.49 (+ Na^+), 1126.47 (+ K^+); **Analysis**, $C_{51}H_{79}N_3O_{22}$, calculated: C, 56.29; H, 7.50; N, 3.86; found: C, 55.93; H, 7.55; N, 3.60; **UV-vis** (water, 5.33×10^{-5} M): λ_{max} = 258 and 366 nm.



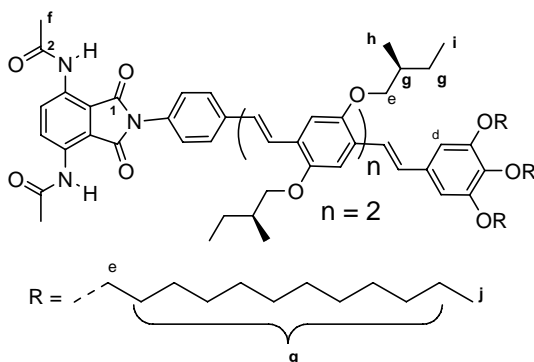
3,6-Bis(acetylamino)-N-(3,4,5-tris((2S)-2-(2-(2-(2-methoxyethoxy))-ethoxy)-ethoxy)-propoxy)-phenyl)-phthalimide (20c). **19** (0.377 g, 1.438 mmol) and amine **21c** (1.333 g, 1.504 mmol) were used. After reflux of the mixture for 17 h, the solvent was evaporated and the residue was purified by column chromatography (silica gel, 20 *v%* heptane in 1,2-dimethoxyethane, R_f = 0.3) yielding **20c** (1.457 g, 1.289 mmol, 90 %) as a viscous yellow oil. R_t (GPC, mixed-D, 254 nm, $CHCl_3$): R_t = 8.38 min. **1H -NMR** (400 MHz, $CDCl_3$): δ = 9.38 (s, 2H, **b**), 8.81 (s, 2H, **a**), 6.62 (s, 2H, **d**), 4.10-4.02 (m, 3H, **e**), 3.90-3.81 (m, 6H, **f**), 3.77-3.69 (m, 6H, **g**), 3.68-3.62 (m, 36H, **h**), 3.56-3.52 (m, 6H, **i**), 3.39-3.37 (m, 9H, **j**), 2.26 (s, 6H, **c**), 1.32-1.29 (m, 9H, **k**); **^{13}C -NMR** (50 MHz, $CDCl_3$): δ = 169.0 and 168.3 (**4**, **5**), 152.9 (**9**), 138.0 (**10**), 133.3 (**2**), 127.5 (**3**), 126.0 (**7**), 113.8 (**1**), 105.6 (**8**), 76.4 (**11**), 75.1 (**12**), 74.4 (**15**), 72.8 (**14**), 72.0 (**18**), 70.9-70.5 (**17**), 68.9 (**16**), 68.6 (**13**), 59.1 (**19**), 24.9 (**6**), 17.7-17.5 (**20**); **FT-IR** σ (cm^{-1}) = 3363 (N-H), 2871 (C-H), 2184, 1754 and 1699 (imide and amide), 1637, 1616, 1598 and 1548 and 1491 (aromatic C-C), 1438, 1393, 1369, 1297, 1239, 1200, 1099, 1016, 978, 906, 845, 762, 688, 665; **MS** (MALDI-TOF), m/z calculated: 1129.58, measured: 1152.65 (+ Na^+), 1169.61 (+ K^+); **Analysis**, $C_{57}H_{87}N_3O_{22}$, calculated: C, 57.38; H, 7.76; N, 3.72; measured: C, 57.41; H, 7.78; N, 3.61; **UV-vis** (water, 4.87×10^{-5} M): λ_{max} = 259 and 367 nm.



3,6-Bis(acetylamino)-N-(2-bromo-5-pyridyl)-phthalimide (20d). **19** (0.524 g, 2.000 mmol) and amine **21d** (0.363 g, 2.100 mmol) were used. After 48 h of reflux the crude reaction mixture was concentrated and filtered over silica gel with 50 v% EtOAc in CHCl₃. Subsequent, crystallization from EtOAc (3 ×) gave phthalimide **6d** (0.564 g, 1.352 mmol, 68%) as yellow fluffy crystals. ¹H-NMR (300 MHz, CDCl₃) δ (ppm) = 9.27 (s, 2H, **a**), 8.82 (s, 2H, **b**), 8.56 (d, 1H, *J* = 2.2 Hz, **c**), 7.71 (dd, 1H, *J*_a = 8.4 Hz, *J*_b = 2.3 Hz, **d**), 7.46 (d, 1H, *J* = 8.2 Hz, **e**), 2.26 (s, 6H, **f**); ¹³C-NMR (CDCl₃) δ (ppm) = 169.1 and 167.5 (**1**, **2**), 147.0 (**3**), 141.0 (**4**), 135.4 (**5**), 133.8 (**6**), 128.6 (**7**), 128.2 (**8**), 127.7 (**9**), 113.4 (**10**), 25.0 (**11**); FT-IR σ (cm⁻¹) = 3366, 3330, 3121, 3061, 1761, 1711, 1692, 1678, 1492, 1464, 1188, 758, 723; MS (MALDI-TOF), *m/z* calculated: 416.02; found: 416.93; **Analysis**, C₁₇H₁₃BrN₄O₄Br, calculated: C, 48.94; H, 3.14; N, 13.43; found: C, 48.74, H, 2.77; N, 12.81.

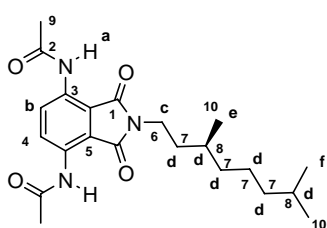


3,6-Bis(acetylamino)-N-OPV3-phthalimide (20e). **19** (0.040 g, 0.154 mmol) and amine **21e** (0.173 g, 0.169 mmol) were used. After 24 h of reflux the reaction mixture was concentrated and purified by column chromatography (silica gel, CHCl₃ to 5 v% EtOAc in CHCl₃) affording **20e** as a yellowish solid (0.178 g, 0.140 mmol, 91%). ¹H-NMR (300 MHz, CDCl₃) δ (ppm) = 9.82 (s, 2H, **a**), 8.76 (s, 2H, **b**), 7.64 (d, 2H, *J* = 8.5 Hz, **c**), 7.52 (d, 2H, *J* = 16.5 Hz, **d**), 7.45 (d, 2H, 8.5 Hz, **e**), 7.36 (d, 2H, *J* = 16.2 Hz, **f**), 7.16 (d, 2H, 16.5 Hz, **g**), 7.08 (d, 2H, *J* = 8.0 Hz, **h**), 7.01 (d, 2H, *J* = 16.2 Hz, **i**), 6.72 (s, 2H, **j**), 4.04-3.82 (m, 10H, **i**), 2.17 (s, 6H, **j**), 2.02-1.92 (m, 2H, **k**), 1.88-1.60 (m, 8H, **l**), 1.50-1.28 (m, 49H, **l**), 1.14-1.12 (d, 6H, **m**), 1.05-1.00 (t, 6H, **n**), 0.91-0.86 (t, 9H, **o**); ¹³C-NMR (CDCl₃) δ (ppm) = 168.9 and 168.2 (**1**, **2**), 153.3 (**3**), 151.5 (**3**), 151.1 (**3**), 138.3 (**4**) (C_{ar}C_{ar}O), 138.2 (**5**), 133.3 (**6**) (C_{ar}N), 133.1 (**7**) (C_{ar}NC=O), 129.7 (**8**), 129.0 (**9**), 127.5 (**10**) (CH_{ar}CH_{ar}), 127.4 (**11**), 127.3 (**12**), 127.0 (**13**), 126.1, 126.1, 125.0, 122.3, 113.7 (C_{ar}C=O), 110.9, 109.9, 105.1, 74.5 and 74.2 and 73.6 (3 × OCH₂CH₂), 69.1 (2 × OCH₂C*H) 35.3 and 35.2 (2 × CHCH₃), 32.0 - 26.2 (CH₂), 24.8 (CH₃), 22.8 (CH₂), 17.0 and 16.9 (2 × C=OCH₃), 14.2 (3 × CH₂CH₂CH₃), 11.6 and 11.5 (2 × CH₃); FT-IR σ (cm⁻¹) = 3365 (N-H), 2957, 2922, 2853, 1699, 1493, 1348, 1239, 1115, 758, 732; MS (MALDI-TOF), *m/z* calculated: 1265.89; found: 1265.86; **Analysis**, C₈₀H₁₁₉N₃O₉, calculated: C, 75.85; H, 9.47; N, 3.32; found: C, 75.73; H, 9.50; N, 2.95; **UV-vis** (CHCl₃, 2.21 × 10⁻⁶ M): λ_{max} = 410 nm (ε = 47999 M⁻¹ cm⁻¹) and 329 nm (ε = 33152 M⁻¹ cm⁻¹); (THF, 1.28 × 10⁻⁵ M): λ_{max} = 402 nm (ε = 58293 M⁻¹ cm⁻¹) and 332 nm (ε = 25346 M⁻¹ cm⁻¹).



3,6-Bis(acetylamino)-N-OPV4-phthalimide (20f). **19** (0.075 g, 0.287 mmol) and OPV-4-NH₂ (**21f**)¹⁴ (0.355 g, 0.274 mmol) were used. After 22 h of reflux the reaction mixture was concentrated and purified by column chromatography (silica-gel, CHCl₃ to 10 v% EtOAc in CHCl₃) rendering **20f** (0.366 g, 0.238 mmol, 87%) as an orange solid. ¹H-NMR¹⁵ (300 MHz, CDCl₃) δ (ppm) = 9.38 (s, 2H, **a**), 8.82 (s, 2H, **b**), 7.66 (d, 2H, *J* = 8.5 Hz, **c**), 6.74 (s,

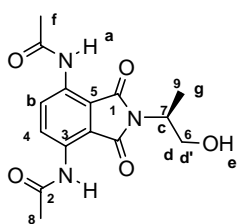
2H, **d**), 4.05-3.83 (m, 14H, **e**), 2.25 (s, 6H, **f**), 2.03-1.61 (m, 14H, **g**), 1.59-1.27 (m, 58H, **g**), 1.13-1.10 (m, 12H, **h**), 1.02 (t, 12H, $J = 7.3$ Hz, **i**), 0.88 (t, 9H, **j**); $^{13}\text{C-NMR}$ (CDCl_3) δ (ppm) = 169.1 and 168.5 (**1**, **2**), 153.4 ($2 \times \text{CH}_{\text{ar}}\text{-CarO}$), 151.6, 151.3, 151.3, 151.1, 138.5 ($(\text{OC}_{\text{ar}})_2\text{CarO}$), 138.3, 133.5, 133.4 (CarNC=O), 129.6, 128.8, 128.3, 127.7 ($\text{CH}_{\text{ar}}\text{CH}_{\text{ar}}$), 127.4, 127.4, 127.2, 127.1 ($2 \times \text{HNC}_{\text{ar}}\text{CH}_{\text{ar}}$), 126.4, 126.2, 125.2, 123.1, 122.614, 113.9 (CarC=O), 111.1, 110.6, 110.0, 109.7, 105.2, 74.7, 74.6, 74.3, 74.1, 73.7, 69.2, 35.3, 35.2, 35.1, 32.1, 30.5, 29.9, 29.9, 29.8, 29.6, 29.5, 26.6, 26.5, 26.3, 25.0, 22.8, 17.0, 16.9 ($2 \times \text{C=OCH}_3$), 14.3, 14.3, 11.7, 11.6, 11.6; **FT-IR** σ (cm^{-1}) = 3367 (NH), 2958, 2922, 2853, 1701 (C=O), 1494, 1199; **MS** (MALDI-TOF), m/z calculated: 1541.09, found: 1541.02; **Analysis**, $\text{C}_{98}\text{H}_{145}\text{N}_3\text{O}_{11}$, calculated: C, 76.37; H, 9.48; N, 2.73; found: C, 76.52; H, 9.34; N, 2.22. **UV-vis** (THF, 1.38×10^{-5} M): $\lambda_{\text{max}} = 432$ nm ($\epsilon = 80188 \text{ M}^{-1} \text{ cm}^{-1}$) and 337 nm ($\epsilon = 27499 \text{ M}^{-1} \text{ cm}^{-1}$); (heptane, 1.41×10^{-5} M): $\lambda_{\text{max}} = 427$ nm ($\epsilon = 78320 \text{ M}^{-1} \text{ cm}^{-1}$) and 333 nm ($\epsilon = 25735 \text{ M}^{-1} \text{ cm}^{-1}$); (CHCl_3 , 1.47×10^{-5} M): $\lambda_{\text{max}} = 433$ nm ($\epsilon = 76008 \text{ M}^{-1} \text{ cm}^{-1}$) and 337 nm ($\epsilon = 26311 \text{ M}^{-1} \text{ cm}^{-1}$).



3,6-Bis(acetylamino)-N-[3(S),7-dimethyl-octyl]-phthalimide (20g). **19** (60.8

mg, 0.232 mmol) and amine **21g** (36.5 mg, 0.232 mmol) were used. After 17 h of reflux the reaction mixture was concentrated. Subsequent purification by filtration (silica gel, CHCl_3) afforded phthalimide **20g** (77.4 mg, 0.193 mmol, 83%) as a light yellow solid. $^1\text{H-NMR}$ (300 MHz, CDCl_3) δ (ppm) = 9.23 (s, 2H, **a**), 8.66 (s, 2H, **b**), 3.58 (t, 2H, **c**), 1.66-1.08 (m, 10H, **d**), 0.90 (d,

3H, $J = 5.8$ Hz, **e**), 0.79 (d, 6H, $J = 6.6$ Hz, **f**); $^{13}\text{C-NMR}$ (75 MHz, CDCl_3) δ (ppm) = 169.6 and 169.1 (**1**, **2**), 132.9 (**3**), 127.2 (**4**), 114.4 (**5**), 39.3 (**6**), 37.1 and 36.3 and 35.6 (**7**), 30.7 and 28.0 (**8**), 25.0 (**9**), 24.7 (**7**), 22.8 and 22.7 and 19.5 (**10**); **FT-IR** σ (cm^{-1}) = 3356 (NH), 2925, 1756, 1706 and 1700 (C=O), 1496, 1348, 1171, 771, 764; **MS** (MALDI-TOF), calculated: 401.23 found: 401.22 and 402.22 (+ H^+); **Analysis**, $\text{C}_{22}\text{H}_{31}\text{N}_3\text{O}_4$, calculated: C, 65.81; H, 7.78; N, 10.47; found: C, 65.88; H, 7.83; N, 10.26; **UV-vis** (THF, 1.63×10^{-5} M): $\lambda_{\text{max}} = 278$ nm ($\epsilon = 19910 \text{ M}^{-1} \text{ cm}^{-1}$) and 387 nm ($\epsilon = 5738 \text{ M}^{-1} \text{ cm}^{-1}$); (heptane, 1.36×10^{-4} M): $\lambda_{\text{max}} = 276$ nm ($\epsilon = 19796 \text{ M}^{-1} \text{ cm}^{-1}$) and 389 nm ($\epsilon = 6657 \text{ M}^{-1} \text{ cm}^{-1}$).

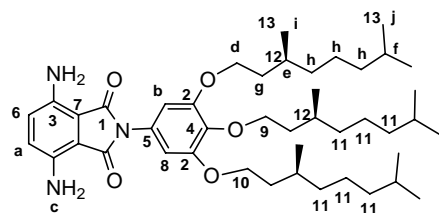


3,6-Bis(acetylamino)-N-(1-methyl-2-hydroxy-ethyl)-phthalimide (20h). **19** (0.054

g, 0.204 mmol) and amine **21h** (0.016 mL, 0.015 g, 0.204 mmol) were used. For solubility reasons a 20 *v*% solution of DMF in dioxane was used as the solvent. After 17 h of reflux the reaction mixture was concentrated *in vacuo*. Filtration over silica gel starting with CHCl_3 ($R_f = 0$) and ending with 50 *v*% EtOAc in CHCl_3 and subsequent drying over MgSO_4 , filtration and concentration of the filtrate gave

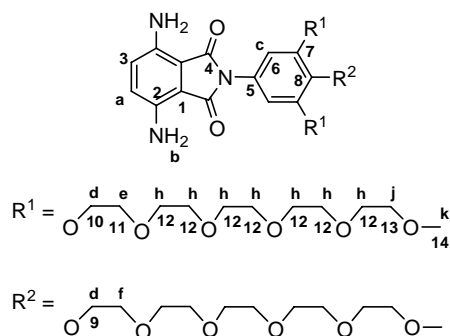
desired **20h** (0.056 g, 0.176 mmol, 86%) as a bright yellow solid. $^1\text{H-NMR}$ (300 MHz, CDCl_3) δ (ppm) = 9.26 (s, 2H, **a**), 8.50 (s, 2H, **b**), 4.56 (m, 1H, **c**), 4.11 (m, 1H, **d**), 3.81 (m, 1H, **d'**), 3.33 (t, 1H, $J = 6.0$ Hz, **e**), 2.23 (s, 6H, **f**), 1.43 (d, 3H, $J = 6.9$, **g**); $^{13}\text{C-NMR}$ (75 MHz, CDCl_3) δ (ppm) = 169.9 and 169.2 (**1**, **2**), 132.8 (**3**), 126.8 (**4**), 114.2 (**5**), 63.6 (**6**), 49.9 (**7**), 24.9 (**8**), 14.7 (**9**); **FT-IR** σ (cm^{-1}) = 3455 (OH), 3345 (NH), 1754, 1683, 1635, 1612, 1488, 1331, 765; **MS** (MALDI-TOF), m/z calculated: 319.11 found: 319.08.

General procedure for the synthesis of 3,6-diaminophthalimides (22a-g). The 3,6-bis(acetylamino)phthalimides (**20a-g**) were dissolved in a solution of 1.6M HCl in dioxane and refluxed. The crude reaction mixture was concentrated and purified by column chromatography over silica gel.

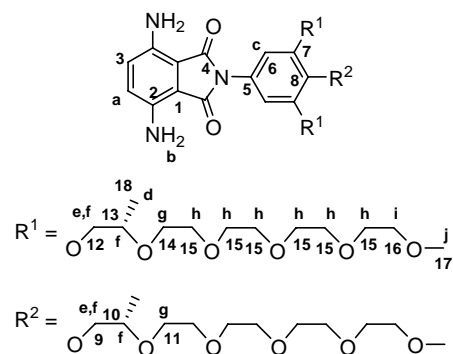


3,6-Diamino-N-(3,4,5-tri-(S)-3,7-dimethyloctyloxyphenyl)-phthalimide (22a).

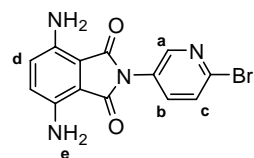
20a (0.095 g, 0.117 mmol) was used. After 2.5 h of reflux the mixture was poured into ice water and the pH was set to ~8 by addition of cold aqueous ammonia. Subsequent to extraction with CH_2Cl_2 (3 \times) the combined organic layers were dried over MgSO_4 . After filtration and concentration the crude mixture was purified by column chromatography (silica gel, 35 *v*% EtOAc in heptane, R_f = 0.3) resulting in **22a** (0.078 g, 0.108 mmol, 91%) as a sticky orange solid. **GPC** (mixed D, CHCl_3 , 254 nm): R_t = 8.91 min. **$^1\text{H-NMR}$** (400 MHz, CDCl_3): δ = 6.78 (s, 2H, **a**), 6.61 (s, 2H, **b**), 4.94 (s, 4H, **c**), 4.03-3.95 (m, 6H, **d**), 1.88-1.82 (m, 3H, **e**), 1.71-1.68 (m, 3H, **f**), 1.67-1.49 (m, 6H, **g**), 1.37-1.12 (m, 18H, **h**), 0.94-0.92 (m, 9H, **i**), 0.88-0.86 (m, 18H, **j**); **$^{13}\text{C-NMR}$** (75 MHz, CDCl_3): δ = 168.9 and 153.5 (**1**, **2**), 138.7 (**3**), 137.9 (**4**), 127.3 (**5**), 125.4 (**6**), 109.7 (**7**), 105.7 (**8**), 72.1 (**9**), 67.7 (**10**), 39.7-36.7 and 25.0 (**11**), 30.2-28.3 (**12**), 23.0-19.9 (**13**); **FT-IR** σ (cm^{-1}) = 3480 and 3361 (NH_2), 2954 and 2924 and 2870 (C-H), 1737 and 1684 (imide, C=O), 1655, 1616, 1591 and 1504 (aromatic C-C), 1489, 1463, 1433, 1381, 1367, 1312, 1293, 1233 (ether, aryl-O-alkyl), 1188, 1114, 1016, 939, 825, 815, 768, 735, 705, 666; **MS** (MALDI-TOF), m/z calculated: 721.54, found: 722.53 (+ H^+); **Analysis**, $\text{C}_{44}\text{H}_{71}\text{N}_3\text{O}_5$, calculated: C, 73.19%; H, 9.91%; N, 5.82%; found: C, 72.75%; H, 10.07%; N, 5.50%. **UV-vis** (CHCl_3 , 4.43×10^{-5} M): λ_{max} = 253 and 445 nm.



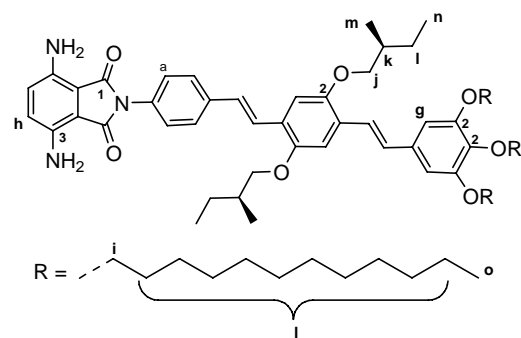
3,6-Diamino-N-(3,4,5-tris(2-(2-(2-(2-methoxyethoxy))-ethoxy)-ethoxy)-phenyl)-phthalimide (22b). **20b** (0.205 g, 0.188 mmol) was used. After 1 h of reflux the reaction mixture was cooled to 0°C and cold aqueous ammonia was added until the pH \approx 8. Water (25 mL) and brine (25 mL) were added. Subsequently, an extraction with CH_2Cl_2 (4 \times 50 mL) was performed. The combined organic layers were dried over MgSO_4 and filtered, followed by concentration *in vacuo*. Purification by column chromatography (silica gel, 5 *v*% heptane in 1,2-dimethoxyethane, R_f = 0.3) gave **22b** (0.158 g, 0.157 mmol, 83%) as a viscous orange oil. **GPC** (mixed D, 254 nm, CHCl_3) R_t = 8.63 min; **$^1\text{H-NMR}$** (400 MHz, CDCl_3): δ (ppm) = 6.81 (s, 2H, **a**), 6.68 (s, 2H, **c**), 4.99 (s, 4H, **b**), 4.18-4.15 (m, 6H, **d**), 3.84 (t, 4H, J = 4.9 Hz, **e**), 3.80 (t, 2H, J = 5.1 Hz, **f**), 3.73-3.68 (m, 6H, **g**), 3.67-3.62 (m, 36H, **h**), 3.56-3.53 (m, 6H, **i**), 3.38-3.37 (ds, 9H, **j**); **$^{13}\text{C-NMR}$** (75 MHz, CDCl_3): δ (ppm) = 168.6 (**4**), 152.9 (**7**), 138.9 (**2**), 138.0 (**8**), 127.7 (**5**), 125.5 (**3**), 109.3 (**1**), 106.9 (**6**), 72.6 (**9**), 72.2 (**13**), 71.1-70.8 (**12**), 69.9 (**11**), 69.2 (**10**), 59.3 (**14**); **FT-IR** σ (cm^{-1}) = 3465 and 3354 (NH_2), 2870 (C-H), 2159, 1732 and 1687 (imide, C=O), 1656, 1619, 1594 and 1494 (aromatic C-C), 1434, 1350, 1292, 1244, 1189, 1093 (ether), 940, 846, 767, 704; **MS** (MALDI-TOF), m/z calculated: 1003.51; found: 1003.28, 1026.28 (+ Na^+), 1043.26 (+ K^+); **Analysis**, $\text{C}_{47}\text{H}_{77}\text{N}_3\text{O}_{20}$, calculated: C, 56.22; H, 7.73; N, 4.18; found: C, 56.12; H, 7.89; N, 4.01; **UV-vis** (water, 3.98×10^{-5} M): λ_{max} = 258 and 447 nm.



3,6-Diamino-N-(3,4,5-tris(2-(2-(2-(2-methoxyethoxy)ethoxy)ethoxy)propoxy)phenyl)phthalimide (22c). **20c** (1.247 g, 1.104 mmol) was used. After 45 min of reflux the reaction mixture was poured into ice water and a satd. aq. NaHCO_3 solution was added until $\text{pH} \approx 8$ was reached. After addition of brine, the aqueous layer was extracted with CH_2Cl_2 (4 \times), the combined organic layers were dried over MgSO_4 . After evaporation of the solvent the residue was purified by column chromatography (silica gel, 10 $v\%$ heptane in 1,2-dimethoxyethane, $R_f = 0.3$) yielding **22c** (1.150 g, 1.099 mmol, 95%) as a thick orange oil. **GPC** (mixed D, 254 nm, CHCl_3): $R_t = 8.58$ min. R_t (HPLC, PDA detector) = 8.93 min., purity $\approx 97\%$. **$^1\text{H-NMR}$** (400 MHz, CDCl_3): $\delta = 6.81$ (s, 2H, **a**), 6.65 (s, 2H, **c**), 5.00 (s, 4H, **b**), 4.08-4.02 (m, 3H, **e**), 3.90-3.78 (m, 6H, **f**), 3.78-3.68 (m, 6H, **g**), 3.68-3.59 (m, 36H, **h**), 3.56-3.53 (m, 6H, **i**), 3.38-3.36 (s, 9H, **j**), 1.31-1.27 (m, 9H, **d**); **$^{13}\text{C-NMR}$** (50 MHz, CDCl_3): $\delta = 168.4$ (**4**), 152.5 (**7**), 138.8 (**2**), 137.1 (**8**), 127.5 (**5**), 125.5 (**3**), 108.3 (**1**), 105.8 (**6**), 76.3 (**9**), 75.0 (**10**), 74.3 (**13**), 72.6 (**12**), 71.9 (**16**), 70.8-70.4 (**15**), 68.8 (**14**), 68.5 (**11**), 59.0 (**17**), 17.7-17.5 (**18**); **FT-IR** σ (cm^{-1}) = 3465 and 3355 (NH_2), 2871 (C-H), 2179, 1732 and 1688 (imide), 1656, 1619, 1595 and 1494 (aromatic C-C), 1434, 1374, 1350, 1292, 1242, 1190, 1094 (ether), 1025, 941, 829, 767, 730, 706; **MS** (MALDI-TOF), m/z calculated: 1045.56, found: 1045.47, 1068.47 (+ Na^+), 1084.45 (+ K^+); **Analysis**, $\text{C}_{50}\text{H}_{83}\text{N}_3\text{O}_{20}$, calculated: C, 57.40; H, 8.00; N, 4.02; O, 30.58; found: C, 57.48; H, 8.14; N, 4.02; **UV-vis** (water, 4.21×10^{-5} M): $\lambda_{\text{max}} = 260$ and 448 nm.

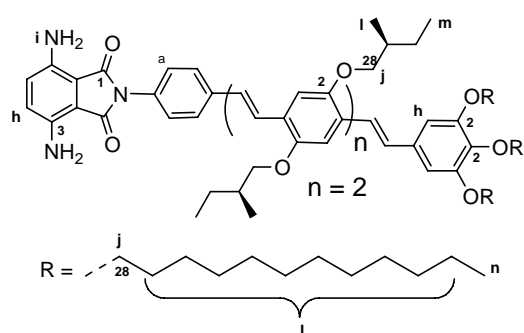


3,6-Diamino-N-(2-bromo-5-pyridyl) phthalimide (22d). **20d** (0.4743 g, 1.134 mmol) was used. After 4 h of reflux the reaction mixture is concentrated *in vacuo* and redissolved in EtOAc and washed with a satd. aq. Na_2CO_3 solution (2 \times). The combined aqueous layers were extracted with CHCl_3 (2 \times). All combined organic layers were dried over MgSO_4 , filtered and concentrated. The remaining orange solid was used as such and contained $\sim 70\%$ of **22d** according to NMR. Purification of **22d** proved to be impossible and was successfully used as such. After derivatization, purification was successful (Chapter 4, compounds **12a,b**). **$^1\text{H-NMR}$** (300 MHz, CDCl_3) δ (ppm) = 8.50 (d, 1H, $J = 2.5$ Hz, **a**), 7.87 (dd, 1H, $J_a = 8.5$ Hz, $J_b = 2.7$, **b**), 7.81 (d, 1H, $J = 8.5$ Hz, **c**), 6.95 (s, 2H, **d**), 6.05 (s, 4H, **e**); **MS** (MALDI-TOF), $\text{C}_{13}\text{H}_9\text{BrN}_4\text{O}_2$, m/z calculated: 331.99, found: 331.92.



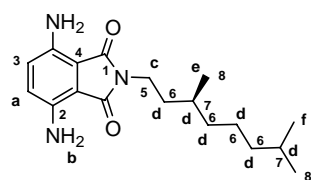
3,6-Diamino-N-OPV3-phthalimide (22e). **20e** (0.146 g, 0.115 mmol) was used. After 5 h of reflux the reaction mixture was concentrated *in vacuo*. The residue was redissolved in CH_2Cl_2 and washed with diluted aq. ammonia (3 \times) maintaining the pH at of the aqueous layer at ~ 8 . Column chromatography (silica gel, 2 $v\%$ EtOAc in CHCl_3 , $R_f = 0.25$) gave desired phthalimide **22e** (0.110 g, 0.093 mmol, 81%) as a yellow solid. **$^1\text{H-NMR}$** (300 MHz, CDCl_3) δ (ppm) = 7.62 (d, 2H, $J = 8.5$ Hz, **a**), 7.51 (d, 1H, $J = 16.2$ Hz, **b** HC=CH), 7.44 (d, 2H, $J = 8.5$ Hz, **c**),

7.39 (d, 1H, $J = 16.5$ Hz, **d** HC=CH), 7.17 (d, 1H, **d** HC=CH), 7.11 (d, 2H, $J = 8.2$ Hz, **e**), 7.03 (d, 1H, $J = 16.5$ Hz, **f** HC=CH), 6.82 (s, 2H, **g**), 6.74 (s, 2H, **h**), 4.05-3.95 (m, 6H, **i**), 3.92-3.83 (m, 4H, **j**), 2.01-1.92 (m, 2H, **k**), 1.87-1.59 (m, 2H, **l**), 1.49-1.42 (m, 6H, **l**), 1.40-1.21 (m, 50H, **l**), 1.12 (d, 6H, $J = 6.6$ Hz, **m**), 1.01 (t, 6H, $J = 7.4$ Hz, **n**), 0.88 (t, 9H, $J = 6.5$ Hz, **o**); $^{13}\text{C-NMR}$ (75 MHz, CDCl_3) δ (ppm) = 168.5 (**1**), 153.4 (**2**), 151.5 (**2**), 151.2 (**2**), 138.6 (**3**), 138.2 (**4**), 137.4 (**5**) ($\text{C}_{\text{ar}}\text{NC}=\text{O}$), 133.3 (**6**), 131.2 (**7**), 128.8 (**8**), 128.0 (**9**), 127.3 (**10**), 127.0 (**11**), 126.6, 126.6, 125.3, 124.3 ($\text{CH}_{\text{ar}}\text{CH}_{\text{ar}}$), 122.6, 110.9, 110.2 ($\text{C}_{\text{ar}}\text{C}=\text{O}$), 109.4, 105.2, 74.5 (OCH_2CH), 74.3 (OCH_2CH), 73.7 (OCH_2 , middle chain), 69.2 (OCH_2 , outer chains), 35.3 (CHCH_3), 35.2 (CHCH_3), 32.0, 30.5, 29.9, 29.8, 29.8, 29.6, 29.5, 29.5, 26.5, 26.5, 26.3, 22.8 ($12 \times \text{CH}_2$), 17.0, 16.9, 14.2, 11.7, 11.6 ($5 \times \text{CH}_3$); **FT-IR** σ (cm^{-1}) = 3470 & 3354 (NH_2), 2956, 2919, 2851, 1736, 1682, 1493, 1377, 1203, 1115, 963; **MS** (MALDI-TOF), m/z calculated: 1181.87; found: 1181.91; **Analysis**, $\text{C}_{76}\text{H}_{115}\text{N}_3\text{O}_7$, calculated: C, 77.18; H, 9.8; N, 3.55; found: C, 77.42; H, 9.90; N, 3.15.



3,6-Diamino-N-OPV4-phthalimide (22f). **20f** (0.154 g, 0.100 mmol) was used. After 3 h of reflux with 0.3 mL instead of 0.2 mL 12 M HCl the reaction was stopped and concentrated *in vacuo*. The residue was dissolved in EtOAc (10 mL) and washed with an aq. satd. solution of NaHCO_3 (3×10 mL), H_2O (10 mL) and brine (10 mL). The organic layer was dried over MgSO_4 followed by filtration and concentration *in vacuo*. Purification by column

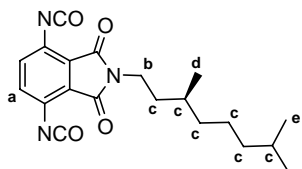
chromatography (silica gel, CHCl_3 to 5 v/v EtOAc/ CHCl_3) furnished **1f** as an orange yellow solid (0.109 g, 0.075 mmol, 75%). $^1\text{H-NMR}$ ¹⁵ (300 MHz, CDCl_3) δ (ppm) = 7.62 (d, 2H, $J = 8.5$ Hz, **a**), 7.54 (s, 2H, **b**), 7.48 (d, 2H, $J = 8.8$ Hz, **c**), 7.40 (d, 2H, $J = 17.3$ Hz, **d**), 7.21 (s, 2H, **e**), 7.13 (d, 2H, $J = 7.7$ Hz, **f**), 7.05 (d, 1H, $J = 16.2$ Hz, **g**), 6.75 (s, 4H, **h**), 4.93 (br s, 4H, **i**), 4.05 - 3.83 (m, 14H, **j**), 1.99 - 1.27 (m, 72H, **k**), 1.13 and 1.11 ($2 \times$ d, 12H, **l**), 1.02 (t, 12H, $J = 7.4$, **m**), 0.89 (t, 9H, $J = 6.5$ Hz, **n**); $^{13}\text{C-NMR}$ (75 MHz, CDCl_3) δ (ppm) = 168.5 (**1**), 153.4, 151.5, 151.3, 151.2 and 151.1 (5×2), 138.6 (**3**), 138.2 (**4**), 137.4 (**5**), 133.4 (**6**), 131.1 (**7**), 128.7 (**8**), 127.95 (**9**), 127.88 (**10**), 127.5 (**11**), 127.0 (**12**), 126.9 (**13**), 126.57 (**14**), 126.55 (**15**), 125.3 (**16**), 124.4 (**17**), 122.8 (**18**), 122.72 (**19**), 122.65 (**20**), 111.0 (**21**), 110.6 (**22**), 110.0 (**23**), 109.7 (**24**), 109.4 (**25**), 105.2 (**27**), 74.59, 74.55, 74.3, 74.2, 73.7, 69.2 (6×28), 35.3, 35.2, 35.1, 32.0, 30.5, 29.9, 29.8, 29.8, 29.6, 29.51, 29.48, 26.52, 26.48, 26.3, 22.8, 17.0, 16.9, 14.2, 11.7, 11.6, 11.5; **FT-IR** σ (cm^{-1}) = 3475 and 3365 (NH_2), 2958, 2921, 2853, 1738, 1687 ($\text{C}=\text{O}$), 1494, 1422, 1202, 1117, 963, 730; **MS** (MALDI-TOF), m/z calculated: 1457.07, found: 1457.09; **Analysis**, $\text{C}_{94}\text{H}_{141}\text{O}_9$, calculated: C, 77.48; H, 9.75; N, 2.88; found: C, 77.35; H, 9.89; N, 2.69.



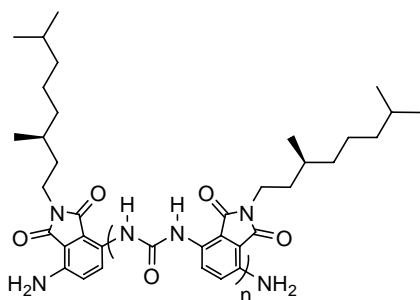
3,6-Diamino-N-[3(S),7-dimethyl-octyl]-phthalimide (22g). **20g** (0.063 g, 0.157 mmol) was used. After 1.5 h reflux EtAOc (20 mL) was added to the reaction mixture and washed with saturated aq. NaHCO_3 (2×20 mL) and water (20 mL). The organic layers were dried over MgSO_4 followed by filtration and concentration of the filtrate *in vacuo*. Purification by column

chromatography (silica gel, CHCl_3 , $R_f = 0.2$) gave **22g** (0.045 g, 0.142 mmol, 90%) as a yellow/orange solid. $^1\text{H-NMR}$ (300 MHz, CDCl_3) δ (ppm) = 6.74 (s, 2H, **a**), 4.80 (br s, 4H, **b**), 3.61 (m, 2H, **c**), 1.69 - 1.09 (m, 10H, **d**), 0.96 (d, 3H, **e**), 0.85 (d, 6H, **f**); $^{13}\text{C-NMR}$ (75 MHz, CDCl_3) δ (ppm) = 169.8 (**1**), 137.9 (**2**), 124.8 (**3**), 110.5

(4), 39.4 (5), 37.2 and 35.9 and 35.7 (6), 30.8 and 28.0 (7), 24.7 (6) 22.8 and 22.7 and 19.5 (8); **FT-IR** σ (cm^{-1}) = 3457 and 3330 and 3198 (NH_2), 2954, 2928, 2859, 1734, 1677 ($\text{C}=\text{O}$), 1630, 1489, 768, 752.; **MS** (MALDI-TOF), $\text{C}_{18}\text{H}_{27}\text{N}_3\text{O}_3$, m/z calculated: 317.21 found: 317.16; **Analysis**, calculated: C, 68.11; H, 8.57; N, 13.24; found: C, 68.05; H, 8.64; N, 12.77; **UV-vis** (CHCl_3): λ_{max} = 262 and 445 nm. UV-vis



3,6-Diisocyanato-N-3(S),7-dimethyl-octyl-phthalimide (23). Diamine **22g** (56.7 mg, 0.187 mmol) in PhCH_3 (1.5 mL) was slowly added to a solution of 20 $w\%$ solution of phosgene in PhCH_3 (2.0 mL, 3.7 mmol). The mixture was stirred for 30 min at rt and subsequently stirred under reflux for 1 h. IR analysis established the conversion from amine to isocyanate. Concentration of the mixture *in vacuo* gave **22g** as an orange solid (63.0 mg, 0.171 mmol, 91%). **$^1\text{H-NMR}$** (300 MHz, CDCl_3) δ (ppm) = 7.13 (s, 2H, **a**), 3.62 (t, 2H, $J = 7.0$ Hz, **b**), 1.66-1.00 (m, 10H, **c**), 0.89 (d, 3H, $J = 6.0$ Hz, **d**), 0.79 (d, 6H, $J = 6.6$ Hz, **e**); **FT-IR** σ (cm^{-1}) = 2955, 2926, 2855, 2266, 2243, 1705, 1539, 1438, 1412, 1378, 1340, 1261, 1217, 1177, 1068, 974, 889, 844, 772, 759.



Amino terminated poly-{3-ureido-N-[(S)-3,7-dimethyloctyl]-phthalimide-N', 6-diyl} (24). Diamine **22g** (51.9 mg, 0.171 mmol), and DMAP (20.09 g, 0.171 mmol) were dissolved in toluene (2.1 mL) and heated to reflux. Diisocyanate **23** (63.0 mg, 0.171 mmol) in PhCH_3 (1.2 mL) was slowly added. The mixture was heated under reflux in an argon atmosphere for 17 h. The reaction mixture was concentrated *in vacuo* and subsequently purified from the remaining DMAP by column chromatography (silica gel, THF). The same chromatography afforded separation between longer oligomers **24a** (35.3 mg) shorter oligomers, **24b** (69.7 mg) and. Both were isolated as light-orange solids. Longer oligomers **24a**. **GPC** (mixed-D, CHCl_3 , 410 nm with polystyrene as the internal standard): 21-4 units. **$^1\text{H-NMR}$** (300 MHz, CDCl_3) δ (ppm) = 25°C and 50°C, broad peaks; (CDCl_3 , 6 drops HFIP): 25°C and 50°C, broad peaks; (THF- d_8): 25°C and 50°C, broad peaks; All spectra did show the presence of characteristic urea protons at ~8.9-8.8 ppm and absorptions that could be attributed to aryl protons in ortho position of the urea functionalities at ~8.6-8.4 ppm. **FT-IR** σ (cm^{-1}) = 3341, 2985, 2926, 2869, 1741, 1672, 1619, 1508, 1480, 1415, 1356, 1277, 1260, 1221, 1094, 1017, 841, 798, 763; Shorter oligomers **24b**. **GPC** (mixed-D, CHCl_3 , 410nm with polystyrene as the internal standard): 13-1 units. **$^1\text{H-NMR}$** (300 MHz, CDCl_3) δ (ppm) = 25°C, 9.3 (s), 8.88-8.83 (br m), 8.56-8.48 (br m), 8.38-8.35 (m), 8.31-7.41 (br m), 7.38-7.35 (br m), 7.22-7.16 (m), 6.98 (s), 6.86 (d), 6.56 (s), 5.58 (s), 5.36-5.34 (m), 5.19-5.01 (br m), 3.89-3.60 (br t), 2.04-0.14 (multiple br m); 50°C, no improvement; **FT-IR** σ (cm^{-1}) = 3344, 2956, 2925, 854, 1740, 1675, 1619, 1509, 1481, 1445, 1358, 1277, 1260, 1222, 1179, 1091, 1017, 841, 798, 764.

2.7 References

- 1) Hill, D. J.; Mio, M. J.; Prince, R. B.; Hughes, T. S.; and Moore, J. S., *Chem. Rev.* **2001**, *101*, 3893-4011.
- 2) van Gorp, J. J.; Vekemans, J. A. J. M.; Meijer, E. W. *Chem. Commun.* **2004**, 60-1.
- 3) van Gorp, J. J. Thesis TU Eindhoven 2004, *Helices by hydrogen bonding*.
- 4) Will, W. *Chem. Ber.* **1895**, *28*, 367.
- 5) Momose, T; Torigoe, M. J. *Pharm. Soc. Jpn.* **1951**, *71*, 977-9.
- 6) Khajavi, M. S.; Nikpour, F.; and Hajihadi, M. J. *Chem. Research* **1996**, 96-7.
- 7) Schmidt, R. R.; Wagner, A. *Synthesis* **1981**, 273-5.
- 8) Schmidt, R. R.; Wagner, A. *Synthesis* **1982**, 958-62.
- 9) Fraile, J. M.; Garcia, J. I.; Gomez, M. A.; Hoz, A. de la; Mayoral, J. A.; Moreno, A.; Prieto, P.; Salvatella, L.; Vazquez, E. *Eur. J. Org. Chem.* **2001**, *66*, 2891-2900.
- 10) Shah, J.; Conner, B. P.; Swartz, G. M. JR.; Hunsucker, K. A.; Rougas, J.; Amato, D. R.; Pribluda, V. and Treston, A. patent WO03014315, 2003.
- 11) Dimroth, O. *Justus Liebigs Ann. Chem.* **1909**, *364*, 183.
- 12) Schwarz, J. S. P. *J. Org. Chem.* **1972**, *37*, 2906-8.
- 13) Verbicky, J. W. Jr., and Williams, L. J. *Org. Chem.* **1981**, *46*, 175-7
- 14) Peeters, E.; van Hal, P. A.; Meskers, S. C. J.; Janssen, R. A. J.; Meijer, E. W. *Chem. Eur. J.* **2002**, *8*, 4470-4.
- 15) All ¹H and ¹³C peaks correspond to previously reported OPV4 species. For a complete assignment of all OPV4 moiety peaks see: Jonkheijm, P.; Hoeben, F. J. M.; Kleppinger, R.; van Herrikhuyzen, J.; Schenning, A. P. H. J.; Meijer, E. W. *J. Am. Chem. Soc.* **2003**, *125*, 15941-9.

Chapter 3

Anthraquinones as a novel backbone

Abstract

Apart from homo-oligomeric foldamers also copolymeric foldamers have been pursued. An attempt has been made to regioselectively incorporate anthraquinone units in the foldameric backbone. However, MALDI-TOF analysis of the polymeric distribution indicated the presence of non-perfectly alternating sequences. A more detailed study established the presence of intermediates that may give rise to urea scrambling. To circumvent these problems the synthesis of a ureidoanthraquinone homopolymer is envisaged. This led to the synthesis of a novel soluble 1,4-diamino-anthraquinone monomer, which in principle could give access to an ureido-anthraquinone homopolymer capable of folding in a helix containing approximately 7 units in one turn. Moreover, lipophilic and hydrophilic 1,8-diaminio-anthraquinones have been developed to generate ureido-anthraquinone based foldamers that would display a helical arrangement, albeit that half the number of units should be accommodated in a helical turn. Polymerization experiments were hampered due to the synthetic inaccessibility of the required corresponding diisocyanates.

3.1 Introduction

The first poly-ureidophthalimide foldamer as was reported by van Gorp (Chapter 1, Figure 1.11) contained all the requirements for folding. The ureidophthalimide core, solubilizing alkyl tails, and chirality to enable CD study. This type of foldamer, arbitrary referred to as type I (Figure 3.1) contained, however, only functionalities that are essential for the folding properties. In chapter 2 a novel synthetic methodology is discussed to arrive at a variety of 3,6-diaminophthalimides (Chapter 2, Table 1). These are the building blocks that give access to a range of new foldamers of the homo-oligomer type which are characterized by peripheral functionalities. This type can be designated as type II, in which the poly-ureidophthalimide backbone forms the scaffold for the organization of the peripheral functionalities.

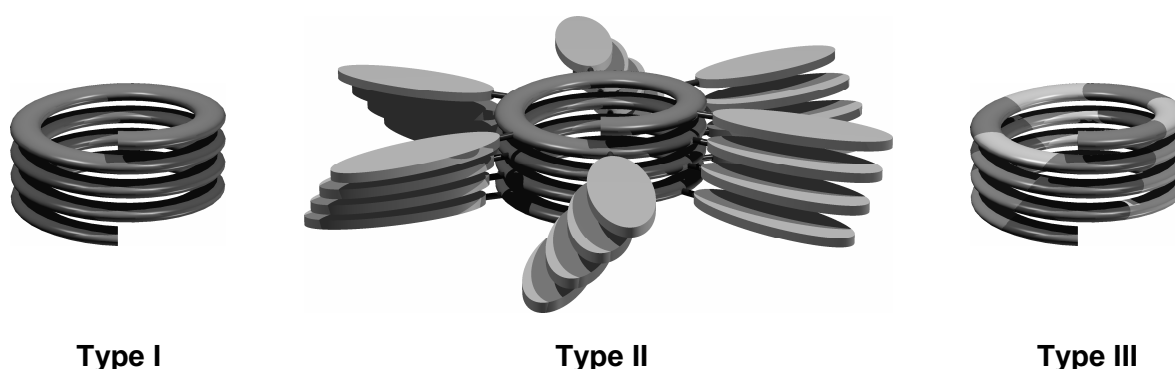


Figure 3.1. Three types of foldamers: single core functionality (type I) and peripheral functionality (type II) and double core functionality (type III).

Although the periphery will influence the properties of the secondary architecture the initial organization is induced by the poly(ureidophthalimide) backbone. Examples of type II will be discussed in chapters 4 and 5.

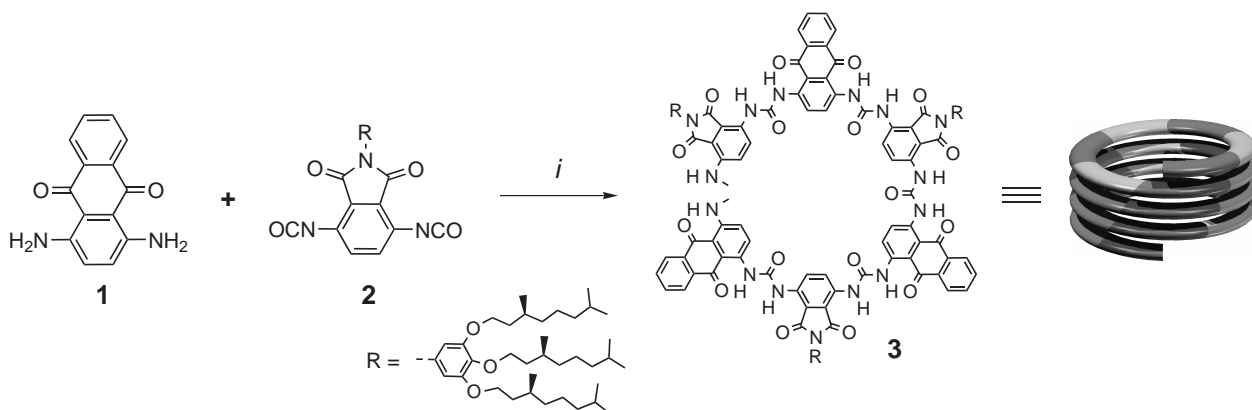
In this chapter the approach towards the introduction of functionality (a chromophore) as a part of the backbone is discussed. We aimed at alternating copolymers consisting of a phthalimide unit as one of the monomeric units. This type of foldamer is represented by type III (Figure 3.1). In contrast to the structural requirements for the introduction of functionality to arrive at type II polymers, synthesis of structures of type III demands the presence of specific structural features in the new polymer building block to maintain the urea as a linker moiety and to fixate its *cisoid* conformation. With such new building blocks combinations of type II and III are feasible in which functionality is introduced in the core as well as in the periphery.

3.2 Alternating anthraquinone-ureidophthalimide co-polymer

To broaden the scope beyond the use of 3,6-diaminophthalimides, and to allow the formation of type III architectures, the use of alternative compounds with similar structural features has been envisaged and provided by van Gorp. Commercial 1,4-diamino-anthraquinone **1** (Scheme 3.1) is

a suitable candidate for use in urea-based foldamers. However, due to the poor solubility of 1,4-diamino-anthraquinone its incorporation in foldamers completely relies on the high solubility of the phthalimide unit (2) in a copolymerization.

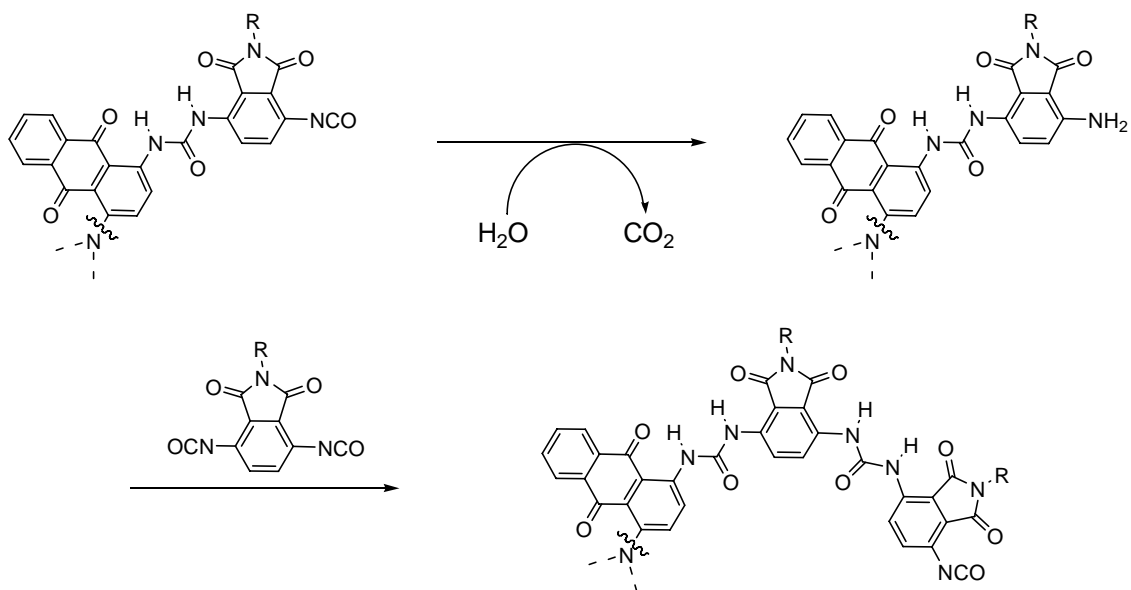
Similar to the employed polymerization conditions for ureidophthalimide polymers, diamino-anthraquinone 1 was copolymerized with diisocyanatophthalimide 2¹ in refluxing toluene in the presence of DMAP, affording copolymer 3.²



Scheme 3.1: Synthetic approach to an alternating ureidophthalimide-anthraquinone co-foldamer 3.² i) DMAP (1.0 equiv.) PhCH₃, reflux 17 h.

Polymer 3 could be fractionated by column chromatography over silica gel with a gradient of 0–3 v% methanol in chloroform as the eluent. Fractions 3a and 3b were analyzed by gel permeation chromatography (GPC) to establish the difference in length and to estimate the poly-dispersity. Besides GPC, ¹H-NMR was used to estimate the average length. Fraction 3a consisted on average of oligomers with sufficient length to make 6 turns. Circular dichroism studies on 3a in dilute solutions showed the presence of ordered structures in heptane although its Cotton effect was much smaller than that of the homopolymer.³ Analysis of the copolymer by MALDI-TOF mass spectrometry indicated the presence of oligomeric species with masses corresponding to non-perfectly alternating sequences. The first source for this unexpected event was thought to be partial hydrolysis of the isocyanate function, especially in view of the expected high electrophilicity in this case. It has been reported that isocyanates are in general already very hygroscopic, and their affinity for water makes handling and storage difficult.⁴ Hydrolysis leads to the formation of an amine, which in turn can attack an isocyanate of the same type of monomer, furnishing a symmetric urea (Scheme 3.2).

Although the polymerization is performed under an argon atmosphere and freshly distilled solvents are used, the presence of traces of water cannot be excluded. Besides hydrolysis another potential cause for non-perfectly alternating sequences in a copolymerization is urea-scrambling. The importance of this possibility and its striking consequences for the copolymerization prompted us to investigate this apparent side reaction in more detail.



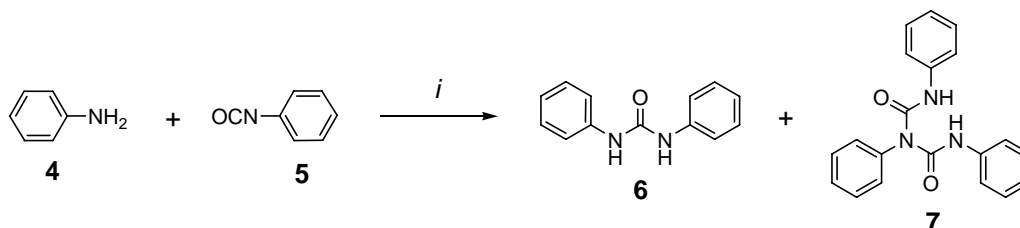
Scheme 3.2: Potential isocyanate hydrolysis resulting in non-perfectly alternating copolymers.

3.3 A brief 'urea-scrambling' investigation

Although it is only noticeable in copolymerization undoubtedly urea-scrambling also takes place during homopolymerization. Attempts to obtain different oligomeric lengths of ureidophthalimides in a semi stepwise^{5,6} approach resulted in the unexpected formation of longer oligomers and even polymeric species.⁷ This may also be attributed to urea scrambling.

To gain more insight into the potential scrambling of urea linkages in the presence of isocyanates at elevated temperatures, several experiments have been designed. Typically, all urea-based foldamers have been synthesized by the polymerization of a diisocyanate with a diamine in refluxing toluene in the presence of DMAP (4-dimethylaminopyridine). The following reactions have all been performed in the absence of DMAP to facilitate analysis. To compensate for the absence of the DMAP, higher temperatures had to be employed. For clarity and to prevent polymerization, only mono-amines and mono-isocyanates have been used.

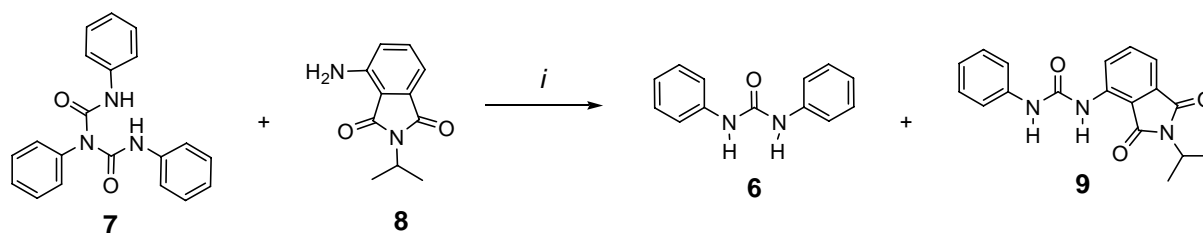
It is thought that the key intermediate in the scrambling process is the biuret species. A biuret is reversibly formed by a reaction of a urea with an isocyanate at elevated temperatures.⁸ Triphenylbiuret (**7**) is obtained by reaction of aniline (**4**) with an excess of the corresponding phenyl isocyanate (**5**) (Scheme 3.3).



Scheme 3.3: Synthesis of diphenylurea **6** and triphenyl biuret **7**. i) **4**, **5** (2.5 equiv.), PhCl, reflux, 59% **6**, 52% **7**.

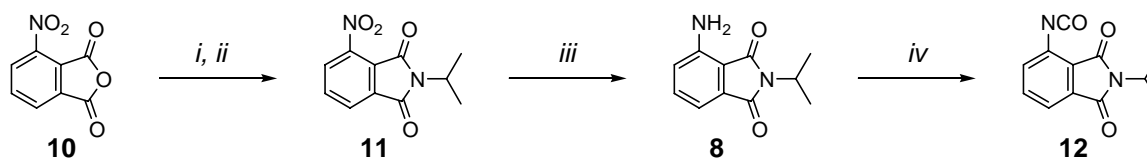
The coupling afforded urea **6** in 59% and biuret **7** in 52% isolated yield based on the amount of aniline. That the sum of the yields exceeds 100% can only be explained by partial hydrolysis of the excess isocyanate.

The reactivity of biuret species **7** is investigated by its exposure to 3-aminophthalimide **8** at elevated temperatures. Analysis of the reaction mixture with electro spray ionization mass spectrometry, a soft ionization technique, established the formation of symmetric urea **6** and asymmetric urea **9** (Scheme 3.4). This provides evidence of the reversibility of the biuret formation, which in this case renders two different urea species.



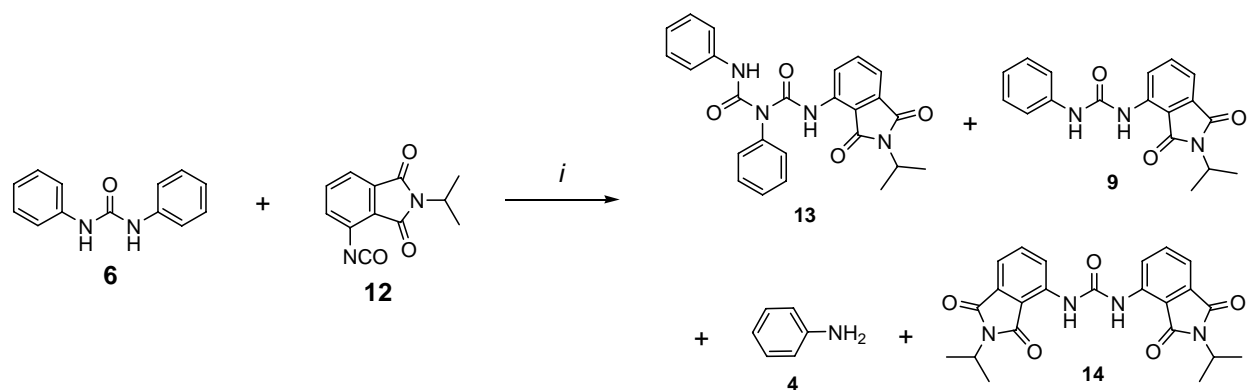
Scheme 3.4: Reaction of biuret **7** with amine **8**. i) PhCl, reflux, 20 h.

3-Aminophthalimide **8** is synthesized starting from 3-nitrophthalic anhydride **10** (Scheme 3.5). Anhydride **10** is converted to 3-nitrophthalimide **11** by reaction with isopropylamine in a two-step procedure. Phthalimide **11** is reduced by palladium-mediated catalytic hydrogenation furnishing 3-aminophthalimide **8**. The amine is converted to the corresponding isocyanate **12**, which is required for the reaction depicted in scheme 3.6, by reaction with phosgene in toluene.



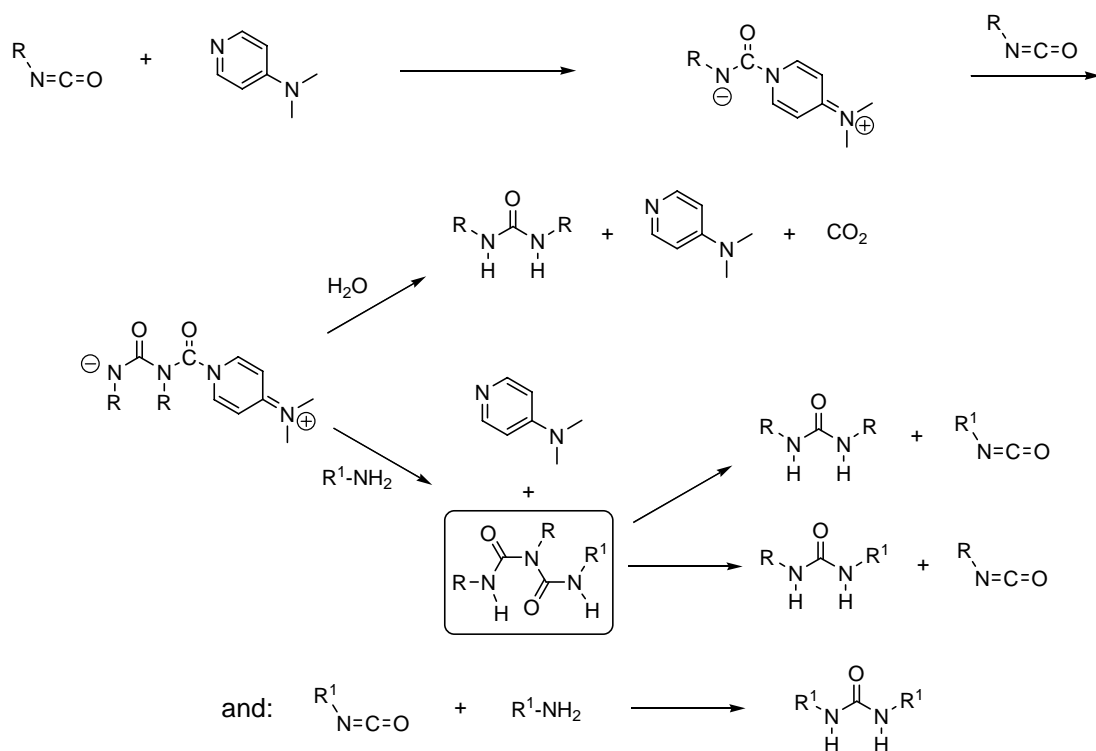
Scheme 3.5: Synthesis of isocyanate **12**. i) H_2N^iPr (2.5 equiv.), CH_3CN , rt, 1 h. ii) Ac_2O , dioxane, $100^\circ C$, 17 h, 60%. iii) H_2 , Pd/C, EtOH/EtOAc, rt, 17 h, 98%. iv) $COCl_2$ (20 equiv.), $PhCH_3$, rt to reflux, 1 h, 100%.

The reactions as described in schemes 3.3 and 3.4 show that biuret species are readily formed and that they are reactive towards primary amines. Interestingly, the reaction of symmetric urea **6** with isocyanate **12** at elevated temperatures (Scheme 3.6) showed the presence of at least four different species according to ESI-MS analysis. The key intermediate necessary for urea scrambling is asymmetric biuret **13**. The reversible nature of biuret formation⁸ gives access to asymmetric urea **9** and symmetric urea **14**.



Scheme 3.6: Formation of biuret **13**, the key intermediate for urea scrambling. i) MIBK, reflux 17 h.

In addition, biuret formation may be enhanced by a Lewis base like DMAP in aromatic solvents.⁹ Isocyanates can react with themselves to urea in the absence of amines by exposure to DMAP at elevated temperatures. In this case the electrophilic isocyanate is converted into the nucleophilic DMAP adduct, which in turn may attack another isocyanate (Scheme 3.7).

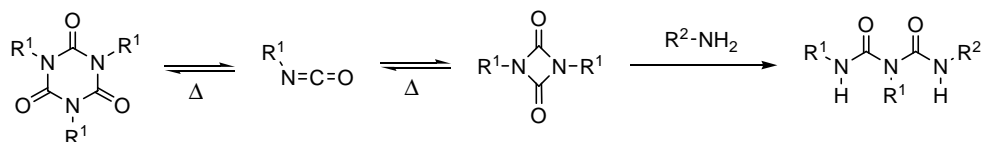


Scheme 3.7: The catalytic influence of DMAP on urea scrambling.

This isocyanate attack on the DMAP adduct yields an unstable species that can be easily attacked by water to give urea, DMAP and CO_2 . However, an asymmetric biuret is formed when the species is attacked by an amine (Scheme 3.7, boxed structure), which in turn will either give a symmetric urea and a new isocyanate or an asymmetric urea and the starting isocyanate. Obviously, the new isocyanate can in turn form a new symmetric urea linkage with

the corresponding amine. In addition, the required DMAP is used in a catalytic fashion. The second cycle is even more complex due to the presence of a new isocyanate species.

Furthermore, it must be noted that isocyanates can also react with themselves in the absence of a catalyst like DMAP. In that case two and three isocyanates may form a dimeric or trimeric species respectively (Scheme 3.8).^{4,10}



Scheme 3.8: Formation of a biuret in the absence of DMAP.

Even the formation of polymers based on this dimerization have been reported.^{4,10} A nucleophilic attack of a primary amine on one of the dimer carbonyls gives an intermediate biuret species, which may lead to products similar to those depicted in scheme 3.6.

Since there is actually no obvious way to circumvent scrambling, functionality is best introduced *via* the phthalimide nitrogen and a homopolymer is aimed at preferentially.

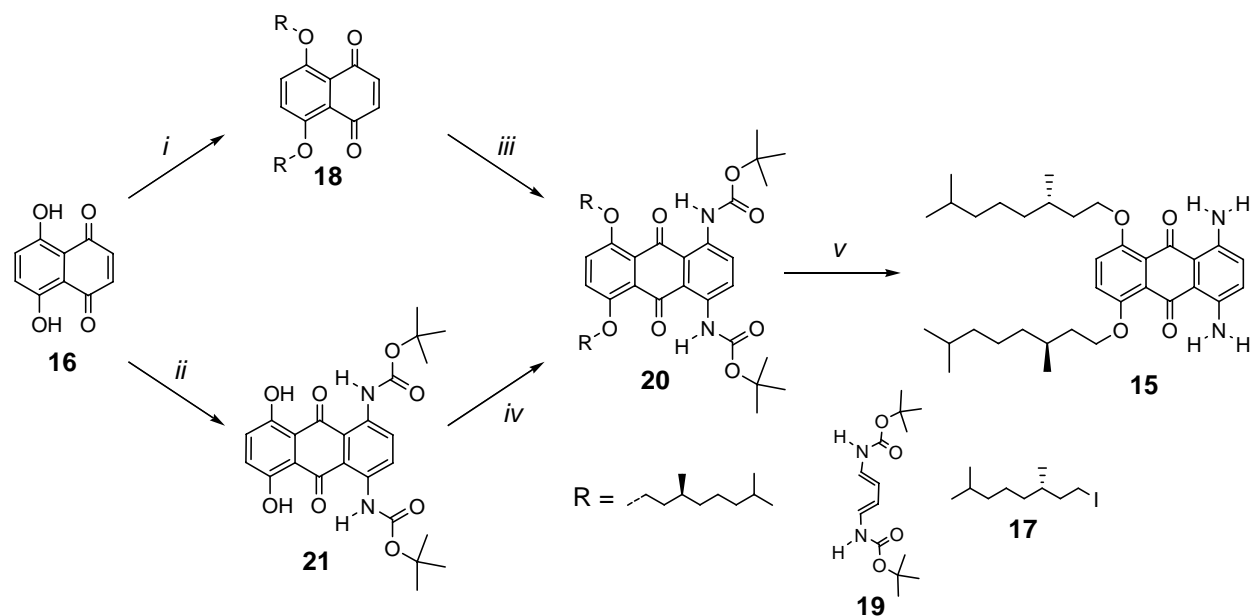
3.4 Towards an anthraquinone homopolymer

Since homopolymerizations do not suffer noticeably from the consequences of the urea scrambling, the synthesis of an anthraquinone homopolymer has been envisaged. However, absence of chirality and low solubility makes commercial diamino-anthraquinone **1** (Scheme 3.1) unsuitable for homo polymerization. This prompted us to investigate synthetic strategies which would give access to novel anthraquinones that contain the required structural features.

The synthesis of anthraquinone was first reported by Laurent¹¹ by oxidation of anthracene with nitric acid and by Fritzsche¹² by oxidation of anthracene with chromic acid. There was little interest in anthraquinone until Graebe and Liebermann reported their findings on the synthesis of alizarin¹³ dye from anthracene, which led to the production of alizarin and marked the start of huge research on anthraquinone and its derivatives. The fundamental scientific basis for the current synthetic process towards anthraquinone was established by Friedel and Crafts by coupling phthaloyl chloride with benzene in the presence of anhydrous AlCl_3 .¹⁴ Preparations of derivatives gave a host of anthraquinone dyes that now constitute the second largest group of commercial colorants. Especially the sulfonated anthraquinones provided a group of bright, fast dyes for wool.¹⁵ For a more detailed history on the synthesis of anthraquinone the reader is referred to a review article.¹⁶

We choose the more recently developed Diels-Alder approach as a key reaction to arrive at the anthraquinone system. The mild conditions for the Diels-Alder methodology are a big

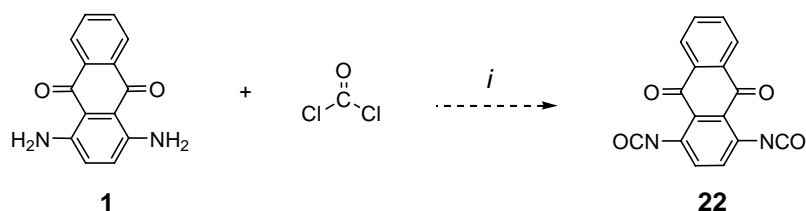
advantage and allow early functionalization of the desired molecules. The synthetic strategy of choice to arrive at suitable anthraquinone building blocks is depicted in scheme 3.9. Two pathways give access to diamino-anthraquinone **15**.



Scheme 3.9: Synthesis of diamino anthraquinone **15**. i) **17** (2.2 equiv.), Ag_2O (2 equiv.), CHCl_3 , reflux, 22 h, 32%. ii) **19** (1.1 equiv.), hydroquinone (1 mol%), DMF, rt, 5 weeks, 35%. iii) **19** (1.2 equiv.), hydroquinone (1 mol%), DMF, 80°C, 32 h, 15%. iv) **17** (2.4 equiv.), Cs_2CO_3 (1.4 equiv.), DMF, 85°C, 1 h, 62%. v) TFA, CH_2Cl_2 , rt, 10 min., 68%.

In the first approach commercial dihydroxynaphthoquinone **16** is alkylated with chiral iodide **17**¹⁷ in the presence of Ag_2O as a base.¹⁸ A subsequent Diels-Alder reaction of alkylated naphthoquinone **18** with diene **19**¹⁹ leads to the Diels-Alder adduct which spontaneously oxidizes (aromatizes) to bis-*N*-Boc protected diamino-anthraquinone **20**.²⁰ The second approach starts with the Diels-Alder reaction of naphthoquinone **16** with diene **19**. Subsequent alkylation of dihydroxy-anthraquinone **21** with chiral iodide **17** in DMF with Cs_2CO_3 as the base furnishes anthraquinone **20**. In spite of the low yielding Diels-Alder step in the second approach, this route is preferred over the first route since the starting compounds are easily accessible. Deprotection of the amino groups of **20** gives the desired 5,8-diamino-anthraquinone **15**.

For the synthesis of an anthraquinone based homopolymer the diamine needs to be converted to the corresponding diisocyanate. Since only a small amount of diamine **15** (Scheme 3.9) is obtained, and the lack of literature precedents, the isocyanate formation has been investigated on commercially available 1,4-diamino anthraquinone **1** (Scheme 3.10).



Scheme 3.10: Anticipated conversion of diamine **1** to diisocyanate **22**. *i*) PhCH_3 , *rt* to reflux.

Unfortunately, instead of the formation of **22**, a totally insoluble compound with a light greenish yellow color was formed. The change of color from dark blue to greenish indicates that a reaction is taking place between 1,4-diamino anthraquinone and phosgene. However, due to its complete insolubility in all common solvents, including DMSO, the formed product could not be analyzed properly. Since the reaction concerns a functional group conversion, infrared (IR) spectroscopy was used to monitor the reaction. The IR spectra (Figure 3.2) show that indeed the amine absorptions at 3390 and 3267 cm^{-1} have disappeared. However, no carbamoyl chloride ($\sim 2150 \text{ cm}^{-1}$) or isocyanate ($\sim 2240 \text{ cm}^{-1}$) peak are observed. The multiple absorptions ranging from 1613-1520 cm^{-1} in the C=O region of the diamino anthraquinone spectrum (Figure 3.2, **a**) have been replaced by what seems to be a single absorption at 1741 cm^{-1} (Figure 3.2, **b**). Furthermore, some absorptions in the fingerprint area are altered.

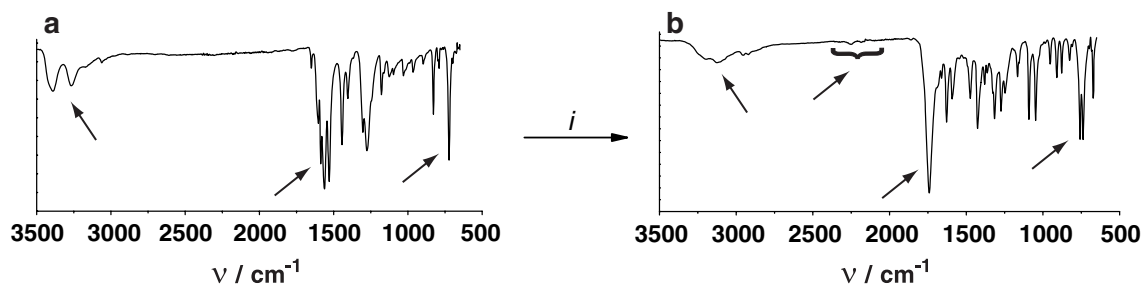
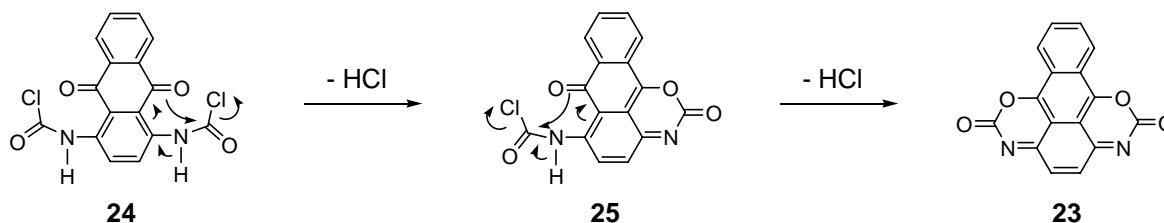


Figure 3.2: IR spectra of a) diamino anthraquinone and the obtained product b) presumably oxazinone **23**. *i*) SOCl_2 (20 equiv.), PhCH_3 , reflux, 4 h.

Conversion of 1,4-diamino-anthraquinone may have led to compound **23** by intramolecular ring closure forming two oxazinones (Scheme 3.11).



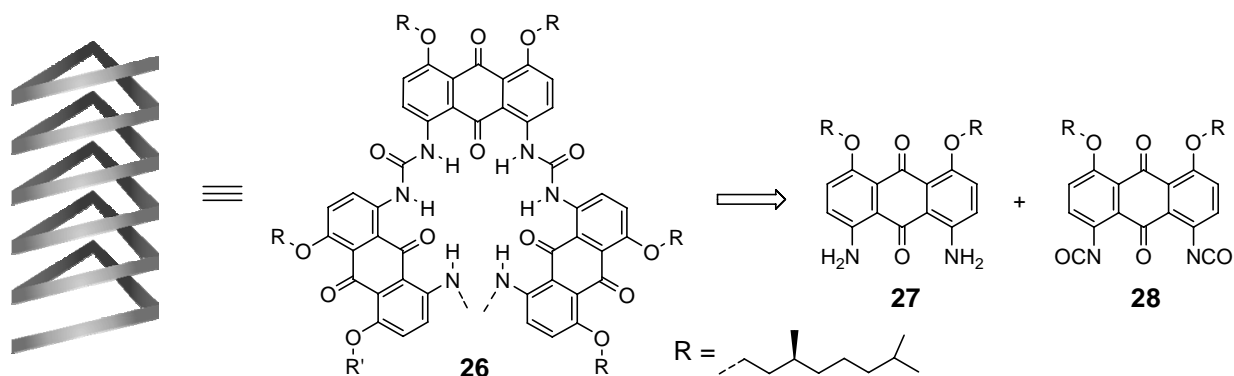
Scheme 3.11: A tentative mechanism for the formation of compound **23**.

A tentative mechanism starts after the formation of the carbamoylchloride intermediate **24**. Intramolecular carbamate formation with concomitant release of HCl could render intermediate **25**, which in turn can expel HCl again furnishing compound **23**. It must be noted that this mechanism can also be applied to the diisocyanate species **22**, via an electrocyclic ring closure.

This conversion is in accordance with the color change. A color change from dark blue (small band gap, high wavelength absorption maximum) to greenish (hypsochromic shift of the absorption maximum) is expected by alteration of the electron releasing NH₂ which is in conjugation with the electron accepting carbonyl. Conversion of either the NH₂ or the carbonyl, resulting in the disruption of the strong donor-acceptor interaction, can only render a compound with a larger band gap. Moreover, the parent anthraquinone system is lost but an aromatic naphthalene system is gained which is in conjugation with the two cyclic carbamate functionalities. Most likely the extended π -system induces a planar conformation. In addition, the construction of a large π -surface is an ideal foundation for π - π stacking interactions, which in turn can account for the insolubility of compound **23**. Although there is no proof yet, the formation of polymeric species by intermolecular reaction is very unlikely in view of the very low concentrations. The formation of a symmetric bis-anthraquinone-urea by reaction of 1-amino-anthraquinone with phosgene has been reported. The poorly characterized urea formed proved to be completely insoluble.²¹

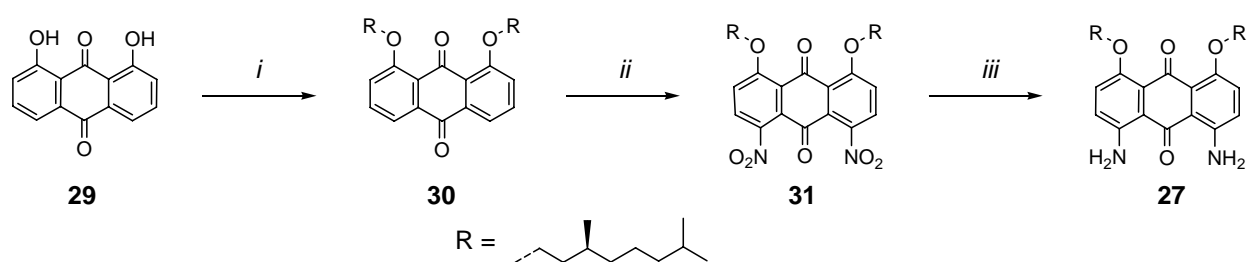
3.5 Towards a triangular helical anthraquinone foldamer

Besides development of novel 1,4-diamino anthraquinones in order to achieve functionalized helices, an attempt was made to synthesize different anthraquinone-based homopolymers. They would show a similar helical arrangement, albeit that they accommodate half the number of units in a helical turn. Scheme 3.12 displays an artist's impression of such a triangular helical architecture **26** and the required building blocks diamino anthraquinone **27** and diisocyanatoanthraquinone **28** in a retrosynthetic approach.



Scheme 3.12: Retrosynthetic approach towards new anthraquinone based helical architectures.

Although anthraquinones are well reported in literature, there is not much known about their synthetic homologues bearing solubility enhancers and different functionalities. The employed synthetic strategy to arrive at diamino-anthraquinone polymer precursor **27** is depicted in Scheme 3.13. Alkylation of commercial dihydroxy-anthraquinone **26**²² with chiral iodide **17**¹⁷ gives dialkoxy anthraquinone **30**. As a base Cs_2CO_3 is used since its solubility in DMF is higher than that of K_2CO_3 . Therefore, the use of a phase-transfer catalyst is not required. After alkylation, nitration was envisaged to obtain dinitro-anthraquinone **31**. Unsubstituted anthraquinone is nitrated in the α position by adding concentrated nitric acid to a solution of anthraquinone in sulfuric acid.²³ However, in this case the rather harsh conditions partly hydrolyze the introduced ether functions. Therefore, milder and more controlled conditions had to be used. Addition of KNO_3 to anthraquinone dissolved in H_2SO_4 at $\sim 0^\circ\text{C}$ does result in the desired dinitro-anthraquinone. The nitration procedure is somewhat laborious due to the high viscosity of the reaction mixture and it requires the use of a mechanical stirrer. It was found that the best results are obtained when the KNO_3 is added portionwise, keeping the overall reaction time as short as possible, e.g. approximately 3 hours. Addition of all KNO_3 at once leads to a high concentration of the reactive nitronium species with concomitant rise in temperature and reduced selectivity for the *para* position. Subsequent reduction of dinitro-anthraquinone **31** by exposure to SnCl_2 ²⁴ in a refluxing solvent mixture of EtOAc/EtOH furnished the desired 4,5-diamino-anthraquinone **27**. Other, reduction attempts with iron dust in H_2SO_4 ²⁵, zinc dust in acetic acid²⁶ and palladium mediated catalytic reduction with H_2 in THF/EtOH/ H_2O or hydrazine²⁷ in $\text{CHCl}_3/\text{MeOH}$ did not afford the desired diamine **27**.



Scheme 3.13: The 3 step synthetic approach to diamino-anthraquinone **27**. i) **17** (2.5 equiv.), Cs_2CO_3 (3.6 equiv), DMF, 80°C , 4 h, 96%, ii) KNO_3 (3 equiv.), H_2SO_4 , 0°C , 3 h, 45%. iii) SnCl_2 (9 equiv.) EtOAc, EtOH, rt, 21 h, 70%.

Dihydroxy-anthraquinone **29** can also be nitrated directly. However, attempts to alkylate after nitration all failed due to the high stability of the phenolate caused by the strong electron withdrawing nitro groups in *para* position. The reactivity is even further lowered due to the ketone functionality in *ortho* position. Both effects are illustrated with the resonance structures depicted in scheme 3.14.

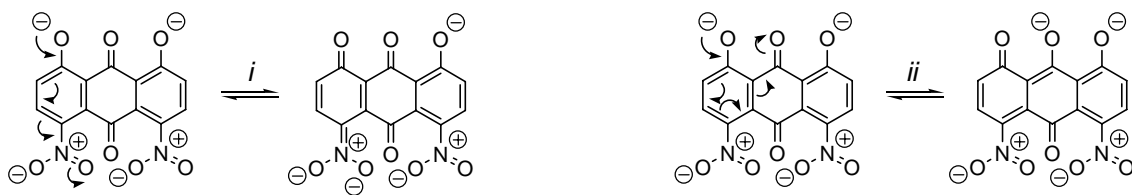
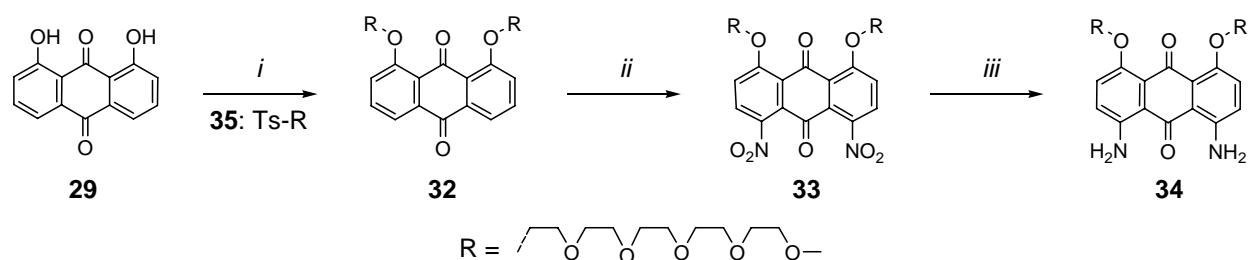


Figure 3.14: Resonance stabilized deprotonated dihydroxy-anthraquinone. i) NO_2 induced resonance. ii) $\text{C}=\text{O}$ induced resonance.

Beside the use of lipophilic tails rendering solubility in most common organic solvents, introduction of hydrophilic tails was also envisaged to ensure solubility in water. This would lead to anthraquinone-based foldamers that allow a study in an aqueous environment. The strategy as employed for the introduction of the lipophilic tails (Scheme 3.13) can be used to decorate anthraquinone with hydrophilic ethyleneoxide tails.

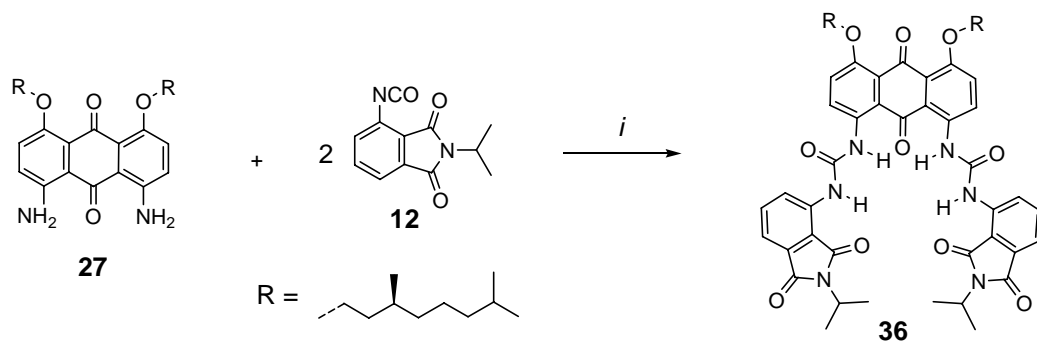
Also in this case the synthetic route starts from dihydroxy-anthraquinone **29**. Alkylation of **29** with tosylated ethylene oxide **35**²⁸ gives anthraquinone **32** (Scheme 3.15). In contrast to the route shown in scheme 3.13 the alkylation is performed in methyl isobutylketone (MIBK) with K_2CO_3 as the base instead of Cs_2CO_3 . However, in this case a phase-transfer catalyst is needed to facilitate deprotonation of the hydroxyl groups. Subsequently, nitration furnishes **33**. It must be noted that nitration proceeds in an easier and more controlled manner than in the case of the anthraquinone decorated with hydrophobic tails, presumably due to the much higher solubility in sulfuric acid thanks to the ethylene oxide tails. In turn, dinitro-anthraquinone **33** is reduced to corresponding hydrophilic diamino-anthraquinone **34**. Purification of **34** by column chromatography proved to be detrimental for the isolated yield. The crude yield was 86% as determined by ^1H NMR, however, after column chromatography only 27% was isolated.



Scheme 3.15: Synthesis of hydrophilic diamino-anthraquinone **34**. i) **35** (2.2 equiv.), K_2CO_3 (4 equiv.), Bu_4Br (5 mol%), MIBK, reflux, 21 h, 33%. ii) KNO_3 (1.2 equiv.), H_2SO_4 , $<4^\circ\text{C}$, 1 h, 90%. iii) SnCl_2 (9 equiv.), EtOAc/EtOH , 30°C , 18 h, (~86%), 27% after column chromatography.

Diamino-anthraquinone **27** was subjected to a reaction with mono-isocyanate **12** furnishing “cotrimer” **35** (Scheme 3.16). Due to its relatively more nucleophilic nature, dialkoxy-diamino-

anthraquinone reacts with an isocyanate even in the absence of the catalyst dimethylamino-pyridine.



Scheme 3.16: Formation of model-compound, "cotrimer" **36**. i) dioxane, reflux, 4 h, 84%.

It would be most interesting to synthesize a foldamer based on alternating anthraquinone **27** and the diisocyanato analogue of phthalimide **12**. Model studies have shown that approximately eleven units would fit in one turn of a helical architecture (Figure 3.3).

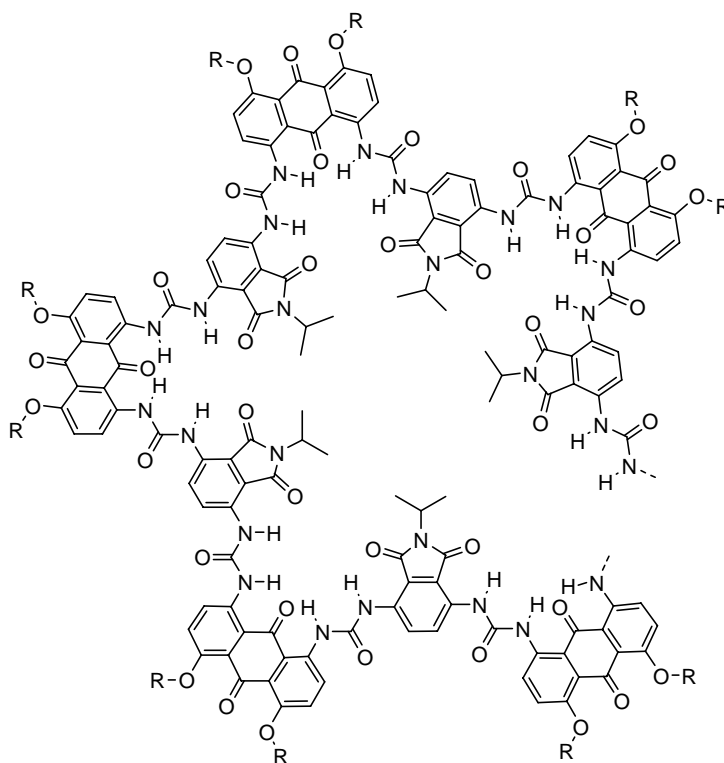
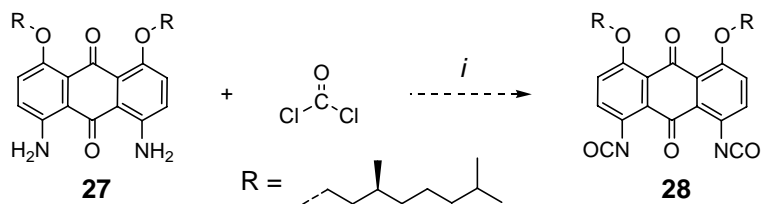


Figure 3.3: Model of an anthraquinone-phthalimide copolymer.

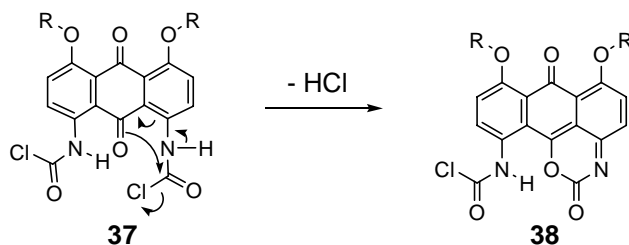
However, at that time the synthesis of diisocyanato phthalimides equipped with an aliphatic unit was still troublesome. In addition, it is best to avoid the 'ureascrambling' problems concerning copolymerization described in section 3.2. Therefore, the envisaged

homopolymerization was investigated. This requires the diisocyanate derivative **28** of diamino-anthraquinone **27** (Scheme 3.17).



Scheme 3.17: Anticipated formation of diisocyanate **28**. *i)* COCl_2 (20 equiv.), PhCH_3 , rt to reflux.

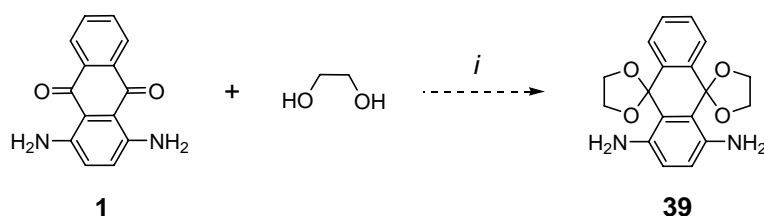
Unfortunately, desired diisocyanate **28** could not be obtained. Also in this case a compound is formed of which the solubility is too low to allow proper characterization. The reaction was followed by infra-red spectroscopy to get more insight on the functional group conversion. The phosgene solution to which diamino-anthraquinone is added at room temperature changes color from red-purple to orange-red. After 30 minutes stirring a sample was examined by IR spectroscopy. The spectrum displays a peak at 1740 cm^{-1} indicative for the formation of the carbamoyl function. However, no clear peak for the accompanying NH absorption was observed. Instead a broad peak around 3000 cm^{-1} and an absorption at 2600 cm^{-1} , which can be attributed to a strongly hydrogen bonded N-H or O-H, are displayed. It seems that all starting compound has reacted. The mixture is heated to reach reflux upon which the color further changes from orange-red to green-black. After almost 2 hours heating IR analysis of a second sample does not show the characteristic NCO absorption. The broad absorption around 3000 cm^{-1} is still present together with a peak that could correspond to a carbonyl absorption. The unknown absorption at 2600 cm^{-1} has disappeared. ^1H NMR analysis reveals the presence of many compounds. A mechanism analogous to that depicted in scheme 3.11 may also apply to this case. However, the intermediate **38**, formed from dicarbamoylchloride **37**, in this case cannot lose a second HCl to form two cyclic carbamates (Scheme 3.18). Formation of the diisocyanate can take place prior to carbamate formation.



Scheme 3.18: A mechanism for the possible formation of **38**.

Assuming the initiating role of the nucleophilic carbonyl oxygen, attempts have been made to prevent the events as depicted in scheme 3.18 by deactivating the carbonyl by a reversible

conversion into a ketal functionality (Scheme 3.19). Commercial diamine **1** is exposed to 1,2-ethanediol in refluxing toluene solution in a flask fitted with a Dean-Stark setup to remove the formed water. Unfortunately, formation of the desired protected anthraquinone **39** was not observed.



Scheme 3.19: Attempt to deactivate the anthraquinone carbonyls by conversion into bis-ketal **39**. i) *p*-TsOH (1 mol%), PhCH₃, reflux.

3.6 Conclusions

In order to extend the scope of the poly(ureidophthalimide), the copolymerization with structurally related diamino-anthraquinone chromophore was envisaged. However, MALDI-TOF analysis indicated the presence of non-perfectly alternating species. It was thought that besides isocyanate hydrolysis, urea scrambling was a potential cause for this unexpected side reaction. A brief investigation on the possible urea scrambling in ureido-based copolymers has indeed led to the establishment of biuret formation, a key intermediate for scrambling. To avoid this difficulty, homopolymerization has to be envisaged.

With a Diels-Alder approach as a key reaction a methodology has been developed for the synthesis of soluble 1,4-diamino-anthraquinones. These may give access to a ureido-anthraquinone based polymer of which the folded architectures is comprised of ~7 units in a turn. The inability to produce the required diisocyanate due to consecutive reaction could not be overcome.

Besides this, another facile synthetic route gave access to novel lipophilic as well as hydrophilic 4,5-diamino-anthraquinones in good yields. These would show a helical arrangement, approximately 3 units in a helical turn. However, at the moment there seems to be no synthetic strategy for the synthesis of the corresponding diisocyanate counterparts. A tentative mechanism is presented explaining the potential formation of cyclic carbamates. Attempts to circumvent this side reaction by protection of the carbonyl functionalities proved to be unsuccessful. Currently a new approach is investigated in our group in which the urea group is introduced *via* a palladium-mediated C-N bond formation under Buchwald conditions.

To conclude, introduction of functionality in the foldamer at this time done best *via* the imide nitrogen of the phthalimide moiety as is described in Chapter 2.

3.7 Experimental

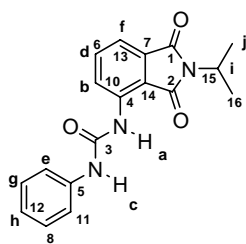
General. See experimental section of chapter 2.

***N,N,N'*-Triphenylbiuret (7) and *N,N'*-diphenylurea (6).** Phenylisocyanate (2.71 mL, 24.91 mmol) was added to a solution of aniline (0.91 mL, 9.97 mmol) in PhCl (20 mL). The mixture was heated to reflux for 6 h. The reaction was monitored by ¹H-NMR (CDCl₃+DMSO). The warm reaction mixture was filtered over a glass filter. The remaining solid was washed with cold PhCl (3 × 10 mL). The filtrate contains mainly triphenylbiuret and was after concentration further purified by column chromatography (silica gel, 2-3 v% EtOAc in CHCl₃ gradient) and gave triphenylbiuret **7** as a white solid (1.73 g, 5.22 mmol, 52%).

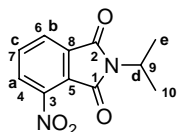
Triphenyl-biuret (7): *R_f* = 0.45 (silica gel, 4 v% EtOAc in CHCl₃); ¹H-NMR (400 MHz, CDCl₃): δ = 8.98 (s, 2H, **a**), 7.61-7.52 (m, 3H, **b/c**), 7.44-7.41 (2x dd, 6H, **d/e**), 7.33 (m, *J* = 8.4 Hz, *J* = 7.3 Hz, *J* = 1.8 Hz, 4H, **f**), 7.13 (m, *J* = 7.7 Hz, *J* = 7.3 Hz, *J* = 1.1 Hz, 2H, **g**); ¹³C-NMR (100 MHz, CDCl₃): δ = 153.5 (**1**), 137.3 (**2**), 136.6 (**3**), 130.6 (**4, 5 or 6**), 129.9 (**4, 5 or 6**), 129.9 (**4, 5 or 6**), 129.0 (**7**), 124.6 (**8**), 120.7 (**9**); **IR:** 3311, 3180, 3144, 3055, 3031, 1705, 1676, 1598/1589, 1527, 1497, 1439, 1318, 1310, 1262, 1241, 1223, 1183, 1110, 1097, 902, 865, 752, 686 cm⁻¹; **MS** (MALDI-TOF): C₂₀H₁₇N₃O₂, *m/z* calculated 331.13 g/mol; found: 331.32 g/mol. **Analysis:** C₂₀H₁₇N₃O₂, calculated: C, 72.49; H, 5.17; N, 12.68; found: C, 71.63; H, 5.06; N, 12.48; The residue on the glass filter was washed with acetone. The precipitate of the filtrate and the remaining solid on the glass filter were combined and dried in vacuo rendering diphenylurea **6** (1.25 g, 5.87 mmol, 59%).

Diphenyl-urea (6): *R_f* ~0.10 (silica, 4 v% EtOAc in CHCl₃); ¹H-NMR (300 MHz, CDCl₃+DMSO): δ = 8.52 (s, 2H, **a**), 7.44 (d, *J* = 8.0 Hz, 4H, **b**), 7.25 (dd, *J* = 7.4 Hz, *J* = 8.2 Hz, 4H, **c**), 6.95 (t, *J* = 7.4 Hz, 2H, **d**); **FT-IR** (NEAT): σ (cm⁻¹) = 3326, 3282, 3194, 3136 tot 3035, 1647, 1593, 1549, 1497, 1448/1440, 1314, 1295, 1231, 894, 752, 696; **Analysis:** C₁₃H₁₂N₂O, calculated: C, 73.56; H, 5.70; N, 13.20; found: C, 73.33; H, 5.59; N, 13.24.

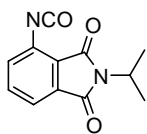
3-Amino-*N*-isopropyl-phthalimide (8). 3-Nitro-*N*-isopropyl-phthalimide **11** (6.62 g, 28.3 mmol) was dissolved in 20 v% EtOH in EtOAc (140 mL) and subsequently purged with argon for 30 min. then 10 w% palladium on carbon (300 mg, 0.28 mmol) was added. The reaction mixture was stirred for 17 h under a hydrogen atmosphere (~1 bar) followed by filtration over hyflo. Concentration of the filtrate gave **8** as a yellow solid (5.68 g, 27.8 mmol, 98%). **M.p.:** 120,4 ± 1,6; ¹H-NMR (300 MHz, CDCl₃): δ = 7.39 (t, 1H, *J* = 7.1 Hz, **a**) 7,06 (d, 1H, *J* = 7.2, **b**) 6,91 (d, 1H, *J* = 8.2 Hz, **c**) 5,21 (s, 2H, **d**) 4.43 (m, 1H, *J* = 6.2 Hz, **e**) 1,47 (d, 6H, *J* = 7.1 Hz, **f**); ¹³C-NMR (75 MHz, CDCl₃): δ = 170.4 (**1, 2**), 145.3 (**3**), 134.9 (**4**), 132.8 (**5**) 120.9 (**6**), 112.3 (**7**), 111.4 (**8**), 42.5 (**9**), 20.2 (**10**); **FT-IR** (NEAT): σ (cm⁻¹) = 3465, 3442, 3359, 2973, 2255, 1751, 1694, 1678, 1595, 1481, 1408, 1355, 1329, 1275, 1191, 1151, 1042, 1026, 993, 906, 871, 817, 727, 681; **MS** (GC-MS): C₁₁H₁₂N₂O₂, *m/z* calculated: 204,09, found: 204.



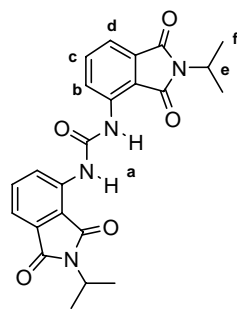
3-Phenylureido-N-isopropylphthalimide (9). Phenylisocyanate (0.37 mL, 3.45 mmol) was added to a solution of 3-amino-N-isopropylphthalimide (0.542 g, 2.65 mmol) in PhCl (5.3 mL). The solution was heated to reflux for 6 h. The reaction was monitored by TLC (silica gel, 80 v% EtOAc in heptane) and $^1\text{H-NMR}$ ($\text{CDCl}_3+\text{dmsO-D}_6$). The presence of isocyanate was checked with IR. The reaction mixture was concentrated *in vacuo* and the remaining solid was purified by column chromatography (silica gel, 15-25 v% EtOAc in heptane gradient). A second purification by column chromatography (silica gel, 2-5 v% MeOH in CHCl_3 gradient, $R_f=0.24$ (silica gel, 5 v% MeOH in CHCl_3)) gave **9** as an off white solid (43%). $^1\text{H-NMR}$ (400 MHz, CDCl_3): $\delta = 9.07$ (s, 1H, **a**), 8.64 (d, $J = 8.4$ Hz, 1H, **b**), 8.18 (s, 1H, **c**), 7.51 (dd, $J = 8.4$ Hz, $J = 7.3$ Hz, 1H, **d**), 7.44 (dd, $J = 8.6$ Hz, $J = 0.9$ Hz, 2H, **e**), 7.34 (d, $J = 7.0$ Hz, 1H, **f**), 7.29 (t, $J = 7.9$ Hz, 2H, **g**), 7.08 (t, $J = 7.3$ Hz, 1H, **h**), 4.40 (m, $J = 7.0$ Hz, 1H, **i**), 1.38 (d, $J = 7.0$ Hz, 6H, **j**); $^{13}\text{C-NMR}$ (100 MHz, CDCl_3): $\delta = 170.5$ and 168.1 (**1**, **2**), 152.7 (**3**), 138.4 (**4**), 137.6 (**5**), 135.5 (**6**), 131.7 (**7**), 129.3 (**8**), 124.7 (**9**), 124.3 (**10**), 121.4 (**11**), 116.7 (**12**), 115.1 (**13**), 43.0 (**14**), 20.2 (**15**); **IR**: 3294, 3143, 3085, 2979, 2971, 1763, 1698, 1669, 1619, 1600, 1549, 1475, 1445, 1349, 1401, 1339, 1292, 1249, 1219, 1150, 1041, 874, 821, 747, 694 cm^{-1} ; **MS** (MALDI-TOF): $\text{C}_{18}\text{H}_{17}\text{N}_3\text{O}_3$, m/z calculated: 323.13, found: 323.31; **Analysis**: calculated: C, 66.86; H, 5.30; N, 13.00; found: C, 66.43; H, 5.24; N, 12.84; **Uv-vis**, CHCl_3 : $\lambda_{\text{max}} = 357$ nm ($\epsilon = 4700 \text{ M}^{-1} \text{ cm}^{-1}$) and $\lambda_{\text{max}} = 266$ nm ($\epsilon = 24 \cdot 10^3 \text{ M}^{-1} \text{ cm}^{-1}$); THF: $\lambda_{\text{max}} = 359$ nm ($\epsilon = 5400 \text{ M}^{-1} \text{ cm}^{-1}$) and $\lambda_{\text{max}} = 270$ nm ($\epsilon = 32 \cdot 10^3 \text{ M}^{-1} \text{ cm}^{-1}$).



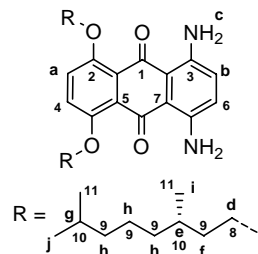
3-Nitro-N-isopropylphthalimide (11). A solution of isopropylamine (10.1 mL, 0.118 mol) in CH_3CN (80 mL) was dropwise added to a solution of 3-nitrophthalic anhydride (**10**) (9.03 g, 49.35 mmol) in CH_3CN (50 mL) at rt. After stirring for 1 h the reaction mixture was concentrated *in vacuo*. The remaining solid was dissolved in hot dioxane (100 mL). Subsequently, Ac_2O (13.4 mL, 0.142 mol) was added. The reaction mixture was heated to 100°C for 17 h under continuous stirring after which it was concentrated. Water (50 mL) was added and extracted with Et_2O (3×50 mL). The combined organic layers were washed with 0.1 M NaOH aq. (50 mL) and subsequently dried over MgSO_4 followed by filtration and concentration of the filtrate. Purification by column chromatography (silica gel, 3 v% EtOAc in CHCl_3 , $R_f = 0.4$) gave **11** as a yellowish solid (6.62 g, 28.3 mmol, 60%). **Melting point**: $106,2 \pm 0,7$; $^1\text{H-NMR}$ (300 MHz, CDCl_3): $\delta = 8,08$ (dd, 2H, $J_{\text{ortho}} = 7.7$ Hz, $J_{\text{meta}} = 2.9$ Hz, **a**, **b**) 7,93 (t, 1H, $J_{\text{ortho}} = 7.8$ Hz, **c**) 4,57 (m, 1H, $J = 6.9$ Hz, **d**) 1,50 (d, 6H, $J = 6.9$ Hz, **e**); $^{13}\text{C-NMR}$ (75 MHz, CDCl_3): $\delta = 166.7$ and 163.0 (**1**, **2**), 145.1 (**3**), 135.3 (**4**), 134.2 (**5**), 128.4 (**6**), 126.8 (**7**), 123.7 (**8**), 44.0 (**9**), 20.0 (**10**); **FT-IR** (NEAT): σ (cm^{-1}) = 3478, 3087, 3043, 2986, 2946, 2881, 2008, 1952, 1777, 1709, 1616, 1538, 1467, 1384, 1352, 1248, 1193, 1156, 1144, 1062, 1048, 1006, 860, 836, 791, 755, 721; **MS** (GC-MS): $\text{C}_{11}\text{H}_{10}\text{N}_2\text{O}_4$, calculated: 234.06, found: 234.



3-Isocyanato-N-isopropylphthalimide (12). A solution of 3-amino-N-isopropylphthalimide (**8**) (0.36 g, 1.76 mmol) was slowly, added dropwise to a 20 w% COCl_2 in PhCH_3 (18.6 mL, 35.16 mmol) at rt. After addition the solution was refluxed for 1 h. Concentration of the reaction mixture *in vacuo* (fumehood!) gave **12** as a yellow solid (0.395 g, 1.72 mmol, 97%) that was used as such. **FT-IR**, $\text{C}_{12}\text{H}_{10}\text{N}_2\text{O}_3$, (NEAT): σ (cm^{-1}) = 3027, 2257, 1777, 1709, 1616, 1522, 1496, 1458, 1387, 1369, 1337, 1197, 1155, 1043, 905, 823, 748, 730, 695.

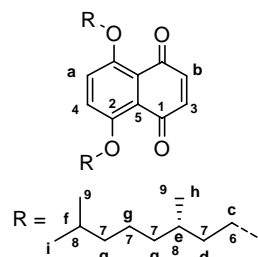


***N,N'*-Bis[3-(*N*-isopropylphthalimidyl)] urea (14).** A solution of 3-amino-*N*-isopropylphthalimide (**8**) (0.162 g, 0.793 mmol) in PhCl (1.6 mL) was heated until completely dissolved. 3-Isocyanato-*N*-isopropylphthalimide **12** (0.219 g, 0.951 mmol) was added and the mixture was heated under reflux for 6 h. The reaction mixture was concentrated *in vacuo*. The remaining solid was triturated with MIBK (3 mL, 2 × 1 mL). The remaining off-white solid was identified as urea **13** (0.344 g, 0.793 mmol, 100%). ¹H-NMR (200 MHz, DMF-d₇): δ = 10.04 (s, 2H, **a**), 8.56 (d, *J* = 8.6 Hz, 2H, **b**), 7.82 (t, *J* = 7.8 Hz, 2H, **c**), 7.52 (d, *J* = 7.0 Hz, 2H, **d**), 4.46 (m, *J* = 7.0 Hz, 2H, **e**), 1.48 (d, *J* = 7.0 Hz, 12H, **f**); FT-IR (NEAT): σ (cm⁻¹) = 3304, 3096, 2981, 2941, 1760, 1732, 1692, 1618, 1544, 1474/1461, 1399, 1334, 1285, 1217, 1190, 1148, 1038, 873, 834/821, 742; **Analysis:** C₂₃H₂₂N₄O₅, calculated: C, 63.59; H, 5.10; N, 12.90; found: C, 63.60; H, 5.02; N, 12.97.



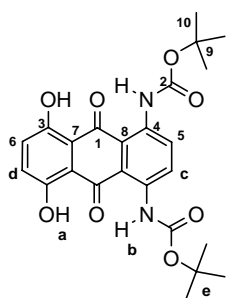
5,8-Diamino-1,4-bis([*S*]-3,7-dimethyloctyloxy)anthraquinone (15). TFA (2 mL) was slowly added to a solution of anthraquinone **20** (0.160 g, 0.213 mmol) in CH₂Cl₂ (2 mL) at rt. Upon addition of TFA the reaction mixture turns from dark orange to dark blue in seconds. After 10 min stirring at rt. The reaction mixture was concentrated *in vacuo* and co-evaporated with toluene (2 × 3 mL). Purification by column chromatography (silica gel, 25 v% EtOAc in heptane + 1 v% Et₃N, R_f = 0.3) gave **15** as a dark purple blue solid (80.1 mg, 0.145 mmol, 68%).

¹H-NMR (300 MHz, CDCl₃): δ = 7.22 (s, 2H, **a**), 6.80 (s, 2H, **b**), 6.60 (br s, 4H, **c**), 4.18-4.06 (m, 4H, **d**), 2.00-1.92 (m, 2H, **e**), 1.73-1.64 (m, 4H, **f**), 1.59-1.43 (m, 2H, **g**), 1.37-1.06 (m, 12H, **h**), 0.96 (d, 6H, *J* = 6.0 Hz, **i**), 0.86 (d, 12H, *J* = 6.6 Hz, **j**); ¹³C-NMR (75 MHz, CDCl₃): δ = 184.9 (**1**), 153.6 (**2**), 143.3 (**3**), 126.4 (**4**), 125.2 (**5**), 121.3 (**6**), 112.7 (**7**), 69.5 (**8**), 39.3, 37.4 and 36.4 (3 × CH₂, **9**), 29.9 and 28.0 (2 × CH, **10**), 24.7 (CH₂, **9**), 22.8, 22.7 and 19.8 (3 × CH₃, **11**); FT-IR (NEAT): σ (cm⁻¹) = 3418 and 3302 (2 × NH₂), 2952, 2925, 2868, 1601 and 1563 and 1542 (C=O), 1460, 1416, 1383, 1299, 1261, 1215 (C_{ar}OCH₂), 1045, 1002, 812, 735; **MS** (MALDI-TOF), C₃₄H₅₀N₂O₄, *m/z* calculated: 550.38, found: 552.09 (+ 2H⁺).

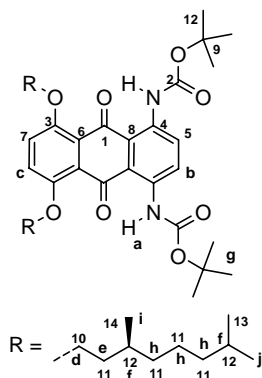


5,8-Bis([*S*]-3,7-dimethyloctyloxy)naphthoquinone (18). A suspension of dihydroxynaphthoquinone **16** (0.244 g, 1.281 mmol) and Ag₂O (0.594 g, 2.562 mmol) in CH₂Cl₂ (2 mL) is sonicated for 5 min. A solution of alkyl iodide **17** (0.756 g, 2.818 mmol) in CH₂Cl₂ was added and the reaction mixture was stirred at reflux for 18 h. TLC shows the presence of **16**, monoalkylated and some dialkylated product. The CH₂Cl₂ was substituted for CHCl₃ (2 mL) and extra Ag₂O (25 mg) was added. The mixture was refluxed for another 22 hours. TLC showed the presence of desired **18** and monoalkylated product. The solvent was then substituted for DMF (2 mL) and the mixture was heated to 85°C for 15 h. TLC showed formation of side products. The reaction was stopped and the crude product was purified by column chromatography (silica gel, 10 v% EtOAc in heptane, R_f = 0.3). ¹H-NMR analysis showed the presence of monoalkylated starting material. The mixture was redissolved in Cl₂C=CCl₂ (1.5 mL) and Ag₂O (0.08 g, 0.35 mmol) and alkyl iodide (0.107 g, 0.400 mmol) were added. After 6 h reflux the mixture was concentrated. Purification by column chromatography (silica gel, 10 v% EtOAc in heptane) gave **18** as a dark orange oil (0.193 g, 0.411 mmol,

32%). $^1\text{H-NMR}$ (300 MHz, CDCl_3): δ = 7.26 (d, 2H, J = 19.5 Hz, **a**), 6.71 (d, 2H, J = 19.5 Hz, **b**), 4.15-4.04 (m, 4H, **c**), 2.00-1.88 (m, 2H, **d**), 1.79-1.73 (m, 2H, **e**), 1.71-1.62 (m, 2H, **d**), 1.60-1.47 (m, 2H, **f**), 137-1.15 (m, 12H, **g**), 0.96 (d, 6H, J = 6.3 Hz, **h**), 0.87 (d, 12H, J = 6.6 Hz, **i**); $^{13}\text{C-NMR}$ (75 MHz, CDCl_3): δ = 184.6 (**1**), 153.3 (**2**), 138.2 (**3**), 121.9 (**4**), 121.3 (**5**), 68.7 (**6**), 39.2, 37.3 and 36.2 ($3 \times \text{CH}_2$, **7**), 29.7 and 27.9 ($2 \times \text{CH}$, **8**), 24.6 (**7**), 22.7, 22.6 and 19.7 ($3 \times \text{CH}_3$, **9**); **FT-IR** (NEAT): σ (cm^{-1}) = 2953, 2935, 2869, 1658, 1622, 1582, 1457, 1284, 1239, 1097, 1047, 1023, 850, 742; **MS** (MALDI-TOF), $\text{C}_{30}\text{H}_{46}\text{O}_4$, m/z calculated: 470.34, found: 472.30 ($\text{M} + 2\text{H}^+$).

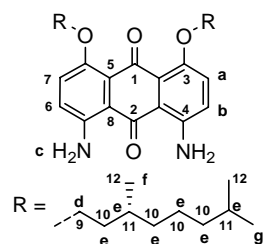


5,8-Bis(*t*-butoxycarbonylamino)-1,4-dihydroxy-anthraquinone (21). A solution of dihydroxynaphthoquinone **16** (0.233 g, 1.227 mmol), diene **19** (0.388 g, 1.364 mmol) and hydroquinone (1.5 mg, 13.6 μmol) in DMF (10 mL) was stirred for 5 weeks at rt in air (the flask was capped with a septum, air was let in *via* a needle). The reaction mixture was concentrated *in vacuo*. Purification by column chromatography (silica gel, 20 v% EtOAc in heptane, R_f = 0.3) provided **21** as an intense purple solid (0.202 g, 0.430 mmol, 35%). $^1\text{H-NMR}$, $\text{C}_{24}\text{H}_{26}\text{N}_2\text{O}_8$, (300 MHz, CDCl_3): δ = 12.88 (s, 2H, **a**), 11.68 (s, 2H, **b**), 8.92 (s, 2H, **c**), 7.28 (s, 2H, **d**), 1.60 (s, 18H, **e**); $^{13}\text{C-NMR}$ (75 MHz, CDCl_3): δ = 157.9 (**2**), 153.1 (**3**), 139.8 (**4**), 129.5 (**5**), 128.2 (**6**), 115.8 (**7**), 113.3 (**8**), 81.7 (**9**), 28.7 (**10**); **FT-IR** (NEAT): σ (cm^{-1}) = 3243, 2925, 2855, 1732, 1603, 1585, 1505, 1452, 1411, 1393, 1350, 1284, 1261, 1217, 1200, 1138, 1074, 1033, 974, 960, 890, 834, 788, 768, 757, 729; **MS** (MALDI-TOF), $\text{C}_{24}\text{H}_{26}\text{N}_2\text{O}_8$, m/z calculated: 470.17, found: 470.04.

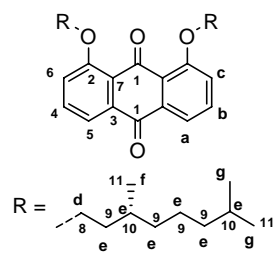


5,8-Bis(*t*-butoxycarbonylamino)-1,4-bis([S]-3,7-dimethyloctyloxy)-anthraquinone (20). *Diels-Alder reaction of 18 with 19.* A solution of naphthoquinone **18** (97.7 mg, 0.208 mmol), diene **19** (49.2 mg, 0.173 mmol) and hydroquinone (0.23 mg, 2.1 μmol) in DMF (0.5 mL) was stirred for 32 h at 80°C. TLC showed several dots and still starting material. The reaction was stopped and the reaction mixture concentrated *in vacuo*. Purification of the residue by column chromatography (silica gel, 10 v% EtOAc in heptane, R_f = 0.3) gave **20** as an orange solid (19.8 mg, 26.3 μmol , 15%). *Alkylation of 21.* A solution of dihydroxy anthraquinone **21** (0.162 g, 0.345 mmol), alkyl iodide **17** (0.241 g, 0.810 mmol) and Cs_2CO_3 (0.427 g, 1.131 mmol) in DMF (1.2 mL) was stirred at 85°C for 1 h. The reaction mixture was concentrated *in vacuo* and redissolved in EtOAc (20 mL). Subsequently, the organic layer was extracted with water (2×20 mL) and a satd. aq. KCl solution (2×20 mL). The organic layer was dried over MgSO_4 and filtered over a glass filter. The concentrated filtrate was purified by column chromatography (silica gel, 10 v% EtOAc in heptane, R_f = 0.25) and furnished **20** as a bright orange solid (0.160 g, 0.213 mmol, 62%). TLC still shows the presence of a small inseparable impurity. $^1\text{H-NMR}$, $\text{C}_{44}\text{H}_{66}\text{N}_2\text{O}_8$, (300 MHz, acetone- d_6): δ = 11.05 (s, 2H, **a**), 8.68 (s, 2H, **b**), 7.46 (s, 2H, **c**), 4.17 (t, 4H, J = 6.0 Hz, **d**), 1.97-1.77 (m, 4H, **e**), 1.69-1.45 (m, 22H, **f**+**g**), 1.43-1.28 (m, 6H, **h**), 1.26-1.16 (m, 6H, **h**), 1.01 (d, 6H, J = 6.3 Hz, **i**), 0.85 (d, 12H, J = 6.6 Hz, **j**); $^{13}\text{C-NMR}$ (75 MHz, CDCl_3): δ = 187.1 (**1**), 153.5 (**2**), 153.3 (**3**), 135.9 (**4**), 126.5 (**5**), 124.2 (**6**), 122.2 (**7**), 119.2 (**8**), 81.0 (**9**), 69.5 (**10**), 39.6, 37.7, and 36.5 (**11**), 30.3, 28.7 and 28.3 (**12**), 25.0 (**11**), 23.0 (**13**) and 20.1 (**14**); **FT-IR** (NEAT): σ (cm^{-1}) = 3279, 2954, 2928, 2870, 1732, 1645, 1598, 1567, 1506, 1458, 1416, 1393, 1367, 1304, 1222, 1205, 1151, 1070, 893, 830, 770, 733; **MS** (MALDI-TOF), m/z

calculated: 750.48, found: 750.61; **Analysis:** C₄₄H₆₆N₂O₈, calculated: C, 70.73; H, 8.86; N, 3.73; found: C, 70.03; H, 9.05; N, 2.96.

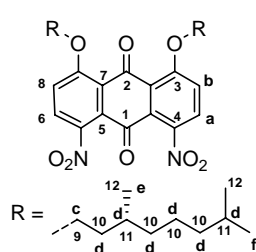


1,8-Di([S]-3,7-dimethyloctyloxy)-4,5-diaminoanthraquinone (27). To a stirring solution of 1,8-di([S]-3,7-dimethyloctyloxy)-4,5-dinitroanthraquinone (**31**) (1.026 g, 1.680 mmol) in 50 v% EtOAc in ethanol (1 mL) at rt. SnCl₂ (2.867 g, 15.12 mmol) was added. The reaction was monitored by TLC (silica gel, 30 v% EtOAc in heptane) and ¹H-NMR. Therefore, a small sample workup was done by extraction with EtOAc/1M aq. NaOH. After 21 h the reaction was concentrated *in vacuo* and the residue redissolved in EtOAc (50 mL) and washed with 1 M NaOH aq. (2 × 50 mL). The combined aqueous layers were extracted with EtOAc (3 × 50 mL). The combined organic layers were washed with brine (50 mL) and subsequently dried over MgSO₄ and filtered over a glass filter. The filtrate was concentrated *in vacuo*. Purification by column chromatography (silica gel, 30 v% EtOAc in heptane, R_f = 0,23) gave **27** as a red-purple solid (0.644 g, 1.169 mmol, 70%). **¹H-NMR** (300 MHz, CDCl₃): δ = 7.14 (d, J = 9.1 Hz, 2H, **a**), 6.85 (d, J = 9.1 Hz, 2H, **b**), 6.47 (s, 4H, **c**), 4.08 (m, J = 3.0 Hz, 4H, **d**), 1.96-1.14 (m, 20H, **e**), 0.99 (d, J = 6.3 Hz, 6H, **f**), 0.90 (d, J = 6.6 Hz, 12H, **g**); **¹³C-NMR** (75 MHz, CDCl₃): δ = 188.6 and 184.8 (**1**, **2**), 150.0 (**3**), 145.2 (**4**), 125.6 (**5**), 125.4 (**6**), 123.0 (**7**), 115.3 (**8**), 70.5 (**9**), 39.6, 37.7 and 36.8 (**10**), 30.0 and 28.2 (**11**), 24.9 (**10**), 22.9, 22.8 and 19.9 (**12**); **FT-IR**, C₃₄H₅₀N₂O₄, (NEAT): σ (cm⁻¹) = 3442, 3328, 2953, 2925, 2868, 1661, 1626, 1531, 1262, 1205; **MS** (MALDI-TOF) m/z, calculated: 550.38, found: 550.32, 551.33 (M+H), 552.34 (M+2H); **Analysis:** C₃₄H₅₀N₂O₄, calculated: C, 74.14; H, 9.15 ; N, 5.09; found: C, 74.05; H, 9.18; N, 5.02; **Uv-vis**, CHCl₃: λ_{max} = 511 nm (ε = 11700 M⁻¹ cm⁻¹) and λ_{max} < 240 nm; Heptane: λ_{max} = 496 nm (ε = 12*10³ M⁻¹ cm⁻¹) and λ_{max} = 232 nm; THF: λ_{max} = 514 nm (ε = 13100 M⁻¹ cm⁻¹) and λ_{max} < 240 nm; ⁱPrOH: λ_{max} = 524 nm, (ε = 12600 M⁻¹ cm⁻¹) and λ_{max} = 234 nm.

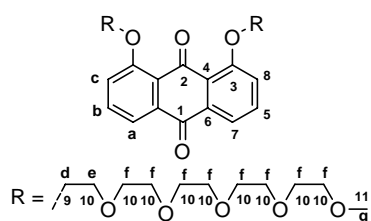


1,8-Di([S]-3,7-dimethyloctyloxy)anthraquinone (30). To a stirring solution of 1,8-dihydroxyanthraquinone (**29**) (5.00 g, 20.80 mmol) in DMF (100 mL) Cs₂CO₃ (25.27 g, 77.60 mmol) was added. The purple solution was brought to 80°C and (S)-3,7-dimethyloctyljodide (**17**) (12.27 g, 45,8 mmol) is added. The temperature was maintained at 80°C for 4 hours. TLC (25 v% EtOAc in heptane) and ¹H-NMR were used to monitor the reaction. The reaction mixture was acidified to pH~4 by adding 1M aq. HCl and subsequently extracted with EtOAc (50 mL). The organic layer was washed with satd. aq. KCl solution (3 × 30 mL). The organic layer was dried over MgSO₄ and filtered over a glass filter. After concentration of the filtrate *in vacuo* purification of the remaining solid by column chromatography (silica gel, 20 v% EtOAc in heptane, R_f=0,36) gave **30** as a yellow solid (10.35 g, 19.87 mmol, 96%). **¹H-NMR** (300 MHz, CDCl₃): δ = 7.81 (dd, J_{ortho} = 7.7 Hz, J_{meta} = 1.0 Hz, 2H, **a**), 7.59 (t, J = 8.1 Hz, 2H, **b**), 7.28 (dd, J_{ortho} = 8.4 Hz, J_{meta} = 1.1 Hz, 2H, **c**), 4.16 (m, J = 3.5 Hz, 4H, **d**), 2.00-1.12 (m, 20H, **e**), 0.98 (d, J = 6.6 Hz, 6H, **f**), 0.86 (d, J = 6.6 Hz, 12H, **g**); **¹³C NMR** (75 MHz, CDCl₃): δ = 184.3 (**1**), 158.9 (**2**), 134.9 (**3**), 133.5 (**4**), 124.8 (**5**), 119.6 (**6**), 118.9 (**7**), 68.4 (**8**), 39.4, 37.5 and 36.0 (**9**), 30.0 and 28.1 (**10**), 24.8 (**9**), 22.8, 22.7 and 19.8 (**11**); **FT-IR**, C₃₄H₄₈O₄, (NEAT): σ (cm⁻¹) = 2953, 2926, 2869, 1671, 1586, 1458, 1440, 1384, 1309, 282, 1233, 1170, 1066, 1030, 967, 903, 868, 840, 789, 744, 733, 677, 662; **MS** (MALDI-TOF) m/z calculated: 520.36, found: 520.13, 521.13 (M+H), 522.15 (M+2H), 543.12 (M+Na); **Analysis:** C₃₄H₄₈O₄,

calculated: C, 78.42; H, 9.29; found: C, 78.42, H, 9.42; **Uv-vis**, CHCl₃: λ_{\max} = 387 nm (ϵ = 7200 M⁻¹ cm⁻¹) and λ_{\max} = 256 nm (ϵ = 26*10³ M⁻¹ cm⁻¹); Heptane: λ_{\max} = 373 nm (ϵ = 7200 M⁻¹ cm⁻¹) and λ_{\max} = 255 nm (ϵ = 26*10³ M⁻¹ cm⁻¹); THF: λ_{\max} = 379 nm (ϵ = 7200 M⁻¹ cm⁻¹) and λ_{\max} = 255 nm (ϵ = 25*10³ M⁻¹ cm⁻¹) ⁱPrOH: λ_{\max} = 385 nm (ϵ = 7300 M⁻¹ cm⁻¹) and λ_{\max} = 255 nm (ϵ = 25*10³ M⁻¹ cm⁻¹).

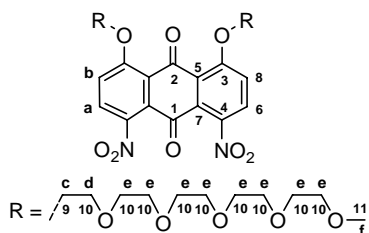


1,8-Di([S]-3,7-dimethyloctyloxy)-4,5-dinitro-anthraquinone (31). A slurry of 1,8-di([S]-3,7-dimethyloctyloxy)anthraquinone **30** (0.522 g, 1.002 mmol) in 95% H₂SO₄ (2 mL) was cooled to 0°C. Potassium nitrate (0.304 g, 3.005 mmol) was added in small portions keeping the temperature at 0°C. The reaction was monitored with TLC (30 v% EtOAc in heptane) and ¹H-NMR, after a sample preparation by EtOAc/water extraction. After 3 hours stirring at 0°C, the mixture was poured into ice water (200 mL) and the aqueous layer was extracted with CH₂Cl₂ (100 mL, and 2 × 50 mL). The combined organic layers were washed with satd. aq. KCl solution (100 mL), dried over MgSO₄ and filtered over a glass filter. After concentration of the filtrate *in vacuo* of the filtrate a yellow-orange solid was obtained. Purification by column chromatography (silica gel, EtOAc/heptane, 1:3, R_f = 0,28) gave **31** as a yellow slightly orange solid (0.281 g, 0.457 mmol, 45%). **¹H-NMR** (400 MHz, CDCl₃): δ = 7.94 (d, J = 9.2 Hz, 2H, **a**), 7.25 (d, J = 9.2 Hz, 2H, **b**), 4.23 (m, J = 6.0 Hz, 4H, **c**), 1.97-1.14 (m, 20H, **d**), 0.99 (d, J = 6.6 Hz, 6H, **e**), 0.87 (d, J = 6.6 Hz, 12H, **f**); **¹³C-NMR** (75 MHz, CDCl₃): δ = 180.8 and 177.3 (**1**, **2**), 160.6 (**3**), 140.2 (**4**), 130.8 (**5**), 129.8 (**6**), 123.5 (**7**), 117.2 (**8**), 68.9 (**9**), 39.2, 37.2 and 35.6 (**10**), 29.8 and 27.9 (**11**), 24.6 (**10**), 22.6 and 22.5 and 19.5 (**12**); **FT-IR**, C₃₄H₄₆N₂O₈, (NEAT): σ (cm⁻¹) = 2953, 2926, 2869, 1692, 1592, 1526, 1460, 1411, 1355, 1290, 1222, 1050, 974, 911, 831, 797, 756, 733, 692; **MS** (MALDI-TOF) m/z calculated: 610.33, found: 550.32, 551.33 (M+H), 552.34 (M+2H); **Analysis**: C₃₄H₄₆N₂O₈, calculated: C, 66.86, H, 7.59, N, 4.59; found: C, 66.85; H, 7.69, N, 4.49; **Uv-vis**, CHCl₃: λ_{\max} = 369 nm (ϵ = 6500 M⁻¹ cm⁻¹) and λ_{\max} = 257 nm (ϵ = 26*10³ M⁻¹ cm⁻¹) Heptane: λ_{\max} = 361 nm, λ_{\max} = 245 nm; THF: λ_{\max} = 372 nm (ϵ = 6300 M⁻¹ cm⁻¹) and λ_{\max} = 254 nm (ϵ = 26*10³ M⁻¹ cm⁻¹) ⁱPrOH: λ_{\max} = 371 nm (ϵ = 6400 M⁻¹ cm⁻¹) and λ_{\max} = 255 nm (ϵ = 27*10³ M⁻¹ cm⁻¹).



1,8-Bis(1,4,7,10,13,16-oxa-heptadecyl)anthraquinone (32). A mixture of tosylated ethylene-oxide **35** (6.013 g, 14.79 mmol), 1,8-dihydroxyanthraquinone (1.615 g, 6.724 mmol), K₂CO₃ (3.717 g, 26.90 mmol) and Bu₄NBr (108 mg, 0.336 mmol) in MIBK (24 mL) was heated under reflux for 21 hours. Based on ¹H-NMR analysis extra tosylated ethylene-oxide (0.683g, 1681 mmol) was added. After 11 h of heating under reflux the reaction was stopped and the mixture was concentrated *in vacuo*. The remaining solid was redissolved in CH₂Cl₂ and the mixture filtered over a glass filter. The filtrate was washed with a water/brine (1:1) mixture. The aqueous layer was then extracted with CH₂Cl₂ (2 ×). The combined organic layers were dried over MgSO₄ followed by filtration over a glass filter. The filtrate was concentrated (yield ~ 90%) and purification by column chromatography (silica gel, 50-80 v% dimethoxy-ethane in heptane gradient, R_f = 0.23 (silica gel, 80 v% dimethoxy-ethane in heptane)) furnished **32** as yellow viscous oil (1.584 g, 2.235 mmol, 33%). **¹H-NMR** (400 MHz, CDCl₃): δ = 7.83 (dd, J = 7.7 Hz, J = 1.1 Hz, 2H, **a**), 7.61 (dd, J = 8.4 Hz, J = 7.7 Hz, 2H, **b**), 7.36 (dd, J = 8.4 Hz, J = 1.1 Hz, 2H, **c**), 4.31 (t, J = 5.1 Hz, 4H, **d**),

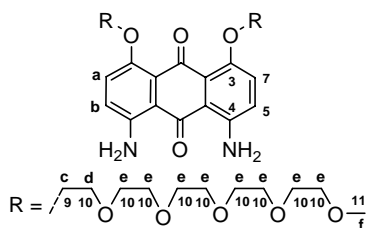
3.99 (t, $J = 5.1$ Hz, 4H, **e**), 3.85-3.52 (m, totaal 32H, **f**), 3.36 (s, 6H, **g**); $^{13}\text{C-NMR}$ (100 MHz, CDCl_3): $\delta = 183.8$ and 182.0 (**1**, **2**), 158.5 (**3**), 134.6 (**4**), 133.6 (**5**), 124.7 (**6**), 120.5 (**7**), 119.4 (**8**), 71.8 (**9**), 71.0 - 69.4 (**10**), 58.9 (**11**); **FT-IR** $\text{C}_{36}\text{H}_{52}\text{O}_{14}$, (NEAT): σ (cm^{-1}) = 2870, 1670, 1586, 1445, 1310, 1278, 1099, 1069, 747; **MS** (MALDI-TOF), $\text{C}_{36}\text{H}_{52}\text{O}_{14}$, m/z calculated: 708.34, found: 708.25, 709.25 (M+H), 710.27 (M+2H), 731.26 (M+Na), 747.25 (M+K); **Uv-vis**, CHCl_3 : $\lambda_{\text{max}} = 381$ nm ($\epsilon = 6700$ $\text{M}^{-1} \text{cm}^{-1}$) and $\lambda_{\text{max}} = 256$ nm ($\epsilon = 26 \cdot 10^3$ $\text{M}^{-1} \text{cm}^{-1}$); H_2O : $\lambda_{\text{max}} = 395$ nm ($\epsilon = 6800$ $\text{M}^{-1} \text{cm}^{-1}$) and $\lambda_{\text{max}} = 256$ nm ($\epsilon = 24 \cdot 10^3$ $\text{M}^{-1} \text{cm}^{-1}$); CH_3CN : $\lambda_{\text{max}} = 379$ nm, ($\epsilon = 6900$ $\text{M}^{-1} \text{cm}^{-1}$) and $\lambda_{\text{max}} = 254$ nm ($\epsilon = 25 \cdot 10^3$ $\text{M}^{-1} \text{cm}^{-1}$); $i\text{PrOH}$: $\lambda_{\text{max}} = 381$ nm ($\epsilon = 6900$ $\text{M}^{-1} \text{cm}^{-1}$) and $\lambda_{\text{max}} = 255$ nm ($\epsilon = 25 \cdot 10^3$ $\text{M}^{-1} \text{cm}^{-1}$).



4,5-Dinitro-1,8-bis(1,4,7,10,13,16-oxa-heptadecyloxy)-anthraquinone

(33). KNO_3 (300 mg, 2.97 mmol and 360 mg, 3.56 mmol) was added in two portions to a suspension of 1,8-disubstituted anthraquinone (**32**) (2.11 g, 2.97 mmol) in 95% H_2SO_4 (15 mL) at $< 4^\circ\text{C}$ which was stirred with a mechanical stirrer. The reaction was monitored with TLC (silica gel, 12 v% MeOH in CHCl_3). After 1 hour the reaction mixture was

poured on ice-water (200 mL). Subsequently, the aqueous layer was extracted with CH_2Cl_2 (3×100 mL). The combined organic layers were washed with satd. aq. NaHCO_3 (100 mL). The aqueous layer was extracted with CH_2Cl_2 (2 \times). The combined organic layers were dried over MgSO_4 followed by filtration over a glass filter after which the filtrate was concentrated *in vacuo*. Purification by column chromatography (silica gel, 5 v% MeOH in CHCl_3 , $R_f = 0.32$) gave **33** as light brown viscous oil (2.13 g, 2.67 mmol, 90%). $^1\text{H-NMR}$ (400 MHz, CDCl_3): $\delta = 7.94$ (d, $J = 9.1$ Hz, 2H, **a**), 7.44 (d, $J = 9.1$ Hz, 2H, **b**), 4.41 (t, $J = 4.8$ Hz, 4H, **c**), 3.98 (t, $J = 4.6$ Hz, 4H, **d**), 3.81 - 3.52 (m, 32H, **e**), 3.36 (s, 6H, **f**); $^{13}\text{C-NMR}$ (100 MHz, CDCl_3): $\delta = 180.5$ and 177.5 (**1**, **2**), 160.5 (**3**), 140.8 (**4**), 130.6 (**5**), 129.7 (**6**), 123.6 (**7**), 118.3 (**8**), 71.8 (**9**), 71.0 - 69.3 (**10**), 58.9 (**11**); **FT-IR** (NEAT): σ (cm^{-1}) = 2872, 1689, 1592, 1531, 1468, 1450, 1412, 1356, 1291, 1096, 1063, 847; **MS** (MALDI-TOF), $\text{C}_{36}\text{H}_{50}\text{N}_2\text{O}_{18}$, m/z calculated: 798.31, found: 799.27 (M+1H), 821.3 (M+Na), 837.28 (M+K); **Uv-vis**, CHCl_3 : $\lambda_{\text{max}} = 369$ nm ($\epsilon = 5900$ $\text{M}^{-1} \text{cm}^{-1}$) and $\lambda_{\text{max}} = 256$ nm ($\epsilon = 26 \cdot 10^3$ $\text{M}^{-1} \text{cm}^{-1}$); H_2O : $\lambda_{\text{max}} = 378$ nm ($\epsilon = 5900$ $\text{M}^{-1} \text{cm}^{-1}$) and $\lambda_{\text{max}} = 259$ nm ($\epsilon = 26 \cdot 10^3$ $\text{M}^{-1} \text{cm}^{-1}$); CH_3CN : $\lambda_{\text{max}} = 375$ nm ($\epsilon = 6000$ $\text{M}^{-1} \text{cm}^{-1}$) and $\lambda_{\text{max}} = 256$ nm ($\epsilon = 26 \cdot 10^3$ $\text{M}^{-1} \text{cm}^{-1}$).

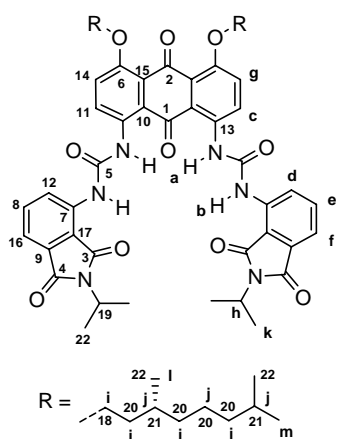


4,5-Diamino-1,8-bis(1,4,7,10,13,16-oxa-heptadecyl) anthraquinone

(34). A solution of dinitro-anthraquinone **33** (0.803 g, 1.005 mmol) in 50 v% EtOAc in EtOH (5 mL) was heated to 30°C . Then, SnCl_2 (1.715 g, 9.047 mmol) was added. The reaction was monitored by TLC (silica gel, 5 v% MeOH in CHCl_3 , $R_f = 0.25$) and $^1\text{H-NMR}$ (CDCl_3). After 18 h the reaction was stopped. Subsequently, the reaction mixture was concentrated *in vacuo* and the residue redissolved in CH_2Cl_2 (150 mL) and the solution washed with 1 M aq. NaOH (150 mL). Brine (100 mL) was added to the aqueous layer and subsequently the mixture was extracted with CH_2Cl_2 (4 \times). The combined organic layers were washed with brine (200 mL), dried over MgSO_4 , filtered over a glass filter. The filtrate was concentrated *in vacuo* and purification by column chromatography (silica gel, 2-6 v% MeOH in CHCl_3 gradient) furnished **34** as a purple highly viscous oil (~ 86% before and

0.200 g, 0.271 mmol, 27% isolated after chromatography). $^1\text{H-NMR}$ (400 MHz, CDCl_3): $\delta = 7.18$ (d, $J = 9.2$

Hz, 2H, **a**), 6.84 (d, $J = 9.2$ Hz, 2H, **b**), 4.19 (t, $J = 4.9$ Hz, 4H, **c**), 3.86 (t, $J = 4.9$ Hz, 4H, **d**), 3.76-3.53 (m, totaal 32H, **e**), 3.37 (s, 6H, **f**); $^{13}\text{C-NMR}$ (75 MHz, CDCl_3): $\delta = 188.3$ (**1**), 184.5 (**2**), 149.7 (**3**), 145.8 (**4**), 126.9 (**5**), 125.7 (**6**), 123.1 (**7**), 114.7 (**8**), 72.0-69.3 (**10**), 59.1 (**11**); **FT-IR** (NEAT): σ (cm^{-1}) = 3439, 3329, 2873, 1668, 1626, 1592, 1535, 1453, 1417, 1349, 1209, 1104, 1063, 833; **MS** (MALDI-TOF), $\text{C}_{36}\text{H}_{54}\text{N}_2\text{O}_{14}$, m/z calculated: 738.36, found: 739.33 (M+H), 740.34 (M+2H), 761.31 (M+Na⁺), **Uv-vis**, CHCl_3 : $\lambda_{\text{max}} = 510$ nm ($\epsilon = 12100$ $\text{M}^{-1} \text{cm}^{-1}$) and $\lambda_{\text{max}} < 250$ nm; H_2O : $\lambda_{\text{max}} = 526$ nm ($\epsilon = 10500$ $\text{M}^{-1} \text{cm}^{-1}$) and $\lambda_{\text{max}} < 240$ nm; CH_3CN : $\lambda_{\text{max}} = 514$ nm ($\epsilon = 11200$ $\text{M}^{-1} \text{cm}^{-1}$) $\lambda_{\text{max}} < 240$ nm; $i\text{PrOH}$: $\lambda_{\text{max}} = 526$ nm ($\epsilon = 12200$ $\text{M}^{-1} \text{cm}^{-1}$) $\lambda_{\text{max}} < 240$ nm.



4,5-Bis(ureido-N-isopropylphthalimidyl-3-ureido)-1,8-di([S]-3,7-dimethyloctyloxy)-anthraquinone (36). A solution of 1,8-di([S]-3,7-dimethyloctyloxy)-4,5-diaminoanthraquinone **27** (370 mg, 0.672 mmol), 3-isocyanato-N-isopropylphthalimide **12** (774 mg, 3.36 mmol) in dioxane (4 mL) was heated under reflux for 4 h or until all diamino-anthraquinone has reacted. The reaction mixture was concentrated *in vacuo* and the residue triturated with CHCl_3 (3×6 mL). The combined CHCl_3 fractions were diluted with EtOAc (50 mL) and the solution washed with 1 M aq. NaOH (2×50 mL). The combined organic layers were dried over MgSO_4 . After filtration and concentration the residue was purified by column chromatography (silica gel, O^iPr_2 , $R_f = 0.28$). A second purification was

necessary. Column chromatography over biobeads (SX-3 (< 2000 g/mol), THF) gave **35** as a red solid (570 mg, 84%). $^1\text{H-NMR}$ (300 MHz, CDCl_3): $\delta = 11.25$ (s, 2H, **a**), 9.20 (s, 2H, **b**), 8.55 (d, $J = 9.6$ Hz, 2H, **c**), 8.49 (d, $J = 8.2$ Hz, 2H, **d**), 7.61 (t, $J = 7.8$ Hz, 2H, **e**), 7.41 (d, $J = 7.1$ Hz, 2H, **f**), 7.38 (d, $J = 9.6$ Hz, 2H, **g**), 4.39 (m, $J = 7.0$ Hz, 2H, **h**), 4.15 (m, $J = 6.2$ Hz, 4H, **i**), 1.97-1.13 (m, totaal 20H, **j**), 1.38 (d, $J = 6.9$ Hz, 12H, **k**), 0.99 (d, $J = 6.3$ Hz, 6H, **l**), 0.87 (d, $J = 6.6$ Hz, 12H, **m**); $^{13}\text{C-NMR}$ (50 MHz, CDCl_3): $\delta = 191.1$ (**1**), 182.4 (**2**), 170.3 (**3**), 167.8 (**4**), 153.4 (**5**), 152.0 (**6**), 137.9 (**7**), 135.4 (**8**), 134.5 (**9**), 131.6 (**10**), 126.6 (**11**), 124.6 (**12**), 124.4 (**13**), 122.8 (**14**), 120.2 (**15**), 117.0 (**16**), 115.6 (**17**), 69.0 (**18**), 43.0 (**19**), 39.4, 37.5 and 36.2 ($3 \times \text{CH}_2$, **20**), 29.9 and 28.0 ($2 \times \text{CH}$, **21**), 24.9 (**20**), 22.8, 22.7, 20.1 and 19.8 ($4 \times \text{CH}_3$, **22**); **FT-IR** (NEAT): σ (cm^{-1}) = 3332, 3242, 2952, 2926, 2869, 1763, 1694, 1619, 1512, 1475, 1338, 1273, 1189, 1038, 747; **MS** (MALDI-TOF), $\text{C}_{58}\text{H}_{70}\text{N}_6\text{O}_{10}$, m/z calculated: 1010.52, found: 1011.67 (M+H), 1033.66 (M+Na), 1034.66 (M+H+Na), 1049.77 (M+K), 1050.63 (M+H+K); **Uv-vis**, CHCl_3 : $\lambda_{\text{max}} = 490$ nm ($\epsilon = 11700$ $\text{M}^{-1} \text{cm}^{-1}$) and $\lambda_{\text{max}} = 354$ nm ($\epsilon = 11900^* \text{M}^{-1} \text{cm}^{-1}$) and $\lambda_{\text{max}} < 300$ nm; Heptane: $\lambda_{\text{max}} = 484$ nm, $\lambda_{\text{max}} = 350$ nm and $\lambda_{\text{max}} < 300$ nm; THF: $\lambda_{\text{max}} = 473$ nm ($\epsilon = 10300$ $\text{M}^{-1} \text{cm}^{-1}$) $\lambda_{\text{max}} = 355$ nm ($\epsilon = 11800^* \text{M}^{-1} \text{cm}^{-1}$) $\lambda_{\text{max}} < 300$ nm; $i\text{PrOH}$: $\lambda_{\text{max}} = 471$ nm, $\lambda_{\text{max}} = 357$ nm and $\lambda_{\text{max}} < 300$ nm.

3.8 References

- 1) van Gorp, J. J.; Vekemans, J. A. J. M.; Meijer, E. W. *Chem. Commun.* **2004**, 60.
- 2) van Gorp J. J.; *Helices by Hydrogen Bonding*, **2004**, Thesis, Chapter 6, Eindhoven University of Technology.
- 3) van Gorp J. J.; *Helices by Hydrogen Bonding*, **2004**, Thesis, Chapter 5, Eindhoven University of Technology.
- 4) Saunders, J. H.; and Slocombe, R. J. *Chem. Rev.* **1948**, *43*, 203-18.
- 5) Aratani, N.; Tsuda, A.; Osuka, A. *Synlett* **2001**, *11*, 1663-74.
- 6) Aratani, N.; Osuka, A. *Macromol. Rapid Commun.* **2001**, *22*, 725-40.
- 7) De Greef, T. F. A. Graduation report: *Towards stepwise synthesis of well-defined ureidophthalimide oligomers*; Eindhoven University of Technology, 2004.
- 8) Dorozhkin, V. P.; Kirpichnikov, P. A. *Doklady Akademii Nauk SSSR* **1986**, *287*, 658-62
- 9) Kleiman, H. *Angew. Makromol. Chem.* **1981**, *80*, 185-94.
- 10) Arnold, R. G.; Nelson, J. A.; Verbanc, J. J.; *Chem. Rev.* **1956**, *57*, 47-67.
- 11) Laurent, A. *Liebigs Ann. Chem.* **1840**, *34*, 287.
- 12) Fritzsche, J. *Jahresbericht über die Fortschritte der Chemie.* (A. Strecker), 1868, p. 403.
- 13) Graebe, C.; and Liebermann, C. *Ber.* **1868**, *1*, 49.
- 14) Friedel, C.; and Crafts, J. M. *Compt. Rend.* **1877**, *84*, 1450.
- 15) "Anthraquinone." Encyclopædia Britannica from Encyclopædia Britannica Premium Service. <<http://www.britannica.com/eb/article-79847>> [Accessed October 29, 2005].
- 16) Phillips, M. *Chem. Rev.* **1929**, *6*, 157-74.
- 17) Palmans, A.; *Supramolecular Structures Based on the Intramolecular H-bonding in the 3,3'-Di(acylamino)-2,2'-Bipyridine Unit*; **1997**, page 89, Eindhoven University of Technology.
- 18) Tolkiehn, K.; Krohn, K. *Ber.*, **1980**, *13*, 1575-83.
- 19) Synthesis and characterization of di-tert-butyl (1*E*,3*E*)-buta-1,3-diene-1,4-diylidicarbamate (**19**) is reported in the experimental section of chapter 2, compound **15a**.
- 20) Schmidt, R. R.; Wagner, A. *Synthesis*, **1981**, 273-5.
- 21) Battegay, M.; Bernhardt, J. *Bull. Soc. Chem. Fr.* **1923**, *33*, 1510-36.
- 22) (a) Murillo, O.; Watanabe, S.; Nakano, A.; Gokel, G. J. *Am. Chem. Soc.* **1995**, *117*, 7665-79. (b) Chen, Z., Schall, O.; Alcalá, M.; Li, Y.; Gokel, G.; Echegoyen, L. J. *Am. Chem. Soc.* **1992**, *114*, 444-51.
- 23) Ullmann, F.; v. d. Schalk, W. *Liebigs Ann Chem.* **1912**, *388*, 199.
- 24) Fieser, L.; Fieser, M. *Reagents for Organic Synthesis* **1967**, John Wiley and sons, inc.; pag. 1113.
- 25) Chang, P.; Cheng, C. *Synth. Commun.* **1995**, *25*, 1893-1900.
- 26) (a) Morris, G.; Mullah, K.; Sutherland, J. *Tetrahedron* **1986**, *42*, 3303-9. (b) Kumar, A.; Sutherland, J.; Thompson, D. J. *Chem. Soc., Perkin Trans. 1* **1987**, 445-7.
- 27) Stefanska, B.; Dzieduszycka, M.; Bontemps-Gracz, M.; Borowski, E. J. *Med. Chem.* **1999**; *42*; 3494-501.
- 28) Brunsveld, L.; Zhang, H.; Glasbeek, M.; Vekemans, J. A. J. M.; Meijer, E. W. *J. Am. Chem. Soc.* **2000**, *122*, 6175-82.

Chapter 4

Foldamers decorated with chromophores

Abstract

From the discussion in chapter 3 it is clear that functionality in poly(ureidophthalimide) is preferentially introduced via the imide nitrogen of the phthalimide monomer. Foldamers that take advantage of the periphery of the putative helical architecture for the organization of functionalities (e.g. chromophores) have not yet been reported. In this chapter we discuss the potential use of this previously unaddressed feature by decoration of our poly-ureidophthalimide foldamer with oligo(phenylenevinylene) (OPV) chromophores. Circular dichroism studies on the novel OPV decorated poly(ureidophthalimides) indicate the presence of helically arranged OPVs in THF. However, such an effect is not observed in CHCl₃. Very remarkable are the measurements in heptane in which a bisignate Cotton effect is observed provided the sample has a THF history. However, with a CHCl₃ history no Cotton effect is observed in heptane. These foldamers decorated with chromophores may be of interest in the field of molecular electronics. Furthermore, a start is made to get more insight into the chiral alignment of peripheral chromophores in this type of architectures with the design of foldamers with peripheral donor-acceptor chromophores.

4.1 Introduction: peripheral functionalization with chromophores

Research on abiotic, non-peptidomimetic oligomers capable of folding started with Hamilton's oligoanthranilamides¹ and was rapidly followed by the first oligo *meta* phenylene ethynylene². The term "foldamer" was defined by Moore^{3e} to categorize dynamic oligomeric systems that are capable of folding into a conformationally ordered state in solution. Since then a variety of synthetic foldamers has been designed, each type utilizing a characteristic combination of secondary interactions to direct the folding. A number of design strategies are prominent in the recent literature. The *m*-phenylene ethynylenes form a class of foldamers that rely on solvophobic interactions in combination with π - π stacking.⁴ In the aromatic oligo-amides reported by Huc⁵, Gong⁶ and others⁷, π - π stacking is combined with hydrogen bonding to direct folding. The latter class is described in more detail in recent reviews.⁸ Less common is the design based on oligo-aromatic ureas: whereas those reported by Gong^b are present in a *cisoid* conformation, those of Zimmerman⁹ are forced into a *transoid* conformation due to intramolecular hydrogen bonding. Recently, we presented a helical foldamer based on poly(ureidophthalimide) in which the urea linkers adopt a *cisoid* conformation due to intramolecular hydrogen bonding.¹⁰ Like the oligoamides, this polyurea engages in intramolecular hydrogen bonding to direct folding and π - π interactions to further stabilize the helical architecture once a turn is completed.

A potential function for helical foldamers is the exploitation of the inner void to host a guest. Depending on the design, helical foldamers may possess an inner void of sufficient size to accommodate ions¹¹ or small molecules^{12,13,14}. The efforts of this research may eventually lead to synthetic trans-membrane ion channels.^b Besides the potential for the exploitation of the inner void, the helical architecture may also be a promising candidate for the organization of peripheral chromophores. To the best of our knowledge this opportunity has not been addressed before. Alignment of chromophores is especially of interest in the field of molecular electronics with potential applications such as organic photovoltaics¹⁵ and organic field effect transistors¹⁶ (Figure 4.1).

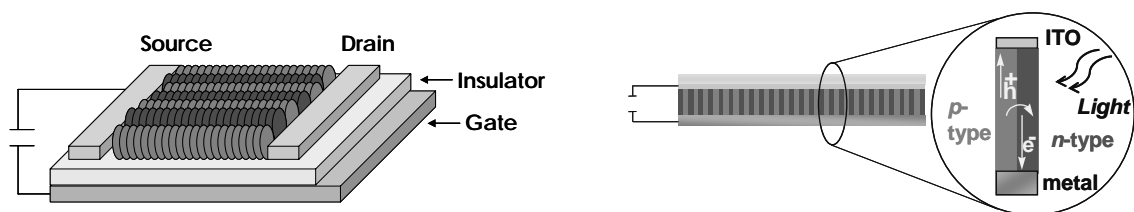


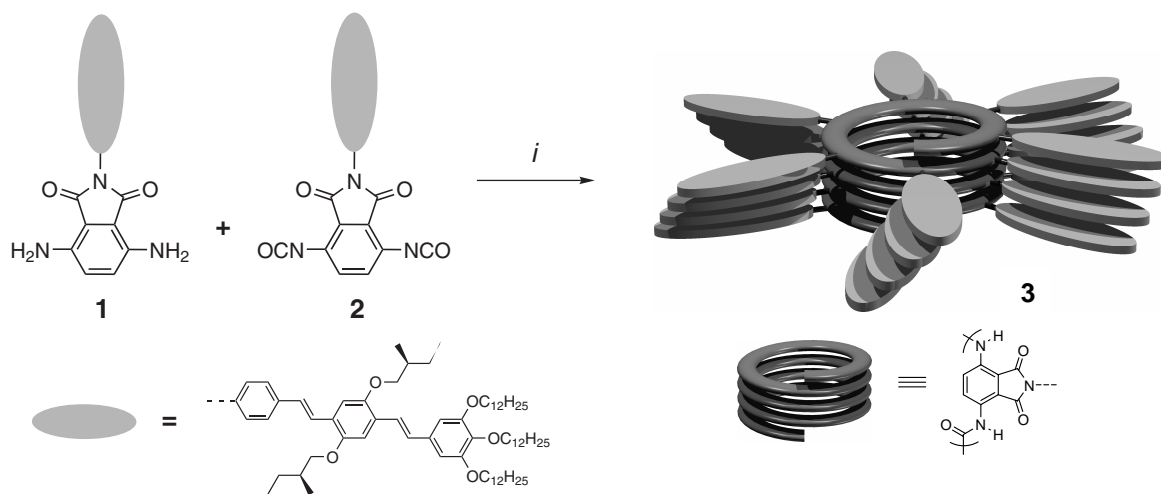
Figure 4.1: Schematic drawings of a FET (left) and an organic solar cell (right) using well-organized nanoscopic morphologies.

In this chapter, we report the synthesis and characterization of the first foldamer that utilizes the periphery to align oligo(*p*-phenylenevinylene) (OPV) chromophores in a chiral fashion. We chose to decorate the previously reported poly(ureidophthalimide) with OPVs since this type of chromophore has been studied in great detail in supramolecular homo-assemblies¹⁷ and hetero-assemblies¹⁸. Furthermore, the extended π -system of OPV chromophores may help to stabilize the helical architecture.

In chapter 2, we reported a general synthetic strategy to obtain an array of 3,6-diaminophthalimides.¹⁹ These are the building blocks that give access to a collection of peripherally functionalized foldamers. A high yielding synthetic methodology is described for the introduction of OPV3 and OPV4 chromophores, both chromophores possessing chiral side chains to allow circular dichroism (CD) spectroscopy studies and additional gallic acid derived moiety guarantees solubility in most common organic solvents.

4.2 Ureidophthalimide foldamer decorated with OPV3 chromophores

Target OPV3 decorated poly(ureidophthalimide) **3** was obtained by reaction of diamine **1**²⁰ with diisocyanate **2** in refluxing toluene in the presence of *p*-dimethylaminopyridine (Scheme 4.1). Diisocyanate **2** is prepared from diamine **1** by exposure to phosgene.



Scheme 4.1: The synthesis of the poly-ureidophthalimide foldamer decorated with OPV3 chromophores **3**. i) DMAP (1.0 equiv.), PhCH₃, 17 h.

After polymerization column chromatography on silica gel with a gradient of chloroform to 10 v% ethyl acetate in chloroform easily removes of the non-migrating *p*-dimethylamino-pyridine and allows separation of the longer from the shorter oligomers. The first fraction **3a** contains oligomers of approximately 6-25 units (~66 w%) whereas the second fraction **3b** consists of oligomers with lengths between 2-7 units (~15 w%) based on GPC analysis (Figure 4.2). Although ¹H-NMR end-group analysis has proven a most reliable method to estimate the average oligomeric length, we found that GPC is more useful in this case since the broad and

overlapping signals in $^1\text{H-NMR}$ hamper proper end-group analysis.²¹ Moreover, $^1\text{H-NMR}$ gives the average length whereas GPC gives more information on the total distribution.

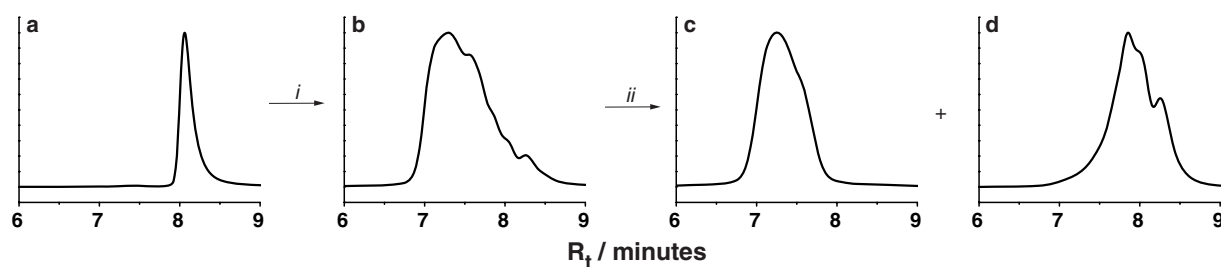


Figure 4.2: GPC analysis of a) monomer **1**, b) crude polymer **3**, c) long fraction **3a** (~66 w%) d) short fraction **3b** (~15 w%) i) polymerization, ii) separation. Measured in CHCl_3 , at 420 nm, mixed-D column against a polystyrene internal standard.

The nature of the solubilizing π -conjugated tails enables UV-vis and CD studies in various solvents. Thus, **3a** is subjected to a study in CHCl_3 , THF, and heptane (Figure 4.3). A chloroform solution of **3a** displays two absorption maxima in the UV-vis spectrum located at 323 nm ($\epsilon = 38700 \text{ M}^{-1}\text{cm}^{-1}$) and 405 nm ($\epsilon = 47800 \text{ M}^{-1}\text{cm}^{-1}$), which can be attributed to the ureido phthalimide moiety and the OPV3 unit, respectively (Figure 4.3a). This solution proved to be CD silent suggesting a random coil conformation for the polymer. When the CHCl_3 solution was concentrated and redissolved in heptane no Cotton effect was observed although in UV-vis a slight red shift of 6 nm was observed for the first maximum to 329 nm ($\epsilon = 30600 \text{ M}^{-1}\text{cm}^{-1}$) and a hypsochromic shift for the highest wavelength absorption to 401 nm ($\epsilon = 37500 \text{ M}^{-1}\text{cm}^{-1}$). However, when the CHCl_3 solution was concentrated and redissolved in THF, two CD effects are observed of which the first is located at 328 nm ($g = -5.0 \times 10^{-4}$) and the second displays a bisignate Cotton effect with a zero crossing at 399 nm and maxima at 379 nm ($g = +4.4 \times 10^{-4}$) and 416 nm ($g = -3.8 \times 10^{-4}$). The zero crossing of this bisignate CD effect coincides with the highest absorption maximum in the UV-vis spectrum at 398 nm ($\epsilon = 43700 \text{ M}^{-1}\text{cm}^{-1}$). This absorption can be attributed to the π - π^* transition of the OPV3 unit, implying a chiral stacking of the OPV3 moieties. It is important to mention that 3,6-bis(acetylamino)-*N*-OPV3-phthalimide (**4**)²², the precursor for diamino monomer **1**, shows no Cotton effect in THF or CHCl_3 . Moreover, THF is known to be a good solvent for isolated OPV3 chromophores and thus, aggregation is not expected. Furthermore, the negative exciton coupling of the bisignate Cotton effect suggests the presence of a left-handed helical arrangement of the transition dipoles of the OPV units.^{23,24} In contrast to the measurement in heptane with a chloroform history, the measurement in heptane with a THF history does show a Cotton effect. This most remarkable observation implies the preservation of the secondary architecture in the solid phase during concentration and its retention when subsequently redissolved in heptane. The maximum of the first Cotton effect is located at 333 nm ($g = -6.6 \times 10^{-4}$). The zero crossing of the bisignate Cotton effect

underwent a minor blue shift and is now positioned at 395 nm with maxima at 373 nm ($g = +3.8 \times 10^{-4}$) and 413 nm ($g = -4.2 \times 10^{-4}$).

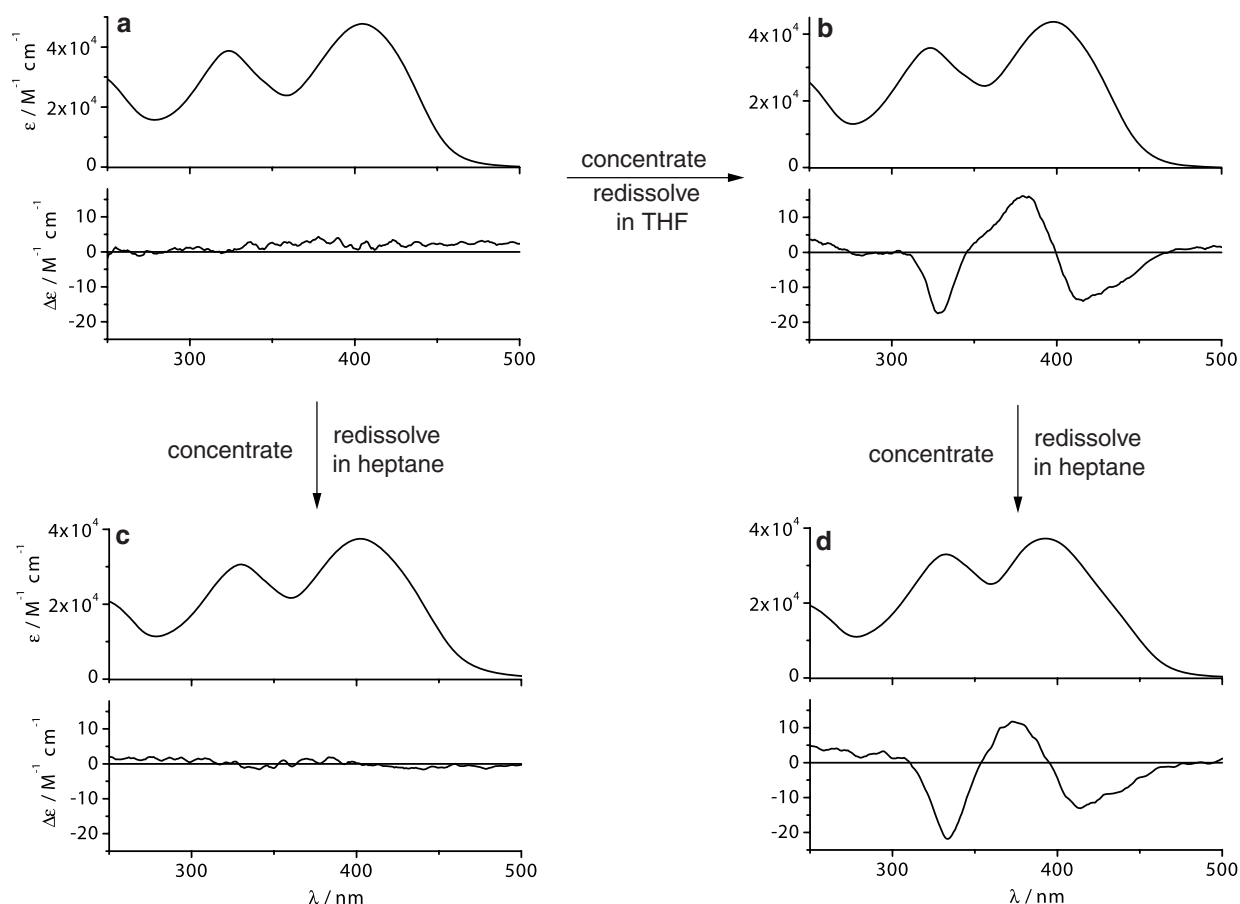


Figure 4.3: UV-vis and CD spectra of longer oligomers fraction **3a** in a) CHCl_3 , 2.4×10^{-5} M. b) THF, 2.9×10^{-5} M. c) heptane, 2.1×10^{-5} M with a CHCl_3 history. d) heptane 2.3×10^{-5} M with a THF history.

The same blue shift is observed for the absorption maximum of the OPV3 unit in the UV-vis spectrum now located at 392 nm ($\epsilon = 37200 \text{ M}^{-1}\text{cm}^{-1}$). Furthermore, a small bathochromic shift to 333 nm ($\epsilon = 33000 \text{ M}^{-1}\text{cm}^{-1}$) is observed for the short wavelength absorption. Besides the remarkable CD results, the UV-vis measurement clearly shows a significantly lower (~20%) molar absorption coefficient for the long wavelength absorption of **3a** in heptane compared to CHCl_3 and THF. This hypochromic (decrease in absorption intensity) effect is an indication for tight π - π stacking that is also observed in DNA and π -stacked polymers.^{25,26} Above all, these experiments demonstrate that heptane is not capable of inducing nor disrupting a chiral secondary architecture but rather dissolves a preformed aggregate. This is in agreement with temperature dependent CD measurements in THF and heptane (Figure 4.4). The gradually decreasing Cotton effect in THF upon increasing the temperature, which is reclaimed upon cooling, demonstrates the dynamics of the secondary architecture in THF. This is in strong contrast to the temperature dependent measurements in heptane that clearly show the

astonishing stability of the secondary architecture. Moreover, similar measurements in dodecane under prolonged heating at 100°C hardly altered the Cotton effect. A melting curve could be constructed from the temperature-dependent Cotton effect at 415 nm in THF and is depicted in figure 4.12 (*vide infra*).

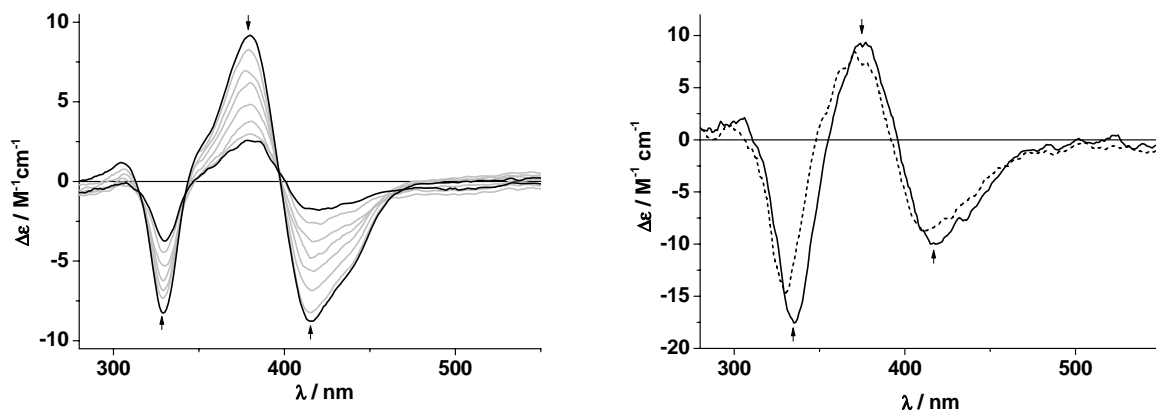


Figure 4.4: Temperature-dependent CD measurements of solution of **3a** in THF, 3.1×10^{-5} M from 20°C (black line) in steps of 5°C (grey lines) to 55°C (black line) (left); and heptane, 3.2×10^{-5} M with a THF history at 20°C (black line) and 85°C (dashed line) (right).

The UV-vis spectra of **3a** in THF at concentrations ranging from 5×10^{-4} M to 5×10^{-6} M display no differences in the position nor in the intensity of the absorption maxima. Despite the minor changes, the concentration dependent CD spectra of **3a** in THF at 20°C reveal an almost concentration independent Cotton effect (Figure 4.5). This suggests that the Cotton effect is the result of an intramolecular organization of the OPV3 chromophores and that aggregation is not responsible for the chirality in the concentration range between 5×10^{-4} M and 5×10^{-6} M.

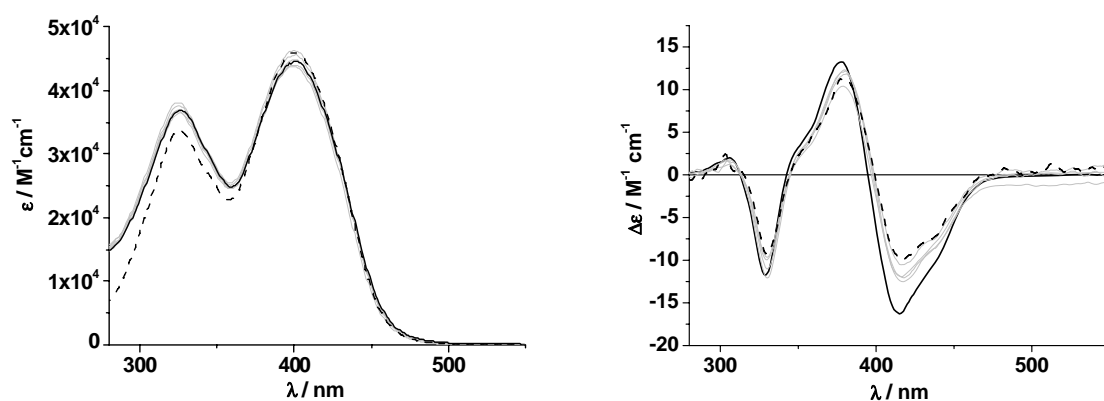


Figure 4.5: Concentration-dependent UV-vis (left) and CD (right) spectra of **3a** in THF at 20°C ranging from 5×10^{-4} M (solid black line) to 5×10^{-6} M (dashed black line) and intermediate steps (grey lines).

To get more insight into the typical urea N-H, C=O and imide C=O vibrations, solid phase infrared (IR) spectra of **3a** from different solvents have been collected (Table 4.1). The

measurements clearly reveal that films of **3a** drop cast from THF and heptane with a THF history, give the same values. But the values differ from drop cast films of **3a** from CHCl₃ and heptane with a CHCl₃ history solution. Although the difference is small, the results are in agreement with the CD spectroscopy results in the sense that both solvents induce a different secondary organization affecting the urea conformation.

Table 4.1: IR absorptions of **3a**, NEAT from different solvents (ν in cm⁻¹).

	Urea-H	imide C=O	Urea C=O
THF	3342	1727	1699
Heptane with THF history	3343	1728	1699
CHCl ₃	3347	1724	1696
Heptane with CHCl ₃ history	3347	1724	1696

A final subjective but noteworthy remark is the observation that solubilizing **3a** in heptane seemed to be easier from a sample with a THF history than from one with a CHCl₃ history. This can be rationalized by considering the putative helical organization in THF which shields the relatively polar ureidophthalimide core from the apolar heptane. However, this is not the case when **3a** has a chloroform history in which there is no such shielding effect of the polar core due to folding.

It is tempting to assume that THF induces or at least facilitates the folding process. A tentative favorable solvent interaction is displayed in figure 4.6. The lone pairs of the spiro oriented THF might participate in a hydrogen bonding interaction with the urea hydrogens. This effect may stabilize the *cisoid* conformation of the urea functionality and hence assist folding.

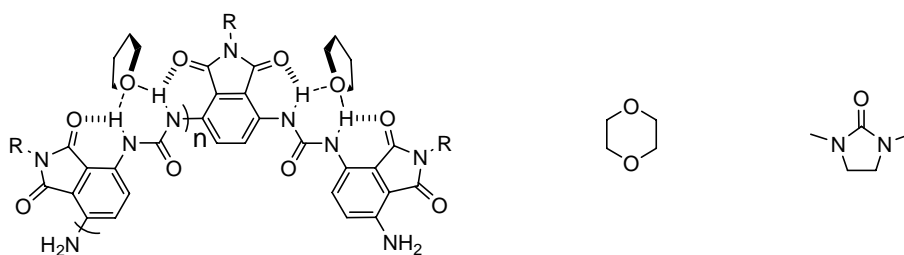


Figure 4.6: Possible templating effect of THF and two solvents with similar structural features as THF, dioxane and 1,3-dimethyl-2-imidazolidinone.

If hydrogen bonding of the THF oxygen to the urea protons is indeed the rationale behind better folding, other solvents with similar hydrogen bonding accepting capabilities might harvest the same effect. Dioxane is structurally related to THF and may, therefore, also be capable of hydrogen bonding with the urea protons. However, when a dioxane solution of **3a** with a CHCl₃ history is analyzed with CD spectroscopy no Cotton effect is observed. Measuring

a dioxane solution with a THF history also displays no Cotton effect. This implies that dioxane is neither capable of inducing helix formation nor preserving a preformed helical architecture. Similar effects have been observed for 1,3-dimethyl-2-imidazolidinone, although it must be noted that the solubility in this solvent is low, resulting in a somewhat turbid solution. Although not explanatory, these results substantiate the unique role of THF in the folding process.

Initial photoluminescence experiments on **3a** in CHCl₃ and THF to get more information on the nature of the stacking of the OPV3 chromophores were hampered due to the very low fluorescence intensity. This is remarkable since other studies revealed the significant emission properties of OPV3.²³ In addition, monomeric precursor 3,6-bis(acetylamino)-*N*-OPV3-phthalimide (**4**)²² (Chapter 2, structure **20e**) also lacks significant fluorescence. The comparison with 3,6-bis(acetylamino)-*N*-OPV3-phthalimide (**4**) is based on the structural resemblance with the monomeric repeating unit in the polymer. These observations indicate the possibility of electron transfer from the OPV3 to the phthalimide moiety. Energy transfer can be excluded since this requires the presence of absorptions at a higher wavelength than the OPV3 absorption maximum. Moreover, this implies that the OPV3-phthalimide system intrinsically comprises the anticipated p- (donor) and n- (acceptor) type material combination required for the use in an organic solar cell. Especially the putative helical arrangement of the secondary architecture is most advantageous since it provides the lamellar organization that is thought to be ideal in organic solar cells (Figure 4.1). Further experiments with photo-induced absorption (PIA) spectrometry must prove whether this phenomenon can indeed be attributed to electron transfer.

To get some information on the surface morphology of the ureido-phthalimide foldamers AFM studies were performed. Solutions of **3a** were dropcast from CHCl₃ and THF on mica and graphite. Unfortunately, no interesting morphologies were observed.

In contrast to the fascinating results obtained with oligomer **3a** in dilute CHCl₃, THF and heptane solutions, fraction **3b**, consisting of the short oligomers, shows no CD effect at all. From the GPC data the average length was estimated to be less than 7 units, which is insufficient to make at least one turn. Still, it was expected that the short oligomers would aggregate into supramolecular chiral architectures in heptane as was the case with the previously reported ureido-phthalimide.¹⁰ Fraction **3b** was subjected to a STM experiment to see whether the claimed curvature, due to the *cisoid* conformation of the urea linkages, could be visualized on a graphite surface. The obtained images show molecules that seem to order in circles as expected, others form worm-like structures (Figure 4.7). However, a number of molecules seem to adopt an undefined conformation. The latter observation can perhaps be attributed to the relatively small size of the OPV3 chromophore, which might induce a too low affinity for the graphite

substrate. In addition, the sample was polydisperse, containing oligomeric lengths ranging from dimeric to heptameric species which may have challenged surface organization.

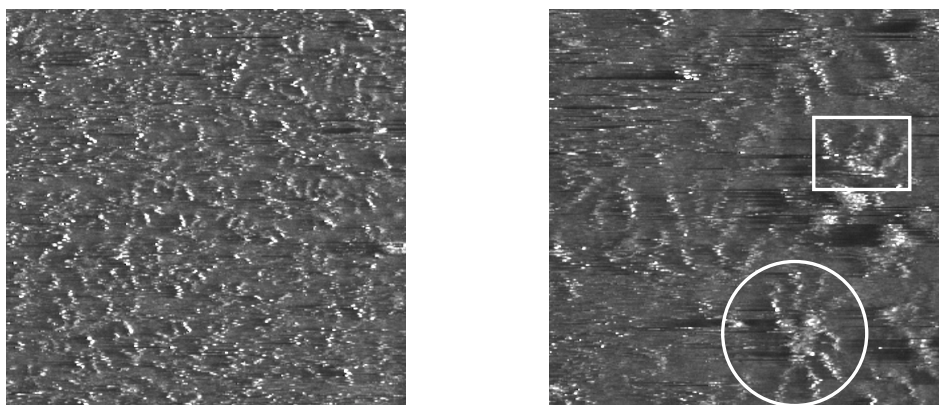
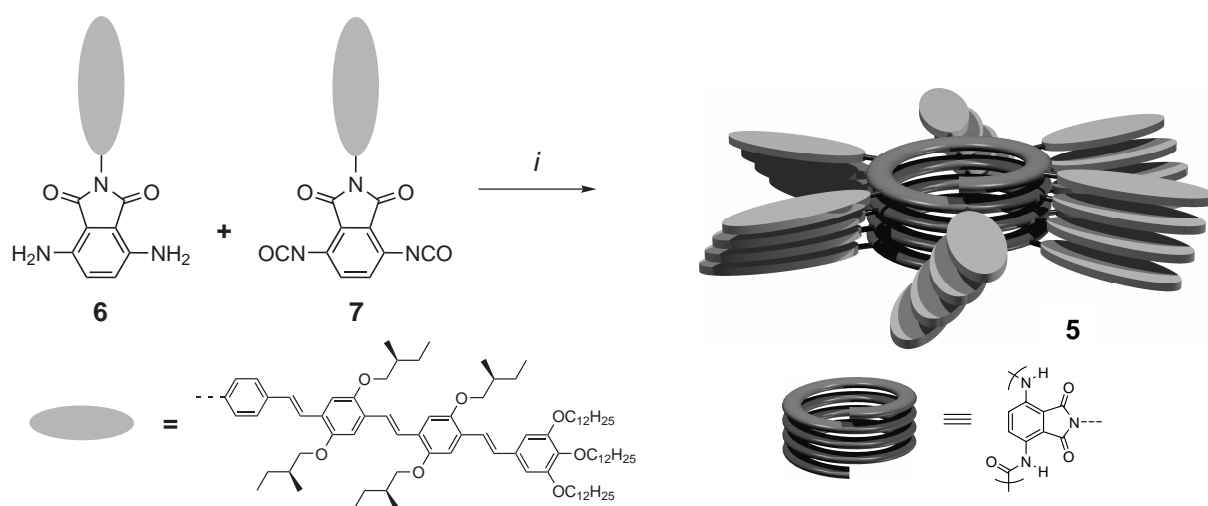


Figure 4.7: STM image of **3b** on graphite (left) and an enlargement (right), circular structures (circle) and worm-like structures (rectangle).

The results obtained with poly(ureidophthalimide) with an OPV3 periphery showed that an extended π -system does not hamper the formation of the putative helical secondary architecture. Thus, even with the non-directed aggregation ability of the OPV3 units based on π - π interactions alone, the directionality in the hydrogen bonding of the ureidophthalimide units precedes the eventual chiral aggregation of the OPV3 chromophores. Moreover, the temperature dependent CD study showed that upon elevation of the temperature the Cotton effect is reduced, but never completely vanishes. Similar results were reported for the first poly(ureidophthalimide) (Chapter 2, Scheme 2.1) foldamer by van Gorp¹⁰ and indicate that in spite of the size, the π -system does not influence the dynamics in THF. Further enlargement of the π -system by introduction of peripheral OPV4 units might affect the formation and/or the stability of the secondary architecture.

4.3 Ureidophthalimide foldamer decorated with OPV4 chromophores

Similar to OPV3-based foldamers, OPV4-decorated poly(ureidophthalimide) **5** was obtained by reaction of diamine **6**²⁷ with diisocyanate **7** in refluxing toluene in the presence of *p*-dimethylaminopyridine (Scheme 4.2). The three dodecyloxy tails ensure solubility in most common organic solvents and the chiral side chains allow for circular dichroism studies.



Scheme 4.2: Synthesis of OPV4 decorated foldamer **5**. i) DMAP (1.0 equiv.), PhCH₃, reflux, 17 h.

Column chromatography over silica gel afforded the fraction of longer oligomers (**5a**) consisting of 5-21 units (61 *w%*) and that with shorter oligomers (**5b**) consisting of 1-5 units (7 *w%*) as was deduced by GPC analysis (Figure 4.8). This demonstrates that simple separation over silica gel is an excellent method to remove the shorter oligomers. Model studies have shown that approximately 7 units may complete one turn.²⁸ From the results obtained with the OPV3 decorated poly(ureidophthalimide) (Section 4.2) we know that the Cotton effect is the result of an intramolecular process. This means that oligomeric lengths shorter than 7 units will presumably not contribute to the Cotton effect. Removal of the shorter oligomers will thereby positively influence the expected Cotton effect of **5a**.

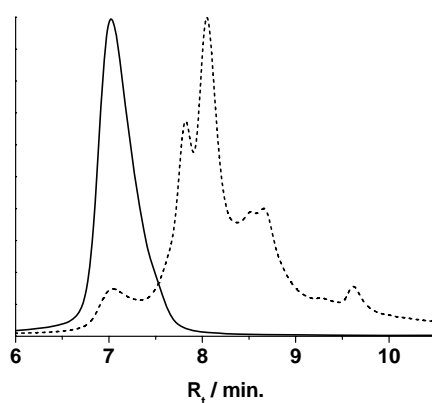


Figure 4.8: Normalized GPC traces of fractions **5a** (black line) and **5b** (dashed line) measured on a mixed-D column, CHCl₃, UV-detection at 254 nm and polystyrene as internal standard.

Fraction **5a** was subjected to a photophysical study in CHCl₃, THF and heptane. The remarkable ‘memory’ effect reported for the OPV3 decorated poly(ureidophthalimide) **3a** (Figure 4.3) is also observed for the OPV4 analogue **5a**. The UV-vis spectrum of a CHCl₃

solution shows two absorption maxima located at 326 nm ($\epsilon = 39500 \text{ M}^{-1}\text{cm}^{-1}$) and 436 nm ($\epsilon = 74000 \text{ M}^{-1}\text{cm}^{-1}$), which can be attributed to the ureidophthalimide moiety and the OPV4 unit, respectively (Figure 4.9). Furthermore, **5a** proved to be CD silent in CHCl_3 , suggesting a random coil conformation.

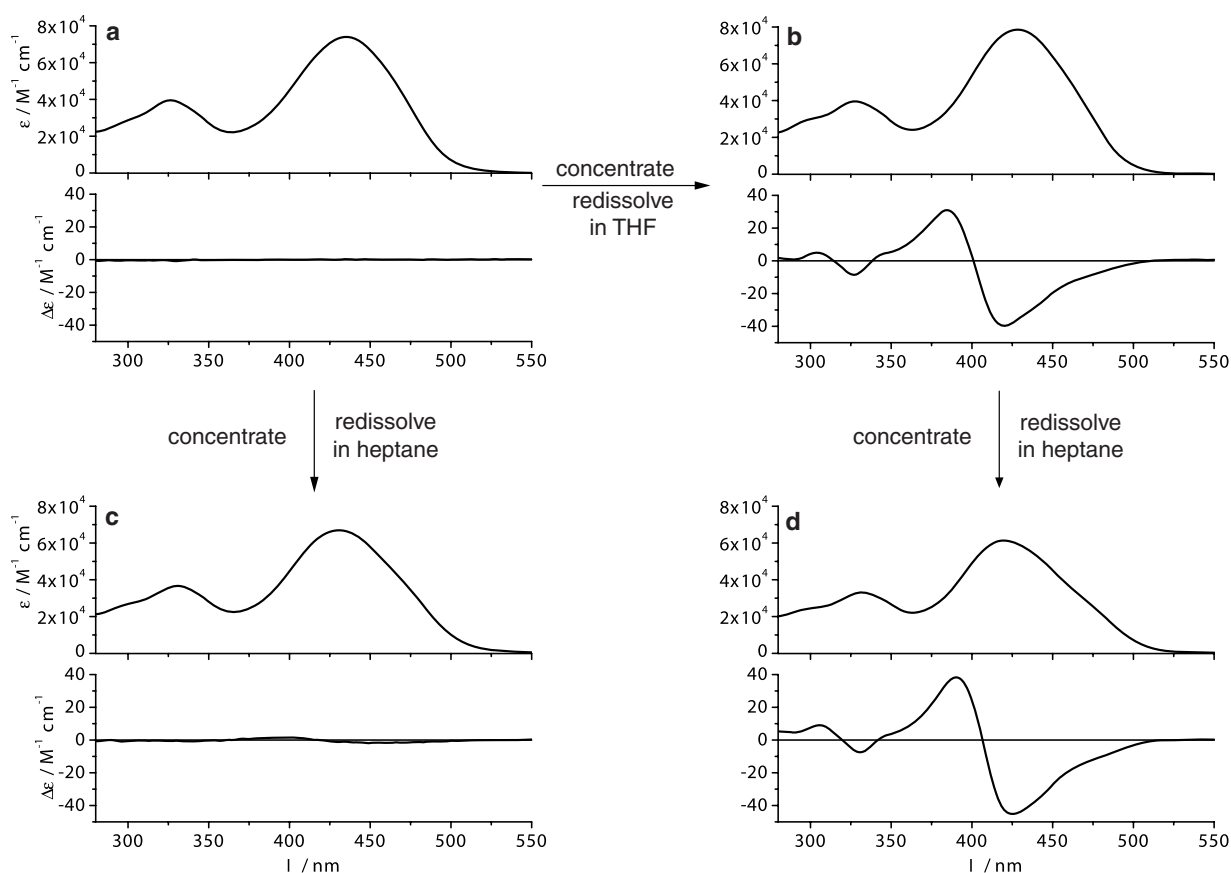


Figure 4.9: UV-vis and CD spectra of **5a** in a) CHCl_3 , $1.3 \times 10^{-5} \text{ M}$. b) THF, $1.5 \times 10^{-5} \text{ M}$. c) heptane, $1.4 \times 10^{-5} \text{ M}$ with a CHCl_3 history. d) heptane $1.4 \times 10^{-5} \text{ M}$ with a THF history.

The UV-vis spectrum of **5a** in THF shows absorption maxima at 328 nm ($\epsilon = 39600 \text{ M}^{-1}\text{cm}^{-1}$) and 429 nm ($\epsilon = 78500 \text{ M}^{-1}\text{cm}^{-1}$). The THF solution reveals two bisignate Cotton effects. The first at 304 nm ($g = +1.6 \times 10^{-4}$) and 328 nm ($g = -2.1 \times 10^{-4}$) with a zero crossing at 314 nm and a second bisignate Cotton effect at 385 nm ($g = +8.9 \times 10^{-4}$) and 420 nm ($g = -5.2 \times 10^{-4}$) with a zero crossing at 401 nm. This is a strong indication for the chiral organization of the OPV4 chromophores. It is unclear why the zero crossing does not coincide with the absorption maximum in UV-vis as was observed for the OPV3 foldamer (Figure 4.3). Moreover, in contrast to the CD measurements on the OPV3 system this system also shows a bisignate Cotton effect in the short wavelength regime which can be attributed to a chiral arrangement of the phthalimide units. A heptane solution with a CHCl_3 history is CD silent with somewhat red-shifted maxima at 330 nm ($\epsilon = 36700 \text{ M}^{-1}\text{cm}^{-1}$) and 430 nm ($\epsilon = 66900 \text{ M}^{-1}\text{cm}^{-1}$), compared to the

UV-vis measurement in CHCl_3 . However, a heptane solution with a THF history reveals two bisignate Cotton effects. The short wavelength bisignate Cotton effect has a zero crossing at 320 nm and maxima at 305 nm ($g = +3.6 \times 10^{-4}$) and 331 nm ($g = -2.2 \times 10^{-4}$). The second bisignate effect has maxima at 390 nm ($g = +1.0 \times 10^{-3}$) and 425 nm ($g = -7.5 \times 10^{-4}$) with a zero crossing at 407 nm. The accompanying UV-vis spectrum shows a minor red-shift of the absorption maxima to 332 nm ($\epsilon = 33100 \text{ M}^{-1}\text{cm}^{-1}$) and 420 nm ($\epsilon = 61300 \text{ M}^{-1}\text{cm}^{-1}$). In addition, the monomeric precursor 3,6-bis(acetylamino)-*N*-OPV4-phthalimide²⁹ is CD silent in CHCl_3 , THF and heptane.

The stability of the putative helical architectures is investigated by subjecting a THF and heptane solution of **5a** to a temperature dependent UV-vis and CD experiment (Figure 4.10). Raising the temperature of the THF solution hardly affects the intensity in combination with an almost negligible hypsochromic shift of the absorption maxima. The Cotton effect, however, does show a marked decrease upon raising the temperature, but reclaims its original value upon cooling and, thereby demonstrating the dynamics of the system in THF.

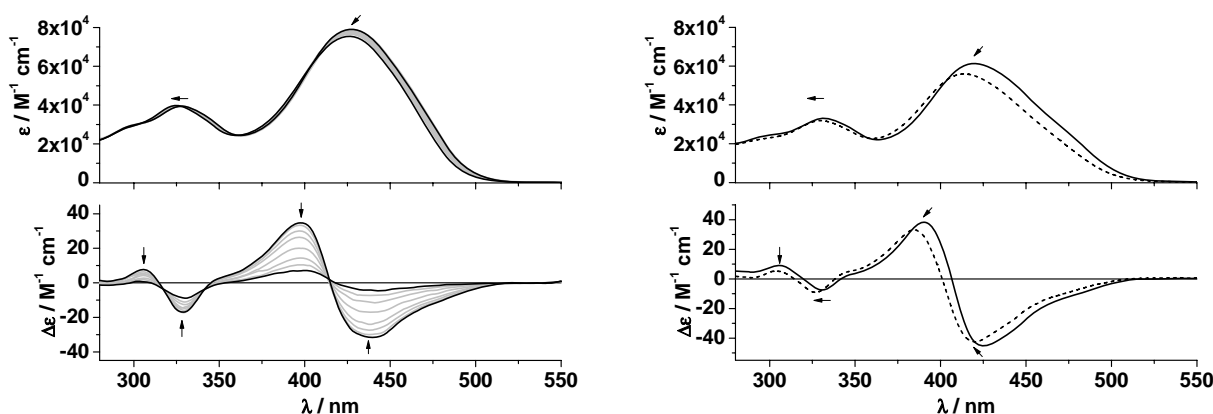


Figure 4.10: Temperature-dependent UV-vis and CD spectroscopy of **5a** in (a) THF, $1.5 \times 10^{-5} \text{ M}$, from 20°C (black line) to 55°C (black line) in steps of 5°C (grey lines); and (b) heptane, $1.4 \times 10^{-5} \text{ M}$, from 20°C (black line) to 80°C (dashed line).

However, elevation of temperature of the heptane solution to 80°C displays only a minor decrease of the Cotton effect, indicating the remarkable stability of the supramolecular architecture in heptane. Furthermore, it seems that the whole spectrum undergoes a shift to shorter wavelength. A similar effect is observed in the UV-vis spectrum. The nature of this effect remains unclear. In addition, prolonged heating of both solutions doesn't affect the Cotton effect any further.

In contrast to the melting curve of **3a** (decorated with OPV3) the melting curve of **5a** (decorated with OPV4) reveals a steeper slope indicating a difference in the change in enthalpy involved in the unfolding process, albeit that the differences are small. (Figure 4.11).

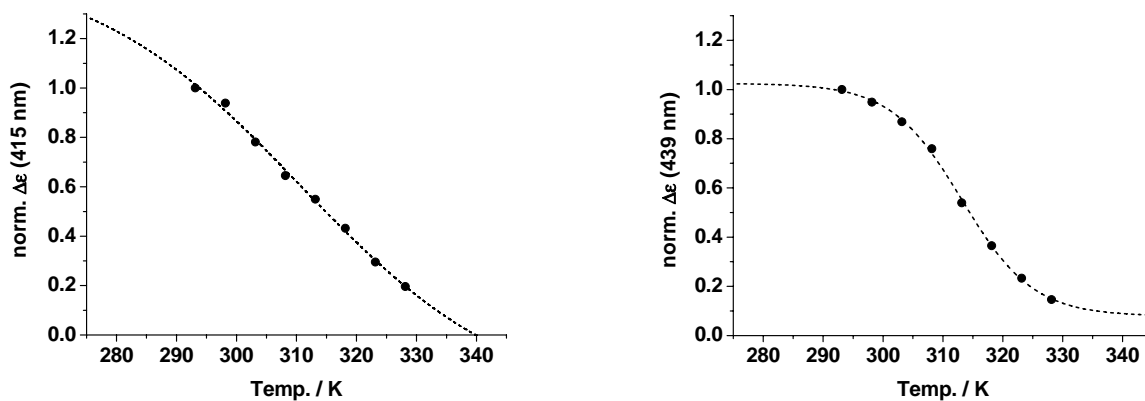


Figure 4.11: Melting curves of the Cotton effect in THF of **3a** (OPV3 decorated) at 415 nm (left), and of **5a** (OPV4 decorated) at 439 nm (right). The curves represent a sigmoidal fit (dashed line) of the data points (black circles).

The almost linear relation between temperature and Cotton effect in **3a** indicates the absence of clear transition between folded and unfolded structures. The difference can be attributed to the larger π -surface in case of the OPV4 decorated foldamer. The slope of the linear part of both curves (~ 0.03) and the melting transition (~ 312 K) are comparable. It must be noted that the Cotton effect in both cases does not reach zero.

The concentration-dependent UV-vis and CD measurements of **5a** in THF display only a minor change in the absorption maxima and Cotton effect over a 100 fold concentration range between 10^{-4} M to 10^{-6} M (Figure 4.12). This observation indicates that the Cotton effect is the result of an intramolecular aggregation.

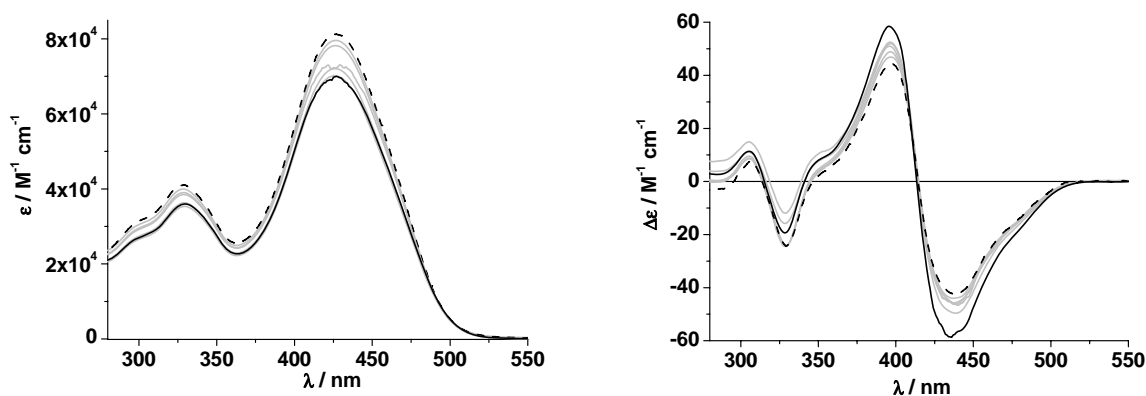
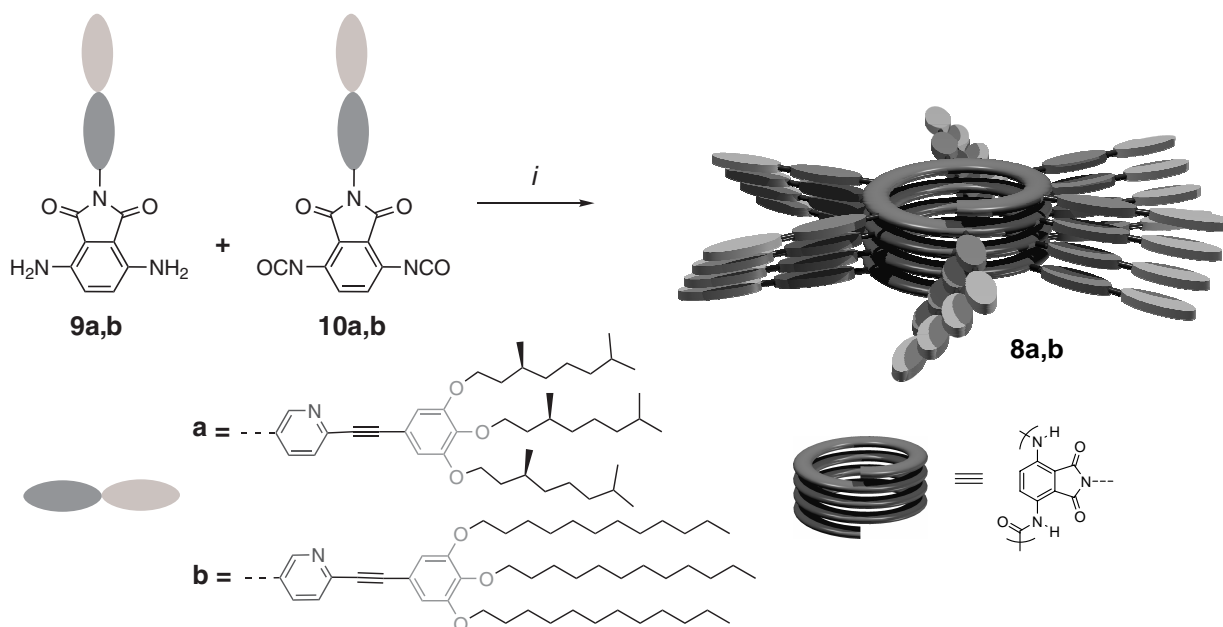


Figure 4.12: Concentration dependent UV-vis (left) and CD (right) spectra of **5a** in THF from 5.1×10^{-4} M (black line) to 5.1×10^{-6} M (dashed line) in six steps (grey lines).

In spite of the presence of a small amount ($<5\%$) of oligomers long enough to make one helical turn, **5b** displayed no Cotton effect in THF. This behavior was expected based on the results obtained with **3b**, the short OPV3 decorated ureidophthalimide oligomers. Future STM experiments must prove whether **5b** reveals a better surface orientation due to the larger π -system.

4.4 Ureidophthalimide foldamer decorated with D- π -A chromophores

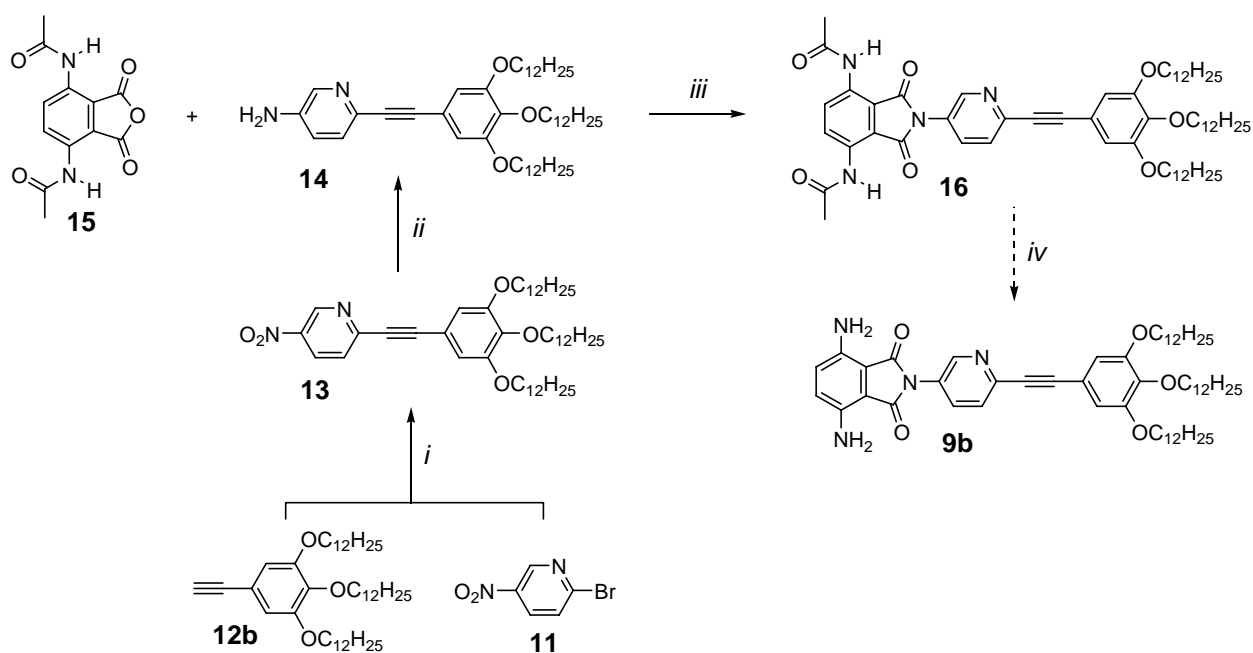
Besides the introduction of OPV chromophores the introduction of a chromophore with a weak donor (D) acceptor (A) interaction was envisaged in cooperation with Guy Koeckelberghs (KU Leuven) (Scheme 4.3). In our design pyridine (weak acceptor) is linked *via* an ethynyl functionality to 3,4,5-tri-alkoxybenzene (donor).



Scheme 4.3: Synthesis of poly(ureidophthalimide) with peripheral D-A chromophores **8a,b**. i) DMAP (1.0 equiv.), $PhCH_3$, 17 h.

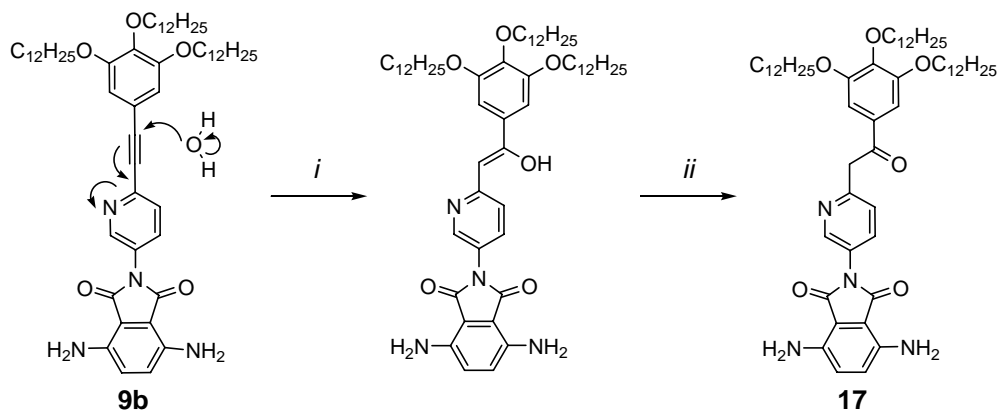
The choice of the ethynyl linker is based on its conjugative properties and the synthetic ease of introduction *via* a robust palladium mediated Sonogashira coupling. In addition, with an ethynyl linker the entire donor-acceptor chromophore is designed as a linear rod, excluding conformational ambiguity, which might disturb the packing of the periphery of the foldamer, such as *cis-trans* isomerization in the case of a vinyl linker. The foldamers decorated with peripheral D-A chromophores **8a** with a chiral periphery and **8b** with an achiral periphery were obtained by the reaction of diaminophthalimide **9** with diisocyanate **10** in refluxing toluene in the presence of 4-dimethylaminopyridine (Scheme 4.3).

The first synthetic approach to arrive at the newly designed donor-acceptor chromophore started with the coupling of commercial 2-bromo-5-nitropyridine **11** with phenylacetylene **12b**³⁰ under palladium mediated Sonogashira conditions (Scheme 4.4). Nitro adduct **13** was then reduced to amine **14** that was subsequently reacted with 3,6-bis(acetylamino)phthalic anhydride **15**³¹ to form 3,6-bis(acetylamino)-phthalimide **16**. The final step towards polymer precursor **9b** was supposed to be the removal of the acetyl functionalities by treatment with aqueous HCl in refluxing dioxane.



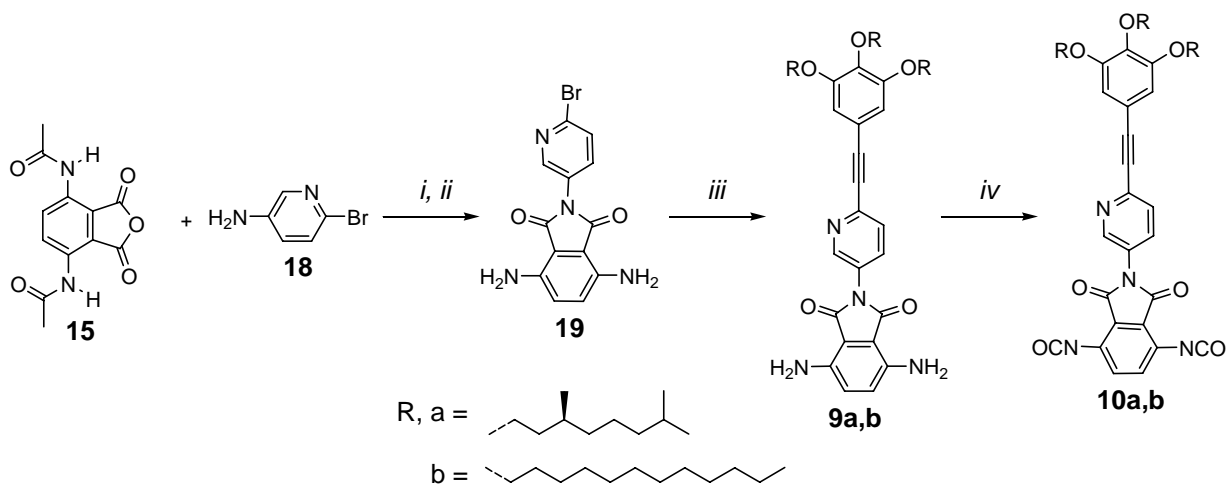
Scheme 4.4: First approach to arrive at polymer precursor **9b**. *i*) $\text{Pd}(\text{PPh}_3)_2(\text{Cl})_2$, CuI , THF , 40°C , 24 h, 89%. *ii*) SnCl_2 (8 equiv.), EtOAc/EtOH , reflux, 1 h, 39%. *iii*) dioxane, reflux, 24 h. *iv*) 1.6 M HCl in dioxane, reflux, 30 min; neutralization.

This however, did not only afford desired **9b** but partly gave the water adduct, ketone **17**. The mixture of diamine **9b** and ketone **17** (Scheme 4.5) proved to be inseparable. The addition of water most likely takes place in a Michael-type addition due to activation of the triple bond by its conjugation with the electron withdrawing pyridine ring. Protonation of the pyridine nitrogen in the acidic environment renders the triple bond even more prone to water addition. Subsequent tautomerization resulted in undesired **17** (Scheme 4.5).



Scheme 4.5: Presumable Michael-addition on **9b** followed by enol-keto tautomerization resulting in **17**. *i*) addition of H_2O . *ii*) tautomerization.

To circumvent the problems during hydrolyses of the amide functionalities, hydrolysis is performed prior to introduction of the acetylene moiety. Thus, 3,6-diaminophthalimide **19**³² is synthesized by reaction of aminopyridine **18** with phthalic anhydride **15**³¹ (Scheme 4.6).



Scheme 4.6: Synthesis of polymer precursors diamines **9a,b** and diisocyanates **10a,b**. i) dioxane, reflux, 17 h, 65%, ii) 1.6 M HCl aq. in dioxane, reflux; neutralization, ~70% iii) acetylene **12a**³⁰ or **12b**³⁰, Pd(PPh₃)₄ (5 mol%), Cul (5 mol%), DMF, DPEA, 80°C, 17 h, **9a**: > 80%, **9b**: >80%. iv) COCl₂, PhCH₃, rt, 1 h, **10a**: ~100%, **10b**: ~100%.

Subsequent introduction of acetylene **12b**³⁰ furnished polymer precursor **9b**. Diamine **9b** is converted into the corresponding diisocyanate **10b** by reaction with phosgene in toluene at room temperature. This successful approach is also employed for the formation of chiral polymer precursors **9a** and **10a**. Column chromatography over silica gel allowed –besides removal of the non-migrating DMAP– separation of the longer chiral oligomers (**8a-I**, ~58 w%) with lengths of 6-29 units from the shorter ones (**8a-II**, ~22 w%) with lengths of 1-27 units (Figure 4.13). GPC analysis indicated only oligomeric lengths of 6-22 units for achiral **8b**.

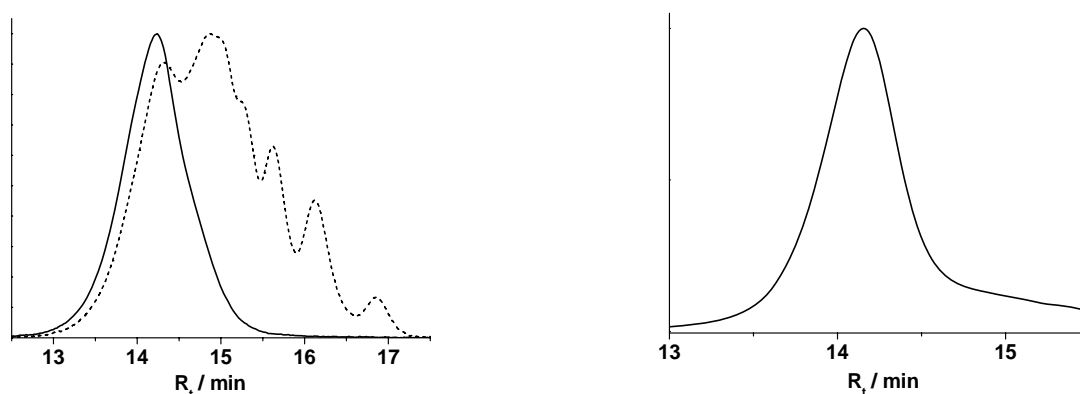


Figure 4.13: GPC traces of chiral fraction **8a-I** (black line) and **8a-II** (dashed line) (left), and achiral oligomers fraction **8b** (right), measured on a mixed-C-D column combination, CHCl₃, detection at 420 nm and polystyrene as internal standard.

Fraction **8a-I** was subjected to a preliminary UV-vis and CD spectroscopy analysis in dilute THF solution (Figure 4.14). Two absorptions are observed with maxima located at 323 nm and 394 nm. Both can be attributed to the phthalimide unit. However, the D-A unit also absorbs in the same wavelength area.

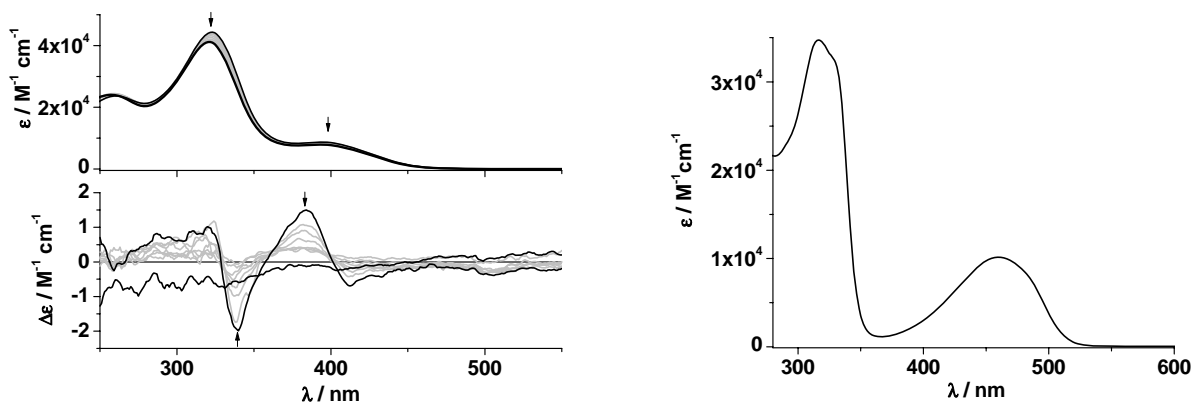


Figure 4.14: Temperature dependent UV-vis and CD spectroscopy of **8a-I**. (left) THF, $4.1 \cdot 10^{-5}$ M, from 15°C (black line) to 55°C (black line) in steps of 5°C (grey lines); and (right) UV-vis spectrum of monomer **9a** in THF, 4.3×10^{-5} M.

The zero crossing of the Cotton effect does not seem to coincide with one of the absorption maxima. A temperature dependent study in THF shows a decreasing Cotton effect upon raising the temperature. The original Cotton effect is reclaimed when the solution is cooled to room temperature again. These observations establish the dynamics of the architecture in THF. Similar measurements in CHCl_3 did not show a Cotton effect.

Further studies must reveal whether the use of nonlinear optics is suitable to strengthen the assumption that poly (ureidophthalimide) based architectures can indeed adopt a helical conformation in solution.

4.5 Conclusions

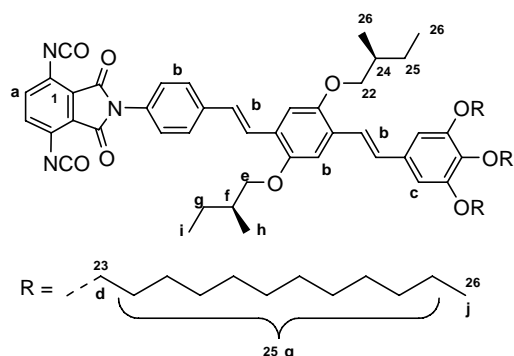
In summary, we have shown that a poly(ureidophthalimide) backbone decorated with OPV chromophores assumes a random coil conformation in CHCl_3 but adopts a putative helical conformation in THF. Measurements in heptane show that the initial secondary organization is preserved depending on the solvent used prior to heptane. Moreover, temperature dependent CD studies establish the dynamics of the secondary architectures in THF and the remarkable stability in heptane. For sure, the intramolecular hydrogen bonding of the phthalimide units is responsible for the initial chiral alignment of the OPV chromophores. However, the rather small Cotton effects might be an indication of the presence of frustrated stacks due to non chiral aggregation of OPV units. Although the role of THF remains undefined it is clear that solvent in general and THF in specific plays an important role in the folding process.

4.6 Outlook

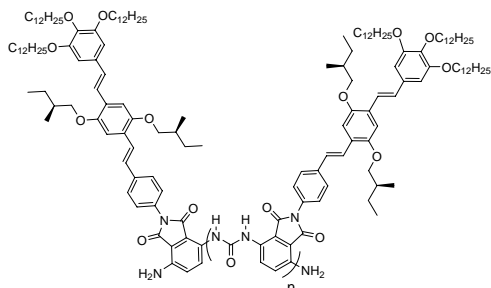
In Sections 4.2 and 4.3 the potential of the ureidophthalimide foldamer as a scaffold for the chiral organization of peripheral chromophores is discussed. CD studies indeed indicated the presence of helical architectures. Of course, with the Cotton effect in CD spectroscopy the expression of chirality is only reflected by the diastereomeric excess of the preferred helical handedness. Nevertheless, $^1\text{H-NMR}$ measurements are in agreement with these observations as was also reported by van Gorp²⁸. The typical downfield shifted urea protons, in combination with the deshielded aromatic protons of the adjacent phthalimide moiety point toward a curved backbone. However, the rather broad spectra, due to the polydisperse nature limit the use of more advanced and powerful NMR techniques like NOESY to establish the folding. There are numerous examples of non-peptidomimetic foldamers of defined length in literature in which NOE interactions confirm the presence of helical architectures.³³ However, with nonlinear optics (NLO) the helical alignment of peripheral chromophores may be further established. This technique requires material comprising a donor-acceptor (D-A) chromophore. The foldamer decorated with D-A chromophores as presented in section 4.4 may be a suitable candidate. Moreover, fluorescence studies on OPV3 decorated foldamer also indicated the presence of a D-A interaction and may therefore also be applicable.

4.7 Experimental

General. See experimental section of chapter 2.



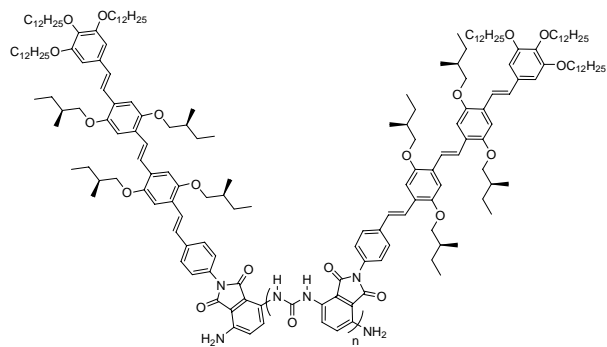
3,6-Diisocyanato-N-OPV3-phthalimide (2). A solution of diamine **1** (53.8 mg, 0.0455 mmol) in toluene (0.5 mL) was added dropwise to a 20 *w*% solution of phosgene in toluene (0.45 mL, 0.9100 mmol) at rt. The reaction was stirred for 30 min. at rt and subsequently refluxed for 30 min. The reaction was monitored by IR. After full conversion the reaction mixture was concentrated (fume hood!) and the residual orange solid was characterized as desired **2** (0.0582 g, 0.0471 mmol, ~100%). $^1\text{H NMR}$ (300 MHz, CDCl_3) δ (ppm) = 7.51 (d, 2H, *J* = 8.2 Hz, **a**), 7.40-6.95 (md, **b**), 6.66 (s, 2H, **c**), 3.97-3.87 (m, 6H, **d**), 3.84-3.74 (m, 4H, **e**), 1.96-1.80 (m, 2H, **f**), 1.78-1.52, 1.42-1.33 and 1.30-1.19 (m, 64H, **g**), 1.05 (d, 6H, *J* = 6.6 Hz, **h**), 0.94 (t, 6H, *J* = 6.2 Hz, **i**), 0.81 (t, 9H, *J* = 6.3 Hz, **j**); $^{13}\text{C NMR}$ (CDCl_3) δ (ppm) = 165.9 (**1**), 153.4 (**2**), 151.5 (**3**), 151.1 (**4**), 138.3 (**5**), 133.2 (**6**), 132.2 (**7**), 129.5 (**8**), 129.0 (**9**), 128.9 (**10**), 127.6 (**11**), 127.4 (**12**), 127.1 (**13**), 126.4 (**14**), 126.3 (**15**), 124.9 (**16**), 123.4 (**17**), 122.5 (**18**), 110.9 (**19**), 110.0 (**20**), 105.2 (**21**), 74.5 and 74.3 (**22**), 73.7 and 69.2 (**23** OCH_2CH_2), 35.3 and 35.2 (**24**), 32.1, 30.5, 29.9, 29.8, 29.8, 29.6, 29.5, 26.6, 26.5, 26.3, 22.8 (**25**), 17.0, 16.9, 14.2, 11.7, 11.6 (**26**); **FT-IR** (ATR) σ (cm^{-1}) = 2957, 2920, 2852, 2245 (N=C=O), 1715 (C=O), 1423, 1384, 1200 (C-O), 1116 (C-O).



Poly-ureido-N-OPV3-phthalimide (3). A solution of diamine **1** (49.5 mg, 41.9 μmol) and DMAP (5.7 mg, 41.9 μmol) in toluene (0.5 mL) was heated to reflux then a solution of diisocyanate **2** (51.7 mg, 41.9 μmol) in toluene (0.3 mL) was added dropwise. The mixture was heated under reflux for 21 h. The mixture was concentrated *in vacuo* and column chromatography (silica gel, gradient of CHCl_3 to 10 *v*% $\text{EtOAc}/\text{CHCl}_3$) afforded removal of the non-migrating DMAP

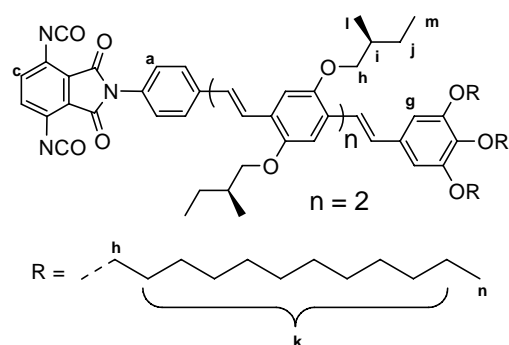
and separation of long oligomers (**3a**) from the short oligomers (**3b**) as orange solids. Long oligomers (**3a**) (66.8 mg, ~66 *w*%) **GPC** (CHCl_3 , mixed-D, 420 nm), R_t (min.) = 7.26; $^1\text{H NMR}$ (300 MHz, CDCl_3) δ (ppm) = only broad peaks at rt. and at 55°C; (33 *v*% HF^iP in CDCl_3) = 8.93 (br s, H_{urea}), 8.70 (br s), 8.49 (br s, H_{ar} phthalimide), 8.18 (br d) 7.70 (br d), 7.59-7.05 (multiple peaks, OPV3 moiety), 4.65-3.36 (br m, $\text{HF}^i\text{P} + 5 \times \text{OCH}_2$), 2.01-0.90 (alkyl tails); **FT-IR** (ATR, NEAT from CHCl_3) σ (cm^{-1}) = 3347, 2958, 2922, 2853, 1724, 1696, 1612, 1578, 1505, 1477, 1423, 1394, 1352, 1261, 1225, 1198, 1180, 1113, 1023, 963, 930, 844, 805, 760, 722; (NEAT from heptane with CHCl_3 history) σ (cm^{-1}) = 3347, 2957, 2922, 2853, 1724, 1696, 1611, 1578, 1505, 1477, 1423, 1393, 1352, 1261, 1225, 1198, 1180, 1113, 1020, 962, 930, 844, 802, 759, 722; (NEAT from THF) σ (cm^{-1}) = 3342, 2958, 2922, 2853, 1727, 1699, 1647, 1610, 1578, 1552, 1504, 1477, 1424, 1405, 1355, 1277, 1261, 1226, 1200, 1180, 1115, 1091, 1022, 961, 930, 846, 805, 757, 742, 722, 697; (NEAT from heptane with THF history) σ (cm^{-1}) = 3343, 2957, 2922, 2853, 1728, 1699, 1646, 1609, 1579, 1553, 1505, 1478, 1424, 1406, 1356, 1260, 1277, 1226, 1200, 1180, 1116, 1092, 1043, 960, 929, 846, 810, 757, 722, 697. Short oligomers (**3b**)

(13.9 mg, ~15 w%), as an orange solid. **GPC** (CHCl_3 , mixed-D, 410 nm), R_t (min.) = 7.86, 8.25; **$^1\text{H NMR}$** (300 MHz, 33 v% HFIP in CDCl_3) δ (ppm) = 8.92 (br s, H_{urea}), 8.71 (br s), 8.46 (br), 8.17, 7.70, 7.57-7.23 (multiple peaks, OPV3 moiety), 7.18 (br d), 6.78 (s), 5.27 (br, NH_2), 4.66-3.59 (HFIP , $\times \text{OCH}_2$), 1.83-1.46 (br m, alkyl tail), 1.29-0.72 (br m, alkyl tail); **FT-IR** (ATR, NEAT from CHCl_3) σ (cm^{-1}) = 3474, 3358, 2956, 2922, 2853, 1735, 1694, 1647, 1613, 1579, 1505, 1483, 1467, 1423, 1389, 1353, 1278, 1226, 1200, 1115, 1041, 963, 931, 846, 812, 760, 742, 722, 697.



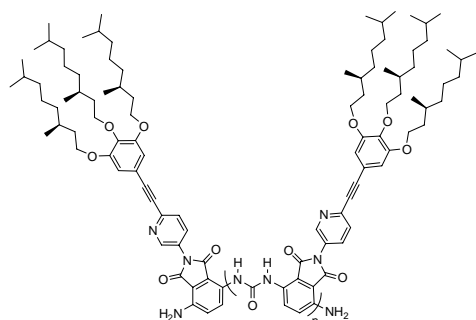
Poly-ureido-N-OPV4-phthalimide (5). A solution of diamine **6** (57.4 mg, 0.039 mmol), diisocyanate **7** (59.3 mg, 0.039 mmol) and DMAP (4.80 mg, 0.039 mmol) was dissolved in toluene (2.0 mL) and heated under reflux for 17 h. After concentration *in vacuo* the crude mixture was purified by column chromatography (silica-gel, CHCl_3 to 30 v% heptane in CHCl_3), affording separation of long oligomers (**5a**) from the short oligomers (**5b**) as orange solids

after concentration. Non-migrating DMAP remained on the silica. Long oligomers (**5a**) (71.5 mg, 61 w%). **GPC** (CHCl_3 , mixed-D, 254 nm), R_t (min.) = 7.02; **$^1\text{H NMR}$** (300 MHz, CDCl_3) δ (ppm) = only broad signals, 8.8-8.2 (2H, $2 \times H_{\text{urea}}$), 7.8-6.8 (16H), 6.74 (br s, 2H, H_{ar} tridodecyloxy benzene), 4.1-3.4 (14H, $7 \times \text{OCH}_2$), 2.1-0.7 (105H, alkyl tails); (300 MHz, 2:1 v/v, CDCl_3 : HFIP) δ (ppm) = better resolution, still broad signals, 8.96 (1H, H_{urea}), 8.51 (1H, H_{ar} , phthalimide), 7.9-7.0 (16H), 6.81 (s, 2H, H_{ar} tridodecyloxy benzene), 4.8-3.4 (HFIP + $7 \times \text{OCH}_2$), 2.1-0.8 (105H, alkyl tails). **FT-IR** (ATR, NEAT from CHCl_3) σ (cm^{-1}) = 3353, 2957, 2922, 2853, 1723, 1694, 1648, 1613, 1578, 1504, 1477, 1421, 1392, 1350, 1277, 1225, 1198, 1181, 1115, 1042, 1009, 963, 931, 852, 842, 813, 760, 722, 686. Short oligomers (**5b**) (8.3 mg, 7 w%). **GPC** (CHCl_3 , mixed-D, 254 nm), R_t (min.) = 7.05, 7.83, 8.05, 8.53 and 8.66; **$^1\text{H NMR}$** (300 MHz, CDCl_3) δ (ppm) = 8.93 (H_{urea}), 8.44 (H_{ar} phthalimide), 7.93, 7.8-7.0 (), 6.74, 5.17 (br s, NH_2), 4.74, 4.2-3.8 ($7 \times \text{OCH}_2$), 3.22, 2.2-0.8 (alkyl tails); (300 MHz, 2:1 v/v, CDCl_3 : HFIP) δ (ppm) = 8.91 (H_{urea}), 8.70, 8.65 (H_{ar} , 3,6-bis(ureido)phthalimide) and 8.50 (H_{ar} , mono ureido phthalimide), 8.14, 7.7-7.1 (H_{ar} + H_{vinyl} , OPV4), 6.84, 6.81 (H_{ar} , tridodecyloxy benzene + H_{ar} , mono amino phthalimide), 6.58 (H_{ar} , diamino phthalimide), 5.26 (br s, NH_2), 4.82 (m), 4.6-3.4 (HFIP + $7 \times \text{OCH}_2$), 3.20 (d), 2.1-0.8 (105H, alkyl tails); **FT-IR** (ATR, NEAT, from CHCl_3) σ (cm^{-1}) = 3474, 3364, 2957, 2922, 2853, 1693, 1649, 1614, 1579, 1536, 1504, 1485, 1466, 1422, 1388, 1341, 1278, 1243, 1225, 1200, 1116, 1043, 1010, 963, 934, 851, 812, 761, 722, 692.



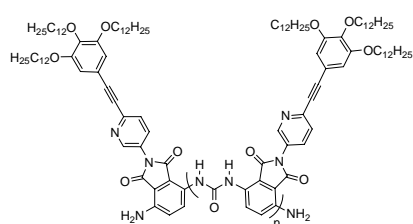
3,6-Diisocyanato-N-OPV4-phthalimide (7). Diamine **6** (57.4 mg, 0.039 mmol) in PhCH_3 (1.5 mL) was added dropwise to a 20 w% solution of phosgene in toluene (0.4 mL, 0.786 mmol) at room temperature. The reaction was monitored by IR. After full conversion the reaction mixture was concentrated (fume hood!) and the residual orange solid was characterized as desired (**7**) (60.3 mg, 0.0399 mmol, ~100%) and used such. **$^1\text{H NMR}$** (300 MHz, CDCl_3) δ (ppm)

= 7.59 (d, 2H, *J* = 8.2 Hz, **a**), 7.51-7.33 (m, 8H, **b**), 7.24 (s, 2H, **c**), 7.17 (d, 2H, *J* = 9.9 Hz, **d**), 7.10 (d, 2H, *J* = 2.5 Hz, **e**), 7.06-6.99 (m, *x*H, **f**), 6.74 (s, 2H, **g**), 4.05-3.81 (m, 14H, **h**), 2.35-1.88 (m, 4H, **i**), 1.86-1.61 (m, 8H, **j**), 1.57-1.27 (m, 60H, **k**), 1.14-1.10 (m, 12H, **l**), 1.02 (t, 12H, *J* = 7.4 Hz, **m**), 0.88 (t, 9H, *J* = 6.5 Hz, **n**); **FT-IR** (ATR) σ (cm⁻¹) = 3062, 2958, 2920, 2852, 2873, 2244, 1786, 1714, 1577, 1540, 1504, 1466, 1423, 1381, 1342, 1242, 1199, 1117, 1044, 964, 902, 855, 824, 809, 753.



Poly-ureido-N-{6-[3,4,5-tris((S)-3,7-dimethyloctyloxy)phenylethynyl]-pyridin-3-yl}phthalimide (8a**).**

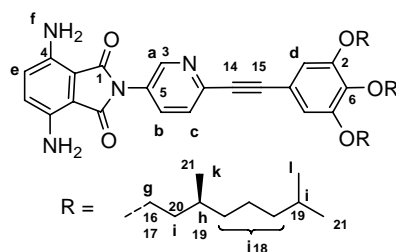
A solution of diamine **9a** (38.9 mg, 47.3 μ mol) and DMAP (5.77 mg, 47.3 μ mol) in toluene (0.8 mL) was added to a solution of diisocyanate **10a** (58.9 mg, 71.6 μ mol) (containing ~30% urea according to ¹H-NMR) in toluene (0.8 mL) and heated under reflux for 17 h. GPC analysis showed oligomer lengths up to ~13 units. The reaction mixture was concentrated and DMAP is removed by column chromatography (silica gel, CHCl₃ to 10 *v*% EtOAc/CHCl₃). In a post-polymerization the isolated residue (0.0886 g) was dissolved in toluene (0.8 mL) and added to a 20 *w*% of phosgene in toluene (0.01 mL, 0.021 mmol) and stirred at rt for 1h. IR indicated the formation of isocyanate. DMAP (2.914 mg, 0.0239 g) was added and the reaction mixture was refluxed for 17 h. GPC showed elongation of the oligomers length. After concentration DMAP was removed by filtration (silica gel 40 *v*% EtOAc/CHCl₃). The mixture was post polymerized 3 more times by extra addition of COCl₂ (0.01 mL, 0.020 mmol, of a 20 *w*% toluene solution) at rt followed by heating under reflux in the absence of DMAP. The reaction was monitored by GPC. The reaction mixture was concentrated. Column chromatography (silica-gel, CHCl₃ to 10 *v*% EtOAc in CHCl₃) afforded separation of the long oligomers (**8a-I**) from the short oligomers (**8a-II**), as orange solids after concentration. Long oligomers (**8a-I**) (57.3 mg, ~58 *w*%), GPC (THF, Mixed-C-D, 420 nm) *R*_t (min) = 14.2, 29-6 units; ¹H NMR (300 MHz, CDCl₃) δ (ppm) = only broad peaks; (33 *v*% HFⁱP in CDCl₃) = 8.96 (br s, *H*_{urea}), 8.62 (s, 2 \times *C*_{phthH}), 8.56 (br, m), 8.43 (d, *C*_{pyrHNpyr}), 8.00 (m, *C*_{pyrHCpyrH}), 7.81 (d, *C*_{pyrHCpyrH}), 7.02 (s), 6.87 (s, 2 \times *C*_{arH}), 6.62, 4.66-3.99 (HFⁱP, and 3 \times OCH₂), 1.89-0.84 (multiple peaks, alkyl tails) **FT-IR** (ATR) σ (cm⁻¹) = 3341, 2954, 2925, 2869, 2215, 1699, 1642, 1611, 1574, 1500, 1474, 1421, 1396, 1361, 1262, 1224, 1178, 1111, 1092, 1043, 1022, 928, 909, 859, 833, 800, 760, 733, 680. Short oligomers (**8a-II**) (22.1 mg, ~22 *w*%), GPC (THF, Mixed-C-D, 420 nm) *R*_t (min) = 14.9, 1-27 units; ¹H NMR (CDCl₃) δ (ppm) = 9.4-8.0 (br m), 8.0-7.8 (br m), 7.7-7.58 (br m), 6.95 (br s), 6.85 (br s), 6.6 (br s), 5.3 (br s, 0.12H, NH₂), 4.35-4.2 (br m), 3.2-3.6 (br m, 6H, 3 \times OCH₂), 2.0-0.5 (br m, 57H, 3 \times alkyl tail); (33 *v*% HFⁱP in CDCl₃) δ (ppm) = 8.97 (), 8.40 (), 8.61 (), 8.56 (), 8.44 (), 8.01 (), 7.81 (), 7.02 (), 6.87 (), 6.62 (), 4.79-3.39 (OCH₂ + HFⁱP), **FT-IR** (ATR) σ (cm⁻¹) = 3447, 2956, 2925, 2869, 2211, 1700, 1642, 1611, 1574, 1500, 1476, 1396, 1364, 1260, 1225, 1180, 1091, 1017, 928, 860, 798, 760.



Poly-ureido-N-{6-[3,4,5-tris(dodecyloxy)phenylethynyl]-pyridin-3-yl}phthalimide (8b**).**

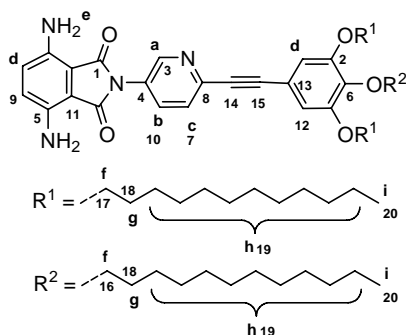
A solution of diamine **9b** (0.0465 g, 0.0513 mmol), diisocyanate **10b** (0.0492 g, 0.0513 mmol) and DMAP (6.267 mg, 0.0513 mmol) was dissolved in PhCH₃ (1.6 mL) and heated under reflux for 17 h. After concentration, DMAP was removed by

filtration (silica gel 40 v% EtOAc/CHCl₃). Concentration the eluted fraction gave a residue that was dissolved in toluene (1.5 mL) and COCl₂ (0.016 mL, 0.0332 mmol, of a 20 w% toluene solution) was added. The mixture was stirred for 30 min at rt and subsequently heated under reflux for 17 h in the absence of DMAP. GPC analysis showed elongation of the oligomeric length. The sequence was repeated two more times until GPC showed no further lengthening. Concentration of the reaction mixture gave (**8b**) (0.0863 g) consisting of 6-27 units as was determined by GPC (THF, mixed-C-D column, 420 nm): Rt = 14.1 min, 6-22. No shorter oligomers were obtained. ¹H NMR (300 MHz, CDCl₃) δ (ppm) = very broad signals: 9.4-7.8 (*H*_{ureum} and *H*_{ar} phthalimide), 7.8-6.2, 4.2-3.4 (6H, OCH₂), 2.0-0.7 (alkyl tails); (300 MHz, 33 v% HFIP in CDCl₃) δ (ppm) = 8.89 (*H*_{ureum}), 8.65, 8.56 (s), 8.47 (d, 1H, *J* = 7.6 Hz, *H*_{pyr}), 8.07 (3H), 7.81 (d, 1H, *J* = 8.0 Hz, *H*_{pyr}), 7.53 (d, 1H, *H*_{pyr}), 7.15, 7.02 (s), 6.86 (s, 2H, *H*_{ar} trialkoxybenzene), 6.61 (s, NH₂), 4.7-3.6 (OCH₂ and HFIP), 2.0-0.8 (alkyl tails). FT-IR (ATR) σ (cm⁻¹) = 3344, 2921, 2852, 2212, 1731, 1699, 1646, 1610, 1574, 1501, 1474, 1422, 1400, 1359, 1278, 1224, 1177, 1115, 1089, 929, 857, 833, 759, 720.



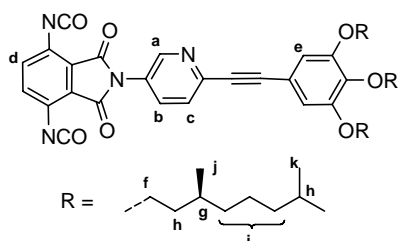
3,6-Diamino-N-{6-[3,4,5-tris((S)-3,7-dimethyloctyloxy)phenylethynyl]pyridin-3-yl}phthalimide (9a**).** Diamine **18**³² (0.0907 g, 0.2723 mmol, ~70% pure), acetylene (**12a**) (0.1383 g, 0.2723 mmol), Pd(PPh₃)₄ (0.0157g, 0.0136 mmol) and CuI (0.0026 g, 0.0136 mmol) were suspended in a mixture of DMF (1.0 mL) and DiPEA (0.75 mL). After freeze-pump-thaw (3 cycles) the suspension was heated at 100°C for

17 h. After concentration *in vacuo* the crude reaction mixture was purified by column chromatography (silica gel, 40 v% EtOAc/CHCl₃, R_f = 0.35) rendering **9a** as an orange solid (0.1347 g, 0.1636 mmol, >85%). ¹H NMR (300 MHz, CDCl₃) δ (ppm) = 8.82 (d, 1H, *J* = 2.5 Hz, **a**), 7.86 (dd, 1H, *J* = 8.5 Hz, *J* = 2.5 Hz, **b**), 7.61 (d, 1H, *J* = 8.5 Hz, **c**), 7.85 (s, 2H, **d**), 6.83 (s, 2H, **e**), 5.01 (s, 4H, **f**), 4.08-3.96 (m, 6H, **g**), 2.23-1.80 (m, 3H, **h**), 1.80-1.40 (m, 9H, **i**), 1.39-1.07 (m, 18H, **j**), 0.94 (t, 9H, *J* = 6.3 Hz, **k**), 0.87 (d, 18H, *J* = 6.6 Hz, **l**); ¹³C NMR (CDCl₃) δ (ppm) = 167.7 (**1**), 153.1 (**2**), 147.1 (**3**), 141.6 (**4**), 139.7 (**5**), 139.0 (**6**), 133.1 (**7**), 128.3 (**8**), 126.8 (**9**), 125.7 (**10**), 116.6 (**11**), 110.6 (**12**), 108.6 (**13**), 90.5 (**14**), 87.4 (**15**), 71.9 (**16**), 67.5 (**17**), 39.4, 39.4, 37.6, 37.4, 37.3, 36.4 (**18**), 29.9, 29.8, 28.1 (**19**), 24.8, 24.8 (**20**), 22.8, 22.7, 19.7 (**21**); FT-IR (ATR) σ (cm⁻¹) = 3468, 3367, 3177, 2954, 2925, 2869, 2211, 1732, 1689, 1657, 1617, 1573, 1492, 1421, 1366, 1266, 1226, 1114, 1070, 967, 942, 830, 760, 750; MS (MALDI-TOF), C₅₁H₇₄N₄O₅, calculated: 822.57, found: 822.42; Analysis, calculated: C, 74.41; H, 9.06; N, 6.81; found: C, 74.00, H, 8.93, N, 6.40. UV-vis (THF, 4.21 × 10⁻⁵ M): λ_{max} = 460 nm (ε = 10160 M⁻¹cm⁻¹) and 317 nm (ε = 34742 M⁻¹cm⁻¹).

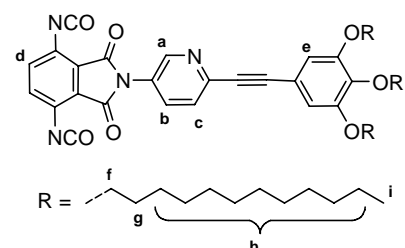


3,6-Diamino-N-6-[[3,4,5-tris(dodecyloxy)phenyl]ethynyl]pyridin-3-yl}phthalimide (9b**).** Diamine **18**³² (0.0726 g, 0.2179 mmol, ~70% pure), acetylene (**12b**) (0.1428 g, 0.2179 mmol) Pd(PPh₃)₄ (0.0126 g, 0.0109 mmol) and CuI (0.0021 g, 0.0109 mmol) were suspended in a mixture of DMF (1.0 mL) and DiPEA (0.75 mL). After freeze-pump-thaw (3 cycles) the suspension was heated at 100°C for 17 h. After concentration *in vacuo* the crude reaction mixture was purified by column chromatography (silica gel, CHCl₃ to 50 v% EtOAc in CHCl₃) which gave **9b** as an orange solid (0.1229 g, 0.1356 mmol, >88%). ¹H NMR (300 MHz,

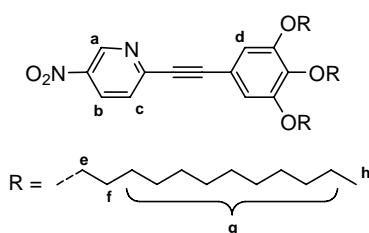
CDCl₃) δ (ppm) = 8.81 (d, 1H, *J* = 2.2 Hz, **a**), 7.86 (dd, 1H, *J* = 8.4 Hz, *J* = 2.4 Hz, **b**), 7.61 (d, 1H, *J* = 8.5, **c**), 6.83 (s, 4H, **d**), 5.00 (s, 4H, **e**), 4.01-3.96 (m, 6H, **f**), 1.86-1.70 (m, 6H, **g**), 1.47-1.21 (m, 54H, **h**), 0.88 (t, 9H, *J* = 6.6 Hz, **i**); ¹³C NMR (75 MHz, CDCl₃) δ (ppm) = 167.7 (**1**), 153.1 (**2**), 147.1 (**3**), 141.6 (**4**), 139.7 (**5**), 139.0 (**6**), 133.1 (**7**), 128.3 (**8**), 126.8 (**9**), 125.7 (**10**), 116.5 (**11**), 110.6 (**12**), 108.7 (**13**), 90.5 (**14**), 87.3 (**15**), 73.7 (**16**), 69.2 (**17**), 32.0 (**18**), 30.4, 29.9, 29.8, 29.8, 29.7, 29.5, 29.5, 29.4, 26.2, 22.8 (10 × CH₂, **19**), 14.2 (**20**); FT-IR (ATR) σ (cm⁻¹) = 3453, 3355, 3175, 2920, 2852, 2210, 1736, 1689, 1658, 1618, 1573, 1492, 1468, 1374, 1267, 1231, 1119, 1078, 968, 942, 827, 759, 749, 721; MS (MALDI-TOF), C₅₇H₈₆N₄O₅, calculated: 906.66; found: 907.62 (+H⁺).



3,6-Diisocyanato-N-{6-[3,4,5-tris((S)-3,7-dimethyloctyloxy)phenylethynyl]-pyridin-3-yl}phthalimide (10a). Diamine **9a** (0.0589 g, 0.0716 mmol) dissolved in PhCH₃ (1.3 mL) was added dropwise to a 20 *w*% solution of phosgene in toluene (0.75 mL, 1.4230 mmol) at room temperature. After all diamine was added, the reaction was monitored by IR. Additional heating to reflux until all amine was converted. The reaction mixture was concentrated (fume hood!) and the obtained orange solid was determined as desired (**10a**) however NMR analysis also showed peaks corresponding to a small amount of urea formation and GPC analysis showed the presence of dimer and trimer. (0.061 g, 0.070 mmol, 97%). The reaction mixture was used as such. ¹H NMR (300 MHz, CDCl₃) δ (ppm) = 8.79 (s, 1H, **a**), 7.86 (d, 1H, *J* = 8.0 Hz, **b**), 7.63 (d, 1H, *J* = 7.7 Hz, **c**), 7.31 (s, 2H, **d**), 6.83 (s, 2H, **e**), 4.01 (m, 6H, **f**), 1.90-1.80 (m, 3H, **g**), 1.78-1.43 (m, 9H, **h**), 1.34-1.07 (m, 18H, **i**), 0.95 (d, 9H, **j**), 0.88 (d, 18H, **k**); FT-IR (ATR) σ (cm⁻¹) = 3353 (small urea absorption) 2954, 2927, 2870, 2248, 1714, 1573, 1516, 1500, 1482, 1384, 1365, 1266, 1229, 1198, 1116, 901, 837, 757.

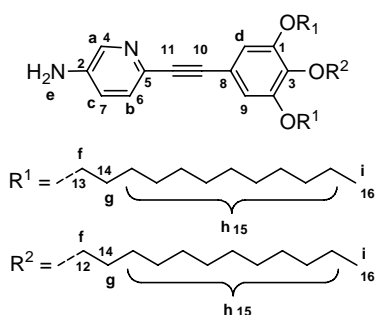


4,7-Diisocyanato-N-{6-[3,4,5-tris(dodecyloxy)phenylethynyl]-pyridin-3-yl}phthalimide (10b). Diamine **9b** (0.0500 g, 0.0552 mmol) dissolved in toluene (1.3 mL) was added dropwise to a 20 *w*% solution of phosgene in toluene (0.55 mL, 1.1034 mmol) at room temperature. The reaction was monitored by IR. When all amine had reacted to isocyanate the reaction was stopped and the mixture concentrated *in vacuo* (fume hood!) which gave **10b** as an orange solid (0.0511g, 0.0533 mmol, 97%). ¹H NMR (300 MHz, CDCl₃) δ (ppm) = 8.79 (d, 1H, *J* = 2.2 Hz, **a**), 7.85 (dd, 1H, *J* = 8.2 Hz, *J* = 2.5 Hz, **b**), 7.63 (d, 1H, *J* = 8.2 Hz, **c**), 7.33 (s, 2H, **d**), 6.83 (s, 2H, **e**), 4.03-3.96 (m, 6H, **f**), 1.86-1.70 (m, 6H, **g**), 1.49-1.09 (m, 60H, **h**), 0.88 (t, 9H, *J* = 6.7 Hz, **i**); FT-IR (ATR) σ (cm⁻¹) = 2923, 2853, 2244, 1716, 1575, 1539, 1503, 1468, 1388, 1267, 1235, 1121, 901, 838, 755.



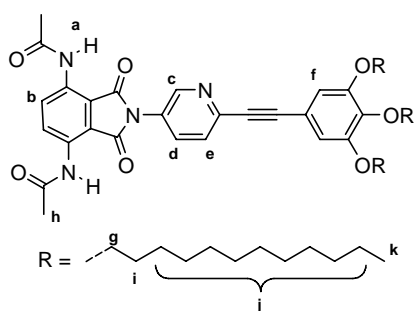
5-Nitro-2-((3,4,5-tris(dodecyloxy)phenyl)ethynyl)pyridine (13). A solution of acetylene **12b** (1.683 g, 2.50 mmol) in THF (13 mL) was added dropwise to a suspension of bromopyridine **11** (0.508 g, 2.50 mmol), CuI (0.0761 g, 0.400 mmol) and Pd(PPh₃)₂ (0.0702 g, 0.100 mmol) in THF (10 mL) at 40°C, that was purged with argon for 30 min prior to use. The temperature was allowed to reach 50°C after complete addition and the

mixture was additionally stirred for 17 h. The reaction mixture was poured into 1 M HCl aq. (50 mL) and the suspension extracted with CH₂Cl₂ (3 × 50 mL). The combined organic layers were washed with satd. aq. NaHCO₃ (50 mL), dried over MgSO₄ and filtered over a glass filter. The filtrate was concentrated *in vacuo* and the residue purified by column chromatography (silica gel, 50 v% CH₂Cl₂ in hexane) to afford **13** as a yellow solid (1.73 g, 2.23 mmol, 89%). ¹H NMR (300 MHz, CDCl₃) δ (ppm) = 9.43 (d, 1H, *J*_{meta} = 2.7 Hz, **a**), 8.48 (dd, 1H, *J*_{ortho} = 8.7 Hz, *J*_{meta} = 2.6 Hz, **b**), 7.66 (d, 1H, *J*_{ortho} = 8.5 Hz, **c**), 6.85 (s, 2H, **d**), 4.03-3.97 (m, 6H, **e**), 1.87-1.71 (m, 6H, **f**), 1.49-1.21 (m, 48H, **g**), 0.89 (t, 9H, *J* = 6.7 Hz, **h**). MS (MALDI-TOF), C₄₉H₈₀N₂O₅, calculated: 776.61; found: 776.57.



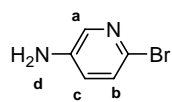
6-[[3,4,5-Tris(dodecyloxy)phenyl]ethynyl]pyridin-3-amine (14). Nitro compound **14** (1.17 g, 1.50 mmol) was dissolved in a warm mixture of EtOAc and EtOH (1:1, 15 mL). Subsequently, SnCl₂·2H₂O (2.708 g, 12.00 mmol) was added and the reaction mixture was heated under reflux for 45 min. The it was poured in to 1 M NaOH aq. (75 mL) and the mixture was extracted with CH₂Cl₂ (4 × 75 mL). The combined organic layers were dried over MgSO₄ and filtered over a glass filter. The filtrate was concentrated *in vacuo* and the residue purified by column

chromatography (silica gel, 5 v% EtOAc in CH₂Cl₂) to give **14** as an orange solid (0.45 g, 0.58 mmol, 39%). ¹H NMR (300 MHz, CDCl₃) δ (ppm) = 7.97 (d, 1H, *J*_{meta} = 1.6 Hz, **a**), 7.19 (d, 1H, *J*_{ortho} = 8.2 Hz, **b**), 6.82 (dd, 1H, *J*_{ortho} = 8.4 Hz, *J*_{meta} = 2.6 Hz, **c**), 6.67 (s, 2H, **d**), 3.93-3.83 (m, 8H, **e**, **f**), 1.75-1.61 (m, 6H, **g**), 1.38-1.00 (m, 48H, **h**), 0.80 (t, 9H, *J* = 6.5 Hz, **i**). ¹³C NMR (75 MHz, CDCl₃) δ (ppm) = 152.9 (**1**), 142.3 (**2**), 139.0 (**3**), 137.5 (**4**), 132.7 (**5**), 127.4 (**6**), 121.0 (**7**), 117.4 (**8**), 110.2 (**9**), 87.9 (**10**), 87.5 (**11**), 73.5 (**12**), 69.1 (**13**), 32.0 (**14**), 30.6 (**15**), 29.8 (**16**), 29.7 (**17**), 29.7 (**18**), 29.6 (**19**), 29.4 (**20**), 29.44 (**21**), 29.41 (**22**), 29.36 (**23**), 26.1 (**24**), 22.7 (**25**), 14.1 (**26**); FT-IR (ATR) σ (cm⁻¹) = 331, 3196, 2921, 2852, 2206, 1631, 1586, 1573, 1500, 1467, 1419, 1354, 1291, 1264, 1232, 1115, 1016, 902, 832, 745, 721. MS (MALDI-TOF), C₄₉H₈₂N₂O₃, calculated: 746.63; found: 747.60 (+ H⁺)



3,6-Bis(acetylamino)-N-6-[3,4,5-tris(dodecyloxy)phenyl]ethynylpyridin-3-ylphthalimide (16). A solution of anhydride **18** (0.131 g, 0.500 mmol), and amine **14** (0.374 g, 0.500 mmol) in dioxane (10 mL) was heated under reflux for 17 h. ¹H-NMR showed the presence of amine while all anhydride had reacted. Extra anhydride (25 mg) was added and the reaction mixture was heated under reflux for an additional 48 h. Then it was poured into 3 M NaOH aq. (100 mL), and the aqueous phase was extracted with Et₂O (4 × 75 mL). The

combined organic layers were dried over MgSO₄ and filtered over a glass filter. The filtrate was concentrated to yield **16** as an orange solid, still containing some anhydride and was used as such for the hydrolysis of the acetyl functions. ¹H NMR (300 MHz, CDCl₃) δ (ppm) = 9.32 (s, 2H, **a**), 8.93 (s, 2H, **b**), 8.85 (d, 1H, *J*_{meta} = 2.2 Hz, **c**), 7.82 (dd, 1H, *J*_{ortho} = 8.2 Hz, *J*_{meta} = 2.5 Hz, **d**), 7.65 (d, 1H, *J*_{ortho} = 8.5 Hz, **e**), 6.83 (s, 2H, **f**), 4.01-3.70 (m, 6H, **g**), 2.24 (s, 6H, **h**), 1.83-1.72 (m, 6H, **i**), 1.47-1.21 (m, 48H, **j**), 0.88 (t, 9H, *J* = 6.5 Hz, **k**).



6-Bromopyridin-3-amine (18). A mixture of 2-bromo-5-nitropyridine (**10**) (2.03 g, 10.0 mmol) and $\text{SnCl}_2 \cdot 2\text{H}_2\text{O}$ (18.05 g, 80.00 mmol) in EtOAc and EtOH (1:1, 60 mL) was heated under reflux for 1 h. The reaction mixture was poured into 4 M NaOH aq. (300 mL) and subsequently the aqueous layer was extracted with CH_2Cl_2 (5×200 mL), The combined organic layers were dried over MgSO_4 and filtered over a glass filter. Concentration of the filtrate *in vacuo* afforded pyridine **18** as a yellow solid (1.57 g, 9.09 mmol, 91%). $^1\text{H NMR}$ (CDCl_3) δ (ppm) = 7.84 (d, 1H, $J_{\text{meta}} = 2.7$ Hz, **a**), 7.21 (dd, 1H, $J_{\text{ortho}} = 8.5$ Hz, $J_{\text{para}} = 0.6$ Hz, **b**), 6.87 (ddd, 1H, $J_{\text{ortho}} = 8.4$, $J_{\text{meta}} = 3.2$, $J_{\text{para}} = 1.2$ Hz, **c**), 3.72 (br s, 2H, **d**).

4.8 References

- 1) Hamuro, Y.; Geib, S. J. and Hamilton, D. A. *J. Am. Chem. Soc.* **1996**, *118*, 7529-41.
- 2) Nelson, J. C.; Saven, J. G.; Moore, J. S.; and Wolynes, P. G., *Science* **1997**, *277*, 1793-6.
- 3) Review articles on foldamers: (a) Block, M. A. B.; Kaiser, C.; Khan, A.; Hecht, S. *Top. Curr. Chem.* **2005**, *89*. (b) Sanford, A. R.; Yamato, K.; Yang, X.; Han, Y.; and Gong, B. *Eur. J. Biochem.* **2004**, *271*, 1416-25. (c) Huc, I. *Eur. J. Org. Chem.* **2004**, 17-29. (d) Schmuck, C. *Angew. Chem. Int. Ed.* **2003**, *42*, 2448-52 (e) Hill, D. J.; Mio, M. J.; Prince, R. B.; Hughes, T. S.; Moore, J. S. *Chem. Rev.* **2001**, *101*, 3893-4011. (f) Gellman, S. H. *Acc. Chem. Res.* **1998**, *31*, 173.
- 4) (a) Matsuda, K.; Stone, M. T.; and Moore, J. S., *J. Am. Chem. Soc.* **2002**, *124*, 11836-7. (b) Brunsveld, L.; Meijer, E. W.; Prince, R. B.; and Moore, J. S. *J. Am. Chem. Soc.* **2001**, *123*, 7978-84. (c) Prince, R. B.; Brunsveld, L.; Meijer, E. W.; and Moore, J. S., *Angew. Chem. Int. Ed.* **2000**, *39*, 228-30. (d) Prince, R. B.; Saven, J. G.; Wolynes, P. G.; and Moore, J. S., *J. Am. Chem. Soc.* **1999**, *121*, 3114-21.
- 5) (a) Dolain, C.; Jiang, H.; Léger, J. M.; Guionneau, P.; and Huc, I. *J. Am. Chem. Soc.* **2005**, *127*, 12943-51. (b) Berl, V.; Huc, I.; Khoury, R. G.; and Lehn, J. M. *Chem. Eur. J.* **2001**, *7*, 2798-2809.
- 6) (a) Yuan, L.; Zeng, H.; Yamato, K.; Sanford, A. R.; Feng, W.; Atreya, H. S.; Sukumaran, D. K.; Szyperski, T.; and Gong, B. *J. Am. Chem. Soc.* **2004**, *126*, 16528-37. (b) Yang, Z.; Yuan, L.; Yamato, K.; Brown, A. L.; Feng, W.; Furukawa, M.; Zeng, X. C.; and Gong, B. *J. Am. Chem. Soc.* **2004**, *126*, 3148-62.
- 7) (a) Hunter, C. A.; Spitaleri, A.; Tomas, S., *Chem. Commun.* **2005**, 3691-3. (b) Tanatani, A.; Yokoyama, A.; Azumaya, I.; Takakura, Y.; Mitsui, C.; Shiro, M.; Uchiyama, M.; Muranaka, A.; Kobayashi, N.; and Yokozawa, T., *J. Am. Chem. Soc.* **2005**, *127*, 8553-61. (c) Hamuro, Y.; Geib, S. J.; and Hamilton, A. D., *J. Am. Chem. Soc.* **1997**, *119*, 10587-93.
- 8) (a) Huc, I., *Eur. J. Org. Chem.* **2004**, *1*, 17-29. (b) Sandford A. R.; Yamato, K.; Yang, X.; Yuan, L.; Han, Y.; and Gong, B. *Eur. J. Biochem.* **2004**, *271*, 1416-25.
- 9) Corbin, P. S.; Zimmerman, S. C.; Thiessen, P. A.; Hawryluk, N. A.; and Murray, T. J. *J. Am. Chem. Soc.* **2001**, *123*, 10475-88.
- 10) Van Gorp, J. J.; Vekemans, J. A. J. M.; and Meijer, E. W., *Chem. Commun.* **2004**, 60-1.
- 11) Maurizot, V.; Linti, G.; and Huc, I., *Chem. Commun.*, **2004**, 924-5.
- 12) (a) Goto, K.; and Moore, J. S., *Org. Lett.* **2005**, *7*, 1683-6. (b) Stone, M. T.; and Moore, S. J., *Org. Lett.* **2004**, *6*, 469-72. (c) Tanatani, A.; Hughes, T. S.; and Moore, J. S., *Angew. Chem. Int. Ed.* **2002**, *41*, 325-8. (d) Prince, R. B.; Barnes, S. A.; and Moore, J. S., *J. Am. Chem. Soc.* **2000**, *122*, 2758-62.
- 13) Garric, J.; Léger, J. M.; Huc, I., *Angew. Chem. Int. Ed.* **2005**, *44*, 1954-8.
- 14) Hou, J. L.; Shao, X. B.; Chen, G. J.; Zhou, Y. X.; Jiang, X. K.; and Li, Z. T., *J. Am. Chem. Soc.* **2004**, *126*, 12386-94.
- 15) Recent reviews: (a) Segura, J. L.; Martin, N.; Guldi, D. M. *Chem. Soc. Rev.* **2005**, *34*, 31-47. (b) Hoppe, H.; Sariciftci, N. S. *J. Mater. Res.* **2004**, *19*, 1924-45.
- 16) Recent reviews: (a) Horowitz, G. *Adv. Mater.* **1998**, *10*, 365-377. (b) Dodabalapur, Ananth; Katz, Howard E.; Torsi, L. *Adv. Mater.* **1996**, *8*, 853-855. (c) Sun, Y.; Liu, Y.; Zhu, D. *J. Mater. Chem.* **2005**, *15*, 53-65. (d) Kraft, A. *Chem. Phys. Chem.* **2001**, *2*, 163-165.
- 17) A selection: (a) Hoeben, F. J. M.; Herz, L. M.; Daniel, C.; Jonkeijm, P.; Schenning, A. P. H. J.; Silva, C.; Meskers, S. C. J.; Beljonne, D.; Phillips, R. T.; Friend, R. H.; Meijer, E. W. *Angew. Chem. Int. Ed.* **2004**, *43*, 1976-9. (b) Ajayaghosh, A.; George, S. J.; Praveen, V. K. *Angew. Chem. Int. Ed.* **2003**, *42*, 332-5. (c) Schenning, A. P. H. J.; Jonkheijm, P.; Peeters, E.; Meijer, E. W. *J. Am. Chem. Soc.* **2001**, *123*, 409-16.
- 18) A selection: (a) Wolffs M.; Hoeben F. J. M.; Beckers E. H. A.; Schenning A. P. H. J.; Meijer E. W. *J. Am. Chem. Soc.* **2005**, *127*, 13484-5. (b) Schenning, A. P. H. J.; van Herrikhuyzen, J.; Jonkheijm, P.; Chen, Z.; Würthner, F.; Meijer, E. W. *J. Am. Chem. Soc.* **2002**, *124*, 10252-3. (c) Beckers, E. H. A.; van Hal, P. A.; Schenning, A. P. H. J.; El-Ghayoury, A.; Peeters, E.; Rispens, M. T.; Hummelen, J. C.; Meijer, E. W.; Janssen, R. A. J. *J. Mater. Chem.* **2002**, *12*, 2054-60.

-
- 19) Sinkeldam, R. W.; van Houtem, M H. C. J.; Koeckelberghs, G.; Vekemans, J. A. J. M.; and Meijer, E. W. *Org. Lett.* **2005** submitted.
 - 20) The synthesis and characterization of 3,6-diamino-*N*-OPV3-phthalimide (**1**) is reported in the experimental section of chapter 2, compound **22e**.
 - 21) Dolain, C.; Grelard, A.; Laguerre, M.; Jiang, H.; Maurizot, V.; Huc, I. *Chem. Eur. J.* **2005**, *11*, 6135-6144.
 - 22) The synthesis and characterization of 3,6-bis(acetylamino)-*N*-OPV3-phthalimide (**4**) is reported in the experimental section of chapter 2, compound **20e**.
 - 23) Jonkheijm, P.; Hoeben, F. J. M.; Kleppinger, R.; van Herrikhuyzen, J.; Schenning, A. P. H. J.; Meijer, E. W. *J. Am. Chem. Soc.* **2003**, *125*, 15941-9.
 - 24) Davydov, A. S. *Zh. Eksp. Teor. Fiz.* **1948**, *18*, 210-8.
 - 25) Nakano, T.; Yade, T. *J. Am. Chem. Soc.* **2003**, *125*, 15474-84.
 - 26) Schuster, G. B. *Acc. Chem. Res.* **2000**, *33*, 253-60.
 - 27) The synthesis and characterization of 3,6-diamino-*N*-OPV4-phthalimide (**9**) is reported in the experimental section of chapter 2, compound **22f**.
 - 28) van Gorp J. J.; *Helices by Hydrogen Bonding*, **2004**, Thesis, Chapter 5, Eindhoven University of Technology.
 - 29) The synthesis and characterization of 3,6-bis(acetylamino)-*N*-OPV4-phthalimide is reported in the experimental section of chapter 2, compound **20f**.
 - 30) Schenning, A. P. H. J.; Franssen, M.; Meijer, E. W. *Macromol. Rapid Commun.* **2002**, *23*, 265-70.
 - 31) The synthesis and characterization of 3,6-bis(acetylamino)phthalic anhydride (**18**) is reported in the experimental section of chapter 2, compound **9**.
 - 32) The synthesis and characterization of **22** and its precursor are reported in the experimental section of chapter 2, compounds **22d** and **20b**, respectively.
 - 33) Examples of the use NOE NMR in the characterization of foldamers: (a) Chang, K.; Kang, B.; Lee, M.; Jeong, K. *J. Am. Chem. Soc.* **2005**, *127*, 12214-5. (b) Gong, B.; Zeng, H.; Zhu, J.; Yuan, L.; Han, Y.; Cheng, S.; Furukawa, M.; Parra, R. D.; Kovalevsky, A. Y.; Mills, J. L.; Skrzypczak-Jankun, E.; Martinovic, S.; Smith, R. D.; Zheng, C.; Szyperki, T.; Zeng, X. *Proc. Natl. Acad. Sci. U.S.A.* **2002**, *99*, 11583-8. (c) Gon. B. *Chem. Eur. J.* **2001**, *7*, 4336-42.

Chapter 5

Helical architectures in water

Abstract

In chapter 4 poly(ureidophthalimide) foldamers decorated with chromophores are discussed. In this chapter the naturally occurring α -helix is mimicked by decoration of the poly(ureidophthalimide) with ethyleneoxide sidechains, which ensure solubility in aqueous media. The novel hydrophilic polymer has been studied with UV-vis and circular dichroism (CD) spectroscopy. The foldamers show a putative helical arrangement in water as well as in THF. Temperature and concentration dependent CD measurements in water have revealed an almost temperature and concentration independent Cotton effect, indicative for a strong intramolecular organization. Similar studies in THF demonstrate the dynamic character of the foldamer. In that case, CD spectroscopy reveals the loss of the Cotton effect upon raising the temperature. In addition, the bisignated Cotton effect in water is opposite in sign to that in THF, suggestive of a solvent dependent preference for one helical handedness. Titration experiments prove the dominance of water in determining the handedness of the helical architecture. Thus, the solvent governs the supramolecular synthesis and allows for control over the helical architecture.

5.1 Introduction: inspired by nature

The intriguing shapes of helical biomolecules, with the α -helix as one of the most abundant secondary architectures in Nature, have always fascinated chemists. Therefore, it is logical to exploit native peptides to investigate the interactions that determine the formation of helical architectures. The numerous interactions that govern folding in natural systems have prompted chemists to design synthetic analogues to give more insight into the requirements for folding.¹ The closest related to natural α -helices are the helical secondary structures based on β -peptides.² Investigations of Gellman and Seebach illustrated that modification of the β -amino acid building blocks gives more control over the secondary architecture.^{3,4} Even more fascinating is the finding that helical architectures comprising of β -peptides proved to be more stable than their α -peptide counterparts⁵, which is encouraging for a completely synthetic approach. Besides the peptides or peptidomimetics also the folding of other synthetic polymers or oligomers into helical architectures can be envisaged.⁶ All of these structures belong to the class of foldamers, according to Moore, being structures that fold into a conformationally ordered state in solution.^{6e} In many cases folding relies on solvophobicity. The folding can be directed by intramolecular hydrogen bonding and additional π - π stacking may stabilize the secondary architecture. Many strategies have been reported to arrive at non-natural foldamers. Prominent architectures are based on donor-acceptor couples⁷, *m*-phenylene-ethynylenes⁸ and their backbone rigidified analogues⁹, aromatic oligoamides^{10,11,12}, aromatic oligoureas^{13,b}, aromatic oligohydrazides¹⁴ and aromatic iminodicarbonyls¹⁵. Depending on their design they may possess an inner void of sufficient size to host ions or small molecules. Obviously, mimicking nature with abiotic foldamers demands solubility in water. Natural helices constructed from α -peptides can rely on their intrinsic bipolar zwitter ionic state to ensure solubility in water. However, synthetic foldamers often contain structural elements that hamper solubility in water. The use of ionic groups in non-natural foldamers is not without consequence since it will probably also affect folding. *m*-Phenylene-ethynylenes (*m*PEs) are known for their helical secondary architectures. However, there is ambiguity as to whether or not their amphiphilic ionic counterparts adopt a helical conformation besides an extended, or all *trans* conformation on the air water interface¹⁶ or in aqueous solutions¹⁷. The best strategy is probably the use of non-ionic functionalities like ethylene oxides to guarantee solubility in water. To our knowledge only Moore and coworkers have reported on a strategy to solubilize *m*PE foldamers in water/acetonitrile solution by decoration with chiral¹⁸ and achiral¹⁹ ethylene oxide chains and in water by longer achiral²⁰ ethylene oxide chains. In the later case, preference of one handedness over the other is realized by addition of a chiral guest, a small organic molecule, which fits in the inner void of the foldamer. This beautiful example demonstrates the potential of synthetic foldamers as candidates for mimicking biological functions. Besides the use of *m*PEs as a host, similar experiments albeit not in water, with aromatic oligoamides have been

reported.²¹ With the use of oligo (ureido-*meta*-phenylene) even mimicking of trans-membrane ion channels is anticipated.^b In that case the urea functions adopt a *cisoid* conformation due to intramolecular hydrogen bonding between the urea hydrogens and the carbonyl of an adjacent ester functionality. Van Gorp previously reported a poly (ureido-*para*-phthalimide) foldamer in which the urea functions adopt a *cisoid* conformation.²² In that case the consecutive monomeric units introduce a curvature in the ureidophthalimide backbone due to intramolecular hydrogen bonding of urea protons with the adjacent imid carbonyls. This interaction renders a bend of approximately 120°, and thus nucleates folding (Figure 5.1). Due to the *para* substitution in the phthalimide unit a larger inner void is created upon folding compared to the oligo (ureido-*meta*-phenylene) system.

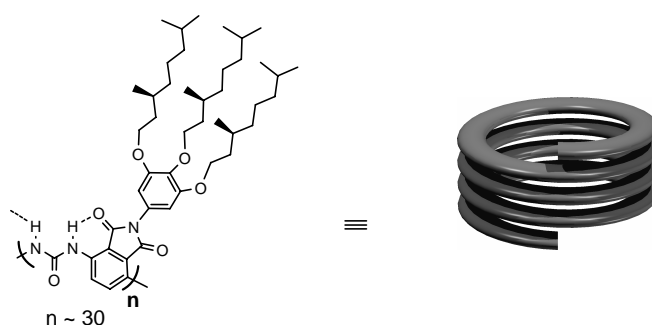


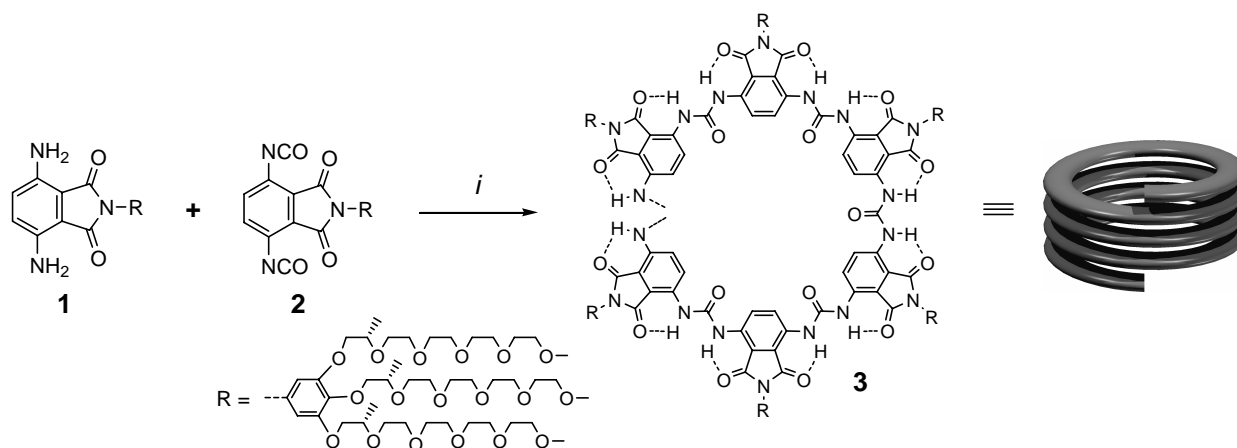
Figure 5.1: Intramolecular hydrogen bond-induced folding in oligo (ureidophthalimide).

CD studies of the polymer (Figure 5.1) in THF indicated folding into a helical architecture. Moreover, studies in heptane proved the stacking of shorter oligomers to larger chiral aggregates. However, the same compound dissolved in CHCl_3 proved to be CD silent. Model studies have shown that by folding an inner void is constructed with dimensions comparable to Moore's *m*-phenylene ethynylene system²³ and that should therefore be suited to host a small molecule.

Similar to the work of Moore, the oligo (ureidophthalimide) foldamer presented in this chapter also relies on oligo(ethylene oxide) functionalities to ensure solubility in water. In chapter 2, we reported a general synthetic strategy directed towards an array of 3,6-diaminophthalimides²⁴, the building blocks for the foldamers. In this way chiral oligo (ethylene oxide) side chains have been incorporated in the foldameric structure enabling a CD study of the polymer.

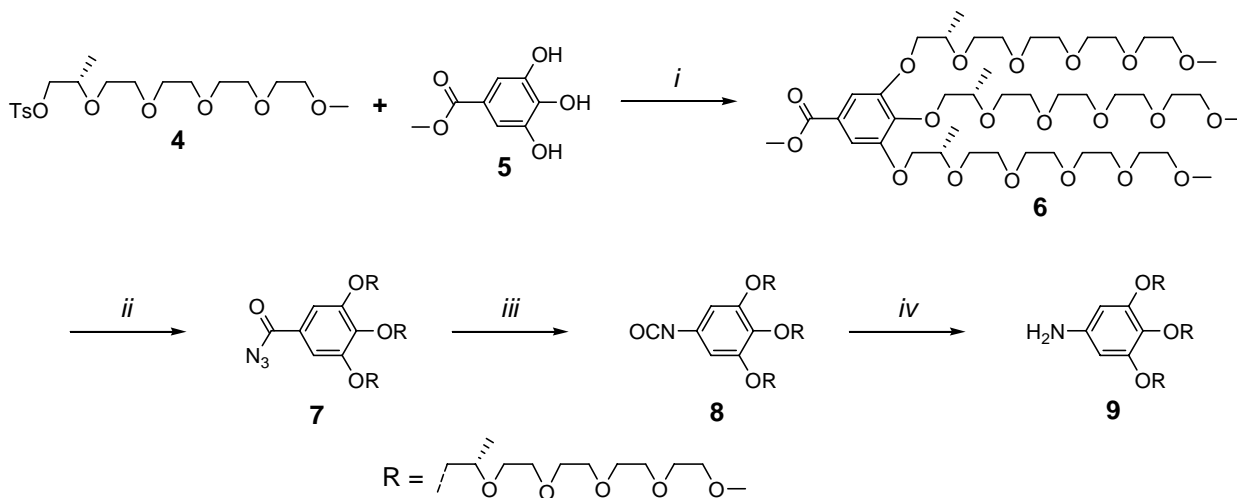
5.2 Synthesis

The ureidophthalimide based polymer **3** as synthesized by Michel van Houtem is obtained by reaction of diamine **1** with diisocyanate **2** in refluxing dioxane in the presence of one equivalent of dimethylaminopyridine (DMAP) (Scheme 5.1).



Scheme 5.1: Polymerization of diamine **1** with diisocyanate **2**. i) DMAP (1 equiv.), dioxane, reflux, 17 h.

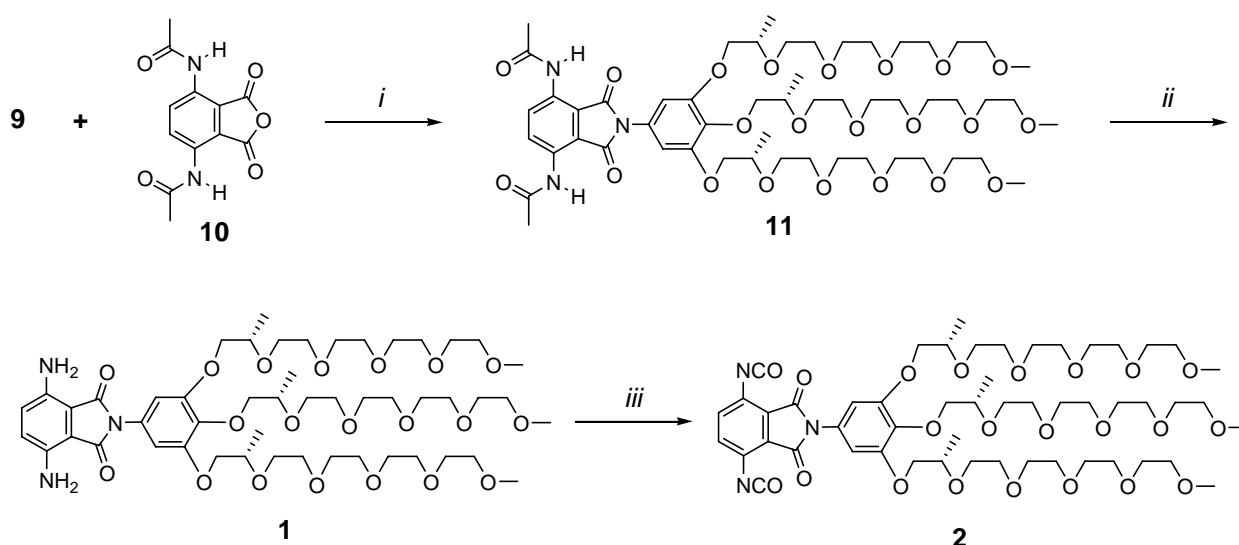
Previously, an efficient synthetic approach to tosylated (2*S*)-2-methyl-3,6,9,12,15-pentaoxahehexadecanol (**4**) and its coupling to methyl gallate (**5**) have been described (Scheme 5.2).²⁵ Subsequently, methyl ester **6** is hydrolyzed and the acid converted to the acid chloride, which reacted with sodium azide to give acyl azide **7**. Curtius rearrangement in dioxane at elevated temperatures renders isocyanate **8**, which in turn is hydrolysed to the corresponding amine **9** by slow addition to aqueous potassium hydroxide in dioxane at 90°C.



Scheme 5.2: Synthesis of amine **9**. i) **4** (3.05 equiv.), **5**, K_2CO_3 (6.2 equiv.), Bu_4NBr (5 equiv.), MIBK, reflux, 6 h. ii) KOH (3.3 equiv.), EtOH/ H_2O (1:1), reflux, 17 h; 0.1 M HCl until pH ~ 3, 95%; $(CO)_2Cl_2$ (1.2 equiv.), DMF (5 drops), CH_2Cl_2 , rt, 17 h, 99%; NaN_3 (18 equiv.), THF/ H_2O (1:1), 5°C, 1 h, 99%. iii) dioxane, reflux, 4 h, ~100%. iv) KOH (160 equiv.), H_2O , 90°C, 30 min., 97%.

Amine **9** is converted into the phthalimide synthon **11** by reaction with 3,6-bis(acetylamino)phthalic anhydride (**10**) (Scheme 5.3). Removal of the acetyl functions to give the corresponding diamine **1** is achieved by exposure of diamide **11** to 1.5 M aqueous HCl in refluxing dioxane. A subsequent exposure of diamine **1** to a 20 *w*% phosgene solution in toluene affords diisocyanate

2. The conversion could be monitored by infrared spectroscopy and proved to be complete and quantitative after 30 minutes stirring at room temperature.



Scheme 5.3: Syntheses of polymer building blocks **1** and **2**. i) dioxane, reflux, 17 h, 90%. ii) dioxane/water/HCl (12 M) (6:1.5:1 v/v), 90°C, 45 min., 95%. iii) COCl₂ (40 equiv.), PhCH₃, rt, 2.5 h, ~100%.

Polymerization of diamine **1** with diisocyanate **2** according to Scheme 5.1 furnished ureidophthalimide polymer **3**. Monitoring the polymerization by IR spectroscopy indicated that it was finished after 17 hours in refluxing dioxane when all diisocyanate was consumed. The non-migrating DMAP was removed by filtration over silica gel with a solvent mixture of 10% methanol in 1,2-dimethoxyethane. A separation of shorter and longer oligomers is effectuated by column chromatography over silica gel with a solvent mixture gradient of 1 to 10% methanol in 1,2-dimethoxyethane. Due to the polar nature of the oligo(ethylene oxide) tails, the first fraction (**3a**) is a mixture of predominantly short oligomers with a small amount of longer oligomers. The second fraction (**3b**), containing only oligomers longer than 8 units. The difference in oligomeric distribution was established by the longer elution time for **3a** (5.69 min) on GPC (CHCl₃, mixed-E column, detection at 310 nm) compared to that of **3b** (4.73 min). Furthermore, from ¹H-NMR endgroup analysis of the latter, an average length was deduced of 20 units.

5.3 UV-vis and CD spectroscopy

Until now the study of ureidophthalimide based polymers was restricted to organic solvents such as heptane, chloroform and THF. For these systems the largest Cotton effect was observed in THF. However, the polar nature of the ethylene oxide tails of **3b** ensures solubility in water. Thus, a dilute aqueous solution of the high molecular weight fraction **3b** is subjected to a UV-

vis and CD study. Since water itself does not absorb in the 200 nm region the spectral width covers the region from 190 nm to 500 nm. The UV-vis spectrum shows three distinct absorption maxima located at 209 nm with a shoulder at 230 nm, 312 nm and 398 nm (Figure 5.2).

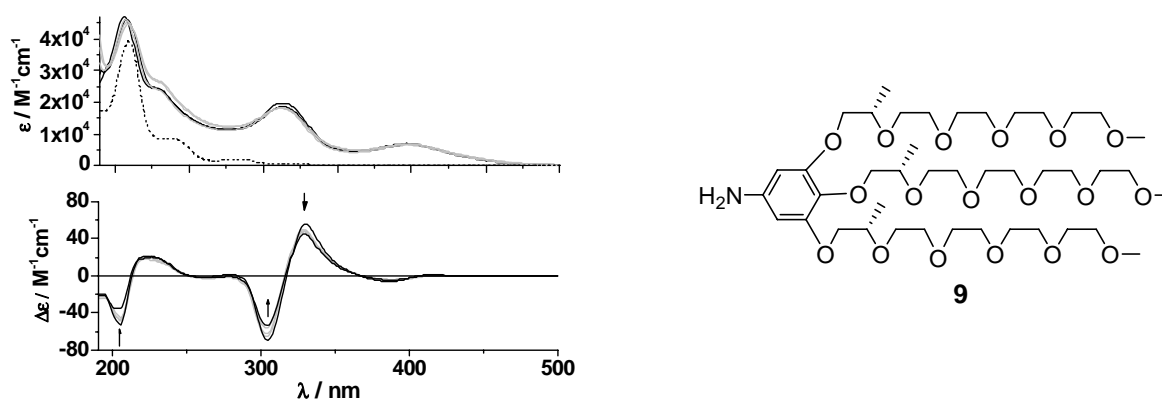


Figure 5.2: Temperature dependent UV-vis and CD spectra of **3b** in water (4.7×10^{-5} M), 15°C (black line), 55°C (black line), 65°C, 80°C and 90°C (grey lines), and amine **9** (dotted line in UV-vis, no Cotton effect observed).

The absorptions located at 310 nm and 398 nm can be attributed to the phthalimide part. The absorption spectrum of amine **9** which lacks the long wavelength absorptions establishes the different contributions to the absorption spectrum. In CD spectroscopy two bisignate Cotton effects are observed. The first bisignate effect displays maxima with $\Delta\epsilon = -53 \text{ M}^{-1}\text{cm}^{-1}$ ($g_{\text{abs}} = -0.0012$) at 205 nm and $\Delta\epsilon = +21 \text{ M}^{-1}\text{cm}^{-1}$ ($g_{\text{abs}} = 0.0009$) at 222 nm (Figure 5.2). The zero-crossing at 213 nm coincides with the absorption maximum in the UV-vis spectrum. The second bisignate Cotton effect displays maxima of $\Delta\epsilon = -69 \text{ M}^{-1}\text{cm}^{-1}$ ($g_{\text{abs}} = -0.0040$) at 304 nm and $\Delta\epsilon = +56 \text{ M}^{-1}\text{cm}^{-1}$ ($g_{\text{abs}} = 0.0045$) at 330 nm. The zero-crossing at 318 nm coincides with the absorption maximum of the phthalimide unit. A small negative CD effect is observed that relates to the absorption at 398 nm.

The appearance of a Cotton effect in water is remarkable since the folding is directed by intramolecular hydrogen bonding of the urea protons with the imide carbonyls. Apparently, water is not capable of disrupting H-bonding and preventing folding. It is safe to state that initial folding is driven by shielding the apolar core from the polar solvent. This solvophobic effect creates a hydrophobic microdomain which allows the expression of subtle hydrogen bonding interactions. Once initiated the system is templated towards folding since the favorable hydrophobic pocket is already there. In addition, although variations are observed, the intensity of the Cotton effect is hardly affected by raising the temperature. The remarkable stability of this folded structure in water contrasts to many native helix-forming proteins which are only marginally stable in water.^{26,27} The extreme stability in water is easily explained by the strong hydrophobic forces and π - π interaction hampering the structure to be water-soluble in its

unfolded form. The significant CD effects are the result of supramolecular chirality and a strong indication for the presence of a helical architecture.

The nature of the oligoethylene oxide rich periphery of **3b** does not restrict the solubility of **3b** to water alone. Thus, a dilute solution of **3b** in THF has been subjected to a UV-vis and CD spectroscopy study. The width of the spectral window is reduced since THF absorbs below 250 nm. The UV-vis spectrum reveals two absorption maxima located at 315 nm and 394 nm (Figure 5.3).

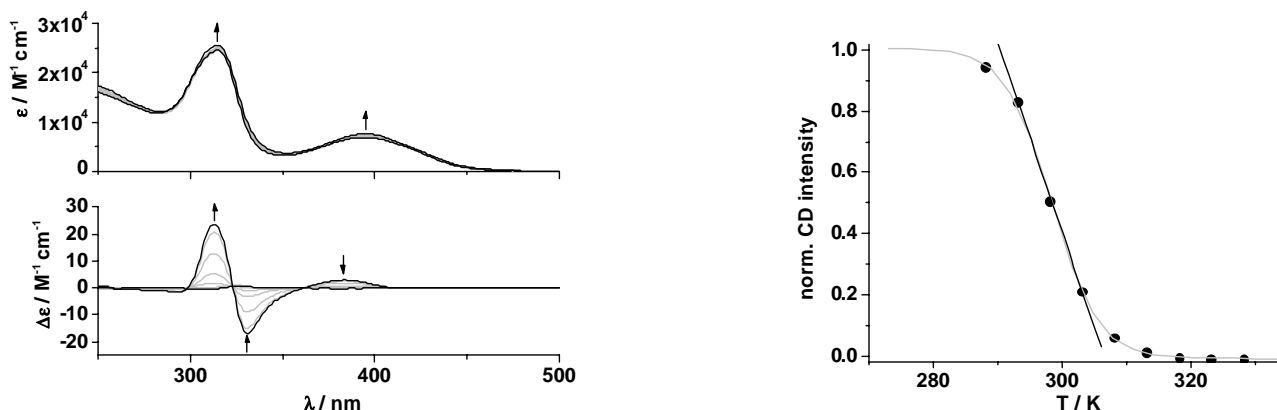


Figure 5.3: (Left) Temperature dependent UV-vis (top) and CD (bottom) spectra of **3b** in THF (5.0×10^{-5} M) from 15°C (black line) to 55°C (black line) with steps of 5°C (gray lines). (Right) melting curve constructed from the CD intensity at 320 nm at different temperatures (black circles), a fitted exponential curve (gray line) and a straight line representing the slope (black line).

The CD spectrum of the same solution shows a Cotton effect with a $\Delta\epsilon$ of $+24 \text{ M}^{-1}\text{cm}^{-1}$ ($g_{\text{abs}} = 0.0009$) at 313 nm and $\Delta\epsilon = -17 \text{ M}^{-1}\text{cm}^{-1}$ ($g_{\text{abs}} = 0.0017$) at 331 nm, respectively, with a zero-crossing at 323 nm. In contrast to the temperature dependent CD measurements in water, the Cotton effect in THF decreases upon raising the temperature and completely vanishes at 55°C. The original value is reclaimed upon cooling to room temperature, illustrating the dynamics of the system in THF. The loss of the Cotton effect at elevated temperatures may be attributed to the unfolding of the helical architecture into a random coil conformation or mark the attained equilibrium between P and M helices. The latter seems to be in agreement with the spectral behavior at different temperatures. Elevation of the temperature does not result in a shift of the absorption maximum, which implies that there is no evidence for a change in the aromatic packing.²⁸ Moreover, the presence of an isodichroic point throughout the temperature dependent measurements in THF indicates that the structure does not adopt other conformations or aggregation states.^{18a} A melting curve (Figure 5.3, right) could be constructed from the temperature dependent CD data. An exponential function represented by a grey line adequately fits the data points. The slope of the curve, denoted by the black line, enables

estimation of the change in enthalpy involved in this process. Applying the formula $\Delta H = \text{slope} * T^2$ gives $\Delta H = -5.5 \text{ kJ/mol}$.

The comparison of **3b** in THF and in water shows that the Cotton effect in THF is smaller and of opposite sign compared to the measurement in water. The lower intensity of the CD effect in THF can point to a less tight packing of the chromophores and/or less intermolecular aggregation of the helical architectures. The latter possibility is addressed with concentration dependent CD studies in water and THF, which revealed the absence of a correlation between concentration and CD intensity over a 100 fold concentration range (10^{-4} to 10^{-6} M), implying that in both cases only monomolecular species are present (Figure 5.4).

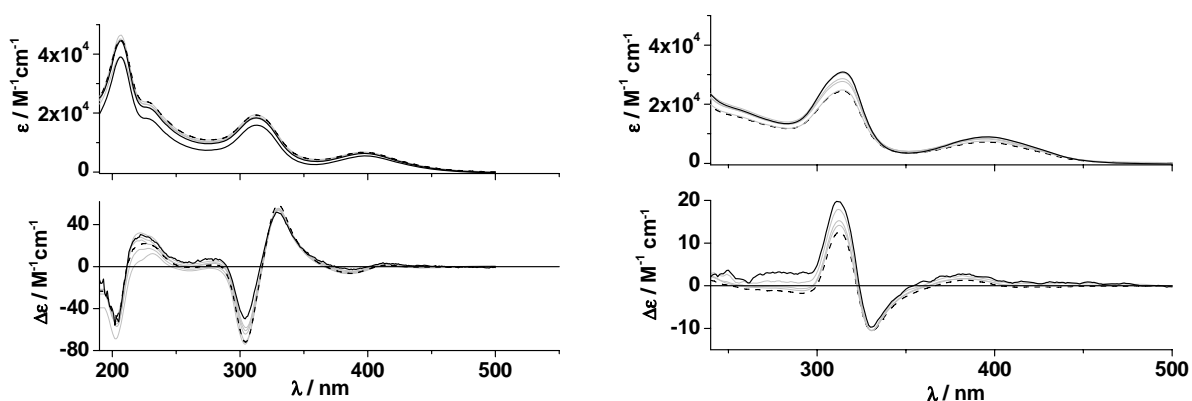


Figure 5.4: Concentration dependent UV-vis and CD measurements of **3b** at 20°C from 5.0×10^{-4} M (black line) to 5.0×10^{-6} M (dashed line) in 5 steps (grey lines) in water (left) and in THF (right).

Hence, the less intense Cotton effect in THF can most likely be attributed to looser packing of the aromatic system. This is supported by a 23% higher molar extinction coefficient of **3b** at 314 nm in THF compared to the overall optical density in water. Hypochromicity is a convincing indication of a tighter packing of the chromophores and is also observed in DNA, RNA and other polymers.²⁹ The observed hypochromic effect can be rationalized by the properties of the solvent. THF is a good solvent for both the apolar core and the polar ethylene oxide periphery. However, water can only dissolve the polar ethylene oxide periphery and will force the apolar core to minimize exposure to water by tight folding and as a consequence induces tight packing of the aromatic units.

The opposite sign of the Cotton effect in THF compared to water hints towards inversion of the helical handedness. This effect can be attributed to differences in hydrogen bonding interactions with the two solvents and a different conformation of the chiral ethylene-oxide side chains. There is a preference for a *gauche* conformation along the C-C axis and a *trans* conformation along the C-O axis of the ethyleneoxide tails in water, as has been established by Matsuura *et al.* with detailed IR spectroscopy studies on poly(ethylene-oxide).³⁰ Recently a similar effect was reported in which dendrons decorated with chiral ethylene oxide tails show

an opposite Cotton effect in water compared to THF.³¹ Therein, this effect is explained as a helical M \rightarrow P transition upon going from THF to water. To investigate the relative influence of the solvent on the helical architecture, **3b** was studied in THF-water mixtures, keeping its concentration constant. From the UV-vis spectra it becomes clear that the optical density in pure water is intensified upon addition of the THF solution (Figure 5.5). This suggests loosening of the intramolecular packing, which eventually might permit helix inversion.

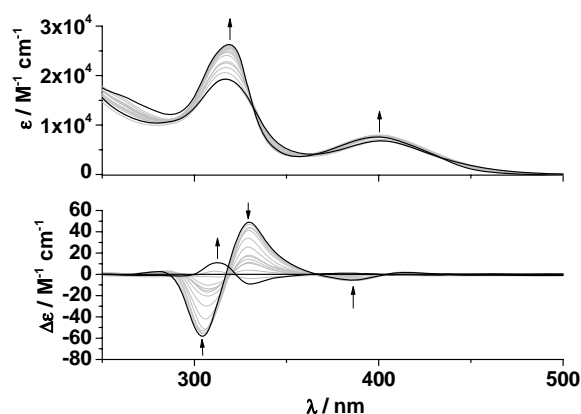


Figure 5.5: UV-vis (top) and CD (bottom) spectra of a titration of **3b** in THF (black line) to a solution of **3b** in water (black line) in 10% steps (grey lines) keeping the concentration constant at 4.15×10^{-5} M.

The accompanying CD spectra show that upon increasing the THF/water ratio the Cotton effect gradually decreases. It is quite remarkable that over 99 v% of THF in water is required to reach inversion of the Cotton effect. These findings demonstrate the outstanding stability and dominance of the conformation of the secondary architecture in water as was also established by the temperature dependent CD experiment in water (Figure 5.2).

5.4 Conclusions

A novel hydrophilic ureidophthalimide polymer was synthesized that establishes a folding dynamics in THF and that reveals outstanding stability of the putative helical architectures in water. Circular dichroism studies at different concentrations show a concentration independent Cotton effect, indicative for intramolecular folding without intermolecular aggregation. The opposite Cotton effect observed in water compared to THF, indicates a solvent induced preference for helical handedness. Titration experiments with water-THF mixtures indicate the dominance of water on the handedness. Furthermore, the assumed helical inversion allows control over the diastereomeric excess. The dimensions of the hollow core created by folding, allow the hosting of ions and may even be suitable for accommodation of small molecules. Our future research will focus on the potential exploitation of the inner void.

5.5 Poly(ureidophthalimide)s: what have we learned?

With the newly developed synthetic approach for the synthesis of 3,6-diaminophthalimides as described in chapter 2, a series of novel poly(ureidophthalimide)s has become available of which their properties in solution are discussed in chapters 2, 4, 5 and by Judith van Gorp^{22,23}. Although an absolute comparison is difficult, the marked differences in their chemical structure (Figure 5.6) might rationalize the results regarding the intensity of the Cotton effect and the stability of the expression of chirality in the various solvents.

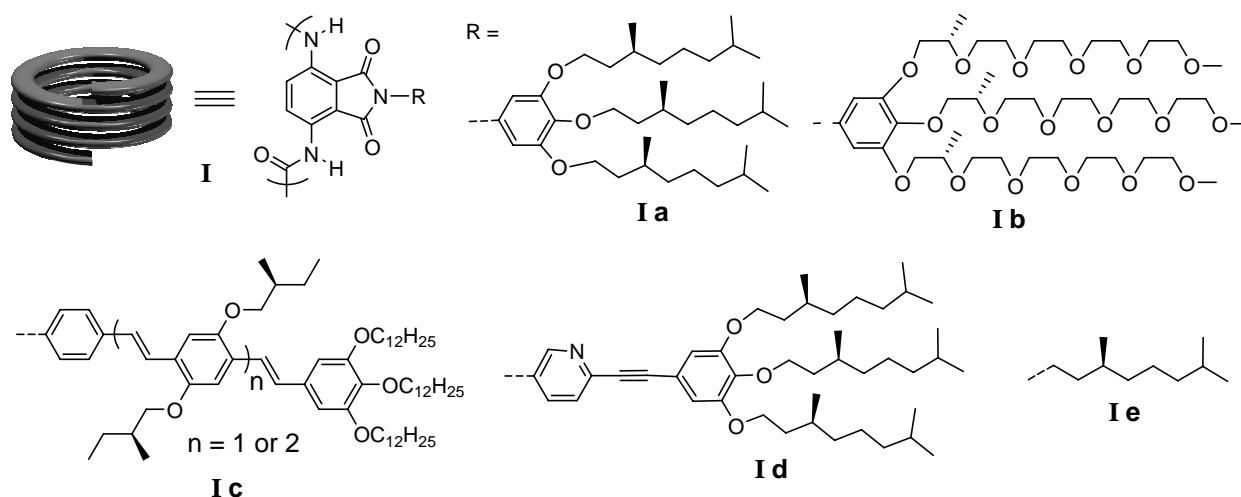


Figure 5.6: The structural differences of the foldameric periphery.

The relative solvophobicity of the core with respect to the periphery is an important factor in the initiation of folding and in the dynamics involved in the folding process. A good solvent like chloroform is capable of dissolving both the core and the periphery. This is reflected in the absence of a Cotton effect in CD for foldamers **Ia-d** in this solvent. Hence, the observed temperature-independent Cotton effect for **Ie** in chloroform is a clear indication that the solubility of the core is no longer ensured by the periphery, resulting in a minimization of solvent exposure by folding. This corresponds with the observation that foldamers **Ia,c,d** show a temperature independent CD effect in heptane. The system has lost its dynamics due to shielding of the relatively polar core from the apolar solvent. Of course, a similar effect is seen for **Ib** in water. In this case the relatively apolar core is shielded from the aqueous surrounding. THF, capable of dissolving the core as well as the periphery in foldamers **Ia-d**, is also the solvent that displays the dynamics of the folding process in temperature-dependent CD measurements. Moreover, it is the dynamics in THF that allows folding of **Ic**, and it is the lack of dynamics in heptane that makes the secondary architecture very stable.

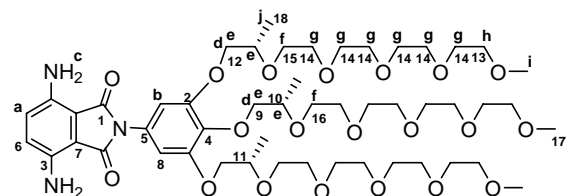
Besides solubility and difference of solvent affinity between core and periphery, the structural properties of the periphery determining the intensity of the Cotton effect, are the

presence or absence of π - π stacking interactions, space confinement and the number and position of chiral centers. An apparently ideal combination can be found in foldamer **Ia** since this structure gives rise to the strongest CD effect. The three chiral tails not only provide the required chirality but also cause extensive space filling which enhances phase segregation, probably essential for a large Cotton effect. Furthermore, the peripheral benzene moiety facilitates additional π - π stacking. The balanced interplay between the aforementioned structural properties is also found in the water soluble variant **Ib**, which displays a large CD effect in water. Extension of the π -system, as in OPV decorated structures **Ic** does not result in an intensification of the Cotton effect. Presumably the smaller CD effect can be attributed to non-helical stacking of the large π -system resulting in 'frustrated stacks'.³² This may also rationalize the weak CD effect of a D- π -A periphery as in **Id**. In addition, the chiral centers in **Ic** are even more remote from the phthalimide core thereby negatively influencing the expression of chirality. Leaving out peripheral π - π interactions as in **Ie** seems to lower the CD effect drastically, despite the close proximity of the chiral center to the core. However, only one chiral chain per monomeric unit is present. This in combination with the limited solubility of **Ie** may explain the small but permanent Cotton effect regardless of solvent or temperature.

With this series of poly(ureidophthalimide)s we have introduced a new scaffold that allows for peripheral organization of a variety of functionalities. Moreover, the hollow core of the water soluble foldamer **1b** may be an interesting candidate for the hosting of ions or small molecules.

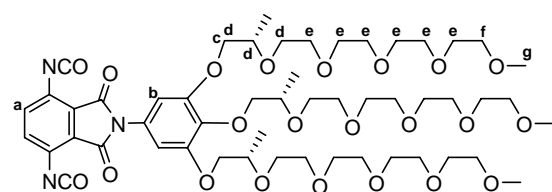
5.6 Experimental

General. See experimental section of chapter 2.



3,6-Diamino-N-(3,4,5-tris[2-(2-{2-[2-(2-methoxyethoxy)ethoxy]ethoxy}ethoxy)propoxy]phenyl)phthalimide (1). Under argon, 3,6-bis(acetylamino)phthalimide **11** (1.247 g, 1.104 mmol) was dissolved in a mixture of dioxane, water and HCl (12 M) (4.2 mL, : 1.1 mL, : 0.7 mL). The stirred reaction

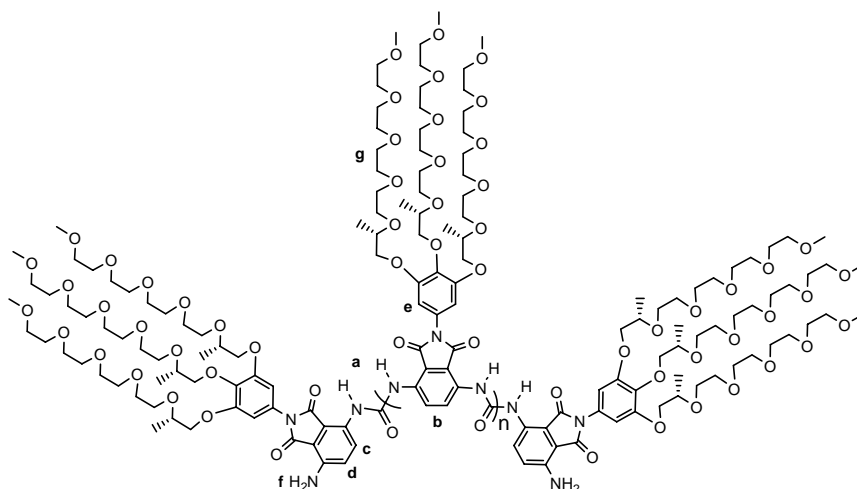
mixture was heated at 90 °C for 45 min, and then poured into ice-water. Subsequently, saturated. aq. NaHCO₃ solution and brine were added, adjusting the pH at 8. The aqueous mixture was then extracted with CH₂Cl₂ (4 × 75 mL), the combined organic layers were dried over MgSO₄ and the filtrate concentrated *in vacuo*. The residue was purified by column chromatography (silica gel, 10 v% heptane in 1,2-dimethoxyethane, R_f = 0.3) yielding **1** (1.150 g, 1.099 mmol, 95 %) as an orange thick oil. **GPC** (mixed D, 254 nm, CHCl₃): R_t = 8.58 min.; **HPLC** (PDA): R_t = 8.93 min. purity ~ 97 %. **¹H-NMR** (400 MHz, CDCl₃): δ (ppm) = 6.81 (s, 2H, **a**), 6.65 (s, 2H, **b**), 5.00 (s, 4H, **c**), 4.08-4.02 (3H, **d**), 3.90-3.78 (6H, **e**), 3.78-3.68 (6H, **f**), 3.68-3.59 (36H, **g**), 3.56-3.53 (6H, **h**), 3.38-3.36 (s, 9H, **i**), 1.31-1.27 (9H, **j**); **¹³C-NMR** (50 MHz, CDCl₃): δ (ppm) = 168.4 (**1**), 152.5 (**2**), 138.8 (**3**), 137.1 (**4**), 127.5 (**5**), 125.5 (**6**), 108.3 (**7**), 105.8 (**8**), 76.3 (**9**), 75.0 (**10**), 74.3 (**11**), 72.6 (**12**), 71.9 (**13**), 70.8-70.4 (**14**), 68.8 (**15**), 68.5 (**16**), 59.0 (**17**), 17.7-17.5 (**18**); **FT-IR** (ATR): σ (cm⁻¹) = 3465 and 3355 (NH₂), 2871 (alkyl C-H), 2179, 1732 and 1688 (imide C=O), 1656, 1619 (NH₂), 1595 and 1494 (aromatic C-C), 1434 (alkyl C-H), 1374, 1350, 1292 (C-N), 1242 (aryl-O-alkyl ether), 1190, 1094 (alkyl-O-alkyl ether), 1025, 941, 829, 767, 730, 706. **Analysis:** C₅₀H₈₃N₃O₂₀, calculated: C, 57.40; H, 8.00; N, 4.02; found: C, 57.48; H, 8.14; N, 4.02; **MS** (MALDI-TOF): calculated: 1045.56. found: 1045.47, 1068.47 (Na⁺ adduct), 1084.45 (K⁺ adduct); **UV-Vis** (water, 4.21 × 10⁻⁵ M): λ_{max} (ε) = 260 nm (13.1 × 10⁴ M⁻¹cm⁻¹) and 448 nm (7.4 × 10⁴ M⁻¹cm⁻¹).



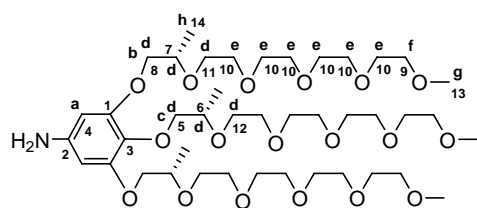
3,6-Diisocyanato-N-(3,4,5-tris[2-(2-{2-[2-(2-methoxyethoxy)ethoxy]ethoxy}ethoxy)propoxy]phenyl)phthalimide (2). Under argon, 3,6-diaminophthalimide **1** (0.185 g, 0.177 mmol) was dissolved in dry toluene (2.0 mL). A phosgene solution

(3.75 ml, 7.09 mmol of a 20 v% solution in PhCH₃) was slowly added to the reaction mixture under continuous stirring. After addition the reaction mixture was stirred for 2.5 h at room temperature. Subsequent concentration *in vacuo* gave **2** (0.165 g, 0.150 mmol, 85 %) as a thick dark-yellow oil that was used as such. **¹H-NMR** (400 MHz, CDCl₃): δ (ppm) = 7.29 (s, 2H, **a**), 6.62 (s, 2H, **b**), 4.08-4.02 (3H, **c**), 3.89-3.69 (12H, **d**), 3.69-3.59 (36H, **e**), 3.58-3.52 (6H, **f**), 3.38-3.37 (9H, **g**), 1.31-1.28 (9H, **h**); **FT-IR** (ATR): σ (cm⁻¹) = 2872, 2246, 1769, 1717, 1597, 1505, 1539, 1437, 1370, 1299, 1239, 1181, 1111, 902, 847, 759, 704.

Amino terminated oligo (3-ureido-*N*-[3,4,5-tris(2S)-2-(2-[2-(2-methoxyethoxy)-ethoxy]-ethoxy)-ethoxy]-pro-poxy]-phenyl]phthalimide-*N'*,6-diyl) (3).

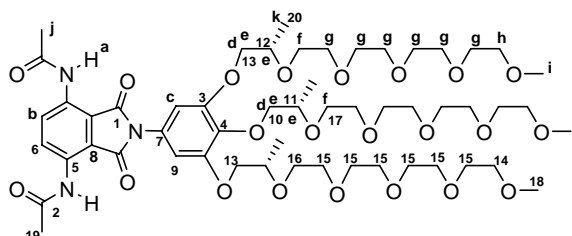


Under argon, 3,6-diaminophthalimide **1** (0.157 g, 0.152 mmol) and dry 3-dimethylaminopyridine (DMAP) (18.3 mg, 0.15 mmol) dissolved in dioxane (0.5 mL) were added to 3,6-diisocyanatophthalimide **2** (0.165 g, 0.150 mmol). The reaction mixture was heated to reflux overnight under continuous stirring followed by evaporation of the solvent *in vacuo*. The DMAP was removed by column chromatography (silica gel, 10 v% MeOH in 1,2-dimethoxyethane) yielding 0.316 g (95 %) of a yellow-orange sticky solid. A second separation by column chromatography (silica gel, 1 to 10 v% MeOH in 1,2-dimethoxyethane gradient) afforded **3a** (0.153 g) containing the shorter oligomers, GPC (CHCl₃, mixed-E, 310 nm), *R_t* (min) = 5.69 min; and **3b** (0.140 g) containing the long oligomers as dark yellow sticky solids. **3b**; GPC (CHCl₃, mixed-E, 310 nm), *R_t* (min) = 4.73 and 4.35, tailing. ¹H-NMR (400 MHz, CDCl₃): δ (ppm) = 9.03-8.70 ((4*n*+2)H, **a** and **b**), 8.44 (d, 2H, *J* = 9.2 Hz, **c**), 6.98 (d, 2H, *J* = 9.2 Hz, **d**), 6.61 (2*n*H, **e**), 5.29 (s, 4H, **f**), 4.10-3.24 and 1.32-1.28 (m, (75*n*+150)H, **g**). MS (MALDI-TOF): Sodium adducts of monomer till 25-mer.



3,4,5-Tris(2S)-2-(2-[2-(2-methoxyethoxy)-ethoxy]-ethoxy)-ethoxy)-pro-poxy]-aniline (9). Under argon, isocyanate **8** (2.292 g, 2.513 mmol) in dioxane (50 mL) was slowly added through a cannula to a hot (60 °C), well-stirred solution of KOH (22.44 g, 0.40 mol) in water (200 mL), which was purged with nitrogen gas for 0.5 h prior to use. After addition of the isocyanate the mixture was stirred at 90 °C for 0.5 h and then concentrated *in vacuo* to remove dioxane. The aqueous residue was extracted with CH₂Cl₂ (3 × 75 mL). The combined organic layers were dried over MgSO₄, filtered and concentrated *in vacuo*. Under argon the residue was mixed with a solution of NaOH (8.0 g, 0.20 mol) in water (100 mL) and dioxane (40 mL), which was purged with nitrogen for 30 min before use. The stirred reaction mixture was heated under reflux for 3 days. Then, the mixture was allowed to reach room temperature and brine (10 mL) was added. Subsequently, the mixture was extracted with CH₂Cl₂ (3 × 75 mL), the combined organic layers dried over MgSO₄ and the suspension filtered. Concentration of the filtrate *in vacuo* gave **9** (2.169 g, 2.447 mmol, 97 %) as a thick brownish oil that was used as such. *R_t* = 0.41 (silica gel, 1,2-dimethoxyethane); HPLC (PDA detector): *R_t* = 2.33 min, purity ≈ 97 %. ¹H-NMR (400 MHz, CDCl₃): δ (ppm) = 5.93 (s, 2H, **a**), 3.99 (m, 2H, **b**), 3.92 (m, 1H, **c**), 3.85-3.69 (12H, **d**), 3.67-3.61 (36H, **e**), 3.58-3.53 (6H, **f**), 3.38 (s, 9H, **g**), 1.28-

1.26 (9H, **h**). $^{13}\text{C-NMR}$ (50 MHz, CDCl_3): δ (ppm) = 153.4 (**1**), 143.2 (**2**), 130.7 (**3**), 94.8 (**4**), 76.8 (**5**), 75.2 (**6**), 74.6 (**7**), 72.8 (**8**), 72.1 (**9**), 71.1-70.7 (**10**), 69.0 (**11**), 68.7 (**12**), 59.3 (**13**), 18.0-17.8 (**14**). **FT-IR** (ATR): σ (cm^{-1}) = 3362, 2870, 2160, 1608, 1507, 1453, 1374, 1350, 1294, 1237, 1200, 1096, 1025, 945, 849, 737. **Analysis**: $\text{C}_{42}\text{H}_{79}\text{NO}_{18}$, calculated C, 56.93; H, 8.99; N, 1.58; found: C, 56.61; H, 9.00; N, 1.53; **MS** (MALDI-TOF), calculated: 885.53, found: 885.73, 908.72 (Na^+ adduct), 924.74 (K^+ adduct).



3,6-Bis(acetylamino)-N-{3,4,5-tris[(2S)-2-(2-{2-[2-(2-methoxyethoxy)-ethoxy]-ethoxy}-ethoxy)-propoxy]-phenyl}-phthalimide (11**)**. Under argon, 3,6-bis(acetylamino)phthalic anhydride (**10**) (0.377 g, 1.438 mmol) and amine **9** (1.333 g, 1.504 mmol) were mixed in dioxane (7.2 mL). After 17 h reflux the mixture was

concentrated *in vacuo* and the remaining residue was purified by column chromatography (silica gel, 25 v% heptane in 1,2-dimethoxyethane) yielding **11** (1.457 g, 1.289 mmol, 90 %) as a yellow thick oil. R_f = 0.3 (silica gel, 20 v% heptane in 1,2-dimethoxyethane); **GPC** (mixed D, 254 nm, CHCl_3): R_t = 8.38 min. $^1\text{H-NMR}$ (400 MHz, CDCl_3): δ (ppm) = 9.38 (s, 2H, **a**), 8.81 (s, 2H, **b**), 6.62 (s, 2H, **c**), 4.10-4.02 (3H, **d**), 3.90-3.81 (6H, **e**), 3.77-3.69 (6H, **f**), 3.68-3.62 (36H, **g**), 3.56-3.52 (6H, **h**), 3.39-3.37 (s, 9H, **i**), 2.26 (s, 6H, **j**), 1.32-1.29 (9H, **k**); $^{13}\text{C-NMR}$ (50 MHz, CDCl_3): δ (ppm) = 169.0 (**1**), 168.3 (**2**), 152.9 (**3**), 138.0 (**4**), 133.3 (**5**), 127.5 (**6**), 126.0 (**7**), 113.8 (**8**), 105.6 (**9**), 76.4 (**10**), 75.1 (**11**), 74.4 (**12**), 72.8 (**13**), 72.0 (**14**), 70.9-70.5 (**15**), 68.9 (**16**), 68.6 (**17**), 59.1 (**18**), 24.9 (**19**), 17.7-17.5 (**20**); **FT-IR** (ATR): σ (cm^{-1}) = 3363, 2871, 2184, 1754 and 1699, 1637, 1616, 1548, 1598 and 1491, 1438, 1393, 1369, 1297, 1239, 1200, 1099, 1016, 978, 906, 845, 762, 688, 665; **Analysis**: $\text{C}_{54}\text{H}_{87}\text{N}_3\text{O}_{22}$, calculated: C, 57.38; H, 7.76; N, 3.72; found: C, 57.41; H, 7.78; N, 3.61; **MS** (MALDI-TOF), calculated: 1129.58; found: 1152.65 (Na^+ adduct), 1169.61 (K^+ adduct); **UV-Vis** (water, 4.87×10^{-5} M): λ_{max} (ϵ) = 259 nm ($24.0 \times 10^4 \text{ M}^{-1}\text{cm}^{-1}$) and 367 nm ($4.5 \times 10^4 \text{ M}^{-1}\text{cm}^{-1}$).

5.7 References

- 1) Kritzer, J. A.; Tirado-Rives, J.; Hart, S. A.; Lear, J. D.; Jorgensen, W. L.; Schepartz, A. J. *Am. Chem. Soc.* **2005**, *127*, 167-78.
- 2) Reviews on helical β -peptides (a) Martinek, T. A.; Fülöp, F. *Eur. J. Biochem.* **2003**, *270*, 3657-66. (b) Cheng, R. P.; Gellman, S. H.; DeGrado, W. F. *Chem. Rev.* **2001**, *101*, 3219-32. (c) DeGrado, W. F.; Schneider, J. P.; Hamuro, Y. *J. Peptide Res.* **1999**, *54*, 206-17.
- 3) Reuping, M.; Mahajan, Y. R.; Jaun, B.; Seebach, D. *Chem. Eur. J.* **2004**, *10*, 1607-15.
- 4) (a) Appella, D. H.; Christianson, L. A.; Karle, I. L.; Powell, D. R.; Gellman, S. H. *J. Am. Chem. Soc.* **1996**, *118*, 13071-2. (b) Appella, D. H.; Christianson, L. A.; Klein, D. A.; Powell, D. R.; Huang, X.; Barchi Jr, J. J.; Gellman, S. H. *Nature*, **1997**, *387*, 381-4.
- 5) Seebach, D.; Matthews, J. L. *Chem. Commun.* **1997**, 2015-22.
- 6) Reviews on foldamers: (a) Block, M. A. B.; Kaiser, C.; Khan, A.; Hecht, S. *Top. Curr. Chem.* **2005**, *89*. (b) Sanford, A. R.; Yamato, K.; Yang, X.; Han, Y.; Gong, B. *Eur. J. Biochem.* **2004**, *271*, 1416-25. (c) Huc, I. *Eur. J. Org. Chem.* **2004**, 17-29. (d) Schmuck, C. *Angew. Chem. Int. ed.* **2003**, 2448-52 (e) Hill, D. J.; Mio, M. J.; Prince, R. B.; Hughes, T. S.; Moore, J. S. *Chem. Rev.* **2001**, *101*, 3893-4011. (f) Gellman, S. H. *Acc. Chem. Res.* **1998**, *31*, 173-80.
- 7) Nguyen, J. Q.; Iverson, B. L. *J. Am. Chem. Soc.* **1999**, *121*, 2639-40.
- 8) Nelson, J. C.; Saven, J. G.; Moore, J. S.; Wolynes, P. G. *Science*, **1997**, *277*, 1793-6.
- 9) Yang, X.; Yuan, L.; Yamato, K.; Brown, A. L.; Feng, W.; Furukawa, M.; Zeng, C. X.; Gong, B. *J. Am. Chem. Soc.* **2004**, *126*, 3148-62.
- 10) (a) Gong, B. *Chem. Eur. J.* **2001**, *7*, 4337-42. (b) Ernst, J. T.; Becerril, J.; Park, H. S.; Yin, H.; Hamilton, A. D. *Angew. Chem. Int. Ed.* **2003**, *42*, 535-9. (c) Jiang, H.; Léger, J. M.; Huc, I. *J. Am. Chem. Soc.* **2003**, *125*, 3448-9.
- 11) Hamuro, Y.; Geib, S.; Hamilton, A. D. *J. Am. Chem. Soc.* **1996**, *118*, 7529-41.
- 12) (a) Berl. V.; Huc, I.; Khoury, R. G.; Lehn, J. M. *Chem. Eur. J.* **2001**, *7*, 2798-2809. (b) Dolain, C.; Maurizot, V.; Huc, I. *Angew. Chem. Int. Ed.* **2003**, *42*, 2738-40.
- 13) Corbin, P. S.; Zimmerman, S. C.; Thiessen, P. A.; Hawryluk, N. A.; Murray, T. J. *J. Am. Chem. Soc.* **2001**, *123*, 10475-88.
- 14) Hou, J. L.; Shao, X. B.; Chen, G. J.; Zhou, Y. X.; Jiang, X. K.; Li, Z. T. *J. Am. Chem. Soc.* **2004**, *126*, 12386-94.
- 15) Masu, H.; Sakai, M.; Kishikawa, K.; Yamamoto, M.; Yamaguchi, K.; Kohmoto, S. *J. Org. Chem.* **2005**, *70*, 1423-31.
- 16) Arnt, L.; Tew, G. N. *J. Am. Chem. Soc.* **2002**, *124*, 7664-5.
- 17) Arnt, L.; Tew, G. N. *Macromolecules* **2004**, *37*, 1283-8.
- 18) (a) L. Brunsveld, L.; Meijer, E. W.; Prince, R. B.; Moore, J. S. *J. Am. Chem. Soc.* **2001**, *123*, 7978-84. (b) Prince, R. B.; Brunsveld, L.; Meijer, E. W.; Moore, J. S. *Angew. Chem. Int. Ed.* **2000**, *39*, 228-30.
- 19) Prince, R. B.; Barnes, S. A.; Moore, J. S. *J. Am. Chem. Soc.* **2000**, *122*, 2758-62. (b) Prince, R. B.; Saven, J. G.; Wolynes, P. G.; Moore, J. S. *J. Am. Chem. Soc.* **1999**, *121*, 3114-21.
- 20) Stone, M. T.; Moore, J. S.; *Org. Lett.* **2004**, *6*, 469-72.
- 21) Garric, J.; Léger, J. M.; Huc, I. *Angew. Chem. Int. Ed.* **2005**, *44*, 1954-8.
- 22) van Gorp, J. J.; Vekemans, J. A. J. M.; Meijer, E. W. *Chem. Commun.* **2004**, 60-1.
- 23) van Gorp, J. J.; Thesis, Eindhoven University of Technology: *Helices by Hydrogen Bonding*, **2004**.
- 24) Sinkeldam, R. W.; van Houtem, M. H. C. J.; Koeckelberghs, G.; Vekemans, J. A. J. M.; Meijer, E. W. *Org. Lett.* **2005**, *8*, 383-5.
- 25) Brunsveld, L.; Zhang, H.; Glasbeek, M.; Vekemans, J. A. J. M.; Meijer, E. W. *J. Am. Chem. Soc.* **2000**, *122*, 6175-82.
- 26) Shoemaker, K. R.; Kim, P. S.; Brems, D. N.; Marqusee, S.; York, E. J.; Chaiken, I. M.; Steward, J. M.; Baldwin, R. L. *Proc. Natl. Acad. Sci. U.S.A.* **1985**, *82*, 2349-53.
- 27) Marqusee, S.; Robbins, V. H.; Baldwin, R. L. *Proc. Natl. Acad. Sci. U.S.A.* **1989**, *86*, 5286-90.

- 28) Prince, R. B.; Brunsveld, L.; Meijer, E. W.; Moore, J. S. *Angew. Chem. Int. Ed.* **2000**, *39*, 228-30.
- 29) (a) Barr, G. C.; Norman, D. *Techniques Applied to Nucleic Acids. Nucleic Acids in Chemistry and Biology*, 2nd ed.; Blackburn, G. M. Gait, M. J.; Eds.; Oxford University Press, Inc.: New York, 1996; pp 446-7. (b) Cantor, C. R.; Schimmel, P. R. *Biophysical Chemistry*; Freeman, New York, 1980. (c) Bloomfield, V. A.; Crothers, D. M.; Tinoco, I. *Physical Chemistry of Nucleic acids*; Harper & Row, New York, 1974.
- 30) (a) Wahab, S. A.; Matsuura, H. *Phys. Chem. Chem. Phys.* **2001**, *3*, 4689-95. (b) Begum, R.; Yonemitsu, T.; Matsuura, H. *J. Mol. Struct.* **1998**, *447*, 111. (c) Begum, R.; Matsuura, H. *J. Chem. Soc. Faraday Trans.* **1997**, *93*, 3839.
- 31) Hofacker, A. L.; Parquette, J. R. *Angew. Chem. Int. Ed.* **2005**, *44*, 1053-7.
- 32) Schenning, A. P. H. J.; Jonkheijm, P.; Peeters, E.; Meijer, E. W. *J. Am. Chem. Soc.* **2001**, *123*, 409-416.

Chapter 6

Indigo: synthesis of a new soluble n-type material

Abstract

In the previous chapters the synthetic aspects and potential of new types of foldamers based on a poly(ureidophthalimide) backbone was discussed. The strong indication that these foldamers are capable of aligning peripheral chromophores may contribute to research on organic photovoltaics. This chapter is not focused on the organization of chromophores but on the development of a new n-type chromophore potentially useful in i.e. organic solar cells. The well-known dye indigo is an appealing candidate since it possesses an intrinsic long-wavelength absorption maximum and hence a small band gap. However, the notorious insolubility of the parent indigo required derivatization to ensure processability. Several approaches have been investigated and proven to be unsuccessful except for one. With 5-bromo-N-acetyloxyl as a key precursor a set of novel soluble indigo derivatives have become available. Besides solubility, the novel route allowed introduction of functionality for band gap engineering. The new indigo derivatives have been studied with UV-vis and fluorescence spectroscopy. Photoinduced absorption spectroscopy and atomic force microscopy on N,N'-diacetylindigo revealed its applicability for use in an organic solar cell. However the performance of a solar cell constructed from N,N'-diacetylindigo and poly(phenylenevinylene) has so far been disappointing.

6.1 Introduction

In Chapter 2 a novel synthetic methodology that gives access to polymer building blocks decorated with chromophores is presented.¹ In chapter 4 the peripheral organization of chromophores by exploitation of the secondary structure of poly (ureidophthalimide) is discussed. This system may be of interest for the use in organic solar cells that benefit from highly organized chromophores (Figure 4.1, Chapter 4). This chapter, however, does not concern the controlled organization of chromophores but rather discusses the development of a new type of chromophore for use in an organic solar cell or other applications. The newly developed chromophores may be incorporated in the ureidophthalimide architecture in a later stage of this research.

Nowadays potential applications for dyes, inherently containing long-wavelength absorbing chromophores, lie in the field of molecular electronic devices such as organic photovoltaic cells. This application depends on the efficient conversion of solar radiation into electric current. The AM1.5 (Air Mass 1.5) plot represents the standardized solar spectrum on earth (Figure 6.1). The highest number of photons/m² s⁻¹, the photon flux or photon density, is irradiated in the region between 550-700 nm.

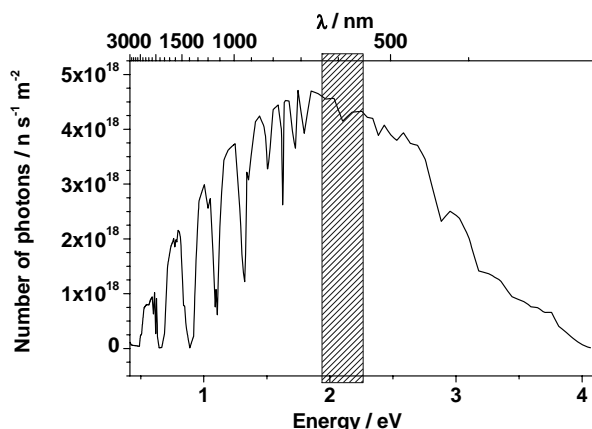


Figure 6.1: AM1.5 plot, the standardized solar spectrum on earth. The wavelength regime in which indigo displays its absorption maximum is highlighted.

Modern successful organic solar cells are based on the 'bulk heterojunction' approach.² The active layer in this cell type is formed by a blend of a p-type and an n-type material. Electron rich/donating (p-type) compounds are most abundant. However, there is a strong demand for more electron poor/accepting (n-type) materials displaying a good electron mobility. The fact that the dye indigo possesses its absorption maximum in the wavelength regime with the highest photon flux (Figure 6.1) makes it an appealing chromophore for application in organic solar cells. Especially the influence of substitution on the band gap may allow optimization of

the indigo chromophore for use in a solar cell. In this chapter a synthetic route to arrive at such a potential candidate based on one of the oldest known dyes: indigo (**1**) (Figure 6.2) for use in organic solar cells is presented.

Organic dyes, like indigo, have been studied ever since the development of organic chemistry. An important application is their use as a colorant for fabrics. Indigo is in that respect an excellent example since it was, and still is widely used in the textile industry for its typical deep blue color with excellent light fastness. In this application its notorious insolubility due to inter as well as intra molecular hydrogen bonding in combination with π - π stacking is an advantage (Figure 6.2).

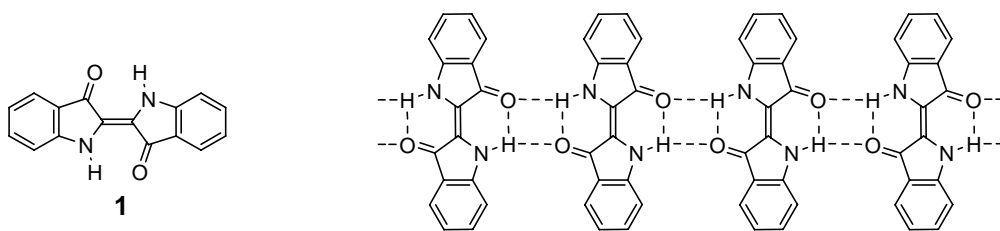
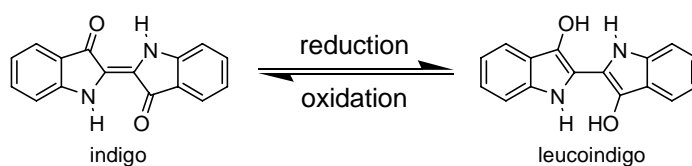


Figure 6.2: Insolubility of indigo (**1**) due to inter- as well as intramolecular hydrogen bonding.

The insolubility of indigo gave rise to a special procedure to dye textile, known as vat dyeing. In this process indigo is converted to leucoindigo (indigo white) by exposure to a reducing agent in a basic aqueous solution (Scheme 6.1). The fabric to be colored is immersed in the vat containing the colorless leucoindigo solution. After this soaking treatment the fabric is pulled out and upon exposure to air the leucoindigo is oxidized to indigo. In this process indigo strongly attaches to the fibers of the fabric. A simple washing procedure removes excess of pigment.



Scheme 6.1: Formation of soluble leucoindigo.

However, insolubility is just one of the characteristics of indigo and not a very enjoyable property for organic chemists since it hampers synthetic derivatization. But this huge disadvantage is compensated by its intriguing dark blue color that reveals its high wavelength absorption maximum in UV-vis absorption spectrometry and hence its intrinsic small band gap. Although depending on the medium, an absorption maximum of typically around 600 nm is observed. The relation between color and constitution of indigo has been the subject of many experimental and theoretical studies.³ Not the benzene rings are most essential for the bathochromic absorption of indigo, but rather the cross conjugated system consisting of the two

donor (nitrogen) and two acceptor (C=O) moieties connected through the central double bond causes the characteristic absorption at 660 nm in the solid phase and ranging from 590 to 630 nm in various solvents.^{4,5} Figure 6.3 shows the influence of π -system elongation on the absorption maximum.^{6,7}

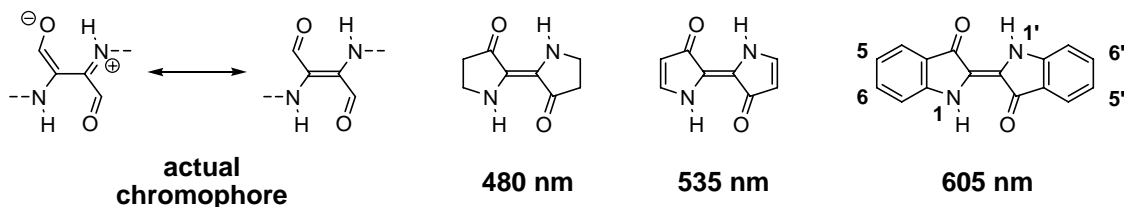
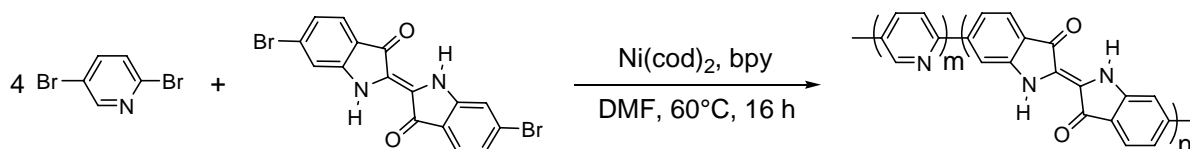


Figure 6.3: Influence of the π -system elongation on the absorption maximum in ethanol.

Another feature of indigo is the possibility to manipulate the band gap by proper substitution.^{4,3c} Electron releasing substituents on the N-1, N-1', C-5 and C-5' positions or the introduction of electron accepting groups on the C-6 and C-6' positions cause a bathochromic shift. However, a hypsochromic shift is obtained by the introduction of an electron withdrawing group on N-1, N-1', C-5 and C-5' or by introduction of electron-releasing substituents on the C-6 and C-6' position. This effect can be rationalized by taking a closer look at the effect of substitution on the strong donor-acceptor interaction within the indigo structure. When electron releasing substituents are placed on N-1, N-1', C-5 and C-5' positions the electron density on the nitrogens is enhanced which therefore becomes a better donor. Introduction of electron withdrawing functionalities on the C-6 and C-6' positions will lower the electron density on the carbonyl moiety which in turn becomes a better acceptor.

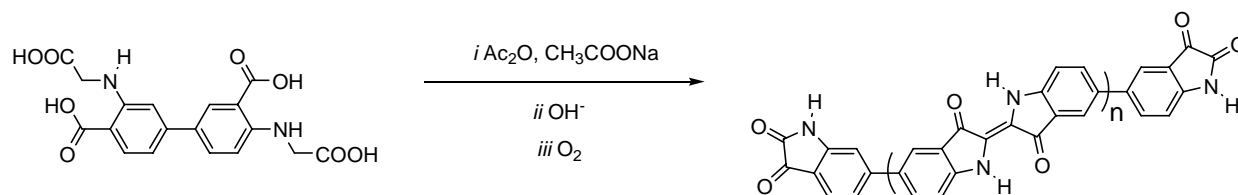
Besides the small band gap, indicated by its absorption maximum at 660 nm, indigo also possesses a relatively low-lying LUMO.⁸ A small band gap together with a low-lying LUMO are two properties that make indigo a new candidate for a small band gap n-type material, eventually appealing for use in organic solar cells. These features have been recognized by Yamamoto who exploited his own Yamamoto coupling to synthesize an indigo-pyridine copolymer (Scheme 6.2).⁹



Scheme 6.2: Synthesis of a pyridine-indigo copolymer.

Obviously, there is no control over the regioselectivity. It is even to be expected that the polymer will consist primarily of pyridine due to the 4 fold excess of 2,5-dibromopyridine and

the latter's much higher solubility in DMF. Moreover, the solubility of this copolymer is limited but does dissolve in formic acid. Another approach to obtain a polymer consisting of only indigo is depicted in scheme 6.3. In two steps the starting compound is converted into the monomer that will readily oxidize in air to give the polymer.¹⁰ The polymer becomes soluble in basic aqueous media and loses its characteristic dark blue color. A similar approach has been patented by the Sun Oil Company.¹¹

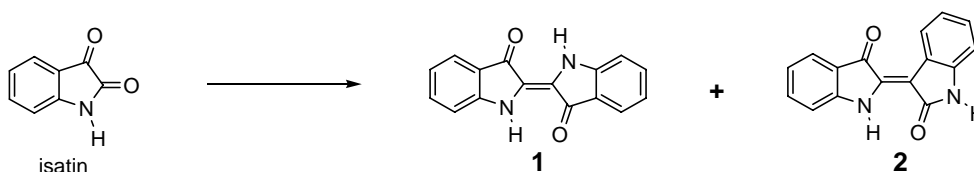


Scheme 6.3: *An indigo homopolymer.*

However, for successful application in the field of molecular electronics, derivatization of indigo is a prerequisite to increase solubility to make indigo processable. This requires a completely new multi-step approach to allow early introduction of solubility and functionalities to alter the absorption maximum. For the potential use as a peripheral chromophore in poly(ureidophthalimide) foldamers (Chapter 4), an asymmetric indigo is required. However, in view of the synthetic challenges the primary focus will be on the synthesis of a symmetric indigo derivative.

6.2 A Brief history on the synthesis of indigo

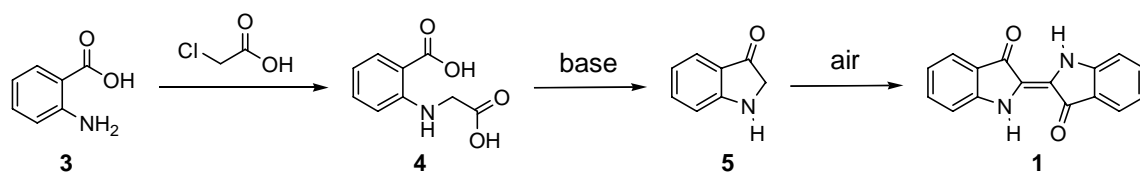
Indigo has been used for over 3500 years as a dye and was known to the ancients of Asia, Egypt, Greece, Rome, Britain, and Peru. The earliest findings were bandages dyed with indigo on Egyptian mummies that date back to 1580 B.C. For a long time the only source of indigo was a natural one. Indigo used to be extracted from the indigo plant: *Indigofera tinctoria*. Indigo (**1**) was first synthesized by Baeyer in 1870 who prepared it from isatin and PCl_3 .¹² Besides indigo, this route also gave isomer indirubin (**2**), a red dye, as a side product (Scheme 6.4).



Scheme 6.4: *Baeyer indigo (1) synthesis and side product indirubin (2).*

The commercial synthetic process is based on the research by Heumann¹³ and adapted to allow large-scale production. This route started from anthranilic acid (**3**) which is reacted with

chloroacetic acid to give intermediate **4**. When heated in the presence of a strong base, indoxyl (**5**) is formed which oxidizes (dimerization) in air giving indigo (**1**) (Scheme 6.5).

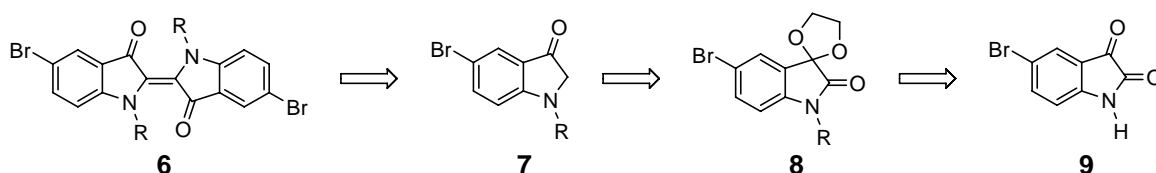


Scheme 6.5: The first synthetic route for the production of indigo.

The insoluble nature of the parent indigo requires introduction of solubility and functionality prior to indigo formation. Although there is a vast number of publications on indigo, little is reported on a general synthetic methodology that addresses solubility and facile substitution for band gap engineering.

6.3 Towards soluble indigo derivatives, the isatin pathway

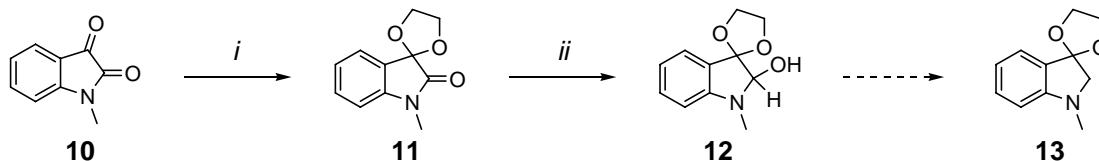
In this strategy we follow the initial approach of Baeyer (Scheme 6.4) to synthesize dibromo-indigo (**6**) (Scheme 6.6) starting from isatin. Since our interest goes beyond indigo itself an anchor point for further derivatization is required. This handle can be found in commercial 5-bromo-isatin (**9**), where the C-Br bond provides an excellent substrate for π -system elongation by modern palladium mediated chemistry. The insolubility of the final indigo can be tackled with the early introduction of solubilizing groups by alkylation¹⁴ or acetylation¹⁵ of bromo-isatin (**9**). To prevent formation of indirubin (**2**) the Baeyer strategy had to be altered. The approach depicted in scheme 6.6 aims at a ketal protection^{15,16} of the carbonyl adjacent to the benzene moiety giving rise to compounds **8**. Finally, reduction of the lactam carbonyl should give access to 5-bromo-indoxyl (**7**) which is the precursor for 5,5'-dibromo-indigo (**6**). Subsequently, the π -system of 5,5'-dibromo-*N,N'*-disubstituted indigo can be elongated by exploitation of the aryl-bromide functionality. Besides this approach, π -elongation of indoxyls **7** may also precede dimerization.



Scheme 6.6: Retrosynthetic approach towards 5,5'-dibromo-indigos (**2**).

To investigate the potential of this route, commercial *N*-methylisatin (**10**) was monoprotected with 1,2-ethanediol in refluxing toluene in the presence of a catalytic amount of *p*-

toluenesulfonic acid to give **11** (Scheme 6.7). Subsequent reduction of the remaining carbonyl gave alcohol **12** but did not afford the anticipated indoxyl **13**. Attempts to force the reduction to completion by changing the reaction conditions to refluxing dioxane gave a mixture of products.

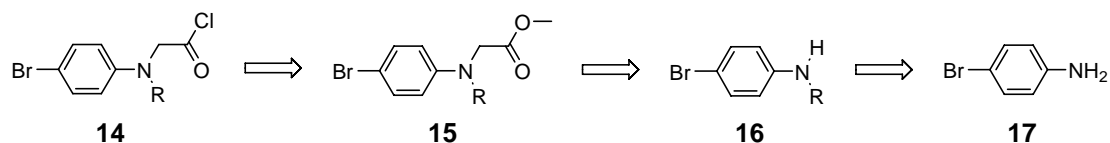


Scheme 6.7: Synthetic approach towards protected indoxyl **13**. i) 1,2-ethanediol (1.2 equiv.), *p*-TsOH (10 mol%), PhCH_3 , reflux, 3 h, 98%. ii) LiAlH_4 (0.5 equiv.), THF, rt, 1 h, 99% of **12**.

Since the synthesis of monoprotected *N*-methyl indoxyl **13** proved to be unsuccessful, another approach was investigated in which the formation of the indoxyl skeleton is part of the synthetic route.

6.4 A Friedel-Crafts precursor as the key intermediate

The exploitation of the Friedel-Crafts procedure for the construction of the indoxyl framework has been previously reported for the synthesis of the closely related structures: thioindoxyl¹⁷, pyrroloindolone¹⁸ and for the formation of isatin¹⁹ derivatives. Similar to scheme 6.5 also this approach leads to *N*-substituted indoxyls of type **7**, the precursor for indigos of type **6**. Indoxyls **7** may become accessible *via* a Friedel-Crafts reaction on the corresponding acid chlorides **14** which may be synthesized in two steps from methyl esters **15** (Scheme 6.8). In turn, esters of type **15** can be constructed from secondary amines **16** by alkylation with methyl bromoacetate. Amines of type **16** should become available by acylation of **17** followed by a reduction.

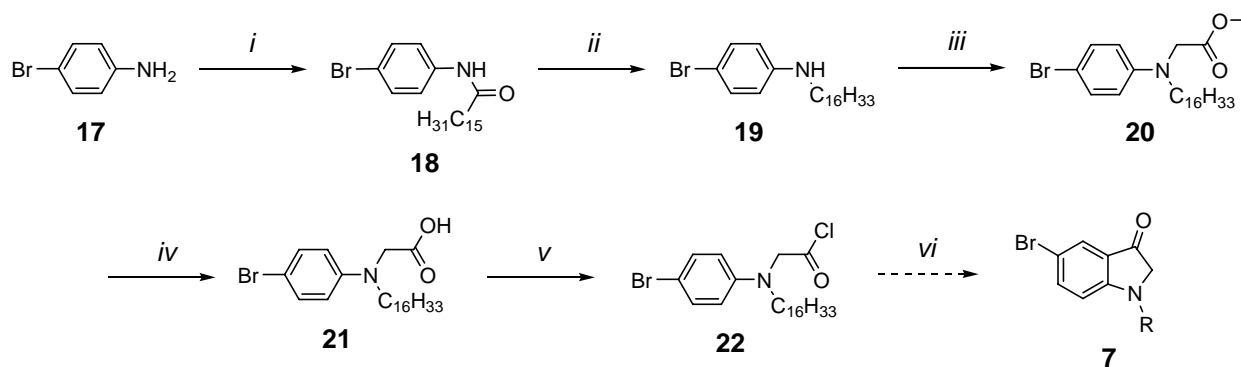


Scheme 6.8: A retrosynthetic approach towards of acid chloride **14**, a precursor for indoxyl **7**.

Acylation of aniline **17** with palmitoyl chloride gave amide **18** which, in turn, is reduced to the corresponding secondary amine **19** (Scheme 6.9). A subsequent alkylation with methyl bromoacetate furnishes tertiary amine **20** that after methyl ester hydrolysis gives acid **21**. By exposure of acid **21** to thionyl chloride, acid chloride **22** is obtained. However, exposure of **22** to AlCl_3 under Friedel-Crafts conditions did not result in the formation of a single product.

After addition of AlCl_3 to a solution of **22** in CHCl_3 under reflux the color changed to dark red, indicative of complex formation between AlCl_3 and the acid chloride. ^1H NMR analysis in

CHCl₃ of a sample after a work up revealed that the singlet at ~4.3 ppm, which can be attributed to the CH₂ located between the nitrogen and the COCl, had disappeared. The aromatic region still displays two doublets instead of the expected singlet and two doublets. Thus, the benzene moiety remained unsubstituted.



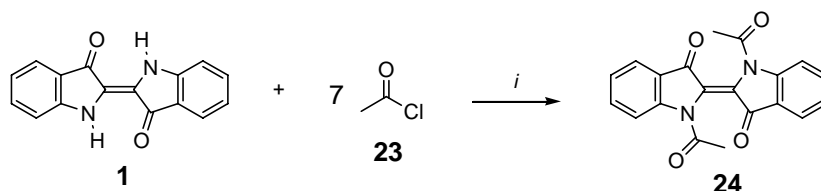
Scheme 6.9: Synthetic route towards indoxyls **7**. i) palmitoyl chloride (1 equiv.), Et₃N (1.1 equiv.), CH₂Cl₂, rt, 3 h, 93%. ii) LiAlH₄ (1 equiv.), rt, 1 h; reflux, 1 h, 97%. iii) NaH (1.5 equiv.) DMF, 40°C, 3 h, then methyl bromoacetate (1 equiv.), 40°C, 17 h, 75%. iv) 1M aq. NaOH (~4 equiv.), THF, rt, 5 h, 100%. v) SOCl₂ (1.2 equiv.), DMF (2 drops), CCl₄, rt, ~100%. vi) AlCl₃ (2 equiv.), CHCl₃,

Moreover, TLC showed the presence of many products. Instead of using CHCl₃, the Friedel-Crafts reaction was performed in nitromethane. Unfortunately, despite limited conversion already several products were formed. Although still unclear, a possible explanation may be the strong interaction of AlCl₃ with the tertiary amine reducing the nucleophilicity of the benzene core.²⁰ In addition, the acid chloride **22** was very unstable judged from degradation after a few days under argon in the dark at room temperature. Finally, attempts have been made to cyclize acid **21** by exposure to poly (phosphoric acid) at 100°C and 150°C.²¹ Also in these cases ¹H NMR revealed an unchanged aromatic region.

It seems that the construction of the indoxyl ring *via* a Friedel-Crafts ring closure is not possible on this system. Therefore, an approach was envisaged in which the indoxyl ring is formed by reaction between two *ortho* positioned substituents on the benzene ring.

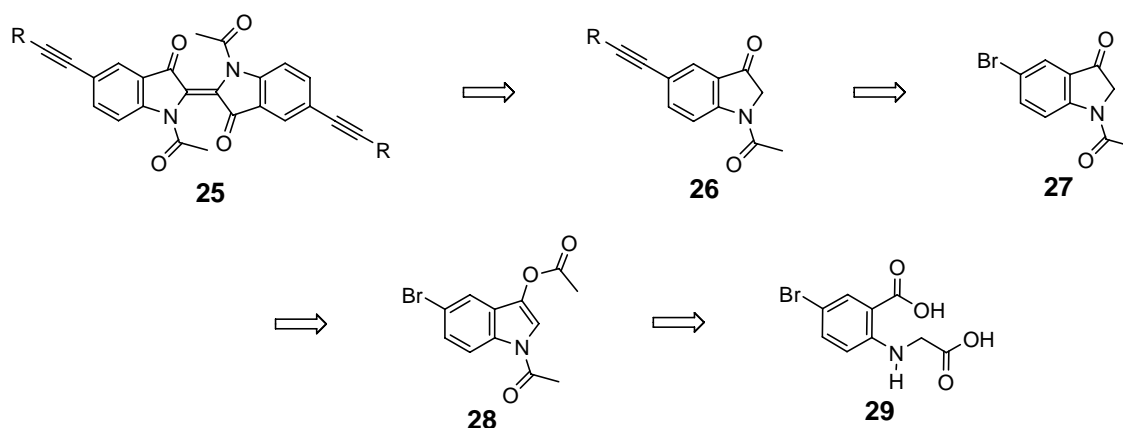
6.5 Soluble *N,N'*-diacetylundigo derivatives

From literature it is known that the solubility of indigo is enormously improved by acetylation of indigo on both nitrogens. The solubility is increased due to breaking up of inter- as well as intramolecular hydrogen bonding. Direct acetylation of indigo **1** with an excess of acetyl chloride **23** in a solvent mixture of *n*-butyl acetate and lutidine at elevated temperatures furnished *N,N'*-diacetylundigo **24** in moderate yields (Scheme 6.10).²² The crude product can be recrystallized from ethyl acetate-hexane resulting in bright dark pink-red crystals.



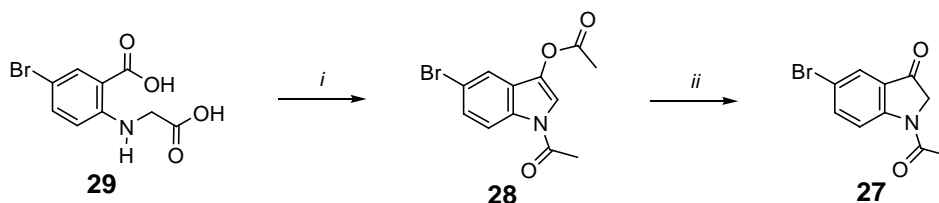
Scheme 6.10: Acetylation of commercially available indigo. i) *n*-BuOAc/lutidine, 80°C, 24 h, 59%.

Although two old patents mention direct bromination of indigo²³ to obtain mono and dibromo-indigo, it is not expected that this process is selective and exclusively would yield 5,5'-dibromo indigo. Obviously, separation of such a mixture will be extremely difficult. Besides these patents no literature is available on the bromination of indigo. However, dibromo-indigo has been constructed from different bromine containing precursors.²⁴ The approach depicted in scheme 6.11 starts from commercial **29** which is converted in *N*-acetylindoxyl **27**. Acetylene linkers are chosen for the extension of the π -system since their introduction relies on the robust, versatile and well documented Sonogashira approach. Thus, 5-bromo-*N*-acetylindoxyl (**27**) was selected as the key synthon since in principle a wide variety of ethynyl derivatives can be introduced to arrive at compounds of type **26**, which in turn should give access to indigo's of type **25**.



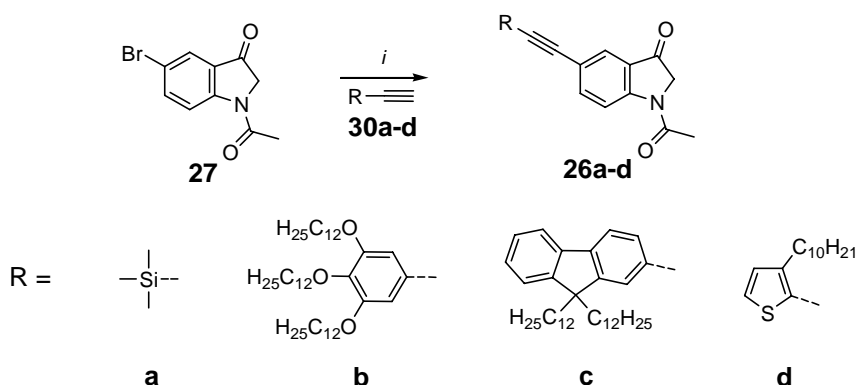
Scheme 6.11: Retrosynthetic approach to 5,5'-bis(ethynyl)indigos **25**.

Acetylation and ring closure in the presence of acetic anhydride and sodium acetate as a base at elevated temperatures converted diacid **29** into indoxyl derivative **28**. A subsequent selective hydrolysis of the ester with Na₂SO₃ in an ethanol/water mixture, leaving the amide intact, furnished key synthon 5-bromo-*N*-acetyl-indoxyl (**27**) (Scheme 6.12).^{25,26} ¹H NMR analysis of compound **27** in CDCl₃ revealed that it is only present in its keto form, despite the aromaticity of the enol form.



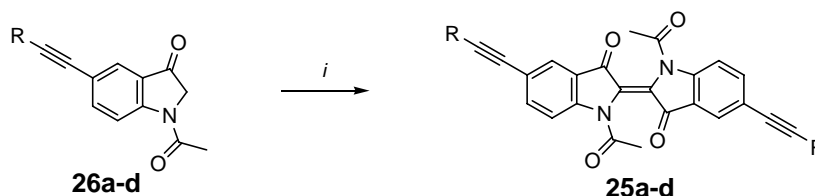
Scheme 6.12: Synthesis of key synthon **27**. i) NaOAc, Ac₂O, reflux, 45 min., 50%. ii) Na₂SO₃ (1.7 equiv.), EtOH/H₂O, reflux, 30 min., 93%.

Brominated indoxyl **27** proved indeed to be a suitable precursor for the palladium catalyzed introduction of various ethynyl derivatives under Sonogashira conditions (Scheme 6.13). The Sonogashira conditions for coupling of **27** with **30a**, **b**²⁷, **c**²⁸, and **d** were optimized for the synthesis of **26a**. These conditions were used without further optimization to obtain **26b-d** but are most likely not ideal as can be judged from the moderate to low yields.



Scheme 6.13: Synthesis of 5-ethynyl-N-acetyl-indoxyl derivatives **26a-d**. i) acetylene **30a** (4 equiv.) **b-d** (1 equiv.), CH₃CN/Et₃N, 80°C, 5-21 h, **a**: 89%, **b**: 44%, **c**: 22% **d**: 16%.

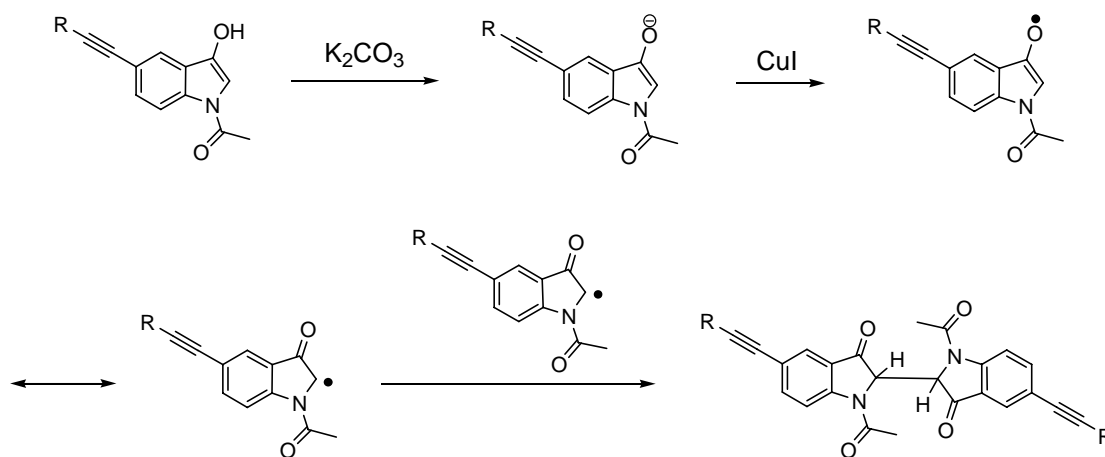
Subsequent exposure of ethynyl derivatives **26a-d** to K₂CO₃ in a THF/water mixture in the presence of CuI at room temperature induced oxidative dimerization to the corresponding indigo analogues **25a-d** (Scheme 6.14).



Scheme 6.14: Dimerization of **26a-d** to the corresponding indigos **25a-d**. i) CuI (1.1 equiv.), K₂CO₃ (0.5 equiv.), THF, H₂O (20 v%), rt, 1 h, **a**: 4%, **b**: 18%, **c**: 2%, **d**: 7%.

The yields of the dimerization are quite disappointing. A tentative mechanism for the dimerization is postulated in scheme 6.15. After keto-enol tautomerization, the enol form can be

easily deprotonated by K_2CO_3 . The oxy-anion is prone to oxidation by exposure to CuI rendering a radical that dimerizes. Tautomerization following oxidation may lead by dehydrogenation to indigo derivatives. The differences in yields are most likely correlated to the solubility of the anionic intermediates, judged from the highest yield for indigo **25b**, possessing three solubility enhancing alkyl chains. In addition, the radical, and therefore uncontrolled nature of the dimerization may also contribute to the low yields.



Scheme 6.15: Tentative mechanism for the dimerization to 5,5'-bis(ethynyl) derivatives of indigo.

Compounds **25a** and **25b** were purified by column chromatography on silica gel, compounds **25c** and **25d**, however, have been purified by preparative TLC on silica gel in view of the small amounts of desired material. Besides a lot of decomposed black tar remaining on the baseline, the preparative TLC-plate showed a large number of colored side products, indicative of the uncontrollable nature of the dimerization reaction and explaining the low yields of desired indigos.

6.6 Photophysical characterization of the novel indigos

Compounds **24** and **25a-d** possess the distinct intense indigo type color, ranging from dark purple to dark blue for compounds **24** to **25d**, respectively. The UV-vis absorption spectra of the indigo analogues **24** and **25a-d** were recorded in THF (Figure 6.4). All compounds showed a short wavelength absorption maximum around 340 nm and a long wavelength absorption at around 560 nm. *N,N'*-diacetylintdigo (**24**) and **25a** did not display a strong absorption in the 340 nm region whereas compounds **25b-d** displayed a strong absorption. Obviously, this can be attributed to the absence of aromatic units connected with the indigo *via* the ethynyl linker in **24** and **25a**. The long wavelength absorption in all indigo derivatives can indeed be attributed to the indigo moiety. Absorption spectrometry on **24** ($\lambda = 550$ nm, $\epsilon = 4500$ M⁻¹cm⁻¹) clearly showed that *N*-acetylation indeed causes a hypsochromic shift of ~45 nm of the absorption maximum

compared to the maximum of the parent indigo at ~ 603 nm ($\epsilon = 13322$ M $^{-1}$ cm $^{-1}$) in CHCl $_3$ ²⁹ (Section 6.1). However, elongation of the π -system with the substituted ethynyl linker in **25a** induced a bathochromic shift (565 nm, $\epsilon = 6400$ M $^{-1}$ cm $^{-1}$). Further lengthening of the π -system in **25b** (568 nm, $\epsilon = 7600$ M $^{-1}$ cm $^{-1}$), **25c** (569 nm, $\epsilon = 6700$ M $^{-1}$ cm $^{-1}$) and **25d** (572 nm, $\epsilon = 5800$ M $^{-1}$ cm $^{-1}$) with various aromatic substituents causes the absorption maximum to red shift even more. Besides a bathochromic shift of the absorption maximum, π -system elongation was also responsible for a hyperchromic effect (Figure 6.4).

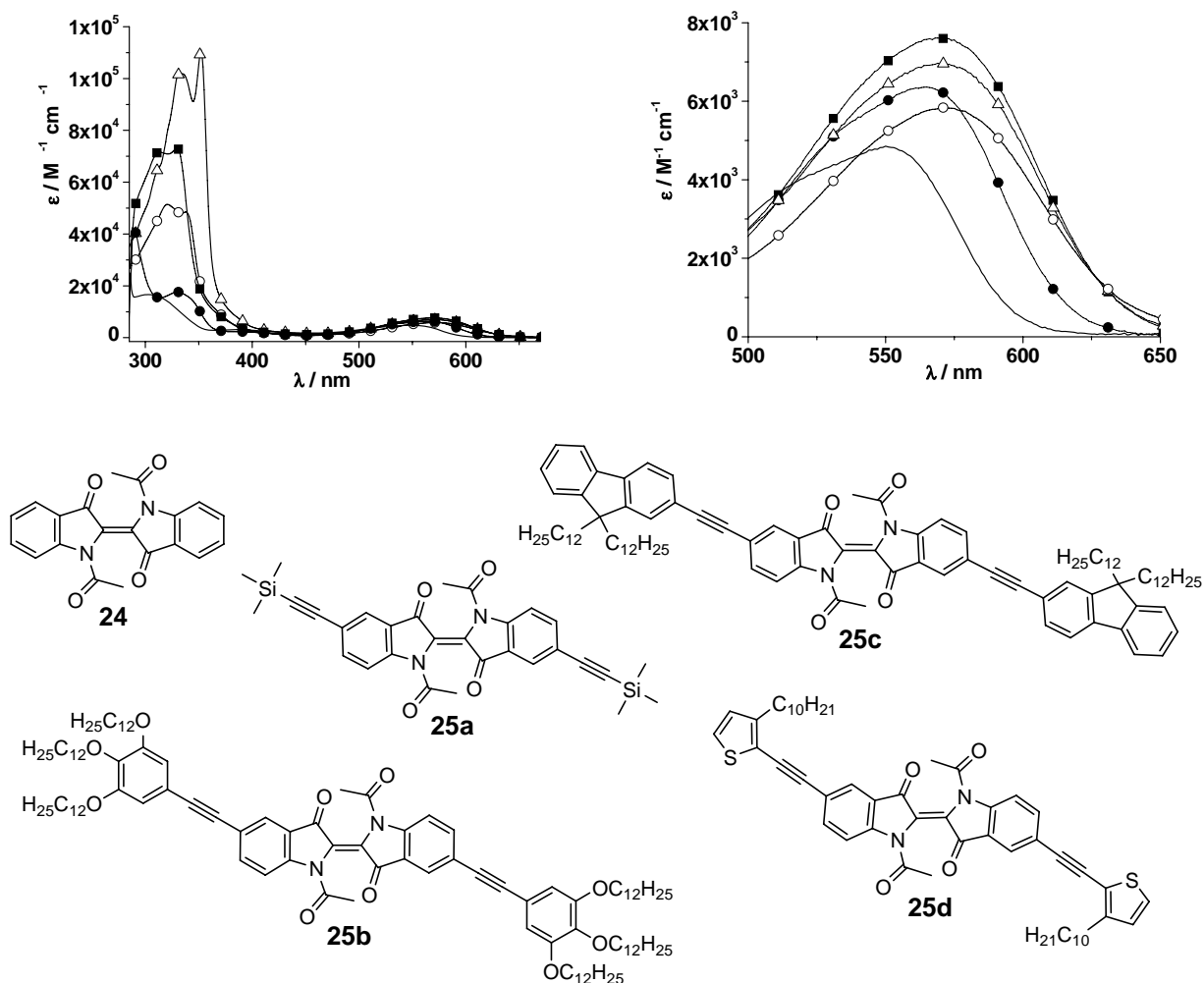


Figure 6.4: UV-vis absorption spectra of indigos in THF (left) and enlargement (right), **24** (straight line), **25a** (filled circle), **25b** (filled square), **25c** (open triangle) and **25d** (open circle).

Compared to *N,N'*-diacetylindigo, (**24**) the molar absorption coefficient for indigo **25b** was increased by a factor 1.6. Clearly, this side effect is an advantage for the use in organic solar cells which may benefit from high molar extinction coefficients.

Photoluminescence spectrometry is performed on solutions of **24** and **25a-d** in THF (optical density ~ 0.1) at 20°C, after excitation at their long wavelength absorption maxima. Remarkably,

only *N,N'*-diacetylindigo (**24**) showed significant emission with a maximum located at 620 nm. The bis-TMS-ethynyl indigo analogue **25a** displayed a fluorescence maximum at 627 nm, but also a 20 fold lower intensity as compared to the fluorescence of **24**, diminishing the fluorescence to almost zero. Indigo analogues **25b-d** lack any observable fluorescence. This effect may be attributed to electron transfer with concomitant formation of a charge separated state (CSS) (Figure 6.5). The fluorescence quenching of indigo in the presence of electron releasing species has been previously reported.^{30,31} In our case the effect can be explained by an intramolecular donor-acceptor interaction. Other possible non-radiative decay pathways for *N,N'*-diacetylindigo are triplet formation³² and *cis-trans* isomerization³³. It is noteworthy to mention that the latter is not likely to occur in unsubstituted indigo (**1**) due to a strong intramolecular hydrogen bond.³⁴ However, in that case a proton transfer from nitrogen to the carbonyl oxygen may take place due to the greatly enhanced ($\sim 10^6$ times) acidity of the aromatic NH groups and the increased basicity of the aromatic carbonyl oxygens in the first excited singlet state.³⁵

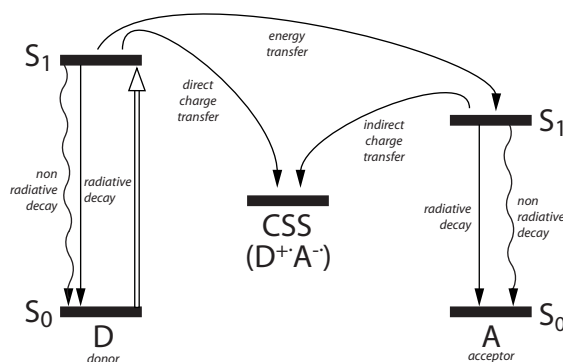


Figure 6.5: Jablonski diagram representing possible photophysical events after excitation (open arrow) in a donor-acceptor (D–A) system.

The potential formation of a CSS of *N,N'*-diacetyl-indigo in the presence of a donor molecule is a prerequisite for its use in organic solar cells, however, it is in competition with alternative processes.

6.7 Is *N,N'*-diacetylindigo a new n-type material suitable for organic solar cells?

A solution of 1 mg/ml *N,N'*-diacetylindigo (**24**) in THF was subjected to a cyclic voltammetry (CV) experiment to gain more insight into the electronic properties. The voltammogram shows the first reduction potential of diacetylindigo at -0.58 V and a second at -1.11 V (Figure 6.6). The values are comparable to those of a recognized n-type material: perylene bisimides³⁶, with a first reduction potential at -0.59 V and a second at -0.92 V for bis *N,N'* alkyl substituted perylene bisimide. The stability of the compound was secured by measuring multiple cycles not

displaying changes in the shape of the voltammogram. The first reduction potential is in agreement with a previously reported value³¹ and in combination with the absorption maximum of indigo, we can conclude that *N,N'*-diacetylintdigo (**24**) is a small band gap molecule with a very low reduction potential.

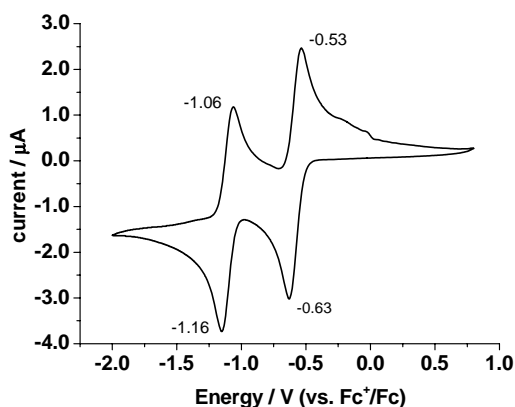


Figure 6.6: Cyclic voltammogram of *N,N'*-diacetylintdigo **24** in THF at a concentration of 2×10^{-3} M, scan rate 25 mV s^{-1} , supporting electrolyte $0.1 \text{ M NBu}_4\text{PF}_6$.

Two types of materials are required for the collection and conversion of sunlight into electrical energy in an organic bulk hetero junction solar cell. In this energy conversion process a charge-separated state (CSS) is formed in which the electron donating material (D) is oxidized ($\text{D}^{\bullet+}$) while the electron accepting species (A) is reduced ($\text{A}^{\bullet-}$) (Figure 6.5). To our best knowledge this is the first observation of a MDMO-PPV (poly[2-methoxy,5-(3',7'-dimethyloctyloxy)]-*p*-phenylene-vinylene) radical cation, indicative for a CSS, in the presence of *N,N'*-diacetylintdigo as the electron acceptor in a photo-induced absorption (PIA) experiment. A solution of both the donor and the acceptor in a 1:1 *w*% ratio in THF does not reveal a detectable charged species. However, a dropcasted film on a quartz plate from the same solution shows unambiguously the presence of a MDMO-PPV cation³⁷ at 0.45 eV suggesting the formation of the radical ion-pair $\text{MDMO-PPV}^{\bullet+} \text{ } N,N'\text{-diacetylintdigo}^{\bullet-}$ (Figure 6.7) in the PIA spectrum, after excitation at 488 nm. The absorption of the radical anion was not observed, probably due to the low extinction coefficient as compared to that of the radical cation species derived from MDMO-PPV.

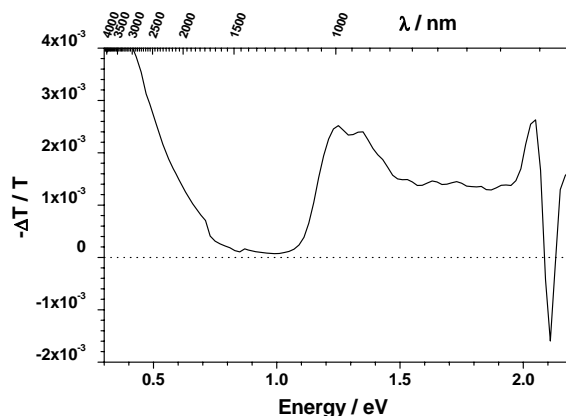


Figure 6.7: Near steady state photoinduced absorption spectrum of a dropcasted thin film of *N,N'*-diacetylidigo/MDMO-PPV blend recorded at 80K. The excitation wavelength is 488 nm, modulation frequency is 33 Hz, laser power 150 mW.

Atomic force microscopy (AFM) is a very powerful tool to investigate the surface morphology of a film, revealing qualitative information about the phase segregation. In this case a film is spin coated on quartz from a THF solution containing both the donor and the acceptor in a 1:1 *w%* ratio. The surface of the resulting optically smooth film with a rms of 34 nm was examined with a NSC100 tip. From the 10 × 10 μm AFM picture, the phase segregation of the two compounds (Figure 6.8) is evidently revealed. Changing the tip for a NSC14 W2C improves resolution and allows zooming in on the surface. The image of a 3 × 3 μm surface clearly displays phase-segregated domains of the two compounds (Figure 6.8). The darker areas mainly contain the MDMO-PPV whereas the lighter areas contain primarily the *N,N'*-diacetylidigo. Within the indigo domain, smaller MDMO-PPV domains are present. This scale of phase segregation has the percolation characteristics desired for solar cell applications.

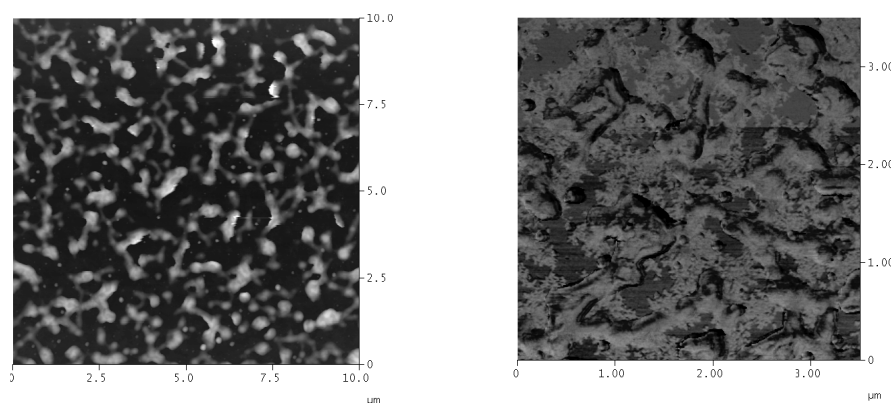


Figure 6.8: AFM phase images of a spincoated film of an *N,N'*-diacetylidigo/MDMO-PPV blend, 10 × 10 μm (left) and an image after zooming in to 3 × 3 μm (right).

The formation of a CSS from the combination of *N,N'*-diacetylidigo and MDMO-PPV in a film with desired percolation properties, justifies the assembly of an organic solar cell. It must be noted that the parent indigo has been used previously in an organic solar cell.³⁸ In that case indigo was sandwiched between an aluminum electrode and a semitransparent gold electrode. In contrast to our findings the authors found that indigo behaves as a p-type material. Furthermore, it was concluded that the cell indeed shows a photovoltaic effect but that the power conversion efficiency is very low. Our solar cell was constructed by first spin coating of an aqueous poly(3,4-ethylenedioxythiophene)/poly(styrenesulfonate) (PEDOT/PSS) dispersion prior to that of a blend of MDMO-PPV/*N,N'*-diacetylidigo (active layer) 1:1 in chlorobenzene on a transparent indium tin oxide (ITO) electrode on glass. Subsequently, an optically smooth aluminum counter-electrode was introduced by vacuum deposition (Figure 6.9). With this procedure two cells have been made that only differ in the rotation speed of the substrate during spin coating (1500 and 1000 rpm). Two other cells have been prepared of which the active layer is a blend of MDMO-PPV/*N,N'*-diacetylidigo in a 1:2 ratio, also spin coated with 1000 and 1500 rpm.

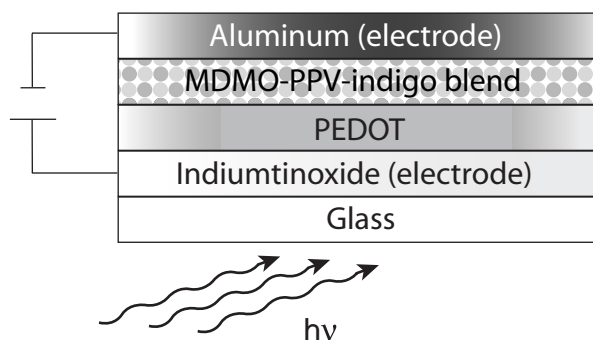


Figure 6.9: Schematic representation of the MDMO-PPV- *N,N'*-diacetylidigo bulk heterojunction solar cell.

The current-voltage characteristics are determined as a measure of the solar cell performance (Figure 6.10). This revealed an extremely low short circuit current (I_{sc}) indicative for the low mobility of the formed charges. Moreover, the high dark current in combination with the low short circuit current negatively affects the open circuit voltage (V_{oc}). The result is a very low fill factor (FF) which is determined by the surface ratio of the small rectangle and the large rectangle. This is a most remarkable observation since fluorescence quenching and the presence of a MDMO-PPV $^{+•}$ in PIA spectrometry proved the formation of charges. Apparently, the mobility of the formed charges is extremely limited in this device. The hole-conducting material MDMO-PPV has previously been successfully used in organic solar cells. Hence, the *N,N'*-diacetylidigo proves to be a very poor electron-conducting material.

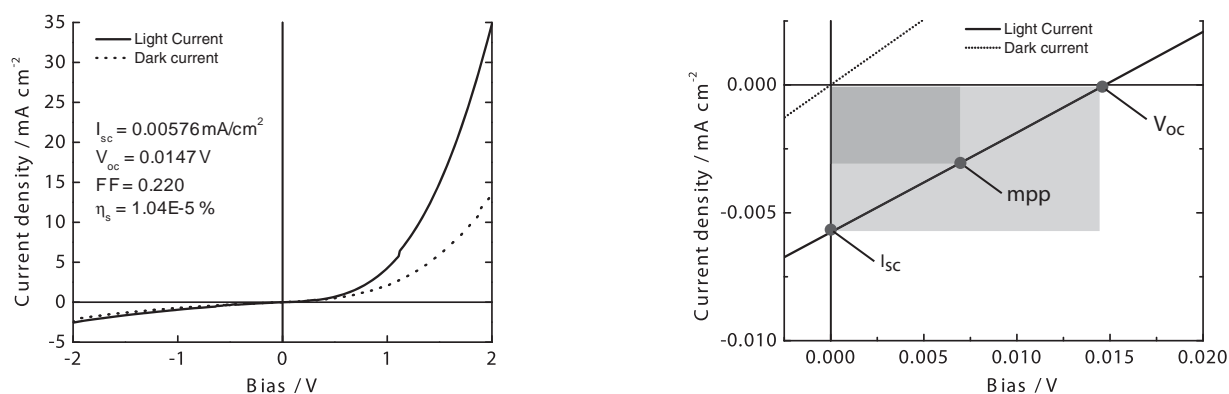


Figure 6.10: *I-V* curve of the MDMO-PPV- *N,N'*-diacetylidigo bulk heterojunction solar cell (left) and expansion with V_{oc} = open circuit voltage, I_{sc} = short circuit current and mpp = maximum power point (right).

Besides MDMO-PPV, also a solar cell with an active layer consisting of poly (3-hexylthiophene), a different donor polymer, and indigo **24** has been investigated. Unfortunately, no improvement of the response could be observed.

Numerous reasons may account for the disappointing results obtained with the solar cell experiments. Only minor improvements can be expected by optimizing the morphology of this particular solar cell. Most likely the intrinsic problems regarding the poor electron mobility of *N,N'*-diacetylidigo hamper its use as a new n-type material in organic solar cells.

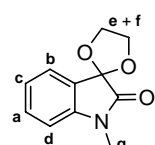
6.8 Conclusions

This is the first time that the bandgap of soluble indigo has been altered by extension of the π -system with the introduction of various ethynyl linkers under Sonogashira conditions. The solubility was ensured by positioning acetyl functionalities on nitrogen. This approach afforded an array of new 5,5'-bisethynyl-*N,N'*-diacetylidigo analogues albeit that the final dimerization step requires optimization. Cyclic voltammetry established the low lying LUMO level which made *N,N'*-diacetylidigo a promising candidate for use in organic solar cells. Photo induced absorption spectrometry on a film of a MDMO-PPV-indigo blend indicated the formation of a CSS. However, preliminary solar cell experiments with *N,N'*-diacetylidigo are rather disappointing which can be attributed to its poor electron conductivity.

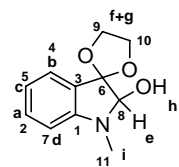
6.9 Experimental

General. General synthetic procedures are described in the experimental section of chapter 2.

Electrochemical measurements: Cyclic voltammetry was measured in THF containing 0.1 M tetrabutylammonium hexafluorophosphate (TBAPF₆) as a supporting electrolyte on an Ecochemie Autolab PGSTAT30 potentiostat. The working electrode was a Pt disk, the counter electrode was Ag bar and a Ag/AgCl electrode was used as referenced electrode. All potentials were measured in a glovebox under nitrogen atmosphere and were reference to the Fc/Fc⁺ (0.47 V) couple. **Near steady-state PIA:** The PIA spectra were recorded between 0.25 and 2.25 eV by exciting with a mechanically modulated cw Ar ion laser ($\lambda = 488$ nm, 33 Hz) pump beam and monitoring the resulting change in transmission of a tungsten-halogen probe light through the sample (ΔT) with a phase-sensitive lock-in amplifier after dispersion by a grating monochromator and detection, using Si, InGaAs, and cooled InSb detectors. The pump power incident on the sample was typically 150 mW with a beam diameter of 2 mm. The PIA ($-\Delta T/T \approx \Delta\alpha d$) was directly calculated from the change in transmission after correction for the photoluminescence, which was recorded in a separate experiment. Photoinduced absorption spectra and photoluminescence spectra were recorded with the pump beam in a direction almost parallel to the direction of the probe beam. The samples were prepared by dropcasting a solution in THF containing both compounds in a 1:1 w/w ratio and were measured in an Oxford cryostat at 80K. **AFM measurements:** Atomic force microscopy images were obtained on a Nanoscope IIIa from Digital Instruments Santa Barbara CA. RTESP-type tips were used. Atomic force microscopy (AFM) measurements were carried out at room temperature with an AFM (Digital Instruments) equipped with a Nanoscope IIIa controller (Digital Instruments) in the Tapping Mode. Quartz substrates were cleaned intensively by rinsing with acetone and ethanol followed by drying under nitrogen flow. Samples were prepared by spincoating from 1:1 w/w (PPV:di-*N,N'*-acetylidigo) mixed solution in THF on quartz.

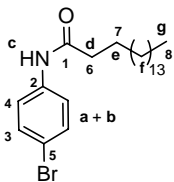


1-Methyl-3H-(3,3-ethylenedioxy)-indol-2-one (11). A flask containing *N*-methyl isatin (**10**) (1.430 g, 8.873 mmol), 1,2-ethanediol (0.60 mL, 0.66 g, 10.65 mmol) and *p*TSOH (0.169 g, 0.887 mmol) in toluene (25 mL) was fitted with a Dean-Stark setup and heated under reflux for 3 h. Concentration of the reaction mixture gave **11** (1.782 g, 8.686 mmol, 98%) as a light orange solid. ¹H NMR (300 MHz, CDCl₃) δ (ppm) = 7.40-7.34 (m, 2H, **a** + **b**), 7.09 (t, 1H, $J = 8.0$ Hz, **c**), 6.79 (d, 1H, $J = 8.2$, **d**), 4.64-4.57 and 4.38-4.30 (2 \times m, 4H, **e** + **f**), 3.13 (s, 3H, **g**); FT-IR (NEAT) σ (cm⁻¹) = 3063, 2956, 2894, 1728, 1616, 1492, 1464, 1374, 1348, 1306, 1283, 1240, 1216, 1112, 1091, 1037, 1021, 1003, 942, 850, 751, 691.

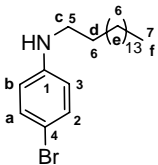


1-Methyl-2-hydroxy-(3,3-ethylenedioxy)-2,3-dihydroindole (12). A solution of 2.3 M LiAlH₄ in THF (0.11 mL, 0.26 mmol) was added to a solution of isatin **11** (0.107 g, 0.522 mmol) in THF (2 mL) at rt and stirred for an additional 1 h. The mixture was dissolved in EtOAc (20 mL) and washed with H₂O (3 \times 10 mL). The organic layer was dried over MgSO₄, filtered. Concentration of the filtrate *in vacuo* gave **12** as a green paste (0.106 g, 0.514 mmol, 99%). ¹H NMR (300 MHz, CDCl₃) δ (ppm) = 7.24 (t, 1H, $J = 7.7$ Hz, **a**), 7.21 (7.21, 1H, $J = 7.1$, **b**), 6.75 (t, 1H, $J = 7.4$ Hz, **c**), 6.50 (d, 1H, $J = 7.6$ Hz, **d**), 4.54 (d, 1H, $J = 11.0$ Hz, **e**), 4.26-4.04 (m, 4H, **f** + **g**),

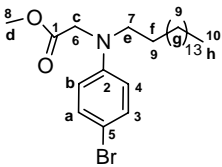
3.07 (d, 1H, *J* = 11.5 Hz, **h**), 2.79 (s, 3H, **i**); ^{13}C NMR (100 MHz, CDCl_3) δ (ppm) = 150.7 (**1**), 131.9 (**2**), 125.0 (**3**), 124.3 (**4**), 119.0 (**5**), 110.8 (**6**), 93.4 (**7**), 93.4 (**8**), 66.3 (**9**) 65.7 (**10**), 32.1 (**11**); FT-IR (NEAT) σ (cm^{-1}) = 3423, 2958, 2892, 1617, 1488, 1472, 1428, 1318, 1294, 1205, 1151, 1105, 1071, 1005, 962, 948, 806, 745, 669.



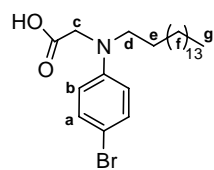
N-(4-Bromophenyl)palmitamide (18). A mixture of 4-bromo-aniline **17** (2.22 g, 12.19 mmol), palmitoyl chloride (3.35 g, 3.7 mL, 12.19 mmol), Et_3N (1.48 g, 2.06 mL, 14.63 mmol) in CH_2Cl_2 (120 mL) was stirred for 3 h at rt. The reaction mixture was concentrated, Et_2O (150 mL) and water (80 mL) were added and the organic layer was washed with water (3×80 mL). The combined organic layers were dried over MgSO_4 and filtered. Concentration of the filtrate gave **18** as a white solid (4.96 g, 12.07 mmol, 93%) that was used as such. ^1H NMR (300 MHz, CDCl_3) δ (ppm) = 7.44 (s, 4H, **a + b**), 7.21 (s, 1H, **c**), 2.36 (t, 2H, **d**), 1.75-1.62 (m, 2H, **e**), 1.27 (s, 26H, **f**), 0.90 (t, 3H, **g**); ^{13}C NMR (75 MHz, CDCl_3) δ (ppm) = 171.5 (**1**), 137.1 (**2**), 132.0 (**3**), 121.4 (**4**), 116.8 (**5**), 37.9 (**6**), 32.0, 29.72, 29.68, 29.5, 29.4, 29.3, 25.6 and 22.8 (**7**), 14.2 (**8**); FT-IR (NEAT) σ (cm^{-1}) = 3313, 2955, 2916, 2849, 1659, 1589, 1522, 1488, 1464, 1395, 1300, 1246, 1176, 1097, 1073, 1013, 959, 844, 819, 726.



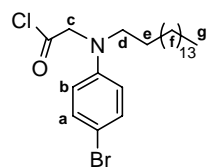
4-Bromo-N-hexadecylbenzenamine (19). A 2.3 M solution of LiAlH_4 in THF (2.13 mL, 4.90 mmol) was added to a solution of amide **18** (2.012 g, 4.894 mmol) in THF (40 mL). The reaction was stirred for 1 h at rt followed by 1 h under reflux. A few drops of 1 M NaOH aq. were added to break up the excess of LiAlH_4 . The reaction mixture was concentrated *in vacuo* and redissolved in Et_2O (100 mL) and water (60 mL) and the organic layer was washed with water (3×60 mL) and brine (60 mL). The combined organic layers were dried over MgSO_4 , filtered. Concentration of the filtrate *in vacuo* gave **19** as an off-white solid (1.88 g, 4.737 mmol, 97%). ^1H NMR (300 MHz, CDCl_3) δ (ppm) = 7.25 (d, 2H, **a**), 6.52 (d, 2H, **b**), 3.06 (t, 2H, *J* = 7.3 Hz, **c**), 1.64-1.55 (m, 2H, **d**), 1.37,-1.11 (m, 26H, **e**), 0.88 (t, 3H, *J* = 7.0 Hz, **f**); ^{13}C NMR (75 MHz, CDCl_3) δ (ppm) = 147.6 (**1**), 132.2 (**2**), 114.7 (**3**), 109.1 (**4**), 44.5 (**5**), 32.3, 30.3, 30.03, 30.01, 29.9, 29.8, 29.7, 29.7, 27.5, 23.1 and 22.9 (**6**), 14.5 (**7**); FT-IR (NEAT) σ (cm^{-1}) = 3407, 2951, 2916, 2847, 1593, 1497, 1479, 1468, 1396, 1377, 1311, 1262, 1246, 1179, 1132, 1072, 998, 812, 769, 747, 720, 691.



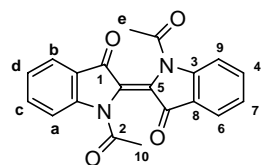
Methyl-2-(N-(4-bromophenyl)-N-hexadecyl)amino-acetate (20). Amine **19** (1.188 g, 2.994 mmol) was added to a suspension of NaH (0.180 g, 4.450 mmol) in DMF at rt. The suspension was heated to 40°C for 3 h upon which the colour changed to dark orange. Methyl bromoacetate (0.687 g, 0.43 mL, 4.490 mmol) was added and the reaction was stirred at 40°C for an additional 17 h. The reaction mixture was concentrated *in vacuo* and purification by column chromatography (silica, 5 v% EtOAc in heptane) afforded **20** (1.053 g, 2.249 mmol, 75%) as a white solid. ^1H NMR (300 MHz, CDCl_3) δ (ppm) = 7.28 (d, 2H, *J* = 9.3 Hz, **a**), 6.50 (d, 2H, *J* = 9.1 Hz, **b**), 4.00 (s, 2H, **c**), 3.72 (s, 3H, **d**), 3.33 (t, 2H, *J* = 7.7 Hz, **e**), 1.26 (m, 2H, **f**), 1.26 (m, 26H, **g**), 0.88 (t, 3H, *J* = 6.7 Hz, **h**); ^{13}C NMR (75 MHz, CDCl_3) δ (ppm) = 171.7 (**1**), 147.3 (**2**), 132.2 (**3**), 114.0 (**4**), 109.2 (**5**), 52.9 (**6**), 52.6 (**7**), 52.4 (**8**), 32.3, 30.02, 30.0, 29.9, 29.8, 29.7, 27.6, 27.4 and 23.0 (**9**), 14.5 (**10**).



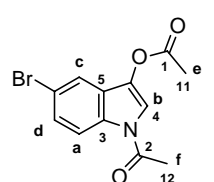
2-(N-4-Bromophenyl-N-hexadecyl)amino-acetic acid (21). 1 M NaOH aq. (4 mL) was added to a solution of ester **20** (0.508 g, 1.086 mmol) in THF (5 mL) and stirred for 5 h at rt. The THF was removed by concentration *in vacuo* and the remaining aqueous mixture was brought to pH~3 by addition of 1 M aqueous HCl. Et₂O (40 mL) was added and the organic layer was washed with water (3 × 40 mL). The combined aqueous layers were neutralized by addition of aqueous saturated NaHCO₃ and extracted with Et₂O (2 × 40 mL). The combined organic layers were dried over MgSO₄ and filtered. Concentration of the filtrate gave **21** (0.493 g, 1.086, 100%) as a white solid. ¹H NMR (300 MHz, CDCl₃) δ (ppm) = 7.22 (d, 2H, *J* = 9.1 Hz, **a**), 6.44 (d, 2H, *J* = 9.1 Hz, **b**), 3.95 (s, 2H, **c**), 3.24 (t, 2H, *J* = 7.7 Hz, **d**), 1.52 (m, 2H, **e**), 1.19 (m, 26H, **f**), 0.81 (t, 3H, *J* = 6.6 Hz, **g**); FT-IR (NEAT) σ (cm⁻¹) = ~3100, 2916, 2850, 1714, 1591, 1501, 1473, 1388, 1359, 1257, 1230, 1202, 1189, 1149, 1086, 944, 883, 796, 720, 688, 620.



2-(N-4-Bromophenyl-N-hexadecyl)amino-acetyl chloride (22). SOCl₂ (0.078 mL, 0.127 g, 1.068 mmol) was added to a solution of acid **21** (0.404 g, 0.890 mmol) in CCl₄ (5 mL) with DMF (2 drops) and stirred for 3 h at rt. Concentration of the reaction mixture *in vacuo* at <30°C to prevent degradation gave **22** (0.43 g, 0.93 mmol, ~104% with traces of DMF judged from ¹H-NMR) that was used as such. ¹H NMR (300 MHz, CDCl₃) δ (ppm) = 7.33 (d, 2H, *J* = 9.0 Hz, **a**), 6.55 (d, 2H, *J* = 8.8 Hz, **b**), 4.43 (s, 2H, **c**), 3.33 (t, 2H, *J* = 7.7 Hz, **d**), 1.60 (m, 2H, **e**), 1.26 (m, 26H, **f**), 0.88 (t, 3H, *J* = 6.4 Hz, **g**).

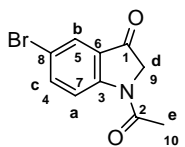


1,1'-Diacetyl-1H,1'H-[2,2']biindolylidene-3,3'-dione, N,N'-diacetylindigo (24). A mixture of indigo (**1**) (1.018 g, 3.880 mmol), 2,6-lutidine (2 mL), *n*-butyl acetate (18 mL) and acetyl chloride (1.9 mL, 2.132 g, 27.157 mmol) was stirred at 100°C for 24 h. Concentration of the reaction mixture followed by column chromatography of the crude solid (silica gel, 50 v% EtOAc in heptane, R_f = 0.4) yielded **24** (0.351 g, 0.983 mmol, 25%) as a dark purple solid which was recrystallized from 50 v% EtOAc in heptane. ¹H NMR (300 MHz, CDCl₃) δ (ppm) = 8.27 (d, 2H, *J* = 8.0 Hz, **a**), 7.77 (d, 2H, *J* = 7.7 Hz, **b**), 7.66 (t, 2H, *J* = 7.8 Hz, **c**), 7.28 (t, 2H, *J* = 7.4 Hz, **d**), 2.56 (s, 2H, **e**); ¹³C NMR (125 MHz, CDCl₃) δ (ppm) = 184.5 (**1**), 170.4 (**2**), 149.5 (**3**), 137.2 (**4**), 126.6 (**5**), 125.6 (**6**), 124.7 (**7**), 122.3 (**8**), 117.5 (**9**), 24.3 (**10**); FT-IR (NEAT) σ (cm⁻¹) = 3026, 2254, 1703, 1678, 1601, 1473, 1458, 1363, 1321, 1300, 1277, 1252, 1202, 1171, 1064, 1008, 925, 754, 730, 710, 678; MS (MALDI-TOF): C₂₀H₁₄N₂O₄, *m/z* calculated: 346.10; found: 346.35. **Analysis**, calculated: C, 69.36; H, 4.07; N, 8.09; found: C, 69.76; H, 4.20; N, 8.07.



1-Acetyl-5-bromo-1H-indole-3-acetate (28). To a suspension of **29** (1.011 g, 3.687 mmol, 90% pure, Aldrich) in acetic anhydride was added NaOAc (0.514 g, 6.268 mmol). The reaction mixture was stirred for 30 min at 80°C. Water (15 mL) was added and the reaction mixture was stirred for an additional 30 min at room temperature. After concentration the residue was washed with water (4 × 20 mL) over a glass filter until the filtrate remained colorless. The residue was dissolved in CHCl₃ (10 mL) and dried over MgSO₄. Filtration and concentration of the filtrate *in vacuo* gave **28** (0.568 g, 1.916 mmol, 59%) as a light yellow solid; (silica gel, 50 v% EtOAc in heptane, R_f = 0.4). ¹H NMR (300 MHz, CDCl₃) δ (ppm) = 8.35 (d, 1H, *J* =

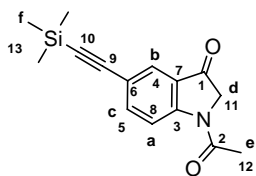
8.8 Hz, **a**), 7.73 (s, 1H, **b**), 7.69 (d, 1H, $J = 1.9$ Hz, **c**), 7.48 (dd, 1H, $J = 8.8$ Hz, $J = 1.9$ Hz, **d**), 2.60 (s, 3H, **e**), 2.39 (s, 3H, **f**); ^{13}C NMR (125 MHz, CDCl_3) δ (ppm) = 168.7 (**1**), 167.7 (**2**), 133.6 (**3**), 131.5 (**4**), 129.1 (**5**), 125.3 (**6**), 120.4 (**7**), 118.2 (**8**), 117.2 (**9**), 114.4 (**10**), 23.9 (**11**), 21.1 (**12**). FT-IR (NEAT) σ (cm^{-1}) = 1756, 1708, 1444, 1372, 1337, 1322, 1193, 932, 889, 809, 770, 715.



1-Acetyl-5-bromo-(2H)-indol-3-one (27). A solution of Na_2SO_3 (2.541 g, 20.164 mmol) in hot water (28 mL) was added to a solution of **5** (3.317 g, 11.202 mmol) in boiling EtOH (14 mL). The reaction mixture was allowed to reflux for about 10 min until TLC (silica gel, 50 v% EtOAc in heptane, $R_f = 0.3$) showed full conversion of the starting material.

The reaction mixture was concentrated *in vacuo* and subsequently dissolved in CHCl_3 (50 mL) and extracted with water (3×30 mL) and brine (30 mL). Drying of the organic layer over MgSO_4 and concentration *in vacuo* of the filtrate gave **27** (2.405 g, 9.446 mmol, 85%) as an off-white solid.

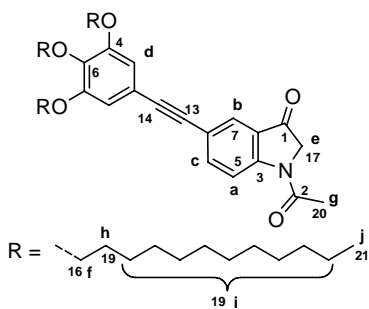
^1H -NMR (300 MHz, CDCl_3) δ (ppm) = 8.48 (d, 1H, $J = 8.8$ Hz, **a**), 7.86 (d, 1H, $J = 2.2$ Hz, **b**), 7.74 (dd, 1H, $J = 8.8$ Hz, $J = 2.2$ Hz, **c**), 4.33 (s, 2H, **d**), 2.32 (s, 3H, **e**); ^{13}C NMR (125 MHz, CDCl_3) δ = 193.3 (**1**), 168.2 (**2**), 152.6 (**3**), 139.9 (**4**), 126.6 (**5**), 126.4 (**6**), 120.3 (**7**), 117.4 (**8**), 56.4 (**9**), 24.3 (**10**). FT-IR (NEAT) σ (cm^{-1}) = 2929, 1715, 1671, 1596, 1460, 1452, 1383, 1351, 1288, 1265, 1191, 825, 659.



1-Acetyl-5-(2-(trimethylsilyl)ethynyl)indolin-3-one (26a). Indoxyl (**27**) (2.257 g, 8.884 mmol) was dissolved in a mixture of acetonitrile (18 mL) and Et_3N (18 mL).

The solution was purged with argon for 30 min and $\text{Pd}(\text{PPh}_3)_4$ (0.371 g, 0.321 mmol) and trimethylsilylacetylene (4.0 mL, 28.3 mmol) were added. The reaction mixture was heated at 80 °C for 4 h. Extra trimethylsilylacetylene (1.0 mL) was added after 1.5 h and 2.5 h. After complete conversion of the starting material, monitored by TLC (silica, 50 v% EtOAc in heptane), the reaction was stopped and concentrated *in vacuo*. Purification of the crude solid by column chromatography (silica gel, 50 v% EtOAc in heptane, $R_f = 0.2$) gave **26a** as an off white solid (2.150 g, 7.92 mmol, 89 %).

^1H -NMR (400 MHz, CDCl_3): δ (ppm) = 8.49 (d, 1H, $J = 8.4$ Hz, 1H, **a**), $\delta = 7.83$ (d, 1H, $J = 1.5$ Hz, **b**), $\delta = 7.73$ (dd, 1H, $J = 8.8$ Hz, $J = 1.8$ Hz, **c**), $\delta = 4.31$ (s, 2H, **d**), $\delta = 2.32$ (s, 3H, **e**), $\delta = 0.26$ (s, 9H, **f**); ^{13}C -NMR (125, CDCl_3): δ (ppm) = 193.8 (**1**), 168.3 (**2**), 153.1 (**3**), 140.7 (**4**), 127.2 (**5**), 124.9 (**6**), 119.4 (**7**), 118.5 (**8**), 103.4 (**9**), 95.6 (**10**), 56.4 (**11**), 24.3 (**12**), 0.0 (**13**). FT-IR (NEAT) σ (cm^{-1}) = 2956, 2156, 1731, 1687, 1243.

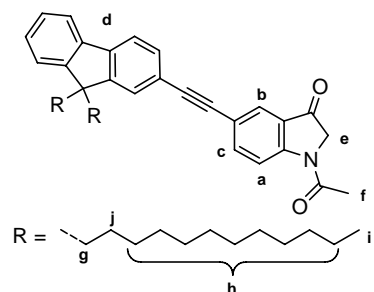


1-Acetyl-5-(3,4,5-tris-dodecyloxy-phenyl-ethynyl)-1,2-dihydro-indol-3-one (26b).

A solution of indoxyl (**27**) (0.255 g, 1.003 mmol), 1,2,3-tris-dodecyloxy-5-ethynyl-benzene²⁷ (0.664 g, 1.013 mmol) in CH_3CN (2 mL) and Et_3N (2 mL) was purged with argon for 30 min. After addition of $\text{Pd}(\text{PPh}_3)_4$ (0.035 g, 0.030 mmol) the reaction mixture was stirred at 80°C for 5 h. The reaction mixture was concentrated *in vacuo*, and purification of the crude solid by column chromatography (silica gel, 33 v% EtOAc in heptane, $R_f = 0.25$) gave **26b** (0.366 g, 0.442 mmol, 44%) as a light brown solid.

^1H NMR (300 MHz, CDCl_3) δ (ppm) = 8.53 (d, $J = 8.5$ Hz, 1H, **a**), 7.86 (d, $J = 1.4$ Hz, 1H, **b**), 7.77 (dd, $J = 8.6$ Hz, $J = 1.6$ Hz, 1H, **c**), 6.71 (s, 2H, **d**), 4.31 (s, 2H, **e**), 3.98 (t, $J = 6.7$ Hz, 6H, **f**), 2.35 (s, 3H, **g**), 1.86-1.69 (m, 6H, **h**), 1.49-1.40 (m, 6H, **i**), 1.30-1.20 (bs, 18H, **i**), 0.88 (t, $J = 6.3$ Hz, 9H, **j**); ^{13}C NMR

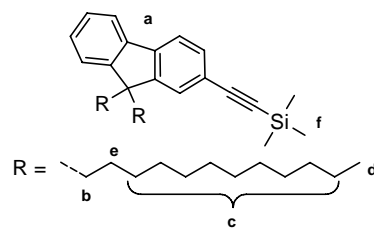
(125.7 MHz, CDCl₃) δ (ppm) = 194.0 (1), 168.2 (2), 153.2 (3), 152.9 (4), 140.3 (5), 139.5 (6), 126.6 (7), 125.1 (8), 119.7 (9), 118.7 (10), 117.1 (11), 110.2 (12), 90.9 (13), 86.7 (14), 73.7 (15), 69.3 (16), 56.5 (17), 32.1 (18), 30.5-29.5 (19 8 \times CH₂), 26.2 (19), 24.3 (20), 22.8 (19), 14.3 (21). FT-IR (NEAT) σ (cm⁻¹) = 2918, 2851, 1724, 1687, 1572, 1502, 1381, 1283, 1118, 839, 826, 721.



1-Acetyl-5-[2-(9,9-didodecyl-9H-fluoren-7-yl)ethynyl]indol-3-one

(**26c**). Pd(PPh₃)₄ (23.9 mg, 20.7 μ mol) was added to a suspension of **30c** (0.364 g, 0.691 mmol) and indoxyl **27** (0.176g, 0.691 mmol) in a mixture of Et₃N (2 mL) and CH₃CN (2 mL), which was de-oxygenated by purging with argon for 30 min. The reaction mixture was heated to 90°C for 18 h. Then it was concentrated and dissolved in EtOAc (10 mL) and washed with water (3 \times 10 mL). The crude solid was purified by column chromatography (silica gel, 33 v% EtOAc in heptane, R_f = 0.25), which

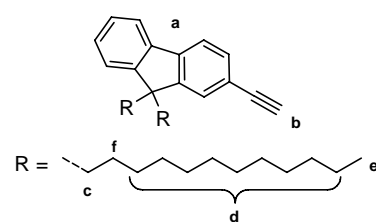
gave **26c** as a light-brown solid (0.079 g, 0.113 mmol, 16%). ¹H-NMR (300 MHz, CDCl₃) δ (ppm) = 8.57 (d, J = 8.8 Hz, 1H, a), 7.9 (d, 1H, J = 1.1 Hz, b), 7.84 (dd, 1H, J = 7.6 Hz, J = 1.6 Hz, c), 7.71-7.30 (3 \times m, 7H, fluorene, d), 4.35 (s, 2H, e), 2.34 (s, 3H, f), 1.97 (t, J = 8.2 Hz, 4H, g), 1.27-1.04 (m, 36H, h), 0.86 (t, 6H, i), 0.61 (m, 4H, j).



9,9-Didodecyl-2-ethynyl-9H-fluorene (30c).

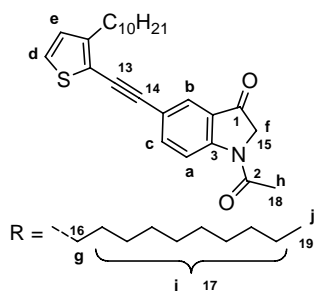
A solution of 2-bromo-9,9-didodecyl-[9H]-fluorene (0.964 g, 1.657 mmol) in Et₃N (4 mL) and THF (4 mL) was purged with argon for 30 minutes. Pd(PPh₃)₄ (0.057 g, 0.050 mmol) and TMS-acetylene (0.488 g, 0.7 mL, 4.966 mmol) were added. The reaction mixture was stirred at 90°C for 18 h and then concentrated *in vacuo*. Purification of the crude reaction mixture with column

chromatography (silica, heptane, R_f = 0.45) resulted in as a slightly orange oil (0.459 g, 0.766 mmol, 46 %) and was used as such; ¹H NMR (300 MHz, CDCl₃) δ (ppm) = 7.72-7.31 (3 \times m, 7H, a), 1.94 (t, 4H, b), 1.26-

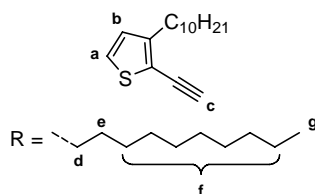


1.03 (m, 36H, c), 0.87 (t, 6H, d), 0.58 (m, 4H, e), 0.29 (s, 9H, f). The compound described above and K₂CO₃ (0.127g, 0.919 mmol) in THF (2.5 mL) and MeOH (2.5 mL) was stirred at rt for 15 h. The mixture was concentrated *in vacuo* and the residue redissolved in Et₂O. Subsequently the organic layer was washed with water (3 \times 10 mL) maintaining the aqueous layer slightly acidic at pH = 6. The organic layer was dried

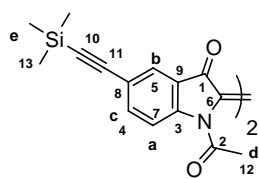
over MgSO₄, filtered over a glass filter. Concentration of the filtrate *in vacuo* afforded **30c** (0.364 g, 0.691 mmol, 90%) as an orange oil. ¹H-NMR showed the presence of a small amount of the starting material <10%; the material was used as such. ¹H-NMR (300 MHz, CDCl₃) δ (ppm) = 7.74-7.32 (3 \times m, 7H, a), 3.1 (1H, b), 1.94 (t, 4H, c), 1.26-1.0 (m, 36H, d), 0.87 (t, 6H, e), 0.58 (br s, f).



1-Acetyl-5-[2-(3-decylthien-2-yl)ethynyl]indolin-3-one (26d). Pd(PPh₃)₄ (69.0 mg, 59.9 μmol) was added to a suspension of 3-decyl-2-ethynylthiophene (*vide infra*) (0.496 g, 1.995 mmol), **27** (0.507 g, 1.995 mmol) and CuI (0.023 g, 0.120 mmol) in a mixture of Et₃N (3 mL) and CH₃CN (3 mL) which was de-oxygenated by applying freeze-pump-thaw (3×) methodology. The reaction mixture was heated at 90°C for 21 h until all 3-decyl-2-ethynylthiophene had reacted. Purification by column chromatography (silica gel, 50 v% EtOAc in heptane, R_f = 0.4) of the concentrated reaction mixture gave **26d** as a light brownish solid (0.185 g, 0.438 mmol, 22%). ¹H NMR (300 MHz, CDCl₃) δ (ppm) = 8.55 (d, 1H, J = 8.8 Hz, a), 7.86 (d, 1H, J = 1.6 Hz, b), 7.77 (dd, 1H, J = 8.7 Hz, J = 1.8 Hz, c), 7.21 (d, 1H, J = 5.2 Hz, d), 6.89 (d, 1H, J = 4.9 Hz, e), 4.33 (s, 2H, f), 2.75 (t, 2H, J = 7.5 Hz, g), 2.34 (s, 3H, h), 1.68-1.13 (2 × m, 16H, i), 0.86 (t, 3H, J = 7.1 Hz, j); ¹³C NMR (125 MHz, CDCl₃) δ (ppm) = 193.9 (1), 168.2 (2), 152.7 (3), 148.4 (4), 139.8 (5), 128.4 (6), 126.5 (7), 126.1 (8), 125.0 (9), 119.5 (10), 118.6 (11), 117.6 (12), 93.6 (13), 83.5 (14), 56.3 (15), 31.9 (16), 30.3-29.3 (17), 24.2 (18), 22.7 (17), 14.2 (19); FT-IR (NEAT) σ (cm⁻¹) = 2924, 2854, 2252 and 2204 (C≡C), 1726, 1673, 1612, 1482, 1440, 1379, 1348, 1264, 906, 839, 728.

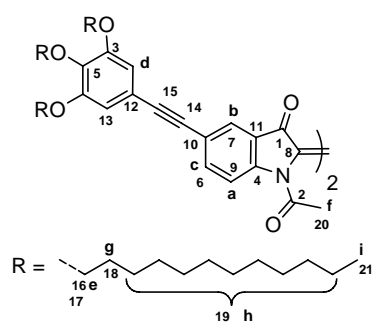


3-Decyl-2-ethynylthiophene (30d). A mixture of 2-bromo-3-decylthiophene (1.832 g, 6.040 mmol), ethynyltriisopropylsilane (1.5 mL, 1.212 g, 6.644 mmol) and CuI (0.058 g, 0.302 mmol) in Et₃N (8.0 mL) was purged with argon for 30 minutes. Pd(PPh₃)₄ (0.140 g, 0.121 mmol) was added and the reaction mixture was heated at 90°C for 18 h. GC-MS analysis showed a conversion of 69% also the presence of homocoupled ethynyltriisopropylsilane and starting material were observed. Extra addition of catalyst and ethynyltriisopropylsilane (1.5 mL, 1.212 g, 6.644 mmol) and a prolonged reaction time at 90°C did not result in a higher conversion. The reaction mixture was filtered over celite and the filtrate concentrated. TLC analysis indicated that purification of TMS protected **30d** by column chromatography was not possible. The crude mixture was dissolved in THF (10 mL) and cooled to 0°C. TBAF (6.4 mL, 6.4 mmol of a 1M solution in THF) was added and the reaction was stirred at 0°C for 1 h allowing the temperature to reach rt. The reaction mixture was concentrated and purification of the remaining solid by column chromatography (silica gel, heptane, R_f = 0.55) gave **30d** as a yellow-orange oil (0.529 g, 2.128 mmol, 35%). ¹H-NMR (400 MHz, CDCl₃): δ (ppm) = 7.14 (d, 1H, J = 5.2 Hz, a), 6.84 (d, 1H, J = 4.9 Hz, b), 3.42 (s, 1H, c), 2.70 (t, 2H, d), 1.61 (m, 2H, e), 1.31-1.20 (m, 14H, f), 0.88 (t, 3H, g); FT-IR (NEAT) σ (cm⁻¹) = 3311, 2955, 2923, 2853, 2101, 1529, 1465, 1418, 838, 722;



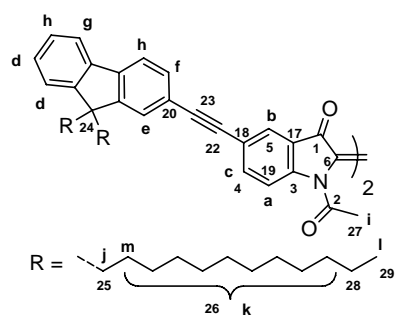
1,1'-Diacetyl-5,5'-bis-trimethylsilylethynyl-1H,1'H-[2,2']biindolylidene-3,3'-dione (25a). See (**25b**) for conditions. A mixture of **26a** (91.8 mg, 0.339 mmol), CuI (64.5 mg, 0.339 mmol), K₂CO₃ (23.4 mg, 0.169 mmol) and H₂O (0.3 mL) in THF (1.6 mL) was used. After column chromatography indigo analogue **25a** was isolated as a blue sticky solid (6.4 mg, 11.9 μmol, 4 %). ¹H NMR (300 MHz, THF-d₈) δ (ppm) = 8.24 (d, 2H, J = 8.8 Hz, a), 7.75 (d, 2H, J = 1.9 Hz, b), 7.68 (dd, 2H, J = 8.7 Hz, J = 1.8 Hz, c), 2.46 (s, 6H, d), 0.20 (s, 18H, e); ¹³C NMR (125 MHz, THF-d₈) δ (ppm) = 183.6 (1), 170.2 (2), 148.6 (3), 140.5 (4), 128.0 (5), 126.5 (6), 122.1 (7), 120.9 (8), 117.4 (9), 103.2 (10), 96.4 (11), 24.3 (12), 0.18 (13); FT-IR (NEAT)

σ (cm^{-1}) = 2959, 2159, 1761, 1684, 1611, 1474, 1302, 1250, 1112, 1069, 891, 842, 777, 761; **MS** (MALDI-TOF): $\text{C}_{30}\text{H}_{30}\text{N}_2\text{O}_4\text{Si}_2$, m/z calculated: 538.17; found: 538.37, 561.37 (+Na⁺), 577.34 (+K⁺).



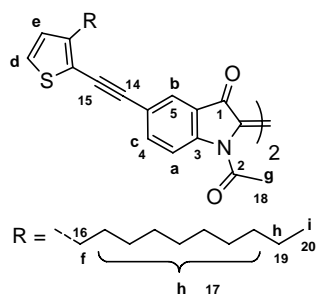
1,1'-Diacetyl-5,5'-bis-(3,4,5-tris-dodecyloxy-phenylethynyl)-1H,1'H-[2,2']biindolylidene-3,3'-dione (25b). H_2O (0.1 mL) was added to a mixture of indoxyl **28b** (0.115 g, 0.139 mmol), CuI (0.026 g, 0.139 mmol) and K_2CO_3 (0.010 g, 0.069 mmol) in THF (0.7 mL). After 2 h stirring at rt the mixture was concentrated *in vacuo*. The residue was dissolved in EtOAc (10 mL) and washed with water (3 × 5 mL). Purification of the crude solid by column chromatography (silica gel, 10 v% EtOAc in heptane, R_f = 0.25) gave **25b** (0.021 g, 0.0126 mmol, 18%) as a dark blue

waxy solid. $^1\text{H NMR}$ (300 MHz, THF- d_8) δ (ppm) = 8.21 (d, 2H, J = 8.5 Hz, **a**), 7.73 (d, 2H, J = 1.9 Hz, **b**), 7.65 (dd, 2H, J = 8.7 Hz, J = 1.9 Hz, **c**), 6.68 (s, 4H, **d**) 3.89-3.81 (6H, **e**), 2.41 (s, 6H, **f**), 1.73-1.56 (12H, **g**), 1.41-1.19 (bs, 108H, **h**), 0.78 (t, 18H, J = 6.6 Hz, **i**); $^{13}\text{C NMR}$ (125 MHz, THF- d_8) δ (ppm) = 184.7 (**1**), 171.2 (**2**), 154.4 (**3**), 149.8 (**4**), 140.9 (**5**), 139.8 (**6**), 128.0 (**7**), 127.2 (**8**), 123.8 (**9**), 121.4 (**10**), 118.4 (**11**), 118.3 (**12**), 111.2 (**13**), 92.0 (**14**), 87.4 (**15**), 74.0 (**16**), 70.0 (**17**), 33.2 (**18**), 31.7, 31.1, 31.1, 31.0, 30.9, 30.9, 30.7, 30.7 and 27.4 (8 × CH_2 , **19**), 23.9 (**20**), 14.8 (**21**); **FT-IR** (NEAT) σ (cm^{-1}) = 2925, 2853, 2210, 1713, 1684, 1575, 1501, 1355, 1302, 1169, 1116, 1069, 835, 722; **MS** (MALDI-TOF), $\text{C}_{108}\text{H}_{166}\text{N}_2\text{O}_{10}$, m/z calculated: 1652.26; found: 1652.28, 1675.25 (+ Na⁺).



1,1'-Diacetyl-5,5'-bis-(9,9-didodecyl-9H-fluoren-2-ylethynyl)-1H,1'H-[2,2']biindolylidene-3,3'-dione (25c). See (**25b**) for conditions. A mixture of **26c** (79.0 mg, 0.1128 mmol), CuI (21.5 mg, 0.1128 mmol), K_2CO_3 (7.8 mg, 0.0564 mmol) and H_2O (0.12 mL) in THF (0.6 mL) was used. Purification by preparative TLC (10 v% EtOAc in heptane, R_f = 0.3) gave **25c** (5.8 mg, 4.1 μmol , 7%) as a dark blue solid. $^1\text{H NMR}$ (300 MHz, THF- d_8) δ (ppm) = 8.24 (d, 2H, J = 8.5 Hz, **a**), 7.79 (d, 2H, J = 1.9 Hz, **b**), 7.72 (dd, 2H, J = 8.7 Hz, J = 1.8 Hz, **c**), 7.62 (4H, **d**), 7.47 (d, 2H, J

= 0.5 Hz, **e**), 7.40 (dd, 2H, J = 7.8 Hz, J = 1.0 Hz, **f**), 7.28 (m, 2H, **g**), 7.20 (m, 4H, fluorene **h**), 2.39 (2 × s, 6H, **i**) (m, 8H, **j**), 1.00 (72H, **k**), 0.75 (t, 12H, **l**), 0.50 (8H, **m**); $^{13}\text{C NMR}$ (125 MHz, THF- d_8) δ (ppm) = 183.6 (**1**), 170.0 (**2**), 151.2 (**3**), 151.0 (**4**), 148.2 (**5**), 142.1 (**6**), 140.4 (**7**), 139.9 (**8**), 130.8 (**9**), 127.8 (**10**), 127.2 (**11**), 127.1 (**12**), 126.4 (**13**), 126.1 (**14**), 123.1 (**15**), 122.2 (**16**), 121.1 (**17**), 120.8 (**18**), 120.2 (**19**), 119.9 (**20**), 117.4 (**21**), 92.1 (**22**), 87.6 (**23**), 55.3 (**24**), 40.4 (**25**), 32.0, 30.2, 29.7, 29.7, 29.5 and 29.4 (**26**), 23.9 (**27**), 22.8 (**28**), 14.3 (**29**); **FT-IR** (NEAT) σ (cm^{-1}) = 2922, 2852, 2209, 1715, 1685, 1613, 1492, 1475, 1467, 1364, 1297, 1273, 1192, 1173, 1109, 1097, 1067, 836, 778, 739; **MS** (ESI), $\text{C}_{98}\text{H}_{126}\text{N}_2\text{O}_4$, m/z calculated: 1395.97; found: 1395.7.



1,1'-Diacetyl-5,5'-bis-(3-decyl-thien-2-ylethynyl)-1H,1'H-[2,2']biindolide-3,3'-dione (25d). See (25b) for conditions. A mixture of **26d** (0.185 g, 0.438 mmol), CuI (91.7 mg, 0.482 mmol), K₂CO₃ (30.3 mg, 0.219 mmol) and H₂O (0.22 mL) in THF (2.2 mL) was used. Purification by preparative TLC (silica gel, 10 v% EtOAc in heptane, R_f = 0.25) gave **25d** (5.7 mg, 6.79 μmol, 2%) as a dark blue solid. ¹H NMR (300 MHz, THF-d₈) δ (ppm) = 8.50 (d, 2H, J = 8.5 Hz, **a**), 8.03 (d, 2H, J = 1.6 Hz, **b**), 7.96 (dd, 2H, J = 1.8 Hz, **c**), 7.52 (d, 2H, J = 5.2 Hz, **d**), 7.12 (d, 2H, J = 5.2 Hz, **e**), 2.97 (t, 4H, J = 7.4 Hz, 4H, **f**), 2.69 (s, 3H, **g**), 1.50 (m, 32H, **h**), 1.04 (t, 6H, J = 6.6 Hz, **i**); ¹³C NMR (125 MHz, THF-d₈) δ (ppm) = 183.5 (**1**), 170.1 (**2**), 149.0 (**3**), 148.4 (**4**), 139.7 (**5**), 128.7 (**6**), 127.1 (**7**), 127.0 (**8**), 126.6 (**9**), 122.3 (**10**), 121.1 (**11**), 117.8 (**12**), 117.6 (**13**), 93.6 (**14**), 84.3 (**15**), 32.2 (**16**), 30.6, 30.1, 30.0, 29.94, 29.92, 29.8, 29.7, 29.6, (**17**), 24.3 (**18**), 23.0 (**19**), 14.4 (**20**); FT-IR (NEAT) σ (cm⁻¹) = 2924, 2854, 2203, 1715, 1685, 1480, 1363, 1298, 1274, 1174, 1107, 1076, 939, 880, 837, 777, 720; MS (MALDI-TOF): C₅₂H₅₈N₂O₄S₂, calculated: 838.38; found: 839.30 (+H), 861.33 (+ Na⁺).

6.10 References

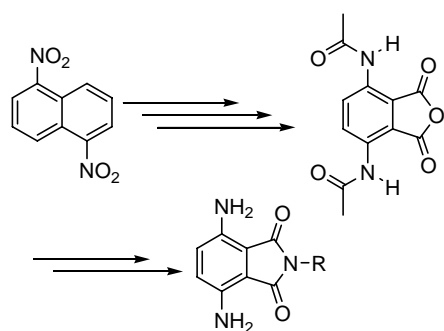
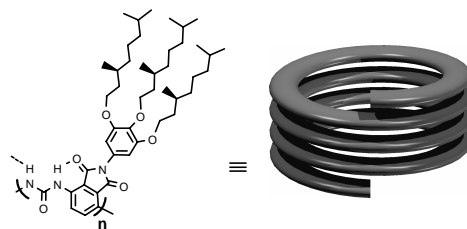
- 1) Sinkeldam, R. W.; van Houtem, M. H. C. J.; Koeckelberghs, G.; Vekemans, J. A. J. M.; Meijer, E. W. *Org. Lett.* **2005** submitted.
- 2) (a) Segura, J. L.; Martin, N.; Guldi, D. M. *Chem. Soc. Rev.* **2005**, *34*, 31-47. (b) Hoppe, H.; Sariciftci, N. S. *J. Mater. Res.* **2004**, *19*, 1924-45.
- 3) (a) Pfeiffer, G. Bauer, H. *Liebigs Ann. Chem.* **1980**, 564-89. (b) Klessinger, K. *Dyes and Pigments* **1982**, *3*, 235-241. (c) Gordon, P. D.; Gregory, P. *Organic chemistry in colour* ©Springer-Verlag **1983**. (d) Lüttke, W.; *J. Mol. Struct.* **1998**, *445*, 277-286.
- 4) Sadler, P. W. *J. Org. Chem.* **1956**, *21*, 316-18
- 5) Lüttke, W.; Klessinger, M. *Ber.* **1964**, *104*, 2342-57
- 6) Klessinger, M.; Lüttke, W. *Tetrahedron* **1963**, *19*, 315-335.
- 7) Klessinger, M. *Tetrahedron* **1966**, *22*, 3355-3365.
- 8) Chen, P. C. *Int. J. Quantum Chem.* **1996**, *60*, 681-687
- 9) Yamamoto, T.; Kizu, K. *J. Phys. Chem.* **1995**, *99*, 8-10.
- 10) Berlin, A. A.; Liogon'kii, B. I.; Zelenetskii, A. N. *et al. Dokl. Chem. (Eng. Trans.)* **1968**, *178*, 156-8.
- 11) Charles, T. L. (Sun Oil Co.) U. S. patent 3,600,401 **1968**.
- 12) Baeyer, A. *Ber.* **1870**, *3*, 514-7.
- 13) Heumann, K. *Ber.* **1890**, *23*, 3043-5.
- 14) Tatsugi, J.; Ikuma, K.; Izawa, Y. *Heterocycles* **1996**, *43*, 7-10.
- 15) Tomchin, A. B.; Fradkina, S. P.; Krylova, I. M.; Khromenkova, Z. A. *J. Org. Chem. (USSR)* **1986**, *22*, 2163-72..
- 16) Papaioannou, N.; Evans, C. A.; Blank, J. T.; Miller, S. J. *Org. Lett.* **2001**, *3*, 2879-82.
- 17) Dalgliesh, C. E.; Mann, F. G. *J. Chem. Soc.* **1945**, 893-909.
- 18) Kazembe, T. C. G.; Taylor, D. A. *Tetrahedron* **1980**, *36*, 2125-32.
- 19) (a) Norman, M. H.; Navas, F.; Thompson, J. B.; Rigdon, G. C. *J. Med. Chem.* **1996**, *39*, 4692-4703. (b) Bryant, W. M.; Huhn, G. F.; Jensen, J. H.; Pierce, M. E.; Stammbach, C. *Synth. Commun.* **1993**, *23*, 1617-25. (c) Peet, N. P.; Sunder, S.; Barbuch, R. J.; *J. Heterocycl. Chem.* **1980**, *17*, 1513-8. (d) Moser, P.; Sallmann, A.; Wiesenberg, I. *J. Med. Chem.* **1990**, *33*, 2358-68.
- 20) Allison, J. A. C.; Brauholtz, J. T.; Mann, F. G. *J. Chem. Soc.* **1954**, 403-8.
- 21) Hurd, C. D.; Hayao, S. *J. Am. Chem. Soc.* **1954**, *76*, 5065-9.
- 22) (a) Setsune, J.; Wakemoto, H.; Matsueda, T.; Matsuura, T.; Tajima, H.; Kitao, T. *J. Chem. Soc. Perkin Trans. 1* **1984**, 2305-9. (b) Blanc, V.; Ross, D. L. *J. Phys. Chem.* **1968**, *72*, 2817-24. (c) Posner, T. *Ber.* **1926**, *59*, 1799-1827. (d) Lieberman, C.; Dickhuth, F. *Ber.* **1891**, *24*, 4130-6.
- 23) (a) Patent: Rahtjen, A.; DE 128575, FTFVA6, Fortschr. Teerfarbenfabr. Verw. Industriezweige **1900**, *6*, 589. (b) Patent: Hoechst Farbwerken, DE 149940, FTFVA6, Fortschr. Teerfarbenfabr. Verw. Industriezweige; **1902**, *7*, 282.
- 24) (a) Friedlaender, P.; Bruckner, S. *Justus Liebigs Ann. Chem.*; **1912**, *388*, 34. (b) Baeyer, A.; Bloem, *Ber.* **1884**, *17*, 966. (c) Einhorn, A.; Gernsheim, A. *Justus Liebigs Ann. Chem.* **1895**, *284*, 145. (d) Kalb, L. *Ber.* **1909**, *42*, 3647, 3653, 3658.
- 25) Su, H. C. F.; Tsou, K. C. *J. Am. Chem. Soc.* **1960**, *82*, 1187-9.
- 26) Holtz, S. J.; Kellie, A. E.; O'Sullivan, D. G.; Sadler, P. W.; *J. Chem. Soc.* **1958**, 1217-22.
- 27) Schenning, A. P. H. J.; Franssen, M.; Meijer, E. W. *Macromol. Rapid Commun.* **2002**, *23*, 265-270.
- 28) Khan, M. S.; Al-Mandhary, M. R. A.; Al-Suti, M. K.; Ahrens, B.; Mahon, M. F.; Male, L.; Raithby, P. R.; Boothby, C. E.; Koehler, A. J. *Chem. Soc. Dalton Trans.* **2003**, 74-84.
- 29) Voss, G.; Schramm, W. *Helv. Chim. Acta* **2000**, *83*, 2884-92.
- 30) Birckner, E.; Paetzold, R.; Haucke, G. *Chem. Phys. Lett.* **1982**, *89*, 22-5.
- 31) Pouliquen, J.; Wintgens, V.; Toscano, V.; Kossanyi, J. *Dyes and Pigments* **1985**, *6*, 163-75.
- 32) Görner, H.; Schulte-Frohlinde, D. *Chem. Phys. Lett.* **1979**, *66*, 363-9.

- 33) (a) Pouliquen, J.; Wintgens, V.; Toscano, V.; Jaafar, B. B.; Tripathi, S.; Kossanyi, J. *Can. J. Chem.* **1984**, *62*, 2478-86. (b) Omote, Y.; Tomotake, A.; Aoyama, H.; Nishio, T.; Kashima, C. *Bull. Chem. Soc. Jpn* **1979**, *52*, 3397-9. (b) Setsune, J.; Wakemoto, H.; Matsukawa, K.; Ishihara, S.; Yamamoto, R.; Kitao, T. *J. Chem. Soc. Chem. Commun.* **1982**, 1022-3. (b) Ross, D. L.; Blanc, J. "Photochromism by *cis-trans* isomerization" in *Photochromism*, edited by Brown, G. H.; Wiley, New York, **1971**.
- 34) (a) Wyman, G. M.; Zarnegar, B. M. *J. Phys. Chem.* **1973**, *77*, 1204-7. (b) Brode, W. R.; Pearson, E. G.; Wyman, G. M. *J. Am. Chem. Soc.* **1954**, *76*, 1034-6.
- 35) (a) Dörr, F. *Applications of Picosecond Spectroscopy to Chemistry* **1984**, 127-38. (b) Kobayashi, T.; Rentzepis, P. M. *J. Chem. Phys.* **1979**, *70*, 886-92. (c) Weller, A. Z. *Electrochem.* **1956**, *60*, 1144.
- 36) (a) Beckers, E. H. A.; Meskers, S. C. J.; Schenning, A. P. H. J.; Chen, Z.; Würthner, F.; Janssen, R. A. J. *J. Phys. Chem. A* **2004**, *108*, 6933-7. (b) You, C.; Würthner, F. *J. Am. Chem. Soc.* **2003**, *125*, 9716-25. (c) Würthner, F.; Sautter, A. *Chem. Commun.* **2000**, 445-446.
- 37) van Hal, P. A.; Beckers, E. H. A.; Peeters, E.; Apperloo, J. J.; Janssen, R. A. J. *Chem. Phys. Lett.* **2000**, *328*, 403-408.
- 38) Uehara, K.; Takagishi, K.; Tanaka, M. *Solar Cells* **1987**, *22*, 295-301.

Summary

The design and synthesis of helical architectures is a fascinating area of research that deals with the chemistry beyond the covalent bond. Foldamers, capable of adopting a helical shape in solution, are just one example in which supramolecular interactions determine the secondary structure. The challenge is to design synthetically achievable systems that possess functionalities capable of directing the primary structure to the helical secondary shape *via* hydrogen bonding and π - π stacking. Poly(ureidophthalimides) are a recent example of foldamers possessing a covalent backbone capable of folding into a helical architecture based on these secondary interactions. Due to the high degree of organization, the use of chromophores in these systems can be of particular interest for the development of 'plastic electronics', *e.g.* field effect transistors (FETs) and organic solar cells. Helical systems soluble in water may be valuable candidates to mimic biological functions.

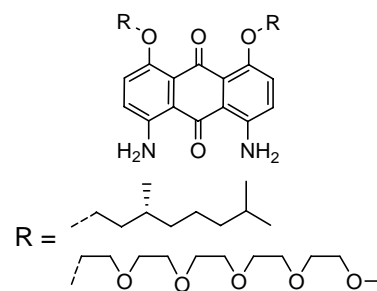
In chapter 1 a brief overview is given of the most studied synthetic foldamer designs of which the β -peptides resemble the naturally occurring α -helix the most. Other widely reported synthetic design principles are based on oligo(*meta*-phenyleneethynylene), aromatic oligoamides, and aromatic oligoureas. The various approaches clearly reveal the importance of the design of the primary structure, since the structural elements therein will govern the secondary shape and properties. Finally, the aim of the thesis is set to be the expansion of the synthetic scope of the poly(ureidophthalimides).



Therefore, in chapter 2, a new synthetic approach is presented that gives high yielding access to novel 3,6-diaminophthalimide building blocks, the precursors for a library of functionalized poly(ureidophthalimides). In addition, a start is made with a synthetic approach circumventing the use of 1,5-dinitronaphthalene as the starting material.

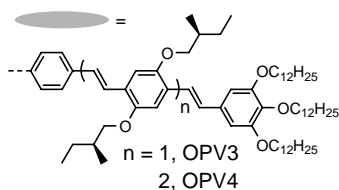
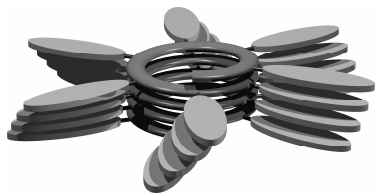
As described in the thesis of Judith van Gorp, attempts to copolymerize anthraquinone and phthalimides resulted in non-perfectly alternating oligomers. A more detailed study on various dimerizations established the formation of intermediates that rationalize scrambling of the urea linker as is presented in chapter 3. To circumvent these problems the synthesis of foldamers consisting of anthraquinones alone was envisaged.

Although the final goals were not achieved due to the inability to synthesize the required



isocyanato polymer precursors, the research led to novel lipophilic and hydrophilic diamino-anthraquinones.

In chapter 4 the potential of the periphery of ureidophthalimides by incorporation of OPV3 and OPV4 chromophores is addressed. CD studies indicated that the chromophores align in a

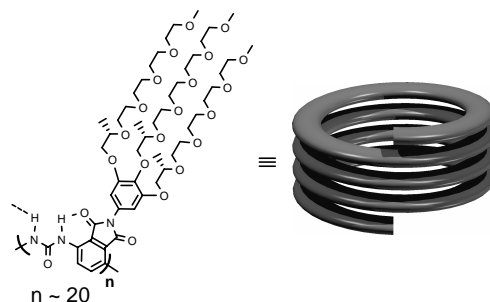


chiral helical fashion along the ureidophthalimide backbone. CD studies in heptane revealed that the solvent history governs the shape of the secondary architecture in this solvent. Temperature dependent CD studies in heptane revealed the remarkable stability of the secondary architectures while temperature studies in THF have shown the dynamics of the systems. Furthermore, there is a strong indication that THF facilitates folding. The somewhat low g -values for the bisignate Cotton effect hint towards the presence of frustrated stacks in which the OPV π - π

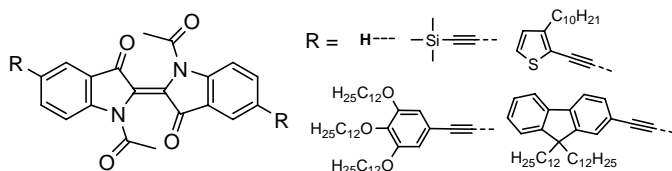
aggregation is not directed by the intramolecular hydrogen bonding of the phthalimide units.

Most foldamer research originates from a desire to understand the requirements for folding in natural systems. To mimic the naturally occurring α -helix solubility in water is a prerequisite.

Therefore, the ureidophthalimide system has been equipped with ethylene oxide chains as is discussed in chapter 5. The CD studies in water and in THF proved the presence of helical architectures. However, their bisignate Cotton effects are opposite in sign. This strongly suggests a solvent-dependent helical handedness preference. This would allow control over the secondary architecture by selecting the right solvent.



In chapter 6 the development of a new processable n -type material based on the notoriously insoluble indigo is described. A multi-step synthetic approach gave access to a



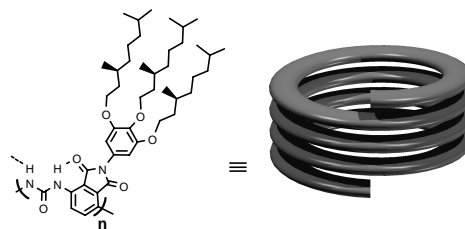
series of novel soluble indigos albeit in low yield. A combination of photophysical and electrochemical experiments led to the construction of an organic bulk-hetero-junction solar cell

with an active layer containing indigo as an n -type material and MDMO-PPV as the p -type material. Unfortunately, the poor electron mobility in N,N' -diacetylindigo is likely to rationalize the weak solar cell performance.

Samenvatting

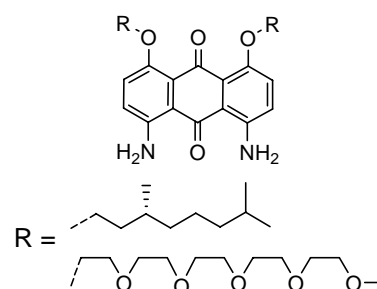
Het ontwerpen en synthetiseren van helices is een fascinerend onderzoeksgebied binnen de chemie dat verder gaat dan covalente interacties alleen. Verbindingen die een helixstructuur kunnen aannemen op basis van secundaire interacties zoals waterstofbrugvorming en π - π interacties behoren tot de foldameren. De poly(ureïdoftaalimides), die in dit proefschrift beschreven worden, behoren tot deze groep. De uitdaging bestaat uit de ontwikkeling van een synthetisch haalbaar ontwerp waarbij de functionele groepen die secundaire interacties mogelijk maken dusdanig gepositioneerd zijn in de primaire structuur dat deze de vorming van een helix induceren. Door de hoge mate van perifere ordening is de helix zeer geschikt voor het uitlijnen van chromoforen. Dit is met name van groot belang voor toepassing in kunststof elektronica, zoals veldeffect transistoren en organische zonnecellen. Daarnaast kunnen wateroplosbare helices waardevolle modelsystemen opleveren om biologische functies te imiteren.

In hoofdstuk 1 wordt een kort overzicht gegeven van de meest bestudeerde synthetische foldameren, waaronder poly(*meta*-fenyleenethynyleen), aromatische oligoamides, aromatische oligoourea, en foldameren gebaseerd op β -peptides. De verschillende synthetische benaderingen onderschrijven het belang van een doordacht ontwerp van de primaire structuur om vouwing tot een helix (secundaire structuur) mogelijk te maken. Dit proefschrift heeft als doel de synthetische mogelijkheden met betrekking tot de poly(ureïdoftaalimides) te verbreden.

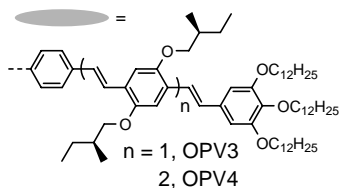
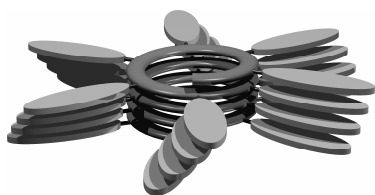


In hoofdstuk 2 wordt een nieuwe synthetische strategie beschreven die in hoge opbrengsten een variëteit aan 3,6-diaminoftaalimide bouwstenen toegankelijk maakt. Deze vormen de precursoren voor nieuwe gefunctionaliseerde poly(ureïdoftaalimides). Eveneens is een begin gemaakt aan de ontwikkeling van een synthetische methode om het gebruik van 1,5-dinitronaftaleen als uitgangsmateriaal te omzeilen.

Judith van Gorp heeft in haar proefschrift beschreven dat de copolymerisatie van anthrachinonderivaten met ftaalimides resulteert in niet perfect alternerende oligomeren. In hoofdstuk 3 wordt een gedetailleerde studie gepresenteerd, die laat zien dat de vorming van specifieke intermediairen tijdens verschillende dimerisatiereacties de *scrambling* van de ureumlinker verklaart. Om deze *scrambling* reactie te omzeilen is de synthese van foldameren die alleen uit anthrachinonen



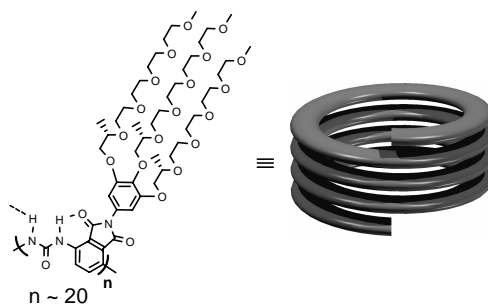
bestaan onderzocht. Ondanks het niet bereiken van het einddoel daar de benodigde isocyaanaten als polymeerprecursor niet synthetiseerbaar bleek, heeft het onderzoek toch geleid tot de synthese van nieuwe hydrofiele en lipofiele diamino-anthrachinonen.



In hoofdstuk 4 is beschreven hoe de periferie van ureïdoftaalimides gebruikt kan worden voor het organiseren van OPV3 en OPV4 chromophoren. Circulair dichroïsme (CD) studies wijzen uit dat de chromophoren zich chiraal ordenen om de ureïdoftaalimide *backbone*. CD studies in heptaan wijzen uit dat de oplosmiddel-geschiedenis de secundaire structuur bepaalt in heptaan. Temperatuurafhankelijke CD studies in heptaan tonen de opvallende stabiliteit aan van de secundaire structuur terwijl de temperatuurstudies in THF juist de dynamiek van het systeem

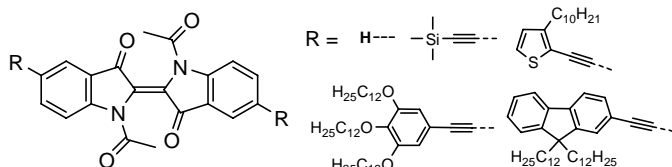
weergeven. Bovendien is er een sterke indicatie dat THF de helixvorming induceert. Het feit dat de g-waarden aan de lage kant zijn duidt mogelijk op de aanwezigheid van slecht geordende structuren waarin de OPV π - π interacties niet gedirigeerd worden door de intramoleculaire waterstofbrugvorming van de ftaalimide-eenheden.

Het meeste foldameeronderzoek richt zich op het vergroten van het begrip ten aanzien van de vouwing van natuurlijke systemen. Om natuurlijke systemen te kunnen imiteren is wateroplosbaarheid een vereiste. Om dit te bereiken is het ureïdoftaalimidesysteem voorzien van oligo-ethyleenoxide groepen. CD studies



in water en THF duiden op de aanwezigheid van spiraalvormige architecturen. Het Cotton-effect in THF is omgekeerd aan dat in water, wat suggereert dat er een oplosmiddelafhankelijke voorkeur voor P- of M-heliciteit is. Daarmee zou door variatie in het oplosmiddel controle over de heliciteit mogelijk zijn.

In hoofdstuk 6 wordt de ontwikkeling van een nieuw n-type chromofoor op basis van het notoir onoplosbare indigo besproken. Een meerstapsynthese leidde tot nieuwe oplosbare



indigoderivaten, zij het in lage opbrengsten. Een combinatie van fotofysische en electrochemische metingen heeft geleid tot de assemblage van een organische *bulk-heterojunction* zonnecel

bestaande uit diacetylundigo als n-type en MDMO-PPV als p-type materiaal. De teleurstellende zonnecelresultaten zijn waarschijnlijk toe te schrijven aan de slechte elektronenmobiliteit van *N,N'*-diacetylundigo.

Curriculum Vitae



René Sinkeldam werd geboren op 19 april 1974 te Purmerend. Na het HLO aan de Hogeschool van Amsterdam afgerond te hebben werd in september 1999 begonnen aan de studie scheikunde aan de Universiteit van Amsterdam. De studie werd afgerond met een afstudeerproject bij prof. dr. H. Hiemstra in the vakgroep organische chemie. Het diploma werd behaald in september 2001. Vervolgens werd in januari 2002 begonnen aan een promotieonderzoek aan de Technische Universiteit Eindhoven in de capaciteitsgroep Macromoleculaire en Organische Chemie onder begeleiding van prof. dr. E. W. Meijer en dr. J. A. J. M. Vekemans. De belangrijkste resultaten van het promotie onderzoek staan beschreven in dit proefschrift.

René Sinkeldam was born in Purmerend, the Netherlands, on April 19th, 1974. After finishing his chemistry study at the Hogeschool van Amsterdam, he started the study chemistry at the University of Amsterdam. The Masters of Science degree was obtained in September 2001 with a graduation project at the laboratory of Organic Chemistry under the supervision of prof. dr. H. Hiemstra. He left for Eindhoven, the Netherlands, in January 2002 to start as a PhD student in the laboratory of Macromolecular and Organic Chemistry at Eindhoven University of Technology under the supervision of prof. dr. E. W. Meijer and dr. J. A. J. M. Vekemans. The most important results of the research are presented in this thesis.

Dankwoord

Met dit dankwoord wordt dit proefschrift, vier jaar onderzoek en een uitermate plezierige tijd afgesloten. Voor de buitenstaander lijkt het wellicht alsof promoveren een eenzame bezigheid is; niets is minder waar. Tijdens de afgelopen vier jaar heb ik hulp gehad van veel mensen.

Bert, bij deze wil ik je graag bedanken voor de mogelijkheid die je mij hebt gegeven om in jouw groep onderzoek te doen. Ik heb mij regelmatig vergaapt aan jouw schier eindeloze kennis van de chemie in de breedste betekenis van het woord. Daarbij heb ik je ervaren als een betrokken en prettige coach in alle 'fase' gesprekken en daarbuiten wanneer het mijn toekomst na SMO betrof. Jef, ik heb heel wat uurtjes, wellicht dagen, bij jou op kantoor gezeten en het hadden er wat mij betreft nog meer mogen zijn. Ik heb zeer veel van je geleerd en mocht altijd graag luisteren naar je ideeën. Tijdens het schrijven van mijn proefschrift, stond je altijd direct voor mij klaar met correcties en aanbevelingen. Bedankt! Verder wil ik de gehele vaste staf bedanken die altijd bereikbaar was voor het beantwoorden van vragen. Ook wil ik Judith en Tom bedanken voor hun pionierend onderzoek op het gebied van de ureïdoftaalimiden wat mij een laagdrempelige instap in dit fascinerende onderzoeksveld bood.

Verder wil ik prof.dr.ir. René Janssen, prof.dr. Jim Feast en prof.dr. Henk Hiemstra bedanken voor het kritisch lezen van mijn proefschrift en wil ik ze tezamen met dr. Albert Schenning en prof.dr. Bert Hulshof bedanken voor hun deelname aan mijn promotiecommissie.

Het is waanzinnig prettig dat de onderzoekers binnen SMO zo in de watten worden gelegd met de ondersteuning van Hanneke, Ingrid, Joke, Carine, Hans, Henk en Hannie. Zij staan altijd voor iedereen klaar om te faciliteren in het onderzoeksproces.

Het lab is de thuisbasis voor de chemicus. Derhalve wil ik bij deze alle huidige en vroegere collega's van Lab 2 bedanken voor de goede werksfeer. In het bijzonder wil ik Jolanda (de enige constante factor op lab 2) even noemen. Ondanks het feit dat onze muziekkieuzes wel eens wat uiteen liepen, wil ik je bedanken voor de altijd strakke organisatie. Dit is ook een goed moment om de medebewoners van STO4.31 van de afgelopen vier jaar: Judith, Pauline, WJ, Ingrid, Theresa, Patrick en Martijn te bedanken en succes te wensen met hun onderzoek of werk. Theresa, thanks a lot for the very nice artwork you created for my thesis and the pleasant conversations we used to have about the differences between The States and The Netherlands. I wish you and James all the best in your careers at Corning.

Geen onderzoek zonder de feed-back van collega's in de vele meetings. Bij deze wil ik graag alle deelnemers van de Apronics- en Helixlunch bedanken voor hun luisterend oor en commentaar.

Aan het eind van mijn indigoproject, wat nogal synthetisch van aard was, kreeg ik veel hulp op weg naar de onvermijdelijke plastic zonnecel. Edwin, Pascal en Waldo bedankt voor jullie tijd en expertise op het gebied van respectievelijk PIA spectroscopie, AF microscopie en de assemblage van een plastic zonnecel.

Dit proefschrift is tevens ook het geboortekaartje van een groot aantal nieuwe verbindingen. De totstandkoming daarvan heb ik mede te danken aan de studenten die ik met veel plezier heb mogen begeleiden. Als eerste wil ik Michel bedanken. Ik weet zeker dat je door het indigo-onderzoek verslaafd bent geraakt aan de synthese. Je hebt dit fantastisch bewezen met al het werk dat beschreven is in hoofdstuk 5. Je bent een slimme kerel en ik ben er van overtuigd dat je eigen promotieonderzoek een succes wordt. Never a dull moment met (radio) Wouter op het lab. Onverstoorbaar energiek en continu pratend zette jij menig anthrachinonmolecule in elkaar. Bedankt! Inge, de resultaten van jouw onderzoek hebben geleid tot de ontwikkeling van

een nieuwe route voor de synthese van 3,6-diaminoftaalimides. Bedankt, en veel succes in je werk bij Mercachem. Hiroko, your stay in The Netherlands was too short. I still think that the project you worked on has a lot of potential. Thank you for your contribution and good luck with your graduate research.

De kortstondige samenwerking met Guy en de gratis OPV's van Freek en Maarten P. hebben mijn onderzoek zeker versneld. Bedankt! Ik hoop dat ik mijn koosnaam 'the OPV destruction plant' heb kunnen goedmaken met de resultaten beschreven in hoofdstuk 4.

Natuurlijk wil ik bij deze ook Ralf, Lou en Joost bedanken voor hun sterk analytisch inzicht. Ik heb veel geleerd van de discussies over de interpretatie van GPC, en MS data. Jos, bedankt voor je Excel sheets en je flexibele instelling als ik weer eens een sample tussendoor wilde meten.

Verstoken van elke vorm van civilisatie merk je dat de individualisering wat minder is doorgedrongen in de zuidelijke gewesten. Als snel bleek dat veel collega's ook buiten de zaak om fantastisch gezellig waren en dat de grootstedelijke infrastructuur en de metropolistische 'feel' van Amsterdam niet nodig waren voor zeer gemakkelijke avonden. Zo werd er heel wat gegeten, pilsjes gedronken en pilsjes gedronken wat weer aanleiding gaf tot het voeren van goede gesprekken. Uiteraard snoven we wat cultuur op met menig concert, film, een goed glas whisky (bedankt Linda!) en natuurlijk carnaval.....oh nee, geen polonaise aan mijn lijf! Hoewel de samenstelling wel eens wisselde zijn de meest kroeg(k)uren doorgebracht met Beckers, Herrik, Fransen, Steve, Chris, Sergé en Pascal. Bedankt! Dit selecte gezelschap was ook vaak terug te vinden in de mannenhoek aan de koffietafel, alwaar politiek en ethiek werden bediscussieerd. Geregeld was daar vrouwelijk tegenwicht aanwezig in de persoon van Patje, Hinke en Linda. Hopelijk zal de jeugd: Arjan, Maarten S. en Michel v. H. deze traditie onder de bezielende leiding van oudgediende Fransen voortzetten. Steve and Chris, thanks a lot for all the on- and off-duty time we spent together. Steve, I enjoyed the days we roamed through Amsterdam and Boston a lot. Chris, you enriched my knowledge of the American culture with the Philly cheese steak sandwich. The world becomes smaller everyday and I am sure we will keep in touch. Op kerstborrels en de altijd weer gezellige SMO-uitjes werd het een ware sport meneer Wienk uit de tent te lokken met heftige maatschappelijke discussies. Mijn debating skills bleken echter niet opgewassen tegen deze verbale overmacht.

Alle pilsjes werden er ook weer afgesport. Op de fiets tezamen met Beckers, de Herrik, Sander en Anouk zijn verreweg de meeste kilometers gereden. Chris, I still vividly remember the times we spent in the gym: "come on Chris, one for the neck".

Uiteraard wil ik bij deze mijn familie en vrienden bedanken voor hun aanhoudende interesse voor mijn onbegrijpelijke onderzoek, mijn leven als chemicus en alles wat daarbij komt kijken.

Deze laatste laatste regels zijn gereserveerd voor degene die ik het meest dankbaar ben. Noek samen met jou vliegt de tijd. Wherever, forever!

Later (später),

René.